

Large Organic Molecules for Quantum Interference Experiments

Inauguraldissertation

zur

Erlangung der Würde eines Doktors der Philosophie
vorgelegt der
Philosophisch-Naturwissenschaftlichen Fakultät
der Universität Basel

von

Lukas Felix
aus Braunau (TG), Schweiz

Basel, 2015

Originaldokument gespeichert auf dem Dokumentenserver der Universität Basel
edoc.unibas.ch

Genehmigt von der Philosophisch-Naturwissenschaftlichen Fakultät

auf Antrag von:

Prof. Dr. Marcel Mayor

Prof. Dr. Andreas Pfaltz

Basel, den 8. Dezember 2015

Prof. Dr. Jörg Schibler

Dekan

Dedicated to:

Paula

Abstract

Matter-wave dualism is a fundamental concept in quantum physics. The observation of wave properties of heavy organic molecules can be used to approach the borderline between classical and quantum physics. Up to which mass and size do particles or molecules still have wave properties? This question is subject to be answered within this thesis and as part of the international nanoquestfit-project where many researchers of different disciplines are involved.

This thesis is a summary of the work done within a research collaboration between the group of Prof. Dr. Marcel Mayor (University of Basel) and the group of Prof. Dr. Markus Arndt (University of Vienna). The work is mainly focused on the development of novel quantum interference experiments that imply the development of new synthetic strategies towards tailor-made molecules. Novel interferometers have been developed by the Arndt group and therefore the molecular requirements changed strongly within the past years. The syntheses of these tailor-made molecules were performed by the author in the laboratories of Prof. Mayor in Basel. Quantum interference experiments and the preliminary investigations described within this work, namely the thermal stability test, the desorption studies and the laser-induced acoustic desorption have been performed by the Arndt group in Vienna.

Investigations at the interface of quantum and classical physics are a fascinating part of the research. The final goal is to approach the quantum-to-classical transition by the observation of quantum properties of large and complex molecules. In order to study the wave nature of such particles—a purely quantum mechanical phenomenon—synthetic procedures towards tailor-made compounds are developed to improve the observation of this phenomenon through matter-wave experiments.

At the starting point of this work, a series of highly fluorinated porphyrin-monomers set a new benchmark in high-mass quantum interference experiments. The highest masses of particles used in quantum interference experiments were around 10'000 g/mol. Thus, our objective was to reach masses up to 25'000 g/mol with the suitable features for the quantum interferometry experiments.

In the first chapter of this thesis, the principle of interferometry, the development and evolution of this technology are presented. In the subsequent chapters, the different synthetic approaches of the tailor-made molecules designed to improve the measurements and achieve the goal of this thesis are described.

The main part of this thesis is focused on the synthesis of tailor-made molecules for quantum interference experiments. In a first part, the synthesis of a novel, more massive fluorinated phthalocyanine is presented. That phthalocyanine was used in far-field quantum interference experiments. Unfortunately, the molecular requirements could not be tuned to observe wave-particle duality in these experiments. The second part focuses on the synthesis of three different molecular libraries. Molecular libraries are mixtures of molecules having the same core but a to some extent random number of long perfluorinated chains. The individual members within the library were observable in MALDI-TOF mass spectrometry. We attached the chains to three different cores to obtain three different molecular libraries. To produce a first generation of libraries we used diacetylene bond porphyrin-dimer. The rather limited reaction scope of diacetylene bond porphyrins was enhanced by the second generation of tetramers and pentamers. To compare the modularity of the synthesis of oligo-porphyrin systems two additional cores, a porphyrin-dimer and a porphyrin-trimer, have also been synthesized. The possibility to produce a molecular beam with the three molecular-libraries has been investigated by thermal studies, desorption experiments and laser-induced acoustic desorption.

The last part of the thesis is focused on the synthesis of photocleavable tags that can be attached to model compounds. These tags are synthesized since novel quantum interference experiments are based on light gratings where a mass difference is supposed to be observed at the detector level upon cleavage. The final idea is, in the near future, to attach these molecules to large particles, such as metal-nanoparticles, clusters or proteins. It is expected to enable the detection of mass differences of the intact clusters and the clusters with the cleaved tags. Three different model compounds have been synthesized. The cleavage of the tags was proven in solution upon irradiation of UV-light in solution, where a constant and reproducible decay was observed. In future quantum interference experiments, the cleavage should be performed in gas-phase as a final prove of concept. The molecules are currently under investigations in the Arndt group.

Acknowledgements

Firstly, I would like to acknowledge Prof. Dr. Marcel Mayor for having me in his group and the opportunity to explore a fascinating field of science. I enjoyed all the discussions we had during the past five years.

In addition, I would like to thank Prof. Dr. Andreas Pfaltz for co-refereeing this thesis and Prof. Dr. Markus Arndt for being external expert. Prof. Dr. Dennis Gillingham is acknowledged for chairing the examination committee.

Not all the work would have been possible without the great help and support of our collaborators in Vienna. I thank Prof. Dr. Markus Arndt and his group members Uğur Sezer, Nadine Dörre, Johannes Horak, Lisa Wörner, Philipp Schmid, and Christian Knobloch for all the extremely interesting discussions and the time we spend together within the Nanoquestfit-project. I hope we meet again in future. Furthermore, I would like to thank Dr. Jens Tüxen for all the support and the preliminary work in the field.

Many thanks to all the current and past members of the Mayor-group. Especially I want to mention my lab-neighbors: Dr. Federica Reinders, Dr. Markus Gantenbein, Dr. Jens Hermes, Dr. Fabian Sander, Dr. Ulrike Fluch, Mario Lehmann-Alvarez, Dr. Almudena Gallego-Gonzales, Dr. Pascal Hess, Kevin Weiland, Kenan Li, Linda Bannwart, and Lorenzo Delarue Bizzini. I greatly enjoyed our scientific and non-scientific discussions. Michel Rickhaus is acknowledged for graphical artwork. Moreover, I thank the students who visited my lab during their undergraduate studies: Simona Hübner, Jan Hanusch, Fabian Bisseger, Marc Müller, and Tanja Amport.

I would like to thank Dr. Daniel Häussinger, Heiko Gsellinger and Kaspar Zimmermann for performing NMR-experiments, Dr. Heinz Nadig for mass spectroscopic analyses and Sylvie Mittelheiser for the elemental analyses. I also want to thank the technical staff from the “Werkstatt”: Andreas Koller, Markus Ast, Manuel Hermida, and Andreas Sohler. Moreover, I would like to thank Markus Hauri and Roy Lips from the “Materialausgabe” and the secretaries Brigitte Howald and Beatrice Erismann.

I thank Dr. Loïc Le Pleux, Dr. Almudena Gallego-Gonzales, Linda Bannwart and my father for proofreading this thesis.

Finally, I would like to thank my family, my mother Katharina, my father Hansrudolf, my sister Theres, her husband Kevin and their son Thierry for the constant support during my studies and my PhD-work. Paula, thank you for being my wife, your love and support.

Table of Contents

1	Introduction	1
1.1	Matter Wave Interferometry	1
1.1.1	Far-Field and Near-Field Interferometry	3
1.1.2	Molecular Far-Field Interferometry	4
1.1.3	Molecular Near-Field Interferometry.....	7
1.2	Research Projects.....	15
2	Fluorinated Phthalocyanines for Far-Field Interferometry.....	17
2.1	Molecular Design	18
2.2	Syntheses and Characterization	21
2.3	Quantum Interference Experiments.....	32
2.4	Conclusion	35
3	Near-Field Interferometry: 1st Generation Porphyrin-Systems	36
3.1	Molecular Design	37
3.2	Statistical Nucleophilic Aromatic Substitution Reaction	40
3.3	Syntheses and Characterization	42
3.4	Thermal Stability Tests.....	51
3.5	LIAD Experiments	54
3.6	Conclusion	57
4	Near-Field Interferometry: 2nd Generation Porphyrin-Systems	59
4.1	Design of Oligo-Porphyrin-Systems	60
4.2	Syntheses of Oligo-Porphyrin-Systems.....	63
4.3	Desorption Experiments	73
4.4	Conclusion	76
5	Photocleavable Tags.....	77
5.1	Photocleavable Protection Groups.....	78
5.2	Molecular Design	81
5.3	Syntheses and Characterization	84
5.4	Cleavage Experiments	101

5.5	Conclusion	108
6	Summary and Outlook.....	110
6.1	Far-Field Interferometry	110
6.2	Near-field Interferometry	111
6.3	Photocleavable Tags	116
6.4	General Summary and Outlook	118
7	Experimental Part	119
7.1	General Remarks	119
7.2	Synthetic Procedures	122
8	List of Abbreviations.....	199
9	Literature	200
11	Appendix	207
11.1	Contributions.....	207
11.2	Publications.....	207
11.3	Curriculum Vitae	Fehler! Textmarke nicht definiert.

1 Introduction

1.1 Matter Wave Interferometry

Waves are all around us and play an important role in our life. Classical wave behavior like waves on a lake or the sound waves, is well known and understood. The phenomenon called interference occurs due to superposition of two waves, which leads to the combined sum of both waves. The first one observing the phenomena of constructive and destructive interference was Thomas Young in 1802 (drawings in Figure 1).^{1,2}

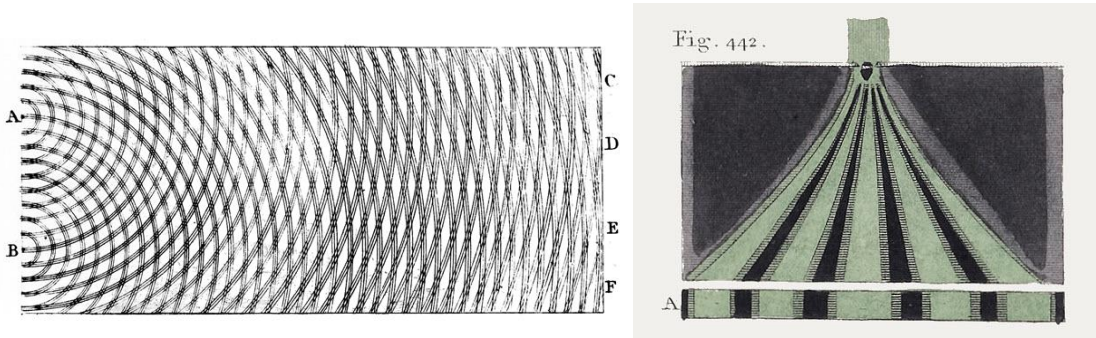


Figure 1. Young's drawing of the wave behavior of light. The images show the propagation of a coherent light diffracted at a double slit (A and B) and detected as a wave at the detector-level (C, D, E, and F).²

Thomas Young used a coherent light source shining on a double slit in a metal plate. Placing a photographic screen behind the double slit, a wave pattern was observed. If photons were described as particles, no wave pattern would be observed on the screen. The constructive and destructive interference of photons is the only explanation of the wave pattern.^{3,4}

This classical physics effect leads to the question whether quantum particles like photons, electrons, neutrons, atoms, molecules, or even large nanoparticles do interfere. In 1924, it was Louis de Broglie proposing the wave particle duality for light, it is also valid for the behavior of electrons.⁵ This theory was the starting point of intense studies towards the observation of wave properties of electrons, neutrons, atoms, and small molecules. Equation 1 is the well-known de Broglie equation, describing that to any particle with a momentum, a wavelength can be assigned.

$$\lambda_{db} = \frac{h}{p} = \frac{h}{m \times v}$$

Equation 1. De Broglie wavelength λ_{db} ; h being the Planck constant, p the momentum, m the mass, and v the velocity.

By observing the wave nature of electrons at a nickel crystal, Davisson and Germer confirmed the theory of de Broglie in 1927.⁶ The observations of Estermann and Stern in 1930 were a breakthrough in quantum interference.⁷ They described the interference of helium-atoms and of dihydrogen-molecules for the first time, measuring the diffraction at a lithium fluoride crystal. The wave nature of neutrons was then observed by Halban and Preiswerk in 1936.⁸

It is very interesting that 150 years passed after the first experiments of Thomas Young, until the next experiments using double slits were performed.¹⁻⁴ Jönsson used a double slit to diffract beams of electrons in 1961.⁹⁻¹¹ In 1988 Zeilinger calculated the diffraction of cold neutrons at double slits.¹² These calculations were verified by adaption of Youngs' double slit experiment for helium atoms by Carnal in 1991.¹³ They used a simple atom interferometer with a double slit, such as Young did in 1802. Keith observed for the first time the wave pattern of sodium atoms in 1988, using a fabricated gold transmission grating.¹⁴

Based on Estermann and Stern's experiments with helium and dihydrogen in 1930, Schöllkopf and Toennies observed the interference of clusters of He₂, H₂, and D₂ in 1994.¹⁵ The clusters are only held together by weak Van der Waals forces. This was the starting point of investigations about various molecules (mostly diatomic ones) such as I₂, Na₂, K₂, and D₂.¹⁶⁻²⁰ Finally, the breakthrough regarding interferometry with complex organic molecules happened in the year 1999, when Arndt *et al.* performed quantum interference experiments (QIE) with the buckminsterfullerene C₆₀.²¹

On the following pages, experimental setups and molecular designs based on the 1999 experiment in the group of Prof. Dr. Markus Arndt at the University of Vienna, which is still working in this field, are summarized. The difference between far-field and near-field interferometry is described in section 1.1.1. The experiments and molecular designs used for far-field and for near-field interferometry are presented in section 1.1.2 and 1.1.3 respectively. A new evaporation technique for the production of molecular beams is also presented in section 3.5.

1.1.1 Far-Field and Near-Field Interferometry

In the original double slit experiment in 1802, Thomas Young observed interference. The diffraction and interference of light is a typical experiment in the far-field regime, which is also known as the Fraunhofer regime.²² Nearly all the early interference experiments are based on the double slit setup used by Young. As shown in Equation 2 in the far-field regime the slit opening (a) is small. In addition to this, the distance (L) between the double slit (diffraction element) and the screen (observation element) is large compared to the wavelength (λ) of the observed element.

$$\frac{a}{L * \lambda} \ll 1$$

Equation 2. Far-field approximation: a is the slit size; L is the distance between the diffraction element and the observation element; λ is the wavelength.

Using far-field conditions no curvature of the propagating steady wave and therefore the wave front is planar.

In contrast to the far-field regime, near-field experiments need a large slit opening (a), and the distance (L) between the double slit (diffraction element) and the screen (observation element) is small compared to the wavelength (λ) of the observed element. This behavior is described in Equation 3.

$$\frac{a}{L * \lambda} \geq 1$$

Equation 3. Near-field approximation: a is the slit size; L is the distance between the diffraction element and the observation element; λ is the wavelength.

The near-field regime is also known as the Fresnel-regime.²² Clauser and Li introduced a near-field interferometer for potassium atoms in 1994.²³ Progress, advantages and disadvantages of both regimes are described in the two following pages.

1.1.2 Molecular Far-Field Interferometry

Initially, it could be expected that the buckminsterfullerene C_{60} , shown in Figure 2, must have particle behavior. However, in 1999, Arndt *et al.* proved the wave properties of C_{60} .²¹ The buckminsterfullerene was chosen since it has an already nearly classical body and the fullerene is readily available in large amounts.^{24,25}

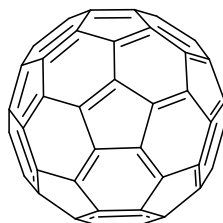


Figure 2. Buckminster fullerene C_{60} .

The experimental setup used for the first experiment is shown in Figure 3. The interferometer consisted of four main parts, the thermal source (oven), the collimation slits, a diffraction grating, and the detection unit. By keeping the interferometer under vacuum (5×10^{-7} bar) the collisions of the beam with background gas can be minimized.

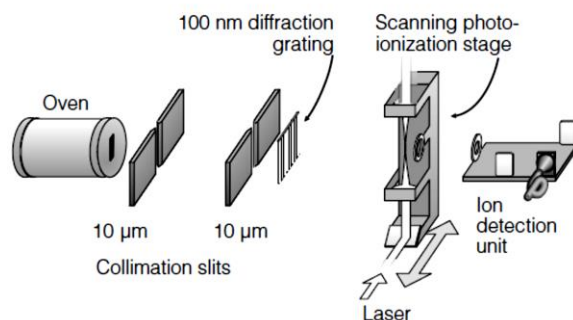


Figure 3. Far-Field interferometer used for the experiments with buckminsterfullerene C_{60} . Containing an oven as a thermal source, two collimation slits, a diffraction grating, and the detection unit.²¹

Sublimation of the C_{60} molecules was done in the oven at 900-1000 K. The sublimed molecules are moving in all directions with different velocities. The most probable velocity is 220 ms^{-1} , corresponding to the de Broglie wavelength of 2.5 nm (Equation 1) and can be determined by time-resolved detection of the chopped molecular beam.^{26,27} To obtain a coherent focused beam, delimitation was done using a slit-opening at the oven and the two $10 \mu\text{m}$ collimation slits. The diffraction grating with grating distance of $100 \mu\text{m}$ was used to obtain an interference-pattern of the C_{60} particles.

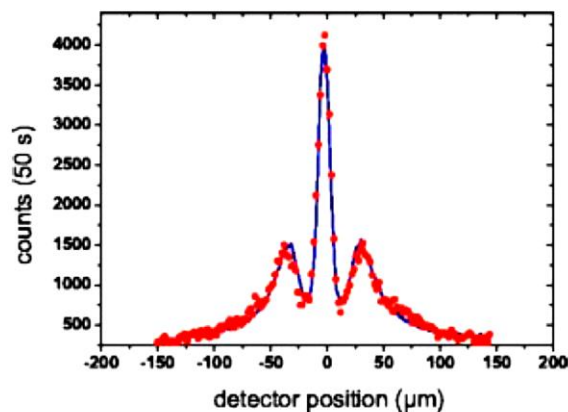


Figure 4. Interference pattern of C_{60} . The detector position (μm) is displayed *versus* the counts of ions in 50 s.²⁶

Using a laterally shifted scanning photoionization stage, the interference pattern was detected by scanning the ions as a function of the detector positions as shown in Figure 4. The broad velocity distribution within the molecular beam was a limitation for the experiment. Using a gravitational selection, the velocity distribution of the molecules within the beam could be delimited, improving the relevance of the interference pattern strongly.²⁸ In the improved setup, it was possible to measure the interference not only for the buckminsterfullerene C_{60} but also for the slightly larger C_{70} fullerene.²⁸ Another drawback of the experiment are Van der Waals interactions between the fullerenes and the material gratings. This could lead to dephasing of the molecular beams as well as to obstruction or destruction of the material gratings. To overcome this problem a standing light wave grating was proposed to substitute the material gratings.^{29,30}

Kapitsa and Dirac were the first describing the diffraction at a standing light wave in 1933.³¹ The theory by Kapitsa and Dirac was confirmed experimentally in 1983 by Moskowitz *et al.*³² The so called Kapitsa-Dirac effect, which describes that electrons are acting like waves when diffracted at a light wave grating, was described in 2001 by Freimund *et al.*³³ The Kapitsa-Dirac effect is still one of the most used phenomenon in far-field and near-field interferometry.³⁴

In 2010, the next milestone in far-field interferometry was set in the Arndt group in Vienna. New concepts were used to adapt the far-field interferometry to large molecules.³⁵ In the year 2012 a novel setup was used observe far-field interference of two phthalocyanine molecules (see Figure 5d and e for molecular structures)³⁶ Figure 5 shows the experimental setup used in 2012 to observe quantum interference with fluorescent dyes.

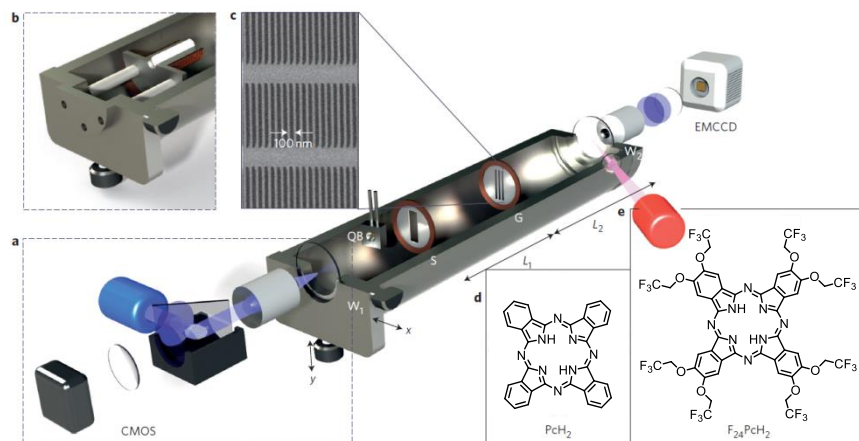


Figure 5. Interferometer setup for laser evaporation, interference and detection. (a) Blue laser (445 nm, 50 mW) focused on a glass plate that was coated with molecules on the inner part; (b) Collimation slits to obtain a coherent molecule beam; (c) Diffraction grating made of SiN_x with a period of 100 nm; (d) PcH_2 ($\text{C}_{32}\text{H}_{18}\text{N}_8$, mass = 514 g/mol); (e) $\text{F}_{24}\text{PcH}_2$ ($\text{C}_{48}\text{H}_{26}\text{F}_{24}\text{N}_8\text{O}_8$, mass = 1298 g/mol).³⁶

The interferometer consists of four different parts. A blue laser was used to produce a molecular beam (Figure 5a) that was delimited at the collimation slits (Figure 5b) to produce a coherent matter wave. The coherent matter wave was diffracted at the diffraction grating (Figure 5c) and finally the fluorescence was detected by a red laser at the detection level. The interference pattern obtained for the two molecules are shown in Figure 6.

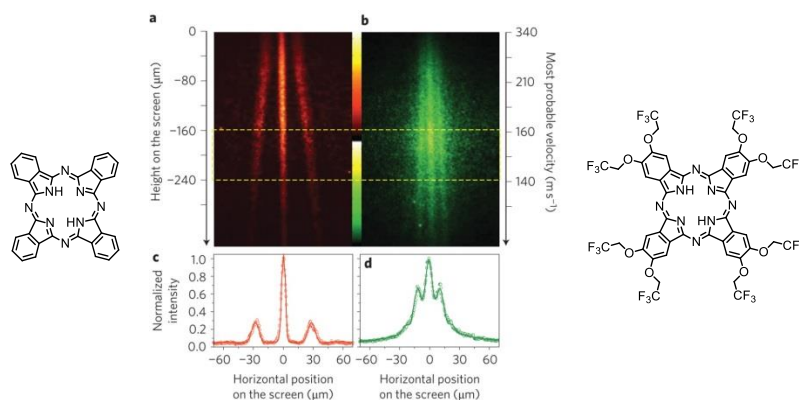


Figure 6. Interference pattern obtained in the interferometer. (a) and (b) showing the screen, (c) and (d) showing the diffraction obtained from the grating.³⁶

Both molecules that were investigated interfere at the grating level. The interference intensity for PcH_2 is well defined in contrast to the intensities for $\text{F}_{24}\text{PcH}_2$. Up to this date the fluorinated phthalocyanine derivative is the heaviest molecule that showed wave behavior in a far-field experimental setup.

Even though the near-field experiments set the first milestone in molecular quantum interference in 1999, these experiments have main drawbacks.²¹ The discussed problem with the material grating, and the small slit width set limits. Thus, adaptation for larger and larger molecules is not possible. With regard on these problems, near-field interferometry progressed fast in the past years and new milestones were set. The progress in molecular near-field interferometry is discussed below.

1.1.3 Molecular Near-Field Interferometry

Interferometry in the near-field regime has major advantages over interferometry in the far-field regime. The biggest advantage of this method can be defined by the Talbot-effect. It describes the diffraction of light at a grating, producing a self-image after the grating in the Talbot-distance.³⁷ To observe the self-image, the distance between the grating and the detector screen has to be a multiple of the Talbot-distance L_T . The definition of the Talbot-distance is shown in Equation 4.

$$L_T = \frac{d^2}{\lambda_{dB}}$$

Equation 4. Talbot-distance L_T , which is defined by the grating period d and the de Broglie wavelength λ_{dB} .

To investigate the difference between far-field and near-field interferometry, an imaginary calculation example is given. Doubling the molecular mass, having a constant Talbot-distance ($L_T = const.$) and the knowledge from Equation 1, Equation 2 and Equation 3, one can determine that the grating distance is reduced in far-field experiments by a factor of 2 and in near-field experiments just by a factor of $\sqrt{2}$. Therefore, the requirements in near-field interferometers are much easier to fulfill than in far-field experiments when the molecular mass is increased.

In 1948 Lau enhanced this theory by the use of a second grating.³⁸ In these experiments, the first grating is supposed to be in Talbot-distance L_T to the diffraction grating, which is still in Talbot-distance L_T to the screen. When the screen is scanned transversally, the interference pattern can be detected. This development allows the use of incoherent matter-waves, since the first grating acts as a collimation grating. It describes the second big advantage over far-field experiments. In Talbot-Lau interferometers (TLI), thermal sources (like an oven) can be used without collimation gratings.^{39,40}

In a next step, it is essential to prove that the periodic pattern on the screen is not only a self-image of the second grating, which is reproduced at the detector level, but occurs due to interference. The effect of the reproduced self-image at the detector level is well understood and described as Moiré-fringes.⁴¹ To prove that the pattern is produced by interference, fringe visibility and its dependence on different velocities of the molecules is investigated. Using a TLI and fullerene C_{70} , the first organic molecule used in the near-field regime, the Arndt group showed good agreement between calculated and experimental data.⁴²

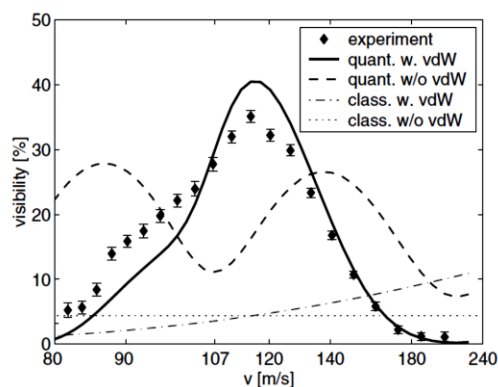


Figure 7. Comparison of the calculated and experimental values of visibility [%] vs. velocity [m/s] of C_{70} .⁴²

If only Moiré-fringes show up on the detector level, the visibility would only be weakly influenced by the velocity of the particles. In contrast, the visibility of the real interference pattern would be highly influenced by the velocity. This could be shown comparing the experimental and calculated values for fullerene C_{70} .

Since the optimized TLI was designed to observe quantum interference of even larger molecules, fluorinated fullerene $C_{60}F_{48}$ and tetraphenylporphyrin (TPP) were exposed to the interferometer.⁴³

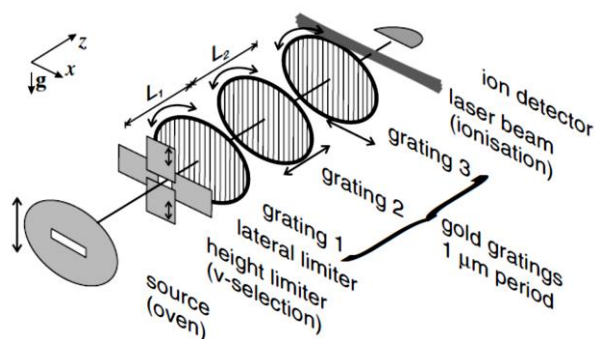


Figure 8. TLI used to produce the interference pattern of fullerene C_{70} , fluorinated fullerene $C_{60}F_{48}$ and tetraphenylporphyrin (TPP).^{42,43}

The apparatus, as shown in Figure 8, consists of an oven source to produce the molecular beam, which is delimited first by a lateral limiter and secondly by a first grating (grating 1, collimation grating). The next grating is in Talbot-distance L_T to the collimation grating and is defined as the diffraction grating (grating 2). The self-image of the diffraction grating can be observed at grating 3, which is the detector level. By moving grating 3 perpendicularly to the molecular wave direction, the interference pattern was detected. The particles were finally ionized by a laser beam and counted with an ion detector. The ionization laser was strong enough to ionize and detect the fullerene C_{70} .⁴² However, the larger molecules $C_{60}F_{48}$ and tetraphenylporphyrin (**TPP**, Figure 9) could also be ionized by the ionization laser but their ionization energy exceeded the binding energy and the molecules decompose. Therefore, a new detection method had to be developed.

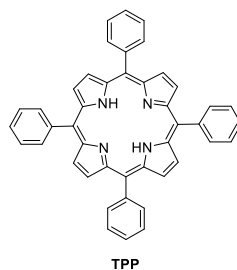


Figure 9. Chemical structure of tetraphenylporphyrin (**TPP**).

The Arndt group solved this problem by using electron impact (EI) ionization.⁴³ Since this method would also ionize the residual gas in the vacuum chamber and thus would finally be detected. The required mass selection was obtained by the installation of a quadrupole mass spectrometer, which allowed tracking of the mass selection within the interferometer and detection of the ions after ionization. This new detection and diffraction methods conducted to major improvements towards QIE with massive particles.

However, detection of molecules by ionization is rather limited, and the Arndt group considered fluorescence detection as a suitable alternative. The first molecule used in a TLI with fluorescence detection was **TPP**. In this case, detection consisted of a quartz-surface situated in Talbot-distance to the diffraction grating.⁴⁴ However, when coming to larger particles similar problems as in far-field interferometry occur. The material-gratings tend to interact with the molecules, additionally, the larger the particles are, the stronger their polarizability turns out to be. The stronger the polarizability the stronger are the interactions with the interferometer walls. Far-field interferometry was the solution to solve these problems. The use of optical gratings

invented by Kapitza and Dirac helps to prevent interactions with gratings.^{29,31} This knowledge was used in 2007 to design a new interferometer named after the two effects and known as the Kapitza-Dirac-Talbot-Lau interferometer (KDTLI).⁴⁵ This interferometer is specially designed for large and highly polarizable molecules. Within the next years, several important experiments have been performed using a KDTLI in the Arndt group. The KDTLI was used as a complementary tool in mass spectroscopy by Gerlich *et al.* in 2008.⁴⁶ The interferometer shows different visibilities on the detector screen for molecules with different mass or polarizability. In 2009 the functionality of the KDTLI was fully described in theory by Hornberger *et al.*⁴⁷ The influence of molecular dynamics on the interference pattern was investigated by Gring *et al.* in 2010 using fluorinated azobenzenes.⁴⁸ Knowing the interferometer distinguishes between molecules with different polarizabilities and different molecular dynamics, two constitutional isomers have been synthesized.⁴⁹

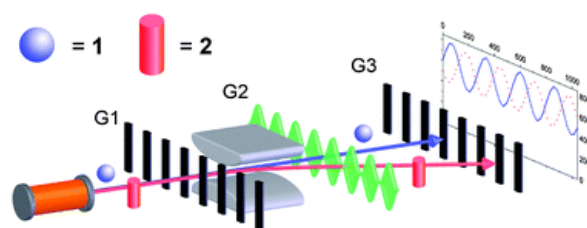


Figure 10. The two constitutional isomers used in a KDTLI equipped with an electric field generator between material grating G1 and wave grating G2.⁴⁹

The interferometer used for these experiments is a variation of the KDTLI. An oven was used to sublime the molecules and produce a molecular beam. The interferometer consists of three gratings, the first collimation grating G1, a standing wave (532 nm) grating G2 and the lateral moving grating G3. Additionally in this interferometer, an electric field is applied between grating G1 and G2, this interaction between the molecule and the electric field yielded a shift of the interference pattern. Molecular beam techniques progressed a lot within these years. Special tailor-made molecules were found crucial for the production of a molecular beam. In 2007 the thermal properties and the use of porphyrins in interferometry was presented.⁵⁰ In the same year the perfluorination of the molecules with regard to Van der Waals interactions between the molecules was investigated.⁵¹ In a next step, molecules had to be immobilized on a surface.⁵² In particular, zinc-**TPP** was bonded to a surface that exposes pyridine moieties. This functional group helps to bring the molecules softly into gas-phase and to mobilize them. Another part of the

interferometer was optimized in 2009 by Marksteiner *et al.*⁵³ It was shown that vacuum ultra violet (VUV) ionization is sensitive enough to detect biomolecules and molecular clusters.

In 2011, in the Arndt group the next milestone in quantum physics was set.⁵⁴ The results and syntheses are further discussed in three publications.^{55–57} For the first time interference was observed between tailor-made molecules. The molecular masses ranged up to 6910 g/mol, and it was shown that molecules with more than 1000 degrees of freedom can pass through an interferometer with nearly no decoherence. The molecules that were used for this study are shown in Figure 11.

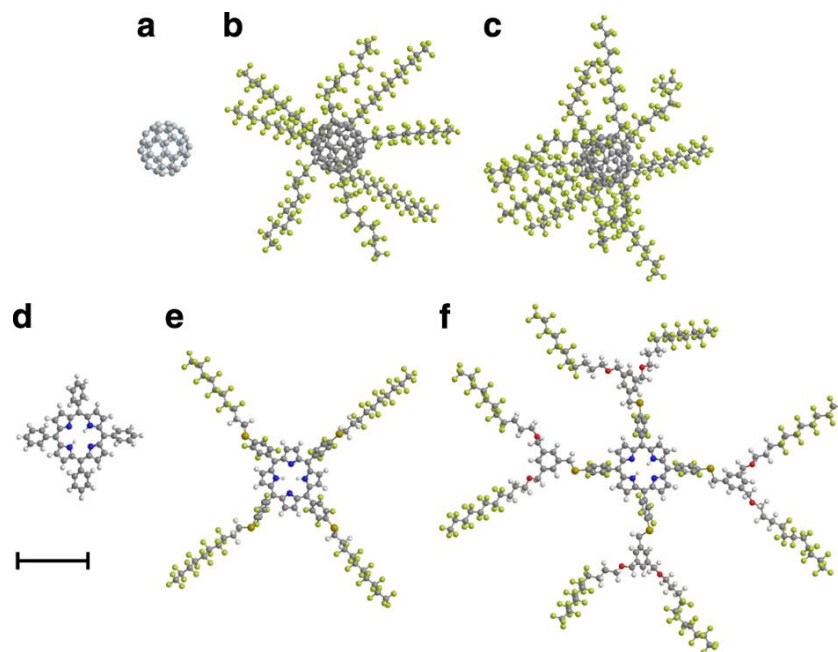


Figure 11. Molecular structures used for the QIE. (a) Buckminsterfullerene C_{60} ($m=720$ g/mol, 60 atoms) was used for calibration; (b) perfluoroalkylated Buckminsterfullerene C_{60} ($C_{60}[C_{12}F_{25}]_8$, $m=5672$ g/mol, 356 atoms), a carbon cage bearing eight perfluoroalkyl chains; (c) the equivalent to (b), but with ten perfluoroalkyl chains ($C_{60}[C_{12}F_{25}]_{10}$, $m=6910$ g/mol, 430 atoms); (d) TPP ($C_{44}H_{30}N_4$, $m=614$ g/mol, 78 atoms), which was used in comparison to the tailor made molecules (e) TPPF84 ($C_{84}H_{26}F_{84}N_4S_4$, $m=2814$ g/mol, 202 atoms) and (f) TPPF152 ($C_{168}H_{94}F_{152}O_8N_4S_4$, $m=5310$ g/mol, 430 atoms). The two porphyrins being the largest in the set. All molecules are in scale and the bar corresponds to 10 Å.⁵⁴

The molecules mentioned above were investigated using a KDTLI in the Arndt group. A schematic representation is shown in Figure 12. The molecules were brought neutrally into gas-phase by sublimation out of an oven. The first two collimation slits (S1 and S2) delimit the molecular beam and focuses on the first grating (G1). This grating is a SiNx membrane with a grating distance of 266 nm and used to produce a coherent molecular beam. The next two gratings are in Talbot-distance and in twice the Talbot-distance respectively to the first grating

(G1). Grating G2 is an optical grating produced by a steady wave of a green laser with a wavelength of 532 nm. This produces a grating with a grating distance of 266 nm.

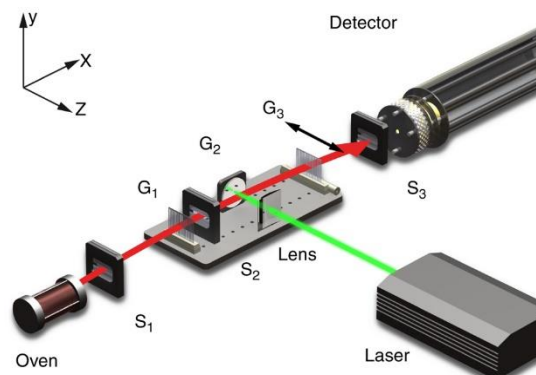


Figure 12. Schematic representation of the KDTLI used in these experiments.⁵⁴

The last grating (G3) is the detector level in this interferometer and similar to grating G1. This grating can be shifted perpendicularly to the molecular beam, and the passing molecules were ionized by EI and were detected using a QMS. The interferograms obtained of the molecules mentioned in Figure 11 are shown in Figure 13.

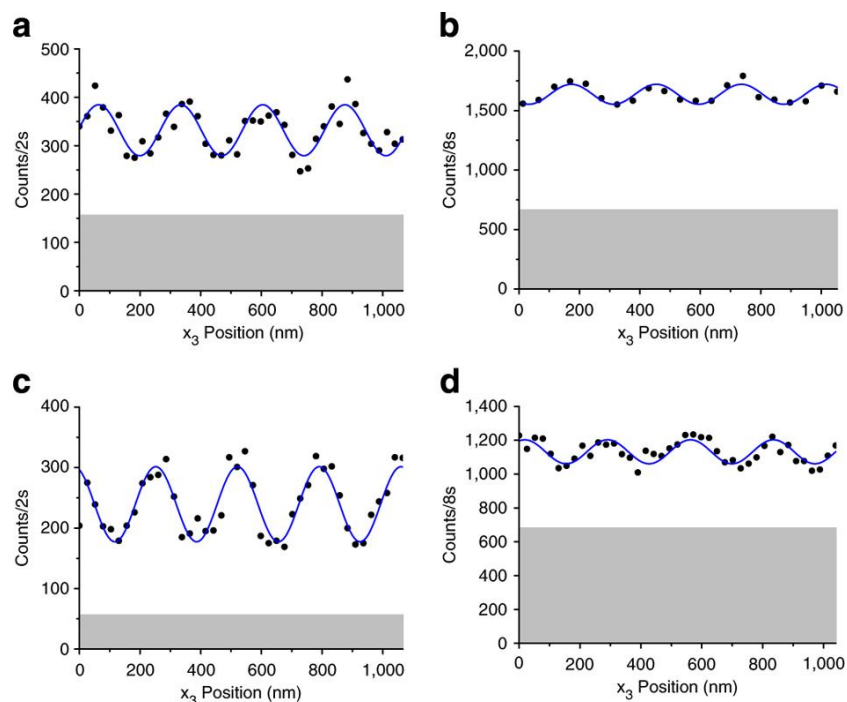


Figure 13. Interferograms obtained in these experiments using (a) Buckminster-fullerene C_{60} , (b) perfluoroalkylated Buckminster-fullerene $C_{60}[C_{12}F_{25}]_8$, (c) TPPF84, and (d) TPPF152.

X-axis: position of grating G3; Y-axis: count of ionized molecules by the QMS passing through grating G3. The black dots indicate the number of counts in each position, the blue line as a sinusoidal fit to the number of counts and the gray part indicates the detector dark rate.⁵⁴

The interferograms of all molecules shown in Figure 11 could be measured. The lowest intensity was obtained for the largest molecules (b and d in Figure 13), which was attributed to the high speed of the molecules.

Even higher molecular masses using the same KDTLI led to a slightly different approach. First of all the problem of high molecular speeds of the large molecules has to be solved. This was done using different ionization techniques described in 2013 by Schmid *et al.*⁵⁸ In most of the mass spectroscopic volatilization processes (such as EI or ESI), the molecules are directly ionized at the source and the particle velocities are around several hundred meters per second. In this study, laser-assisted volatilization produced a sufficiently slow molecular beam without ionization. The molecules were detected by vacuum ultra violet (VUV) ionization and a QMS.

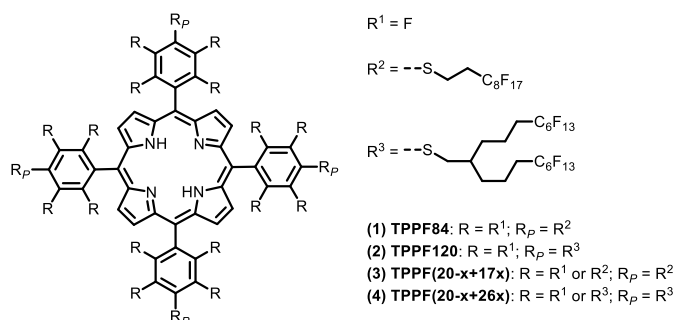


Figure 14. (1) and (2): Monodisperse compounds bearing four fluoroalkylsulfanyl side-chains (R^2 or R^3 respectively) in *para* position (R_p). (3) and (4): Molecular libraries having a various number of fluoroalkylsulfanyl side-chains (R^2 or R^3 respectively), for (3) the most probable $x = 14$ (14 out of 15 positions are substituted) and a mass of 7417 g/mol, for (4) the x ranged from 9 to 12, most probable $x = 11$ and a mass of 9363 g/mol. The monodisperse molecules are obtained in a nucleophilic aromatic substitution reaction in *para* position (R_p) of fully fluorinated TPP (TPPF). The molecular libraries are obtained in a nucleophilic aromatic substitution reaction at TPPF using a large excess of thiol nucleophile.⁵⁸

These newly designed QIEs allowed the use of molecular-libraries (see molecular structures in Figure 14), since the individual members of the library are selected to some extent by speed within the interferometer can be determined by a QMS. The molecular libraries (Figure 14) consisted of a mixture of molecules bearing a variable number of perfluoroalkyl side-chains. Due to the high molecular mass of the side-chains, we obtained well-defined maxima in the mass spectrum. The selection of an interference pattern in a KDTLI by mass spectrometry was shown by Eibenberger *et al.* in 2013.⁵⁹ Libraries were brought into gas-phase in an oven and then delimited by three delimitation slits (D1, D2 and D3) as shown in Figure 15. The delimitation slits were used to obtain a coherent, focused molecular beam.

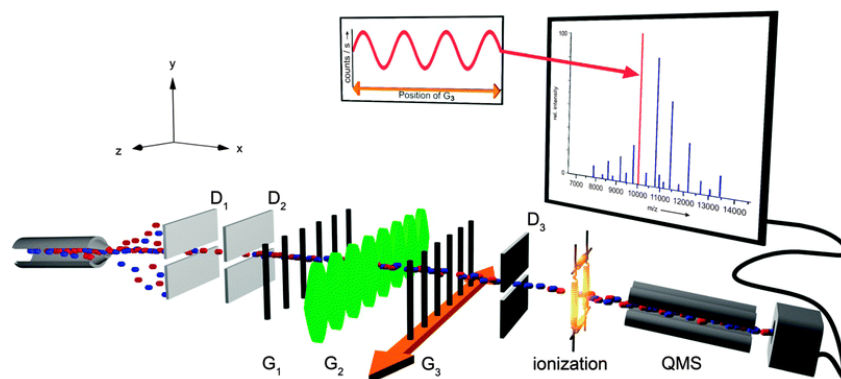


Figure 15. KDTLI used for the selection of interferograms from multi-mass libraries using a QMS.⁵⁹

Grating G₁ produces a coherent matter wave, diffraction and interference of the molecular-beam is done at grating G₂ and the detection is possible by an in z-axis movable grating G₃ as described. The molecular wave is then ionized by EI and the ionized species detected by a QMS. It was possible to obtain interferograms of individual members of the library with masses up to 10'123 g/mol.

At the starting point of this doctoral thesis, a molecular mass of 10'123 g/mol was the maximum mass used in such experiments.⁵⁹ The selection of interfering particles from a library within the interferometers facilitates the possibility of the production of large and heavy tailor made molecules. The question within this chapter about the limits of quantum interference is still unanswered and has to be further investigated.^{60,61} It is also very interesting to investigate softer methods to produce slow and neutral particle-beams, and to observe interference of larger molecules.^{62,63}

The history of quantum interference and the KDTLI is nicely reproduced by Arndt *et al.* in 2010.⁶⁴

1.2 Research Projects

The main goal of this work is to explore the borderline between quantum and classical physics. Is it possible to see interference between particles larger than 20'000 g/mol in the KDTLI near-field interference setup? To answer this question novel tailor made molecules fulfilling all the requirements of the interferometer have to be synthesized. The project herein described is a multidisciplinary project between physics and chemistry. Optimizing towards the production of a coherent, sufficiently intense and slower molecular beam is one of the main goals of this work. Using the optimized interferometers, we needed to adapt the molecular design. Tailor made molecules fulfilling all the requirements for successful QIE need to be synthesized. The main goal within synthetic chemistry is the adaptation of the molecular design for the new QIE.

Novel interfering particles need to have higher masses than the ones described earlier on.⁵⁹ To fulfill this goal, larger systems have to be developed. These higher mass particles can be presented as a molecular library, as described in two recent publications.^{58,59} With larger and higher molecular mass particles also the detection of the molecules in the interferometer need to be adapted.

Not only the before described near-field interferometry made a lot of progress during the past years, also far-field interferometry by the use of a new interferometer opens up a broad field of synthetic chemical activities.³⁶ Is it possible to synthesized molecules fulfilling the requirements of the interferometer having a higher mass than before?

Metalation of **TPPF** (structure shown in Figure 16) and the impact on the flying properties is described. **TPPF** have been found to be an ideal starting point to search for larger molecules and therefore is used as a model compound in this work.

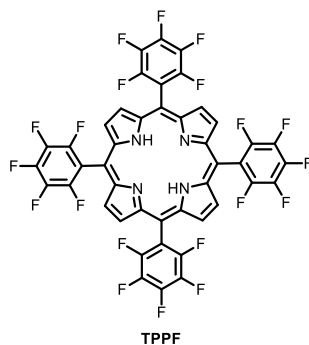


Figure 16. TPPF is used as a model compound and starting point of syntheses.

The production of a sufficiently strong beam of neutral molecules is crucial in QIE. To obtain molecular beams not only the molecular design has to be optimized, but also the experimental setup can be optimized. The source described in the KDTLI is a thermal source, the sublimation temperature of larger systems or biomolecules may be higher than the decomposition temperature. Softer sources to produce sufficiently strong beams of neutral molecules have to be developed.

The last project within this work is also related with the optimization of the detection. The synthetic approach is supposed to be rather different, since a test system, bearing photocleavable tags, is proposed. The question regarding this project is whether the cleavage of the tag in test systems is sufficiently efficient in gas-phase at the irradiated energies. We plan to prove the cleavage properties in solution.

2 Fluorinated Phthalocyanines for Far-Field Interferometry

The first milestone in far-field QIE was reported in 1999 by Arndt *et al.* with the observation of the interference of C_{60} and C_{70} .^{21,28} In a further experiment, a tetraphenyl porphyrin (**TPP**) was then used to observe interference.⁴⁴ Since in far-field experiments individual particles can be observed on the detector level one by one, these experiments are described in literature as “The most beautiful experiments in physics”.^{13,65–68} Our collaborators from the Arndt group in Vienna optimized their far-field interferometer by designing a new Talbot-Lau interferometer using fluorescence detection.³⁶ Therefore, a high fluorescence of the molecule is required. Phthalocyanines seem to have matching optical properties for far-field QIE. The two phthalocyanines shown in Figure 17 fulfilled all the requirements of the interferometer, as it will be explained in the next section, and the fluorinated **F₂₄PcH₂** still retain the world record for far field QIE with a molecular mass of 1298 g/mol.³⁶

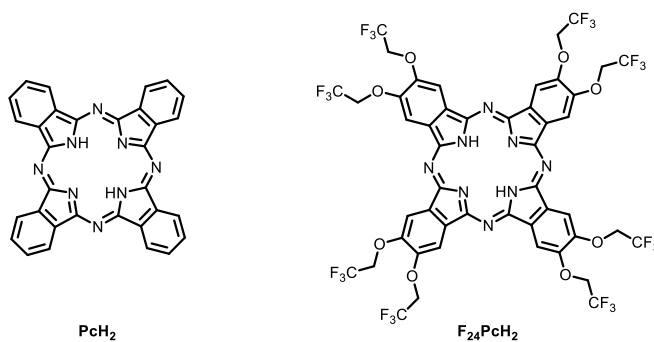
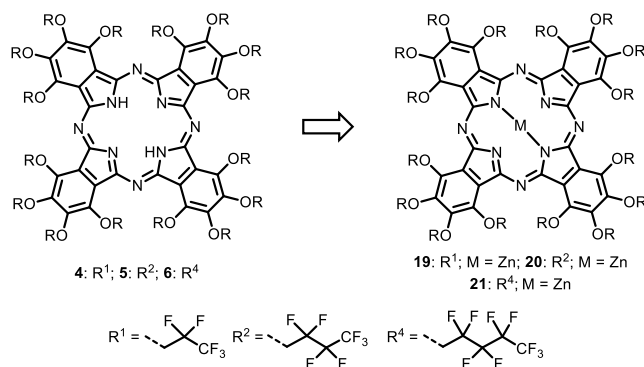


Figure 17. **PcH₂** (molecular formula: $C_{32}H_{18}N_8$, mass = 514 g/mol) and **F₂₄PcH₂** (molecular formula: $C_{48}H_{26}F_{24}N_8O_8$, mass = 1298 g/mol).

will use a central zinc atom, since it was found to be easily cleavable and templates the building up of the macrocycle to obtain higher yields.⁷⁰

Another way to increase the mass of the target molecules with a phthalocyanine core is to increase the number of side-chains attached as shown in Scheme 2 using another phthalonitrile starting material.



Scheme 2. Structure of the perfluoroalkylated phthalocyanines **4**, **5** and **6**, their metallated pendants **19**, **20** and **21**, and the perfluoroalkyl side-chains (R¹, R² and R⁴).

In addition, in this case, the demetallation is planned to be the last step of the synthetic pathway to increase the fluorescence. Using this kind of substituted phthalocyanines, it is possible to reach still fluorescent molecules with masses above 4000 g/mol and obtain molecules that are still fluorescent (Table 1).

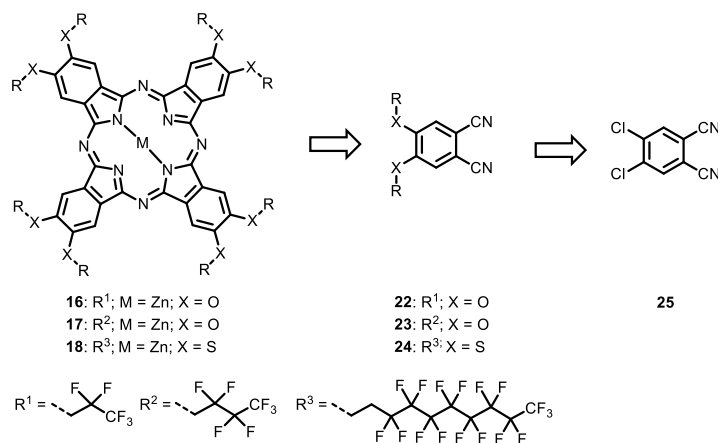
Table 1. Comparison of the masses of the different phthalocyanines.

Molecule	Chain	#Chains	mass (g/mol)	mass ratio
PcH₂	-	0	514	1
F₂₄PcH₂	O-CF ₃	8	1298	2.5
1	R ¹	8	1698	3.3
2	R ²	8	2098	4.1
4	R ¹	16	2082	4.1
5	R ²	16	2882	5.6
6	R ⁴	16	3682	7.2
3	R ⁵	8	4338	8.4

Using the long thiol-chain it is possible to push the mass of the phthalocyanine up to 4338 g/mol, the mass being around 8.4 times bigger than that of the unsubstituted

phthalocyanine. All the proposed phthalocyanine molecules would fit perfectly in one row with the already investigated $F_{24}PcH_2$.

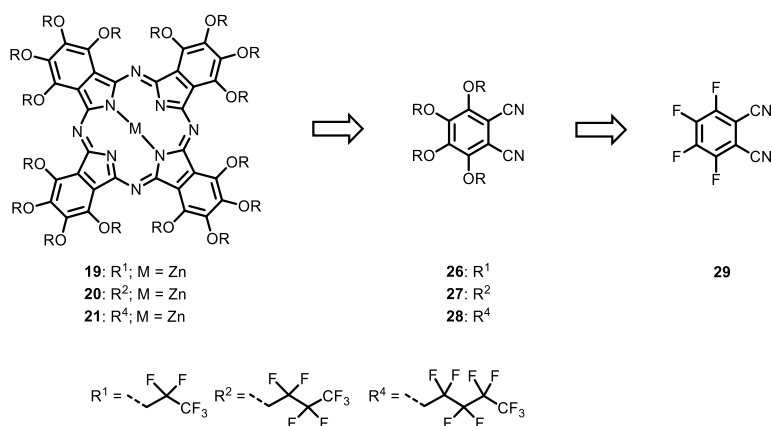
The metallated phthalocyanine molecules (**16**, **17** and **18**) can be obtained from the corresponding phthalonitriles (**22**, **23** and **24**). The phthalocyanine molecules can be obtained using a metal template as shown in Scheme 3.



Scheme 3. Planned reaction pathway from 4,5-dichlorophthalonitrile (**25**) in a nucleophilic aromatic substitution reaction using the three nucleophiles to the fluorinated phthalonitriles (**22**, **23** and **24**). These can be used in metal template mediated reaction to the metal-phthalocyanines (equivalents **16**, **17** and **18**).

Introduction of the perfluoroalkyl side-chains is the first step of the synthesis. It is planned to obtain the phthalonitriles (**22**, **23** and **24**) from 4,5-dichlorophthalonitrile (**25**) in nucleophilic aromatic substitution reactions.

On the other hand, the fully substituted metallated phthalocyanines (**19**, **20** and **21**) can be obtained using a metal template from the corresponding phthalonitriles (**26**, **27** and **28**) as shown in Scheme 4.



Scheme 4. Synthetic pathway towards the fully substituted phthalocyanines (**19**, **20** and **21**) from the corresponding phthalonitriles (**26**, **27** and **28**). These phthalonitriles are planned to be obtained from 3,4,5,6-tetrafluorophthalonitrile (**29**).

The nucleophilic aromatic substitution reaction using the alcohol perfluoroalkyl chains as nucleophile can be performed from the fully fluorinated phthalonitrile **29**.

2.2 Syntheses and Characterization

The first molecule to be synthesized, according to the molecular design described above, is 4,5-dichlorophthalonitrile (**25**), since this molecule is used for the synthesis of the metallated phthalocyanines. A similar reaction pathway was published by Wöhrle *et al.* and was slightly modified to obtain 4,5-dichlorophthalonitrile (**25**).⁷¹

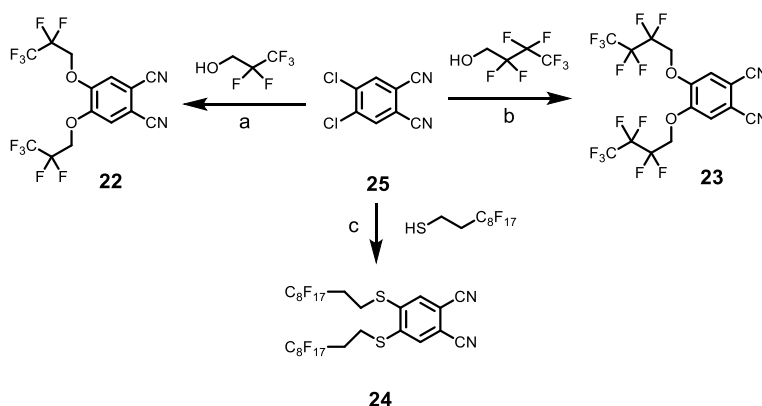


Scheme 5. Synthesis of 4,5-dichlorophthalonitrile (**25**) from 4,5-dichlorophthalic acid (**30**) in four sequential reaction steps. Reagents and conditions: (a) acetic anhydride, 155 °C, 5 h, 94 %; (b) formamide, 160 °C, 3 h, quant.; (c) aq. NH₄OH (25 %), room temperature, 48 h, 89 %; (d) thionyl chloride, -5 °C to room temperature, 30 h, 73 %.

In a first step 4,5-dichlorophthalic acid (**30**) is heated in acetic anhydride at 155 °C for 5 h to obtain benzofuran compound **31** in 94 % yield after filtration without any further purification. Formamide as the source of nitrogen was used to transform the benzofuran **31** at 160 °C to the indol **32** in quantitative yield. Introduction of the second nitrogen was done by the use of liquid

ammonia at a room temperature yielding the phthalamide **33** in 89 % after the ring opening. The compound of the first reaction sequence, 4,5-dichlorophthalonitrile (**25**), was obtained after treatment of phthalamide **33** with thionylchloride in 73 % yield as a colorless solid. This is the starting material for the following nucleophilic aromatic substitution reaction in *para* position to the nitrile at the chlorine.

The nucleophilic aromatic substitution reactions using thiols and alcohols at 4,5-dichlorophthalonitrile (**25**) were performed using modified conditions developed by Wöhrle *et al.* (Scheme 6).

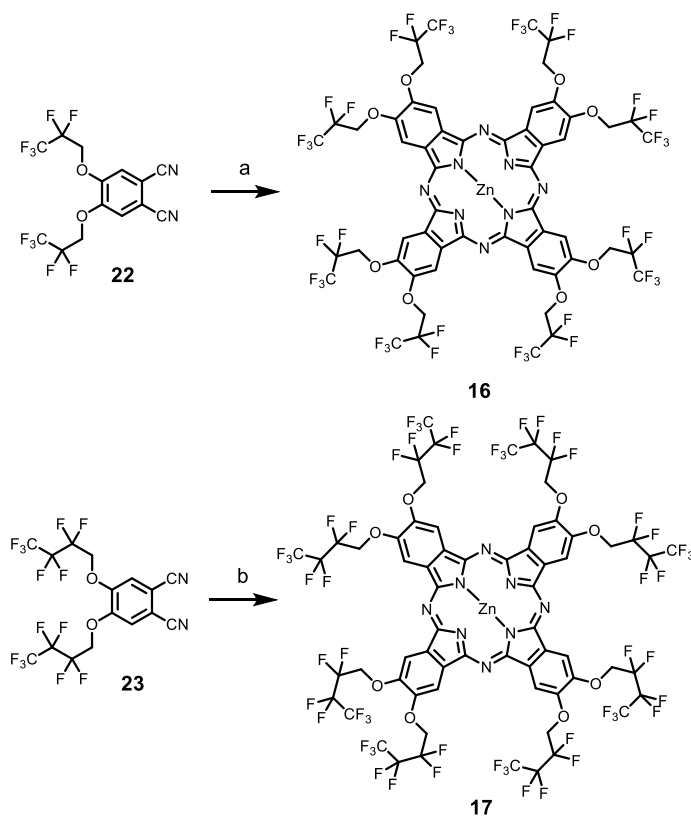


Scheme 6. Nucleophilic aromatic substitution reactions of pentafluoropropane-1-ol, heptafluorobutane-1-ol and 1H,1H,2H,2H-perfluorodecanethiol at dichlorophthalonitrile (**25**). Conditions: (a) pentafluoropropane-1-ol, K₂CO₃; DMSO, MW 100 °C, 1 h, 85 %; (b) heptafluorobutane-1-ol, K₂CO₃; DMSO, MW 100 °C, 3 h, 63 %; (c) 1H,1H,2H,2H-perfluorodecanethiol, K₂CO₃; DMSO, 80 °C, 20 min, 44 %.

The reactions using alcohols as nucleophile were performed in a microwave apparatus, since the heating can be accurately adjusted for the needs of these reactions. Both reactions were done using potassium carbonate as base in dry dimethylsulfoxide (DMSO). DMSO was found to be ideal to mediate the nucleophilic aromatic substitution reactions; the main drawback of the use of DMSO is the limited ability to be heated up, since toxic sulfoxides can be produced. Potassium carbonate was found to be the ideal base for these type of reactions. The use of this base mediated the introduction of the nucleophile and was nicely soluble in warm DMSO. The reaction using pentafluoropropane-1-ol was heated up to 100 °C in the microwave for 1 h to obtain 4,5-bis(2,2,3,3,3-pentafluoropropoxy)phthalonitrile (**22**) in 85 % yield as a colorless solid. It was found that using a longer chain nucleophile such as heptafluorobutane-1-ol decreases the reaction rate tremendously. This can be partly compensated by applying longer reaction times. To introduce heptafluorobutane-1-ol to dichlorophthalonitrile (**25**) a reaction time of 3 h under similar conditions as mentioned above was found to be ideal. Further prolongation of the reaction

time did not lead to higher yields. 4,5-Bis(2,2,3,3,4,4,4-heptafluorobutoxy)phthalonitrile (**23**) was obtained in 63 % yield as a colorless solid after purification by column chromatography. Further prolongation of the perfluoroalkyl side-chain was done using 1*H*,1*H*,2*H*,2*H*-perfluorodecanethiol. Changing the nucleophile from an alcohol to a thiol moiety should in theory increase the yield of the reaction, since thiols are much stronger nucleophiles. In this case, the reaction was performed in DMSO at 80 °C for 20 min. In addition, in this case a longer reaction time did not lead to higher yields. The desired 4,5-bis-(1*H*,1*H*,2*H*,2*H*-perfluorodecylthio)-phthalonitrile (**24**) was obtained in a low yield of 44 %. This may be due to solubility problems during the purification process.

The synthesis of the phthalocyanine molecules from phthalonitriles is well described and understood in literature. We used zinc acetate as the source for the metal template to build up the heteroaromatic ring, 1,8-diazabicyclo[5.4.0]undec-7-ene (DBU) as organic base and pentanol as solvent, since pentanol is base stable and due to its high boiling point, it can be used also at high temperatures.^{70–73}



Scheme 7. Syntheses of phthalocyanines **16** and **17** using a zinc template and DBU in pentanol. Reagents and conditions: (a) zinc acetate, DBU, pentanol, MW 170 °C, 12 h, 21 %; (b) zinc acetate, DBU, pentanol, MW 170 °C, 12 h.

As shown in Scheme 7, phthalocyanine **16** was synthesized from phthalonitrile **22** in 21 % yield as a dark blue solid. The low yield is due to the low solubility of the target compound **22**, this made the purification and analytical processes very troublesome. However, it was not possible to synthesize the phthalocyanine with longer chains **17**. Traces of product could be observed using MALDI-TOF mass spectroscopy, but isolation of target compound **17** was not possible due to extremely low solubility. Analysis of phthalocyanine **16** using MADLI-TOF mass spectroscopy is shown in Figure 18.

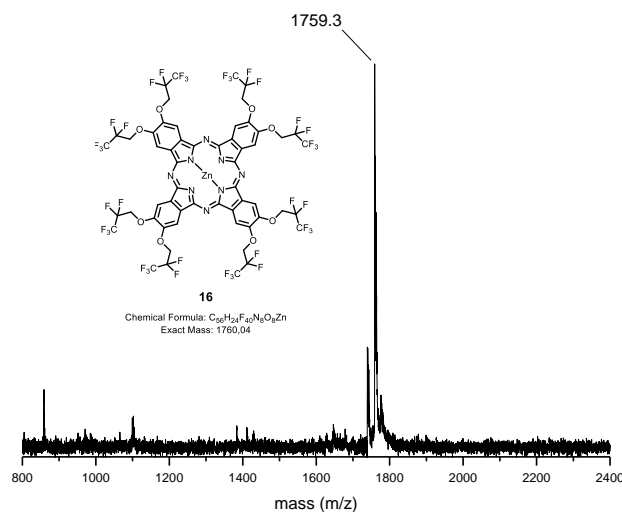
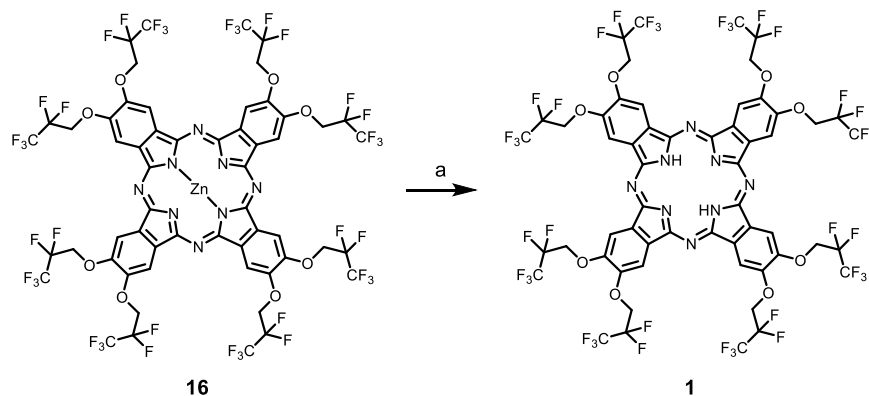


Figure 18. Structure and MALDI-TOF mass spectrum of perfluoroalkylated metal phthalocyanine **16**.

Due to low solubility of metallated phthalocyanine **16** MALDI-TOF mass spectrometry is the only feasible analysis method for these compounds. In order to obtain the desired high fluorescence, the phthalocyanine was demetallated as shown in Scheme 8.



Scheme 8. Demetallation of phthalocyanine **16**. Reagents and conditions: (a) pyridine-HCl, pyridine, 120 °C, 12 h.

The low solubility of zinc-phthalocyanine **16** limited this reaction. The starting material was dissolved in hot pyridine (120 °C) and then pyridine·HCl was added to first bind the zinc atom and secondly protonate the phthalocyanine. While cooling to room temperature the product precipitates in trace amounts. Therefore, no yield could have been determined for this reaction step. Using this small amount of product a MALDI-TOF mass spectrum was taken and the spectrum is shown in Figure 19.

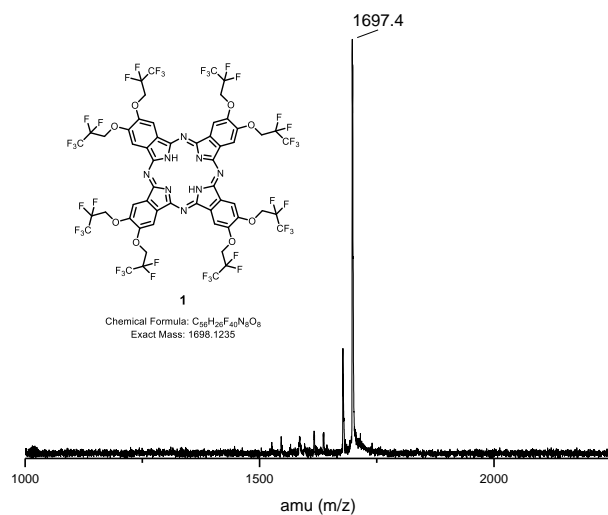
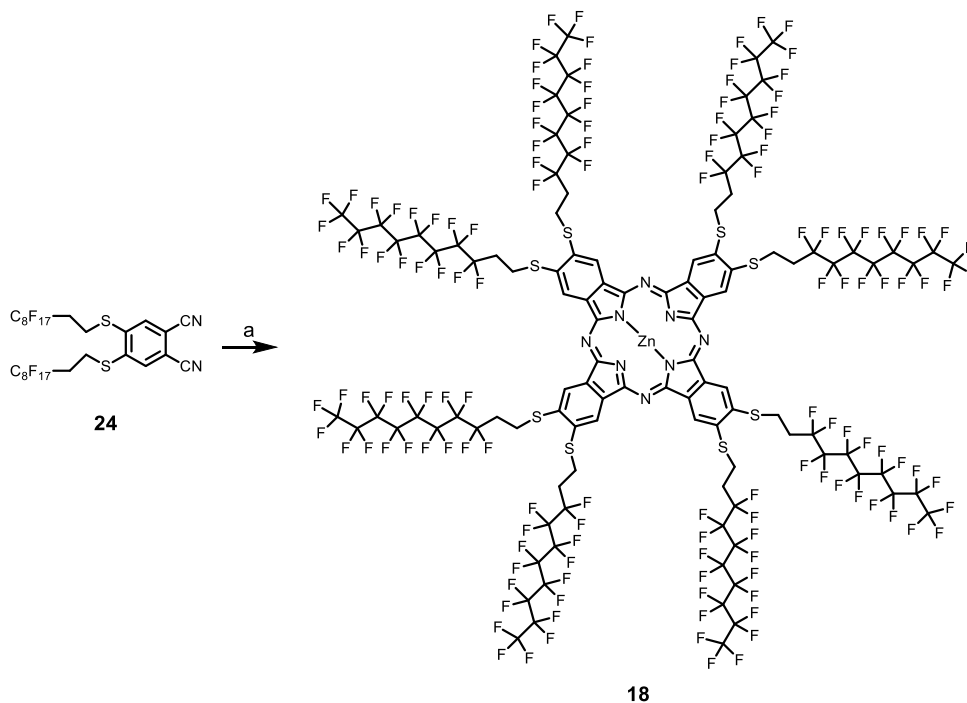


Figure 19. MALDI-TOF analysis and structure of demetallated phthalocyanine **1**.

The precipitate investigated by MALDI-TOF mass spectroscopy was rather pure and thus was the first model compound to be investigated by far-field QIE. It should push the molecular masses of interfering particles in the far-field to around 1700 g/mol.

In order to synthesize molecules with even higher masses, phthalonitrile **24** was used to synthesize a phthalocyanine bearing eight perfluoroalkylated C₁₀ chains. The molecule was synthesized using zinc acetate as the donor of the zinc template as shown in Scheme 9. This microwave reaction was performed in pentanol at 170 °C for 12 h, DBU was used as the organic base.



Scheme 9. Synthesis of perfluoroalkylated phthalocyanine **18** from phthalonitrile **24** using a zinc template. Reagents and conditions: (a) zinc acetate, DBU, pentanol, MW 170 °C, 12 h, 26 %.

When the reaction was cooled down to room temperature, the product **18** immediately precipitated in the reaction flask and therefore the product was hard to isolate and purify. Purification by column chromatography led to the zinc-phthalocyanine **18** in 26 % yield. This low yield can also be attributed to the low solubility of the isolated product. Characterization was done using MALDI-TOF analysis as shown in Figure 20.

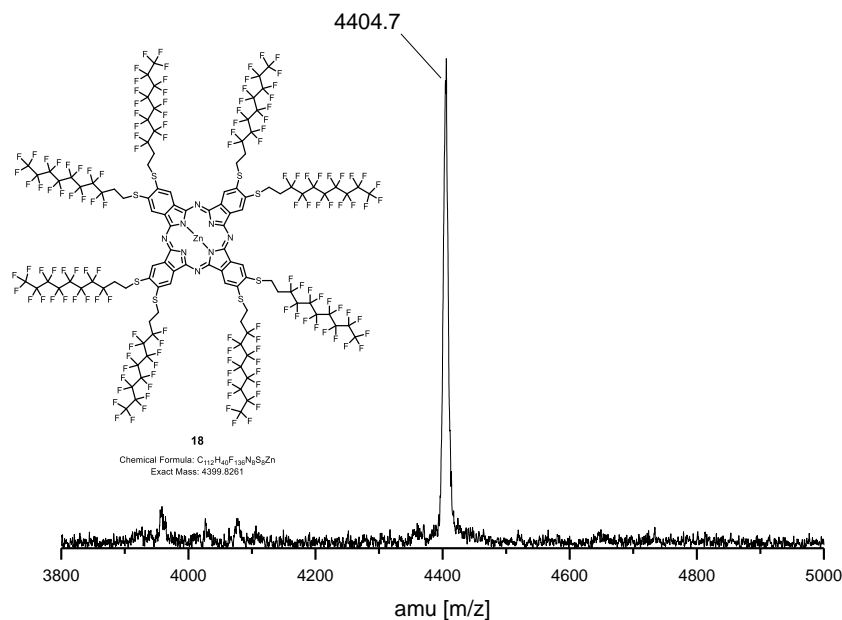
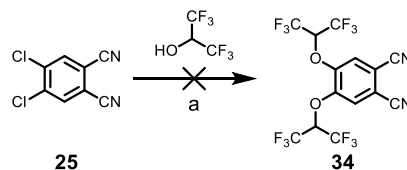


Figure 20. MALDI-TOF analysis and structure of zinc-phthalocyanine **18**.

However, due to low solubility of zinc-phthalocyanine **18** the demetallation reaction could not be performed, therefore this reaction pathway is not useful to synthesize novel highly fluorescent phthalocyanine molecules for far-field experiments

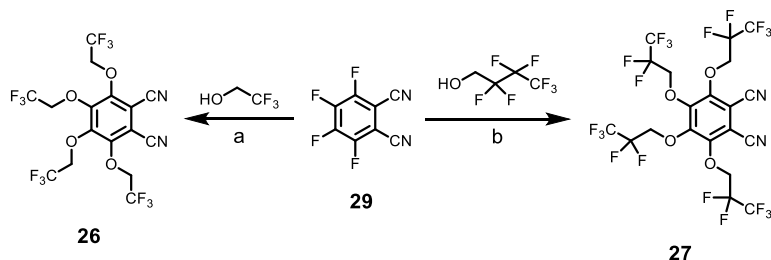
In order to overcome the solubility problems we tried to synthesize phthalonitriles having branched perfluoroalkyl sidechains as shown in Scheme 10.



Scheme 10. Proposed synthesis of a phthalonitrile bearing branched side-chains. Conditions: (a) K₂CO₃, DMSO, MW 100 °C, 1 h.

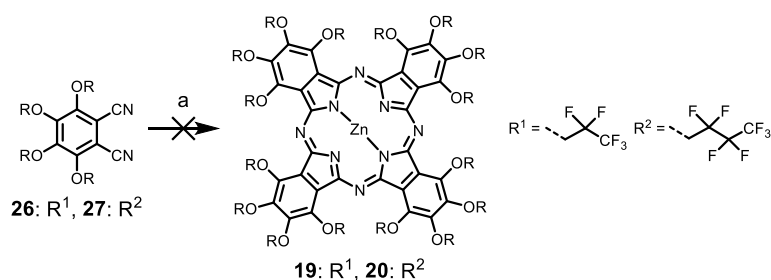
Starting from dichlorophthalonitrile (**25**) and the branched alcohol 1,1,1,3,3,3-hexafluoro-2-propanol (see structure in Scheme 10) using similar conditions as for the nucleophilic aromatic substitution reactions mentioned above branched 4,5-bis((1,1,1,3,3,3-hexafluoro-2-yl)oxy)phthalonitrile (**34**) should be obtained. To our surprise, this nucleophilic attack does not seem to be possible by substitution of the chlorine.

In the synthetic pathway towards phthalocyanines with higher molecular masses, the substitution pattern and the leaving group in the nucleophilic aromatic substitution reaction of the phthalonitrile was changed. Using a fully fluorinated phthalonitrile **29** as shown in Scheme 11 the molecular mass of the molecule can be nearly doubled.



Scheme 11. Fourfold nucleophilic aromatic substitution reaction at 3,4,5,6-tetrafluorophthalonitrile (**29**) using two different alcohol nucleophiles. Conditions: (a) K_2CO_3 , DMF, room temperature, 4 h, 90 %; (b) K_2CO_3 , DMF, room temperature, 4 h, 77 %.

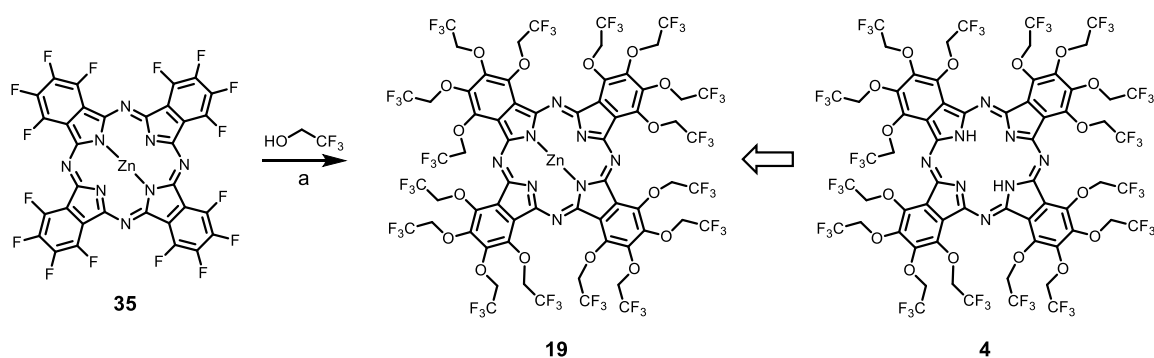
The nucleophilic aromatic substitution reactions shown in Scheme 11 lead to two tetra perfluoroalkyl substituted phthalonitriles. Using 2,2,2-trifluoroethane-1-ol as the nucleophile in the nucleophilic aromatic substitution reaction tetra perfluoroalkyl substituted phthalonitrile **26** was obtained in 90 % yield without any purification step after filtration. Similar reaction conditions using *1H,1H*-pentafluoropropane-1-ol as the nucleophile phthalonitrile **27** was obtained in 77 % yield as a colorless solid. In both nucleophilic aromatic substitution reactions, the nucleophile was used in a tenfold excess and potassium carbonate was used as base to mediate the reaction. Having those two general phthalonitrile building blocks in hand, the fully substituted phthalocyanine molecules can be synthesized using similar conditions as mentioned above.



Scheme 12. Planned syntheses of fully substituted phthalocyanine **19** and **20**. Reagents and conditions: (a) zinc acetate, DBU, pentanol, MW 170 °C, 12 h.

Scheme 12 shows the trial to synthesize the two phthalocyanine molecules **19** and **20** using zinc as the template and DBU as organic base in pentanol at 170 °C in a microwave apparatus.

Unfortunately, this reaction pathway did not lead to the desired product (no trace of the product could be found in the reaction mixture by MALDI-TOF analyses). In order to overcome these problems in the synthetic pathway it was decided to use commercially available zinc 1,2,3,4,8,9,10,11,15,16,17,18,22,23,24,25-hexadecafluorophthalocyanine (**35**) as starting material for the nucleophilic aromatic substitution reaction. Heating phthalocyanine **35** and a fortyfold excess of trifluoroethanol in DMF, using potassium carbonate as base in a microwave apparatus at 100 °C for twelve hours, the 16-fold nucleophilic aromatic substitution reaction was possible as shown in Scheme 13. The reaction could be purified by repeating column chromatography obtaining target phthalocyanine in 47 % yield as a green solid.



Scheme 13. Nucleophilic aromatic substitution reaction of fully fluorinated phthalocyanine **35** and demetallation to phthalocyanine **4**. Conditions: (a) K₂CO₃, DMF, MW 100 °C, 12 h, 47 %.

Analysis of the product was done using ¹H- and ¹⁹F-NMR spectroscopy and MALDI-TOF mass spectrometry. A representative spectrum of zinc-phthalocyanine **19** is shown in Figure 21.

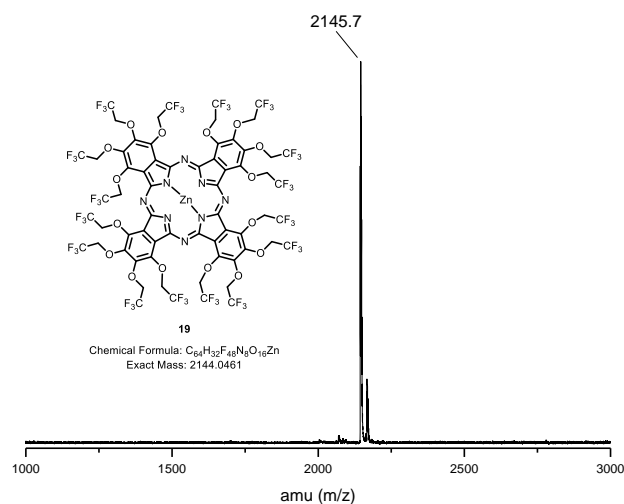
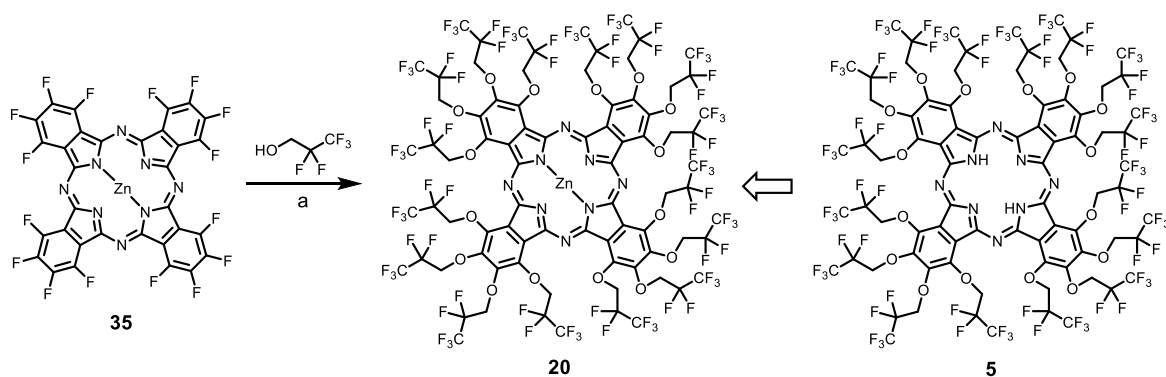


Figure 21. MALDI-TOF analysis and structure of zinc-phthalocyanine **19**.

To enhance fluorescence the demetallated phthalocyanine **4** was supposed to be synthesized as shown in Scheme 13. Unfortunately, it has never been possible to split the central zinc atom of this phthalocyanine. Using our standard conditions mentioned above in pyridine-HCl did only lead to starting material. In addition, harsher conditions such as stirring in concentrated sulfuric acid at room temperature or in boiling sulfuric acid did not lead to the desired product. Strongly zinc-coordinating compounds such as ethylenediaminetetraacetic acid (EDTA) were found to be not coordinating strong enough to break the zinc phthalocyanine bonds.



Scheme 14. Synthesis of the prolonged chain phthalocyanine **20** and the demetallation towards phthalocyanine **5**.
Conditions: (a) K₂CO₃, DMF, MW 100 °C, 12 h, 45 %.

Using similar conditions as for the nucleophilic aromatic substitution reaction with trifluoroethanol towards phthalocyanine **19** also *1H,1H*-pentafluoropropan-1-ol can be introduced to fully fluorinated phthalocyanine **35** as shown in Scheme 14.

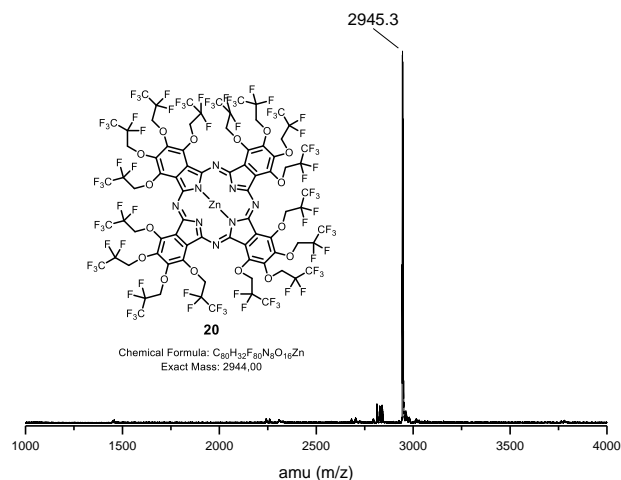


Figure 22. MALDI-TOF analysis and structure of zinc-phthalocyanine **20**.

In addition, in this case the purity of the compound was proven by MALDI-TOF (shown in Figure 22) and NMR analyses. As described above the demetallation of the zinc-phthalocyanine molecules does not seem to be possible in these cases.

2.3 Quantum Interference Experiments

To our delight, it was possible to synthesize larger molecules that can be used in far-field quantum interference experimental setups described in section 1.1.2. The newly synthesized phthalocyanine **1** is shown in Figure 23 in comparison to the phthalocyanines investigated in previous experiments.

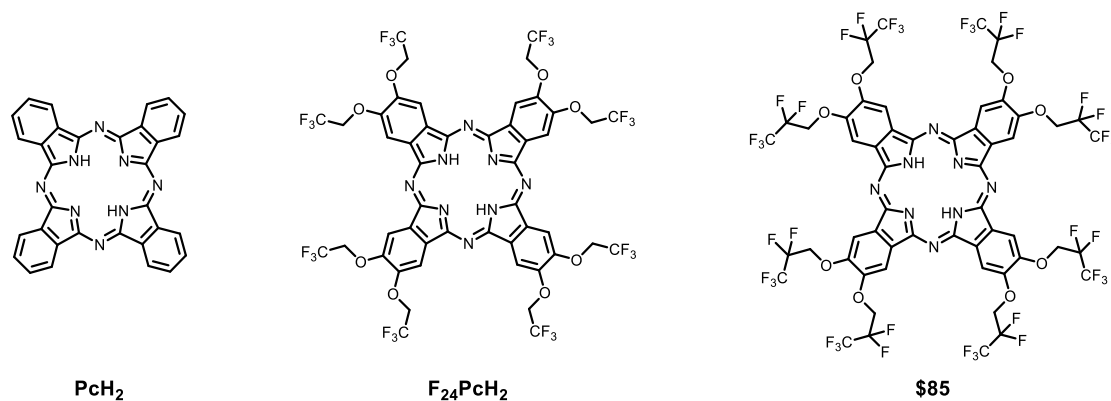


Figure 23. Unsubstituted phthalocyanine **PcH₂** (molecular formula: C₃₂H₁₈N₈; mass: 514.17 g/mol), phthalocyanine **F₂₄PcH₂** (molecular formula: C₄₈H₂₆F₂₄N₈O₈, mass: 1298 g/mol) investigated in earlier studies and the herein synthesized metal-free phthalocyanine **1** (molecular formula: C₅₆H₂₆F₄₀N₈O₈; mass: 1698.12 g/mol).

Using phthalocyanine **1** in QIE would push the mass of interfering particles from 1300 g/mol of the earlier investigated phthalocyanine **F₂₄PcH₂** to nearly 1700 g/mol of the newly synthesized prolonged chain phthalocyanine **1**.

Using the interferometer (Figure 5) phthalocyanine **1** has been investigated. The beam properties of unsubstituted phthalocyanine **PcH₂** and fluorinate phthalocyanine **1** were compared.

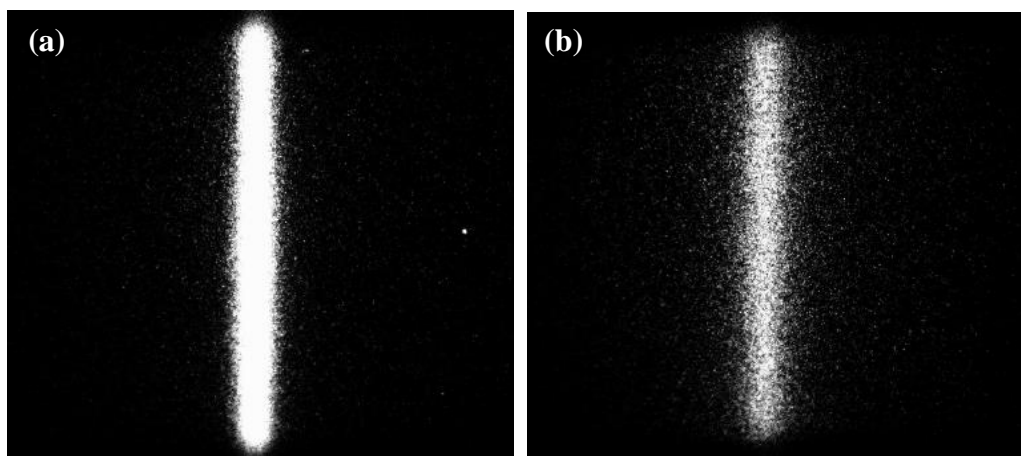


Figure 24. Comparison of the molecular beam of unsubstituted phthalocyanine **PcH₂** (a) and substituted phthalocyanine **1** (b) detected at the detector level by a red fluorescence laser. Each dot indicates a single molecule arriving at the detector level.

Figure 24 shows the molecular beams of unsubstituted phthalocyanine **PcH₂** (a) and phthalocyanine **1** (b) bearing the prolonged fluorinated chains. Increasing the molecular mass the intensity of the molecular beam detected by the red fluorescent laser is decreased strongly. This can be attributed to the lower number of molecules in an equal amount of investigated sample or to a lower fluorescence of phthalocyanine **1** compared to **PcH₂**. In Figure 24 the possibility to produce a sufficiently strong molecular beam is shown, although its intensity is decreased. As expected, the interference pattern can be obtained by the use of a material grating in the case of **PcH₂**. Using these grating in vertical position leads to beam pattern at the detector level as shown in Figure 24. Rotation of the grating leads to interference and the interference pattern should show up at the detector level as shown in Figure 25.

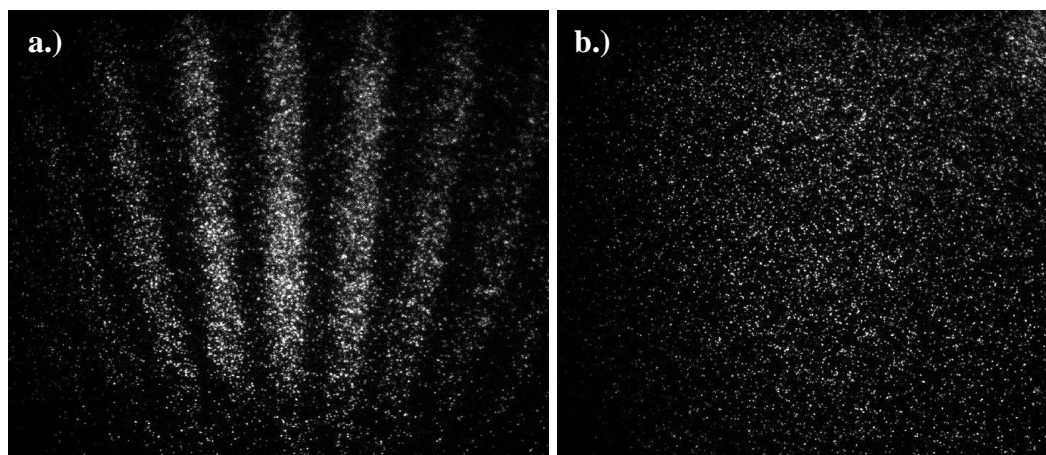


Figure 25. Comparison of detection screen using a 50° rotated grating to observe interference for a molecular beam of unsubstituted phthalocyanine **PcH₂** (a) and substituted phthalocyanine **1** (b) detected at the detector level by fluorescence. Each dot indicates a single molecule arriving at the detector level.

Using a 50° rotated interference grating the interference pattern of unsubstituted phthalocyanine **PcH₂** can be observed (Figure 25a). Using the newly designed and synthesized fluorinated phthalocyanine **1** the interferogram shows a scattering of the detected molecules. The pattern on the screen was compared with a molecule having strong dipole moment such as Rhodamine B.

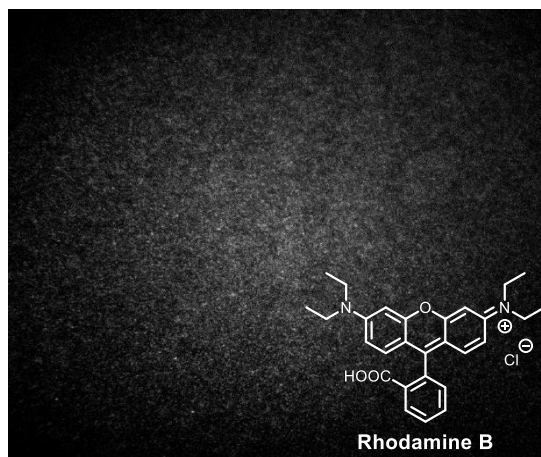


Figure 26. Rhodamine B: structure and interference using a 50° rotated grating.

The scattered interference pattern for phthalocyanine **1** shown in Figure 25 can also be found when the interference of a molecule with a strong dipole moment such as rhodamine B is investigated (Figure 26). Hypothetically, both molecules tend to stack to interference grating and have a broad distribution of speeds. For Rhodamine B we attributed this to the strong dipole moment and for phthalocyanine **1** to the size of the molecule.

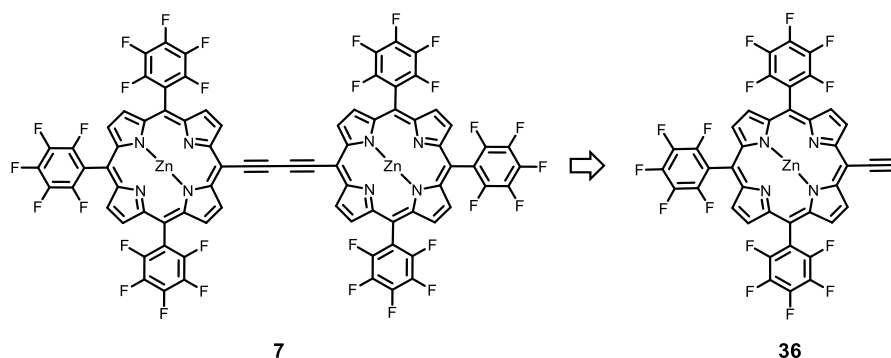
2.4 Conclusion

The syntheses of new and heavier tailor-made phthalocyanine molecules seem to be very challenging. We found the longer chain molecule **16** and its demetallated pendant **1** already being nearly insoluble. This fact also reduces the possibility to handle the molecules in QIE. Syntheses of an even larger molecule such as phthalocyanine **17** and the zinc-free analogue **2** was not possible at all, since only traces of the molecule could be obtained, and purification was impossible due to insolubility. Changing from ether-bridged chains to thioether-bridged chains made it possible to synthesize a novel phthalocyanine **18**. Since the fluorescence of these molecules is quenched in the presence of a heavy metal such as zinc, the central atom has to be removed. However, it was not possible to demetallate phthalocyanine **18** to obtain the hypothetically highly fluorescent phthalocyanine **3** and only starting material was recovered. Using a different approach starting from a fully fluorinated phthalocyanine **35** it was possible to introduce 16 fluorinated chains in nucleophilic aromatic substitution reactions to obtain phthalocyanines **19** and **20**. Unfortunately, it was not possible to demetallate this phthalocyanine to enhance their fluorescence and therefore **1** remained the only molecule that could be investigated in QIE. To our delight, we were able to produce sufficiently strong molecular beams with those molecules, and we were able to detect the molecules in the interferometer by fluorescence. Unfortunately, it was not possible to observe interference using a 50° rotated grating. The scattered interference pattern was similar to an interference pattern of a molecule having a strong dipole moment. The molecules tend to stack to the interference grating and have a broad distribution of speeds within the molecular beam. We attributed this phenomena to the enlarged size of phthalocyanine **1** compared with previously investigated molecules. This leads to the conclusion that investigations of larger molecules in this experimental setup are not possible and the setup needs to be improved to minimize interactions with the interference grating.

3.1 Molecular Design

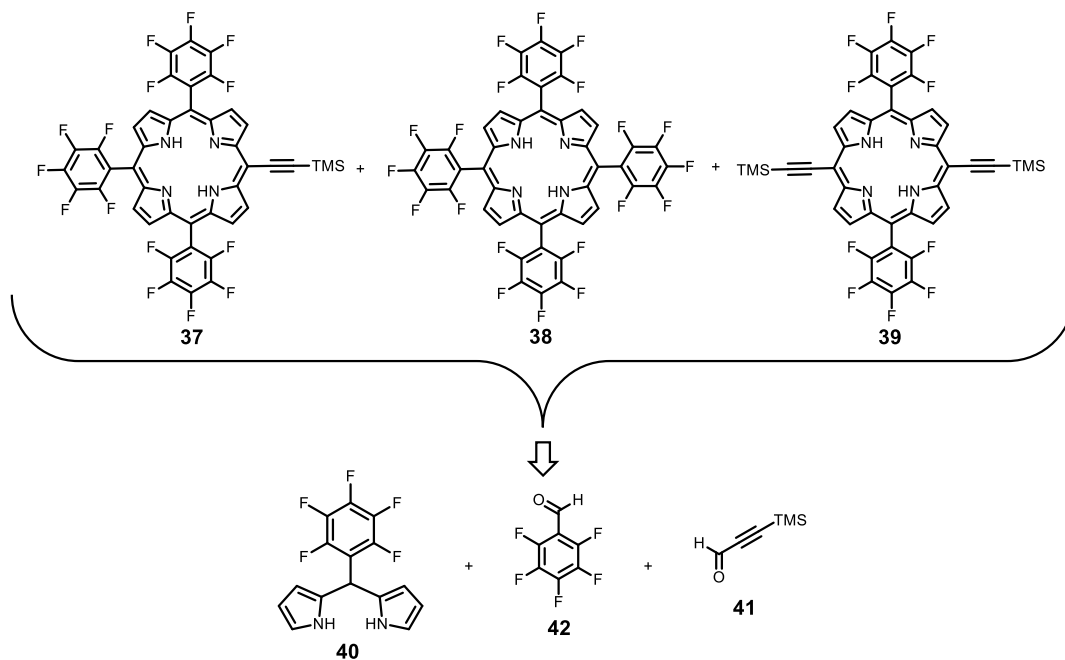
In order to increase the molecular mass of tailor made molecules to be investigated in QIE different strategies are possible. The first and most obvious strategy would be to increase the mass and number of perfluoroalkyl chains attached to the central porphyrin molecule. This strategy seems to be very challenging since fluorinated chains are hard to be synthesized due to their low solubility. On the other hand, it is quite impossible to introduce more side-chains to the molecule since the possibility of their attachment by nucleophilic aromatic substitution reactions is limited. This limitation is due to electronic and to steric reasons, since the large perfluoroalkyl side-chains are rather space demanding. The second strategy would be to synthesize polymeric structures; this would lead to larger structures as described before. This strategy is limited since the distribution of masses in the library mixture would be extremely broad and the masses not well defined. Another strategy could be to use biomolecules such as proteins or DNA strands in QIE. This strategy is discussed in section 5. The fourth strategy is to synthesize porphyrin oligomers, this would increase the number of possible positions for nucleophilic aromatic substitution reactions. Porphyrins showed good beam properties in earlier experiments and the use of multi-porphyrin systems would enable an easy ionization. Beam properties can be tuned, first in the experimental setup by improvement of the volatilization section of the interferometer, and secondly by tuning the molecular properties. The molecules should not be ionized during the volatilization process but finally be ionizable to be able to detect them by MS.

The first molecule that is proposed to fulfill all these requirements is a porphyrin dimer as shown in Scheme 15. Nucleophilic aromatic substitution reactions at the peripheral fluorine atoms should lead to the desired molecular libraries. It would be possible to substitute up to 30 fluorine atoms, which is 1.5 times the amount of binding positions compared to previous examples. The porphyrin dimer **7** shown in Scheme 15 is proposed to be synthesized in an oxidative Glaser-Hay coupling reaction.⁷⁴ These reaction conditions would lead to the dimer from a monomeric unsymmetrical free acetylene porphyrin **36**. Using these coupling conditions, it is necessary to block the central position in the macrocycle to avoid any copper used for the reaction to bind there.



Scheme 15. Planned synthesis of diacetylene coupled porphyrin dimer **7** in a Glaser-Hay oxidative coupling from unsymmetrical porphyrin monomer **36**.

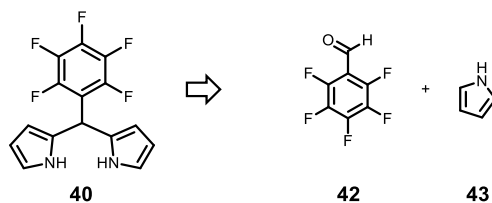
Unsymmetrical porphyrin monomer **36** can be obtained from unsymmetrical porphyrin **37** by binding of a zinc atom and deprotection of the triple bond.



Scheme 16. Synthetic strategy towards unsymmetrical porphyrin **37** and the two symmetrical porphyrins **38** and **39** which can be obtained from dipyrromethane **40**, pentafluorobenzaldehyde (**42**) and TMS-propynal (**41**).

As shown in Scheme 16 it is possible to synthesized unsymmetrical porphyrins in statistical reactions from dipyrromethane compounds and the corresponding aldehydes. If both aldehydes were mixed directly with pyrrole, an even broader distribution of products would have been obtained within this statistical reaction. Therefore, we decided to use a stepwise building-up of the unsymmetrical porphyrin **37**. Within this synthesis we expect to obtain also the symmetrical fully fluorinated porphyrin **38** and the symmetrical porphyrin having two peripheral TMS

protected acetylenes **39**. The synthesis of a porphyrin is an electrophilic aromatic substitution reaction at the pyrroles. In this reaction the dipyrromethane **40** being the nucleophile and the two aldehydes being the electrophiles. Finally, the porphyrinoides have to be oxidized using an oxidizing agent such as modified benzoquinones. Dipyrromethane compound **40** can be obtained as shown in Scheme 17, pentafluorobenzaldehyde (**42**) and TMS-propynal (**41**) are both commercially available.

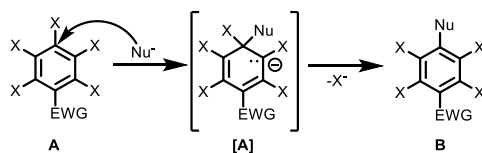


Scheme 17. Proposed synthesis of 5-(pentafluorophenyl)-dipyrromethane (**40**) from pentafluorobenzaldehyde (**42**) and pyrrole (**43**).

In a double electrophilic aromatic substitution reaction at pyrrole (**43**), pentafluorobenzaldehyde (**42**) can be introduced to obtain the desired dipyrromethane compound **40**. This reaction pathway was successfully used for the synthesis of other unsymmetrical porphyrin systems.⁷⁵

3.2 Statistical Nucleophilic Aromatic Substitution Reaction

The most important reaction within the synthesis of molecular libraries as tailor-made molecules for QIE is the statistical nucleophilic aromatic substitution reaction. This reaction was used to introduce a variable number of fluoroalkylsulfanyl side-chains to the porphyrin core. Therefore, we want to focus on the multi-substitution reaction. The nucleophilic attack is depicted in Scheme 18.



Scheme 18. Example of a nucleophilic attack. Nu is the nucleophile, X is fluorine or chlorine and EWG an electron withdrawing group.

The nucleophilic aromatic substitution is, in contrast to the electrophilic aromatic substitution, not dependent on the stabilization of the leaving group (in our case X⁻). The rate-determining step within the reaction is the formation and the stabilization of intermediate [A]. The intermediate [A] is also called the Meisenheimer complex. In this case, the stabilization of the anionic leaving group is not as important as in electrophilic aromatic substitution reactions, but the electronic surrounding in the aromatic system of the intermediate [A]. As shown in Scheme 18 the attack of the nucleophile in A is most probable in the *para* position to an electron-withdrawing group (EWG). This helps to stabilize the lone-pair and the negative charge *ortho* to the nucleophilic attack (+M-effect). Having two atoms next to the leaving group, which tears electrons out of the system, increases the speed of the reaction (-I-effect).⁷⁶⁻⁷⁸ In our case, this would be either a fluorine or a chlorine atom. Since fluorine has a higher electronegativity compared to chlorine the complex is more stable and the rate of the reaction higher. Having two strongly electronegative atoms next to the nucleophilic attack (as in our case), the *para* position to the EWG is the most probable for the primary attack. In our examples shown above and the following examples described within this doctoral thesis, we want to perform multi nucleophilic aromatic substitution reactions. The question is, where does the second nucleophilic attack take place? As shown in Figure 28, molecule B offers two possible binding sites for the second attack of a nucleophile.

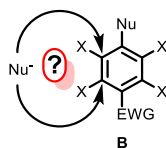
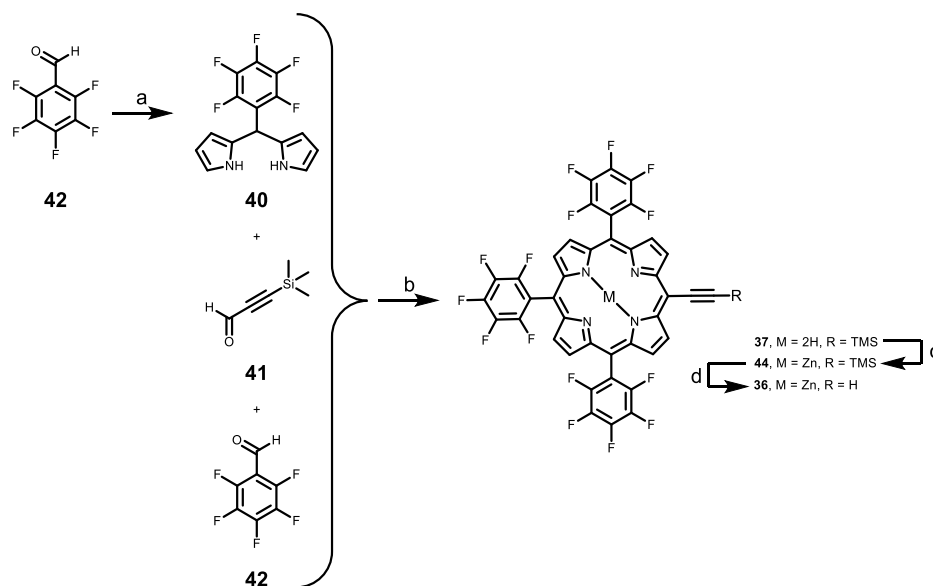


Figure 28. Two possible positions for the second nucleophilic attack at the aromatic system. Nu is the nucleophile, X the leaving group and EWG the electron-withdrawing group.

The attack is possible in two positions, the first position is *ortho* and the second position is *meta* to the already bonded nucleophile. With regard on the described $-I$ -effect of the fluorine and the $+M$ -effect of the EWG for the first attack, with a higher probability the second attack takes place in the *meta* position to the primary nucleophile. The neighboring electronegative fluorine or chlorine stabilizes the negative charge, as well as it is stabilized by delocalization to the EWG. So going back to our molecules, the EWG group helps to stabilize the Meisenheimer complex, and a nucleophilic aromatic substitution reaction is in general possible. Introduction of nucleophiles in theory should be easier at fluorinated aromatic systems than on chlorinated systems. Another effect to keep in mind for the nucleophilic aromatic substitution reaction at multiple positions using large nucleophilic chains is the steric shielding of the individual chains that are already introduced.^{79,80} The introduction of a second perfluoroalkyl side-chain to an aromatic system is sterically hindered due to the size of the perfluorinated chain. Fluorinated chains are sterically more demanding than their hydrogenated counterparts are, since the bond-length of a carbon-fluorine bond of 135 nm is considerably longer than a sp^3 -carbon-hydrogen bond with around 109 nm. In addition, the high electronegativity of fluorine pulls the electron-density to the outer part of the chain. The carbon backbone of the chain can be seen as partially positively charged, and the fluorine atoms as a partially negative charged shield. Combined with the size of the chains, this has a big influence on the number of chains that one can introduce to the newly synthesized porphyrin-systems.

3.3 Syntheses and Characterization

Syntheses towards a novel porphyrin-dimer started with an electrophilic aromatic substitution reaction at pyrrole (**43**) using pentafluorobenzaldehyde (**42**) to obtain the first starting material for the porphyrin synthesis as shown in Scheme 19. The reaction was performed in pyrrole (**43**) as solvent, since these conditions have been found to be ideal by Lee *et al.* in 1994.⁷⁵ 5-(Pentafluorophenyl)-dipyrromethane (**40**) was obtained in 91 % after purification by recrystallization from dichloromethane and cyclohexane as a colorless solid. The purity and structure was confirmed by ¹H-, ¹⁹F- and ¹³C-NMR and electron impact mass spectroscopy (EI-MS) and the obtained values were comparable to literature.⁷⁵



Scheme 19. Synthesis of unsymmetrical porphyrin monomers **36**. Reagents and conditions: (a) pyrrole (**43**), trifluoroacetic acid (TFA), RT, 30 min, 91 %; (b) borontrifluoride diethyltherate (cat.), chloroform, RT, 18 h, then 2,3-dichloro-5,6-dicyano-1,4-benzoquinone (DDQ), RT, 2 h, 15 %; (c) zinc(II) acetate, MeOH, dichloromethane, RT, 24 h, quant.; (d) TBAF (1 M in THF), dichloromethane, 1 h, then MeOH, quant..

The second step shown in Scheme 19 was found to be the key step in this synthetic pathway. There is a broad spectrum of known reaction conditions towards porphyrin systems using dipyrromethanes in literature.^{81–84} The unsymmetrical porphyrin monomer **37** was synthesized from previously synthesized dipyrromethane **40**, TMS-propynal (**41**) and pentafluorobenzaldehyde (**42**). This reaction step suffers from a low yield, therefore the reaction conditions for an unfluorinated porphyrin system developed by Fathalla *et al.* in 2009 were systematically varied.⁸¹ In Table 2, a summary of the varied reaction conditions is shown. The formation of a porphyrin is an equilibrium reaction; therefore, the duration of the reaction is very

important. The porphyrinoid formed before oxidization opens and closes in different isomeric substructures. Addition of the oxidizing agent terminates the reaction and a maximum amount of porphyrin should have been formed at this stage of reaction. Increasing the reaction time raises the yield of this reaction step. If the reaction time is decreased, almost no product will be observed. Changing the oxidizing agent from 2,3-dichloro-5,6-dicyano-1,4-benzoquinone (DDQ) to *p*-chloranil did not lead to higher yields in this step. During these reactions, we found that TMS-propynal (**41**) is more reactive in this step than pentafluorobenzaldehyde (**42**), since a large amount of symmetrical porphyrin **39** was observed. Doubling the equivalents of pentafluorobenzaldehyde (**42**), we obtained the highest yields for this reaction step. Further increasing the equivalents of pentafluorobenzaldehyde (**42**) did not lead to higher yields.

Table 2. Optimization of the conditions to synthesize unsymmetrical porphyrin monomer **37**.^[a]

40 [equiv.]	41 [equiv.]	42 [equiv.]	Time [h]	Oxidizing agent	Yield ^[b] [%]
2	1	1	0.75	DDQ	3
2	1	1	0.33	DDQ	0
2	1	1	1	DDQ	8
2	1	1	18	DDQ	10
2	1	1	18	<i>p</i> -chloranil	7
2	1.1	2	18	DDQ	15
2	1.1	3	18	DDQ	9

[a] All reactions were performed at room temperature and with the same concentration and scale;

[b] Yields are isolated yields.

These optimized reaction conditions were used to synthesize unsymmetrical porphyrin monomer **37** starting from dipyrromethane **40**, TMS-propynal (**41**) and pentafluorobenzaldehyde (**42**). After 18 h stirring at high diluted conditions in chloroform the reaction was oxidized using DDQ and the reaction mixture stirred for another two hours to enable complete oxidization. Subsequent filtration of the crude product through silica and multiple column chromatography allowed separation of the three main products into fractions. In Figure 29, the thin layer chromatography (TLC) plates of the first 50 fraction after column chromatography on silica are displayed. Using different light sources shining on the plates, one can clearly distinguish the fractions of the porphyrins having different substitution pattern.

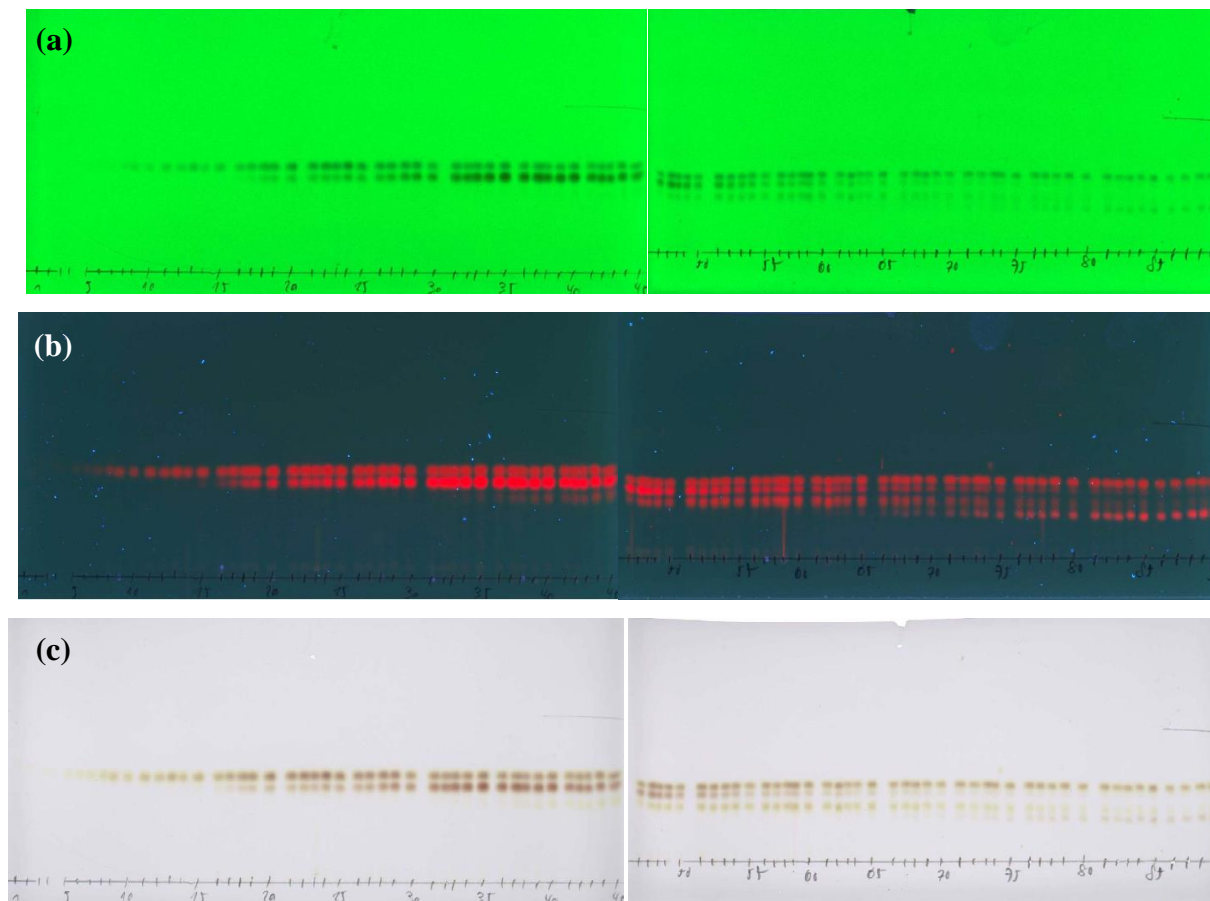


Figure 29. Visualization of spots on the thin layer chromatography (TLC) plates using irradiated light at 254 nm (a), 366 nm (b) and white light (c). The TLC plates show the first 50 collected fractions after column chromatography on silica. The fastest moving product is the double TMS substituted porphyrin **39**, followed by the desired unsymmetrical porphyrin **37** and in the slowest moving spots indicate the fully fluorinated porphyrin **38**.

The first eluted fraction within this purification by column chromatography is the double TMS substituted porphyrin **39**, followed by the desired unsymmetrical porphyrin **37**. The last and least intense spot on TLC is the fully fluorinated porphyrin **38**. The difference between the R_f -values of the different porphyrins equals to 0.01. Due to these difficulties in separation of the different fractions by column chromatography, the purification steps had to be repeated.

Due to the statistical nature of this reaction step, the two undesired symmetrical porphyrin monomers **38** and **39** were obtained in 6 % and in 24 % respectively. The desired unsymmetrical porphyrin monomer **37** was obtained in 15 % yield.

Further modifications at porphyrin monomer **37** are shown in Scheme 19. First a zinc atom was introduced in the porphyrin macrocycle using zinc(II) acetate. In a second step the TMS masked acetylene was deprotected using tetra-butyl-ammonium-fluoride (TBAF). The free-acetylene porphyrin **36** was obtained in quantitative yield over both reaction steps.

The purity of the unsymmetrical porphyrins (**36**, **37** and **44**) was proven by ^1H -, ^{19}F - and ^{13}C -NMR, high-resolution mass spectrometry (HRMS), MALDI-TOF mass spectroscopy, and elemental analysis (EA). Especially the key building block **37** was investigated in detail and should be discussed and compared in this part. In Figure 30 the ^1H -NMR spectrum of this building block is shown and all the signals determined.

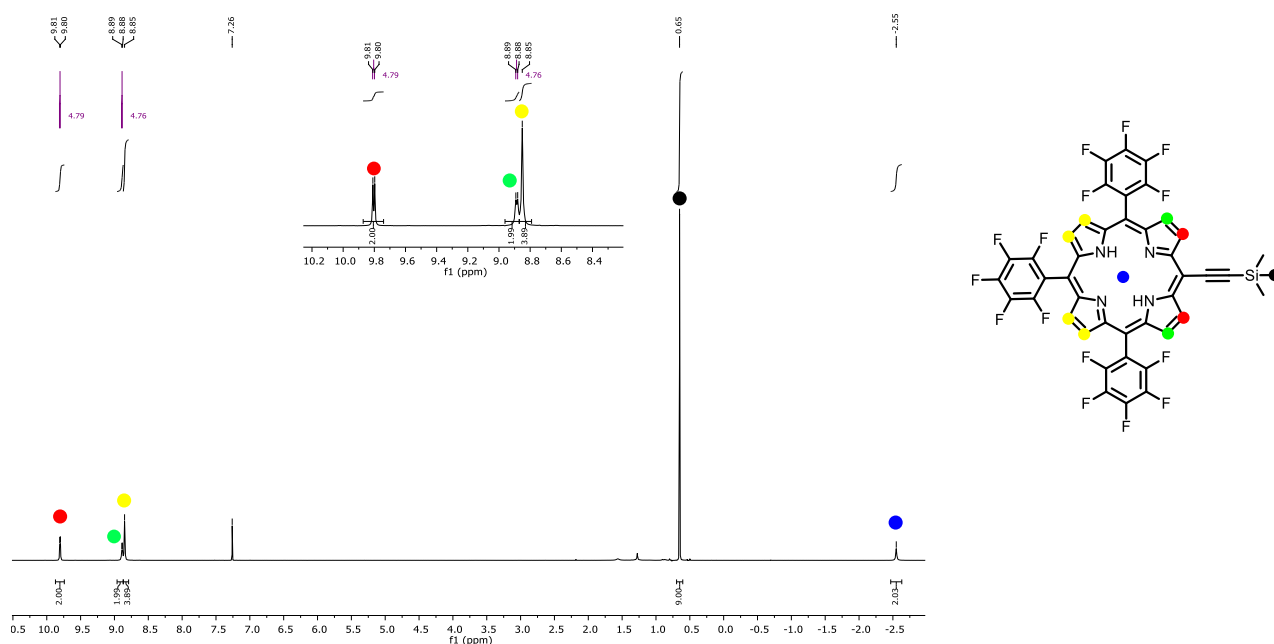


Figure 30. ^1H -NMR spectrum and structure of key building block **37**.

Analyzing the ^1H -NMR spectrum we observed strong and well-defined signals corresponding to all protons in the structure. The aromatic signals originating from the eight protons at the porphyrin macrocycle were found at chemical shifts between 8.85 and 9.81 ppm. The strong low-field shift of the aromatic protons occurs due to the strong electronic effects in the heteroaromatic system. At 8.85 ppm, the signal originating from the protons opposite to the TMS masked acetylene has been found (yellow). This signal does not show any coupling, since both type of protons in this system are similar in the spectrum. Closer to the TMS masked acetylene, the different types of protons can be defined since the chemical shifts strongly vary. Protons in 2-position (red) were found to be strongly shifted in the low field and split into a doublet. This signal showed a $^3J_{\text{H-H}}$ coupling to the protons in 3-position (green). A strong singlet signal at 0.65 ppm indicates the protons of the TMS protecting groups. A porphyrin specific signal of strongly high-field shifted protons of the free base protons (blue) in the center of the macrocycle were found at -2.55 ppm. Using a 600 MHz NMR spectrometer we further determined the fluorine signals in the ^{19}F -NMR spectrum shown in Figure 31.

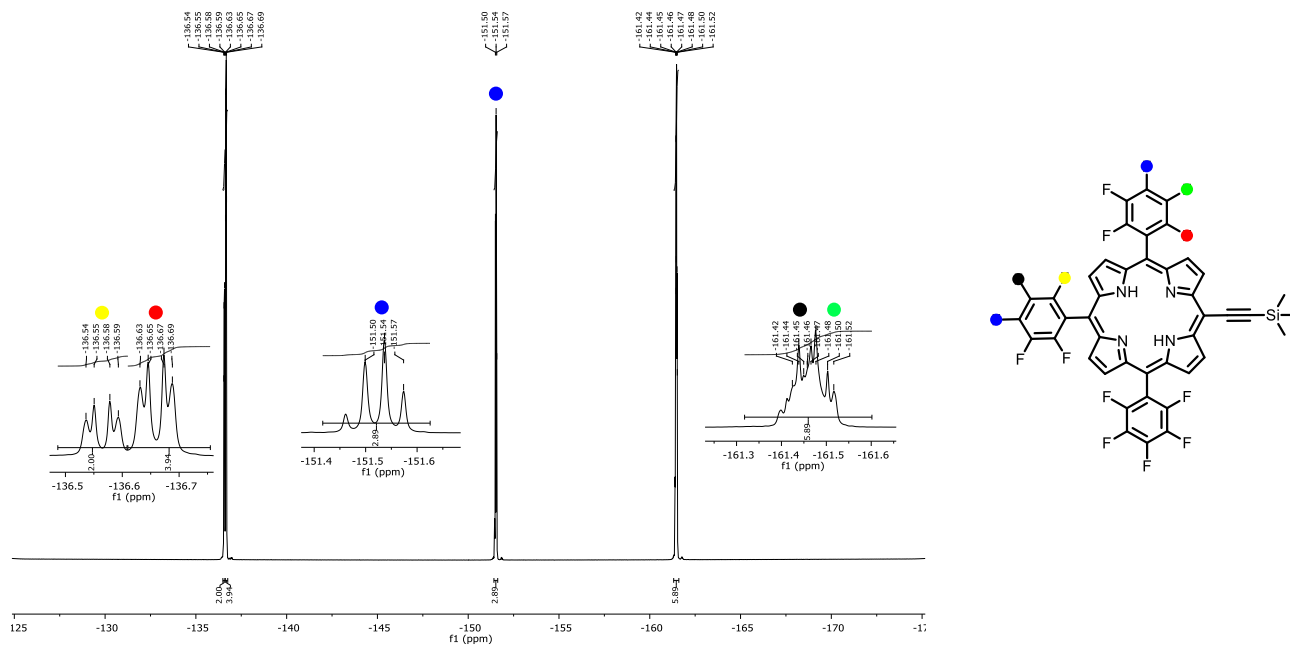
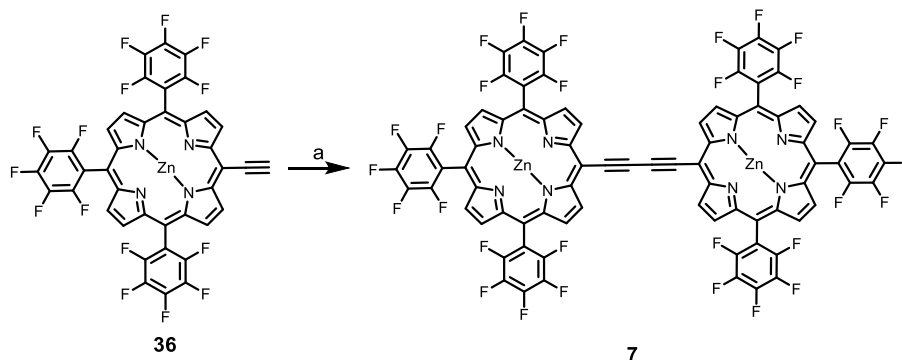


Figure 31. ^{19}F -NMR spectrum and structure of key building block **37**.

The ^{19}F -NMR spectrum showed three main signals occurring from the *ortho*, *meta* and *para* position in the fluorinated aromatic systems. Between -136.5 and -136.7 ppm the signals of the *ortho* protons are found. The signals are split into two doublet of doublets. At a chemical shift of -136.5 ppm the *ortho*-fluorine atom of the aromatic system in 10-position (yellow) can be found. By the integrals found for these signals it was possible to distinguish between the signals of the ring in 10-position to the ones in 5- and 15-position. These *ortho*-fluorine signals were found at -136.7 ppm as a doublet of doublets. The *meta*-fluorine atoms (black and green) could not be distinguished from each other and are overlapped in a multiplet between -161.4 and 161.5 ppm. In addition, the *para*-fluorine atoms are combined in one multiplet between -151.5 and -151.6 ppm.

Having a first unsymmetrical and free acetylene porphyrin **36** in hand we were then able to synthesize a dimeric porphyrin structure under oxidative Glaser-Hay coupling conditions developed by Glaser in 1869 and modified by Hay in 1962.^{85,86} Using these conditions it is crucial to use zinc-porphyrins in order to prevent a copper atom to be bond in the macrocycle. Conditions used for the coupling were modified from previously described conditions by Anderson and co-workers.⁷⁴ It was found that in diacetylene coupled porphyrin dimers the two porphyrin macrocycles are planar with regard to each other. This feature enables the two photon

absorbance of these porphyrin dimers, which may can be used for future detection of the molecules in quantum interference experiments.^{74,87–91}



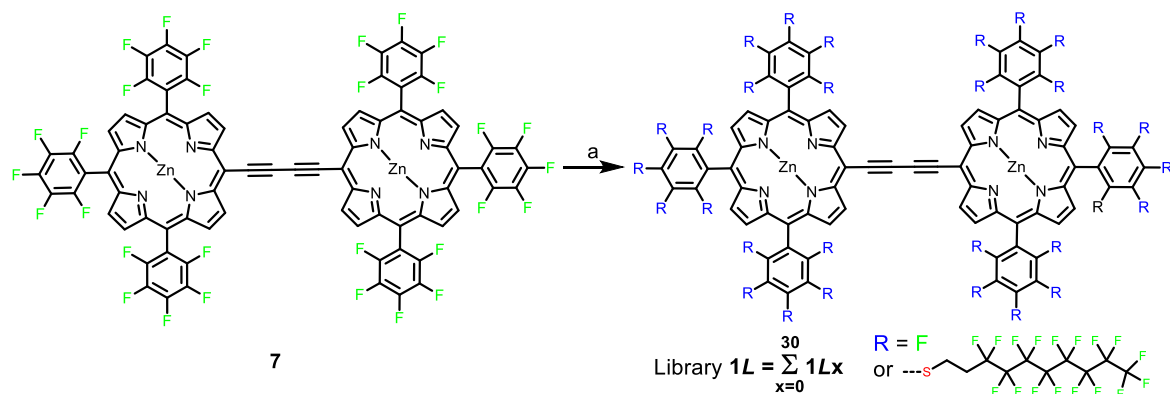
Scheme 20. Oxidative Glaser-Hay coupling to obtain diacetylene coupled porphyrin dimer **7**. Reagents and conditions: (a) Cu(I)Cl, tetramethyl-ethylenediamine (TMEDA), dichloromethane, air, room temperature, 30 min, 95 %.

In an open Erlenmeyer-flask, porphyrin monomer **36** in dichloromethane was stirred vigorously to aerate the solution. An excess of Cu(I)Cl was added, followed by the addition of tetramethyl-ethylenediamine (TMEDA). TMEDA is added to build up the active catalyst. A detailed mechanistic investigation can be found in Fomina *et al.* from 2002.⁹² Subsequent column chromatography of the crude product yielded the desired porphyrin dimer **7** in 95 %. Purity of the obtained dimer **7** was proven by ¹H- and ¹⁹F-NMR spectroscopy and MALDI-TOF mass spectrometry.

As described in the syntheses of earlier tailor-made porphyrins for QIE we try to obtain libraries of molecules by the introduction of a various number of side-chains. This porphyrin dimer **7** exposes 30 fluorine atoms at the periphery for nucleophilic aromatic substitution reactions using perfluoroalkylthiolates. The introduction of peripheral fluoroalkylsulfanyl side-chains to the porphyrin dimer **7**, is not only increasing the molecular mass of the molecule by the production of a molecular library, but also reducing the polarizability of the fluoroalkylsulfanyl side-chains resulting in low Van der Waal interactions and is thus decreasing the intermolecular attraction. Using commercially available *1H,1H,2H,2H*-perfluorodecanethiol the nucleophilic aromatic substitution reaction was performed under weakly basic conditions as described in Table 3. Porphyrin dimer **7** was dissolved dimethylformamide (DMF) and the perfluoroalkylthiolate nucleophile dissolved in ethyl acetate was added to the stirred reaction-mixture. The reaction was started by the addition of diethylamine (DEA). After two hours, the reaction was stopped adding water, the crude product was extracted using diethylether. Analysis

of the obtained library **1L_x** was done use MALDI-TOF mass spectroscopy. The composition of the library is detailed in Table 3.

Table 3. Nucleophilic aromatic substitution reaction at porphyrin-dimer **7** to obtain porphyrin library **1L_x** with *x* being the number of alkylthiol substituents which have replaced a fluorine atom.^[a]



1L_x	x (number of -S(CH ₂) ₂ C ₈ F ₁₇)	Number of F-atoms (= 60-x)	Mass [g/mol]	Calc. Mass [g/mol]	Rel. intensity [%]
1L₄	4	26	3636	3626	25
1L₅	5	25	4084	4086	55
1L₆	6	24	4545	4546	100
1L₇	7	23	5013	5006	63
1L₈	8	22	5481	5466	24

[a] The members of the library have the elemental formula C₈₀H₁₆F_{30-x}N₈Zn₂(S(CH₂)₂C₈F₁₇)_x with *x* = 4 to 8 and the most abundant member (**1L₆**) has *x* = 6 (4545 g/mol). Reagents and conditions: (a) 8 equiv. *1H,1H,2H,2H*-perfluorodecanethiol, diethylamine (DEA), dimethylformamide (DMF), ethyl acetate, room temperature, 2 h.

As we expected only individual members of the library whose masses vary by a difference of $\Delta_m = m(\text{C}_{10}\text{H}_6\text{F}_{17}\text{S}) - m(\text{F}) = 479 - 19 = 460$ are observed within the product mixture. The relatively highest mass was observed for the library **1L₆** with a number of six fluorine atoms substituted by a fluoroalkylsulfanyl side-chain. The number of substituted fluorine atoms varies between four and eight being in a mass range of 3600 to 5500 g/mol. The most abundant signal being library **1L₆** had a mass of 4545 g/mol. It is important to note that the nucleophilic aromatic substitution reaction introducing the fluoroalkylsulfanyl side-chains to the porphyrin dimer **7** is to some extent a random process. The members of the library having a similar *x* (number of side-chains) can also be structural isomers. Some control over the introduction of the side-chain is possible and was already demonstrated in earlier studies.⁵⁷ We observed the introduction at the *para* position to the porphyrin macrocycle being favored and could confirm this by ¹⁹F-NMR spectroscopy.

Table 4 shows five chosen examples of different reaction conditions tested to introduce *1H,1H,2H,2H*-perfluorodecanethiol in a nucleophilic aromatic substitution reaction to the fully fluorinated porphyrin dimer **7**. All the molecular libraries obtained have been investigated by MALDI-TOF analyses. In entry one we used eleven equivalent of thiol and stirred the reaction for three hours in 35 equivalents of diethylamine (DEA) as the base, this procedure led to the introduction of six to nine side-chains. As shown in entry two, increasing the equivalents of thiol to 30 and the equivalents of DEA to 70 together with an increased reaction time of 24 hours, we observed a molecular library with a number of fluoroalkylsulfanyl side-chains ranging from six to eleven. Reducing the reaction time and the equivalents of thiol and DEA led to reduced numbers of side-chains (5-8 in entry three and 4-6 in entry four). To introduce a larger number of fluoroalkylsulfanyl side-chains we changed the solvent to diglyme to be able to heat the reaction mixture to 200 °C. Using 70 equivalents of thiol and 100 equivalents of sodium hydride (NaH) we were able to obtain a library containing individual members with 10 to 21 fluoroalkylsulfanyl side-chains. This investigation enables us to synthesize molecular libraries with specific ranges of fluoroalkylsulfanyl side-chains attached to the molecule.

3.4 Thermal Stability Tests

With molecular library **1Lx** of the porphyrin dimer with fluoroalkylsulfanyl side-chains shown in Table 3 stability tests were performed at the University of Vienna using different temperatures in a quadrupole mass spectrometer (QMS). Thermal stability is essential in QIE in a Kapitza-Dirac Talbot-Lau interferometer (KDTLI) because sublimation is required to produce the molecular beam in near-field experiments. To suit for near-field QIE the molecule should have a sublimation temperature at some hundred degrees Celsius. In a first step, library **1Lx** was heated to 225 °C as represented in Figure 32, and showed a signal of around 1000 counts/s at a molecular mass of 930 amu. This signal is suggested to be twice the mass of the perfluoroalkyl side-chain (2 x 480 amu). The large signal below 500 amu is suggested to show the molecular mass of one perfluoroalkyl side-chain (480 amu) and some decomposition products.

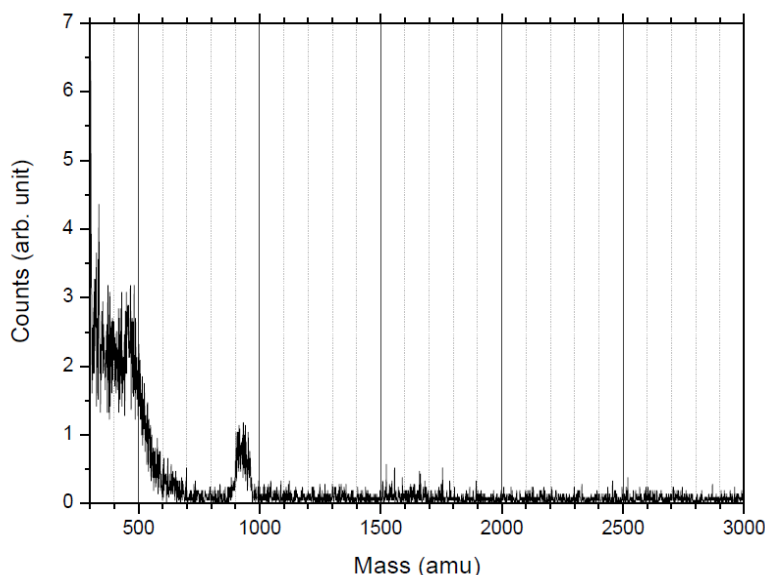


Figure 32. Spectrum of molecular library **1Lx** after heating to 225 °C investigated by a QMS.

Below 300 °C, no signal in the region of 4'000 amu to 5'000 amu could be observed. Concluding in a sublimation temperature higher than 300 °C for library **1Lx** of the diacetylene coupled porphyrin dimer. Above 300 °C, the signal at 930 amu disappears and new signals with higher masses occur. The heating to 384 °C in a first step showed the highest number (about 20'000 counts/s) of counts at a mass of 2'227 amu, which is half of the mass of the six fold substituted member of library **1Lx** that is further described in Table 3. The mass spectrum taken using a QMS after heating to 384 °C is shown in Figure 35.

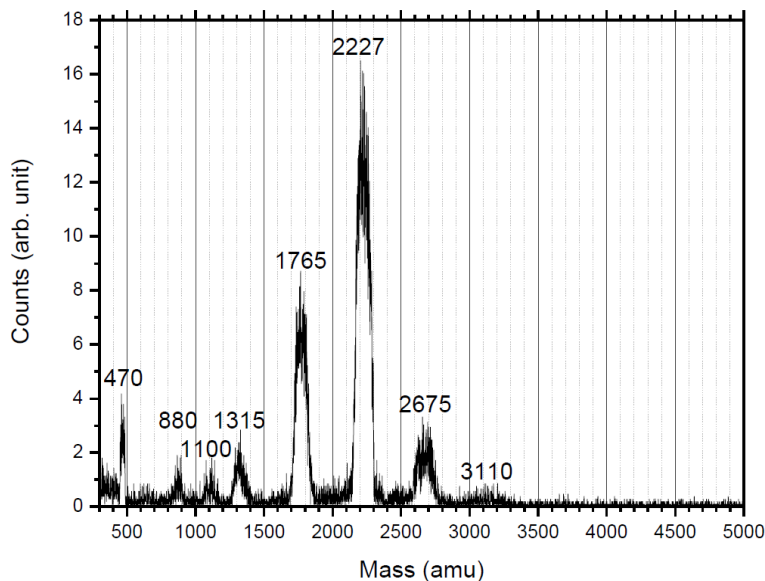


Figure 33. Spectrum of molecular library **1Lx** after heating to 384 °C investigated by a QMS.

The other molecular masses shown in Figure 33 can be attributed to the other decomposed members of the library **1Lx**. 3'110 amu is suggested to be half of the molecular mass of the eight fold substituted dimer, 2'675 amu of the seven times substituted and 1'765 amu of the five times substituted dimer. This observation suggests thermal decomposition by cleaving the diacetylene bond at this temperature in the mass spectrometer.

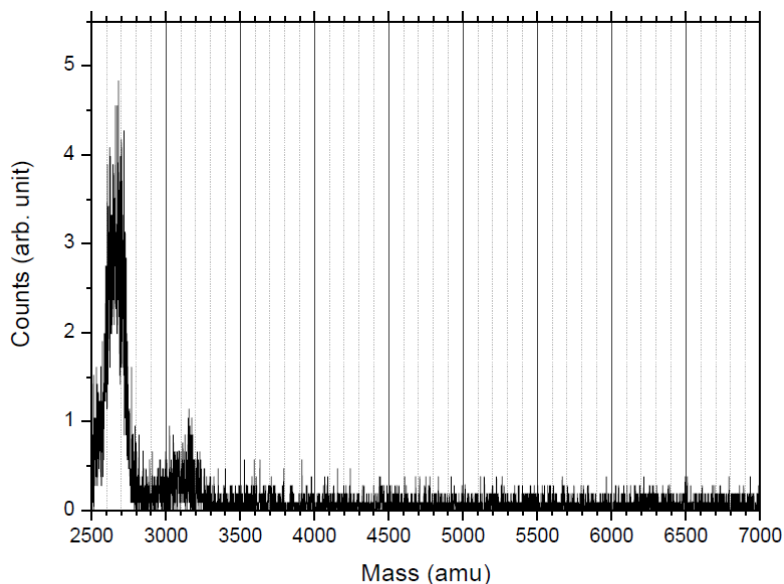


Figure 34. Spectrum of molecular library **1Lx** after heating to 392 °C investigated by a QMS.

Figure 34 shows the results for higher masses at a temperature of 392 °C. No signal for the porphyrin dimers in library **1Lx** was observed. Further heating above 400 °C leads to the disappearance of all signals. It is assumed that the porphyrin core is decomposed at temperatures above 400 °C and therefore the sublimation temperature is probably higher than 400 °C. To access near-field experiments on a KDTLI, the sublimation temperature of the compound needs to be lower than the decomposition temperature. In this case, the sublimation temperature of the entire molecule seems to be higher than the decomposition temperature. This suggestion is supported by the QMS spectrum taken at 384 °C, where half of the molecular masses from the library could be observed.

3.5 LIAD Experiments

As described before the common methods to bring molecules into gas phase, such as sublimation in the Kapitza-Dirac Talbot-Lau interferometer (KDTLI) failed in the case of the molecular libraries produced from porphyrin-dimer **7**. The sublimation temperatures of the molecules and especially of the diacetylene bond between the two porphyrin macrocycles appear to be higher than their decomposition energy level. This leads to major decomposition of the molecules while heating. Methods used in analytical chemistry to bring larger molecules into gas-phase such as matrix-assisted laser desorption ionization (MALDI) or electron spray ionization (ESI) produce charged particles.^{93,94} Our collaborators in the Arndt group developed the idea of laser-induced acoustic desorption (LIAD) to produce neutral or lowly charged molecules that can be transferred into the gas-phase, free from any carrier gas or matrix, in contrast to MALDI or ESI the ionization processes.⁹⁵ This feature enables particle specific detection, such as two-photon ionization. The transfer loss between the source and the mass analyzer are minimized and therefore it is possible to detect very rare samples. The original experiments using LIAD were performed to launch electrons and ions, large polypeptides and DNA strands.⁹⁵⁻⁹⁷ It was also possible to not only launch large molecules but also to transfer the neutral or lowly charged molecules into mass spectrometers.⁹⁸ This technique then enables to launch and detect silicon nanoparticles and biological cells up to a mass of 10^{10} g/mol.^{99,100}

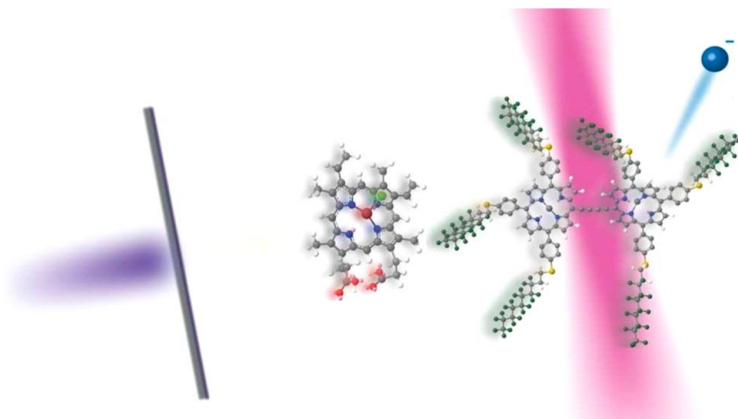


Figure 35. Schematic representation of the LIAD experimental setup. Violet being a short and intense laser pulse, gray represents the metal foil, pink is the vacuum ultra violet (VUV) laser beam ionizing (represented in blue) the represented molecules (a hemin molecule on the left and the herein described library **1Lx**).¹⁰¹

In a LIAD experiment, the molecules are deposited on a several micrometers thick foil. The backside of the foil is brought into motion by a short intense laser pulse. Induced by thermo-mechanical stress in the foil, the molecules are ejected from the front-side of the foil.¹⁰² In our

experiment, we investigated the porphyrin-dimer library **1Lx** in a specially designed LIAD setup. This experiment is of great interest since it enables to access a soft volatilization method for rare unstable samples. Another feature is the low velocity of the large particles detected by the MS. This will be beneficial for matter-wave experiments.^{103,104} In order to investigate the softness of the LIAD volatilization technique, larger biochromophores such as hemin, bilirubin, biliverdin and chlorophyll have been brought into gas-phase. The studies of biomolecules are very interesting with regard on the production of molecular beams with fragile molecules, but also in ionization studies, classical beam deflectometry, or molecular cooling.^{105–108} The investigations on biomolecules are discussed in detail by Sezer *et al.* and will not be investigated within this work.¹⁰¹

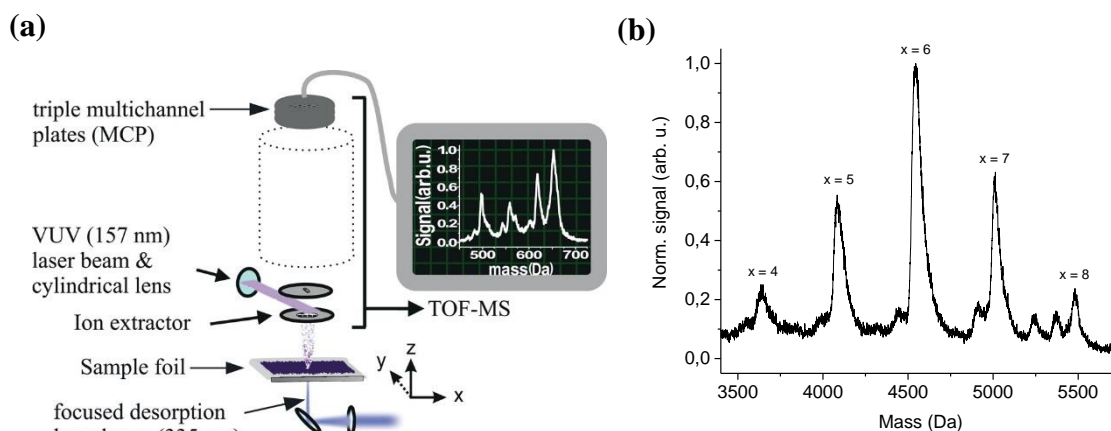


Figure 36. (a): Library **1Lx** is volatilized by LIAD from a surface of a thin metal foil by irradiating its backside with intense pulsed laser light with $\lambda_{\text{des}} = 335$ nm. The produced molecular beam is postionized using vacuum ultra violet (VUV) light with $\lambda_{\text{ion}} = 157.6$ nm and in a last step characterized using a time of flight mass spectrometer (TOF-MS). (b): Representation of the LIAD mass spectrum obtained from the porphyrin-dimer library **1Lx** bearing an amount of x fluoroalkylsulfanyl side-chains.¹⁰¹

In this work we want to focus on the volatilization properties of library **1Lx** in a LIAD setup as shown in Figure 36a. The molecules were deposited on a thin titanium foil with a thickness of 10 ± 2 μm . In a vacuum chamber we shine with a focused desorption laser beam, having an energy of 335 nm, on the backside of the foil. Ions were extracted using an ion extractor before hitting the molecular beam using a vacuum ultra violet (VUV) light with $\lambda_{\text{ion}} = 157.6$ nm. The herein produced ions were then analyzed by a time of flight mass spectrometer (TOF-MS). The mass spectrum found after the LIAD volatilization shown in Figure 36b should be similar to the mass spectrum taken on a regular MALDI-TOF mass spectrometer. Indeed both mass spectra show the same masses and distributions of the mass peaks. The mass difference of two signals is

460±10 and showing a number of fluoroalkylsulfanyl side-chains ranging at library **1Lx** ranging from $x = 4$ to $x = 8$. It was possible to bring the molecules uncharged into gas-phase using LIAD. The molecules were ionized using VUV laser beam at 157 nm and finally the individual members of the library could be detected by a TOF-MS. Using the LIAD technique we found that it is possible to produce molecular beams being around one order of magnitude slower than using matrix assisted laser desorption (MALD). In addition, this behavior is dependent on the material of the substrate material. Using the before described titanium foil we observed most probable velocities of 20 m/s for the fluoroalkylsulfanyl functionalized libraries.

3.6 Conclusion

It was possible to synthesize first porphyrin dimer systems on which a various number of fluoroalkylsulfanyl side-chains we installed in a nucleophilic aromatic substitution. The key step in the reaction pathway towards these molecular libraries was the synthesis of unsymmetrical porphyrin monomer **37**. The reaction conditions were systematically varied to obtain higher yields for this reaction step. A fist multi-porphyrin system was synthesized using a Glaser-Hay coupling. We synthesized a diacetylene coupled porphyrin dimer **7**. Furthermore we were able to introduce long fluorinated chains in a multifold nucleophilic aromatic substitution reaction to the outer part of the fully fluorinated porphyrin dimer. This lead to a first molecular library that was investigated towards QIE in the Arndt group. The library **1Lx** obtained in this last reaction step consisted of five to eight fluoroalkylsulfanyl side-chains being well separated by the mass difference of one side-chain. By variation of the reaction conditions of the nucleophilic aromatic substitution reaction, it was possible to vary the number of side-chains.

Firstly, the porphyrin dimer library **1Lx** was investigated in a sublimation experiment. The substrate was heated stepwise to temperatures above 400 °C and the heated samples investigated using a quadrupole mass spectrometer (QMS). Below 300 °C, it was not possible to sublime the molecule, so it is not possible to produce a molecular beam in a Kapitza-Dirac Talbot-Lau interferometer (KDTLI). By heating to 384 °C the molecules detected after sublimation showed half of the masses found for the molecular library of the intact molecules. This leads to the conclusion that the molecule brakes at the diacetylene bond and cannot be detected intact. Further heating above 400 °C leads to complete decomposition of the sample. Having this information, we decided not to use these molecules in a KDTLI. It would not be possible to produce a molecular beam in the thermal source of this type of interferometer.

Investigations towards softer volatilization techniques brought up the idea of using laser induced acoustic desorption (LIAD). To our delight, it was possible to bring uncharged and fragile molecules into gas-phase using LIAD. We were able to produce sufficiently strong molecular beams of biochromophores and porphyrin dimer library **1Lx**. The library was detected using a time of flight mass spectrometer (TOF-MS) showing an identical mass spectrum as obtained before volatilization in a commercial MALDI-TOF apparatus. This leads to the conclusion that it is possible to produce sufficiently strong molecular beams using small amounts of fragile molecular libraries.

It does not seem to be possible to use the classical KDTLI to investigate these libraries, since a thermal source is used. The sublimation temperature of library **1Lx** is higher than the decomposition energy. Using LIAD it is possible to produce sufficiently strong molecular beams, using postionization it was possible to detect the intact molecules. LIAD seems to be promising to be introduced into QIE. Further development of the experiment needs to be done. Another limitation of library **1Lx** is the number of possible positions in nucleophilic aromatic substitution reaction. In this case, it would only be possible to substitute 30 fluorines by a nucleophile.

4 Near-Field Interferometry: 2nd Generation Porphyrin-Systems

The possibilities to successfully analyze larger porphyrin systems made by Glaser-Hay couplings are rather limited, as this link has proven not to be stable enough. Therefore, we decided to synthesize a second generation of oligo porphyrin-systems. Using new synthetic approaches, we want to avoid the diacetylene bridges between the molecules.

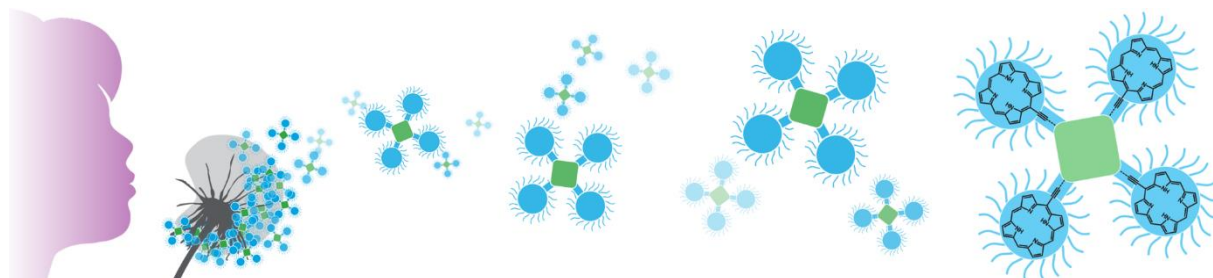


Figure 37. Schematic representation of oligo porphyrin-systems. The porphyrins (light blue) are proposed to be bonded to a central core (green). The porphyrins should be relatively stable and easy to ionize.¹⁰⁹

Herein we present the syntheses of oligo-porphyrin systems that should expose an even larger number of fluorine atoms to be substituted by perfluorinated alkyl thiolates. The linking part between the porphyrins (blue) and the central unit (green) are assumed to be a lot more stable using new synthetic approaches. In order to ease laser evaporation the polarizability/mass ratio should be small to minimize intermolecular interactions. To use laser evaporation the desired compound should be stable enough to survive short time exposure to temperatures up to 1000K during the laser pulses. Earlier experiments using porphyrin monomers showed impressive results regarding the vapor pressure if the molecules are suitably functionalized at the periphery.^{58,59} Using the second generation porphyrin-systems we obtain well defined molecular libraries that have relatively low vapor pressures.¹⁰⁹

4.1 Design of Oligo-Porphyrin-Systems

Herein we present the synthesis of oligo-porphyrin systems as shown in Figure 38. Synthesis of oligo-porphyrins have been widely used before and are well known in literature.^{110–114} We plan the synthesis of oligoporphyrin-systems consisting of two to five porphyrins. The systems should expose a large number of fluorine atoms at their periphery to be able to assemble molecular libraries for QIE. Tailor made porphyrin systems bearing a variable number of perfluoroalkyl side-chains. By the introduction of a metal-ion to the porphyrin macrocycle it should be possible to tune to some extent desorption and post-ionization properties of the target libraries.

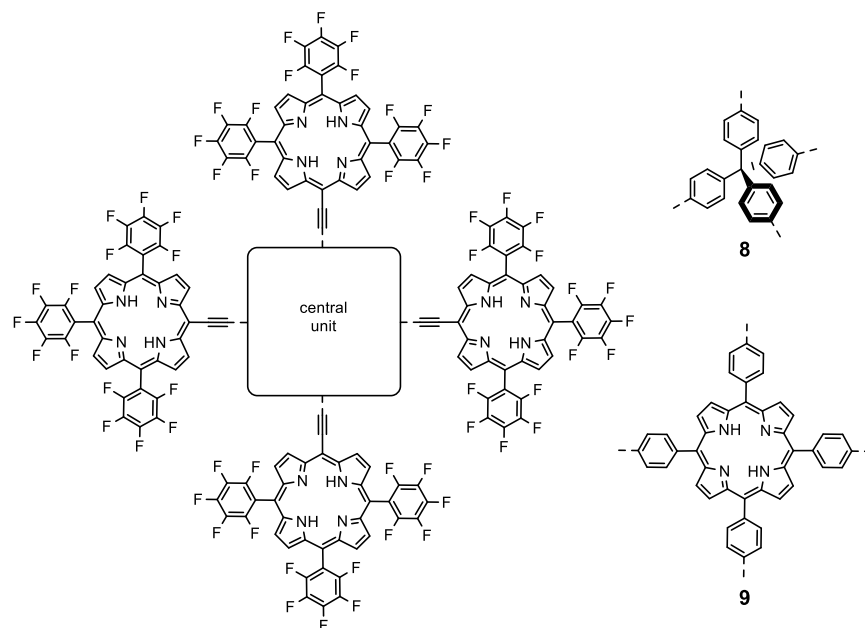


Figure 38. The porphyrin-tetramer **8** and porphyrin-pentamer **9** with two different central units, namely a tetraphenylmethane and a porphyrin, respectively. Both compounds have 60 peripheral fluorine atoms, which are accessible for S_NAr -reactions, allowing to increase their mass by suitable nucleophiles.¹⁰⁹

Of greatest interest to be able to obtain a high molecular mass, the attachment of perfluoroalkyl side-chains to the two oligoporphyrin-systems (**8** and **9**) is of great interest (Figure 38). In both systems, it should be possible to substitute up to 60 fluorine atoms in the periphery in a nucleophilic aromatic substitution reaction by a fluoroalkylsulfanyl side-chain. It should also be possible to obtain libraries with a broad distribution of well-defined individual members. Another very interesting point is the extended conjugation in pentamer **9** compared to tetramer **8**. The porphyrin tetramer **8** has present a sp^3 -hybridized carbon center in the tetrahedral central unit, therefore the conjugation is broken, and all porphyrin units around the central unit can be seen as individual conjugated systems. In comparison, the porphyrin-pentamer **9** is interlinked by ethynyl

bridges in *meso*-position to a central porphyrin unit. Due to a mismatch of π - π and π^* - π^* at the sp^1 - sp^2 connection single acetylene systems are known to have a reduced conjugation. It was previously reported by two groups that porphyrins interlinked directly at the *meso*-position by ethynyl bridges prevent the π -system from twisting out of plane.^{89,91} In our opinion this should extend the conjugation between the different porphyrin macrocycles. In addition, one could hypothesize that the difference in planarity and size of the conjugated systems leads to variations in desorption and photo-ionization behavior obtained from the above-described precursors (**8** and **9**).

In order to develop methods to attach a larger number of porphyrins to a central unit we propose two smaller systems shown in Figure 39.

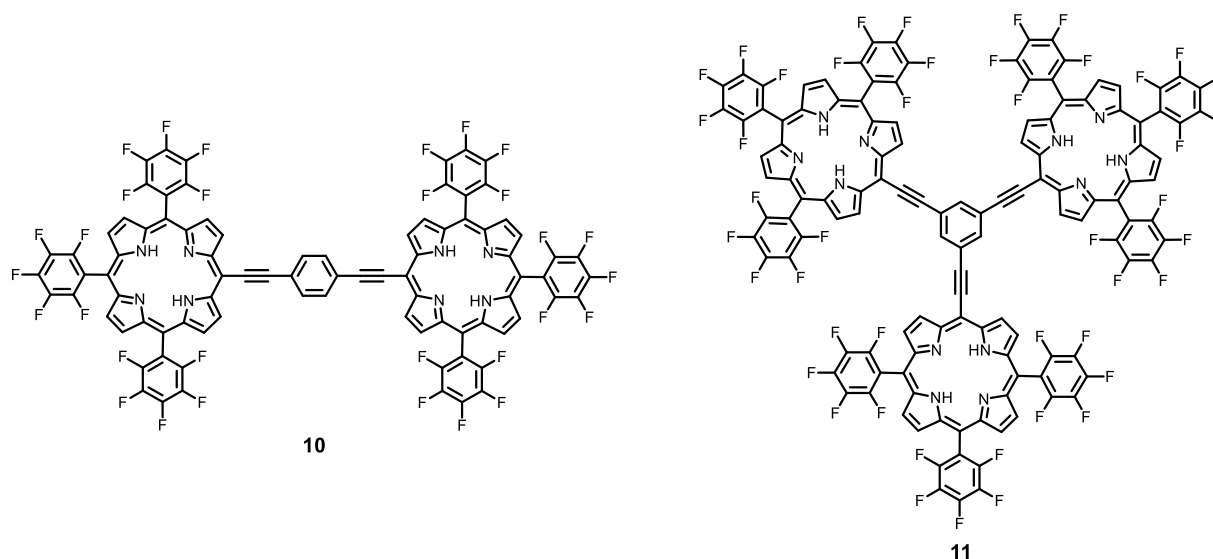


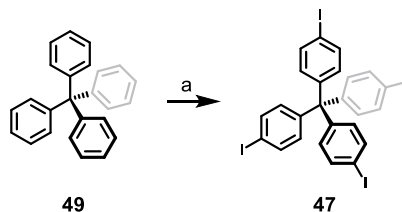
Figure 39. Porphyrin-dimer **10** and porphyrin-trimer **11**. Both are built around a central phenyl unit. Dimer **10** has 30 accessible positions for S_NAr -reactions. The trimer **11** has 45 accessible positions.¹⁰⁹

To push the molecular mass above 20'000 g/mol both the porphyrin-dimer **10** and the porphyrin-trimer **11** are less promising precursors for high-mass libraries compared with tetramer **8** and pentamer **9**. All the molecules shown in Figure 38 and Figure 39 are planned to be synthesized from the same monomeric porphyrin system, which we can obtain from unsymmetrical porphyrin monomer **37** described in section 3. Using Sonogashira cross-coupling reaction conditions it should be possible to connect the peripheral deprotected ethynyl porphyrins to the corresponding iodine central units. Using the commercially available 1,6-diiodobenzene (**45**) and 1,3,5-triiodobenzene (**46**) we plan to optimize the cross-coupling reaction conditions while building up porphyrin-dimer **10** and porphyrin-trimer **11**. Using the optimized conditions

we plan to synthesize porphyrin-tetramer **8** from tetrakis(4-iodophenyl)methane (**47**) attaching the peripheral porphyrins. Tetrakis(4-iodophenyl)methane (**47**) can be obtained via iodination from tetraphenylmethane.¹¹⁵ In order to synthesize porphyrin-pentamer **9** we plan to use *meso*-tetrakis(4-iodophenyl)porphyrin (**48**) as the central unit in the Sonogashira cross-coupling reaction. *Meso*-tetrakis(4-iodophenyl)porphyrin (**48**) can be obtained from pyrrole (**43**) and 4-iodobenzaldehyde (**50**).^{84,116}

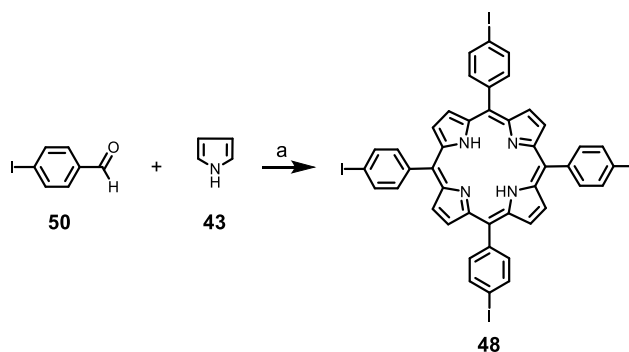
4.2 Syntheses of Oligo-Porphyrin-Systems

To build up the large oligo-porphyrin-systems followed by the molecular libraries we need to synthesize the central units as starting points for the cross-coupling reactions. Due to the higher reactivity of iodine compared to bromine and the number of cross-coupling reactions within one-step (two to four) we decided to focus directly on the iodinated starting materials. The iodinated starting materials are harder to access or more expensive if commercially available, but usually more reactive. The central units to build up the porphyrin-dimer **10** and trimer **11**, 1,6-diiodobenzene (**45**) and 1,3,5-triiodobenzene (**46**) respectively are commercially available and used as obtained. To build up the larger systems we need four iodine binding positions. The first central unit towards the porphyrin-tetramer **8** was synthesized following iodination conditions developed by Aujard *et al.* shown in Scheme 21.¹¹⁵



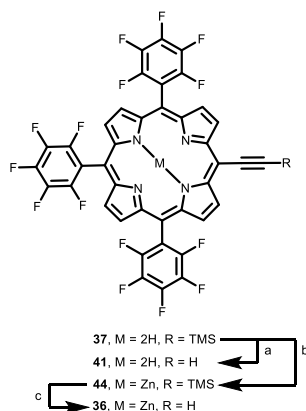
Scheme 21. Synthesis of tetrakis(4-iodophenyl)methane (**47**). Reagents and conditions: (a) [bis(trifluoroacetoxy)iodo]benzene (PIFA), iodine, carbon tetrachloride, reflux, 24 h, 74 %.

The iodination of tetrakis-phenyl-methane (**49**) was done using [bis(trifluoroacetoxy)iodo]-benzene (PIFA) and iodine in carbon tetrachloride to obtain tetrakis(4-iodophenyl)methane (**47**) in 74 % yield as a pink solid without any purification step. The second central unit needed to build up the large porphyrin systems is an iodinated porphyrin. Having this porphyrin in hand, it will be possible to synthesize a porphyrin-pentamer. Conditions developed by Lindsey *et al.* were used as displayed in Scheme 22.^{84,116}



Scheme 22. Synthesis of *meso*-tetrakis(4-iodophenyl)porphyrin (**48**). Reagents and conditions: (a) borontrifluoride diethyl etherate (cat.), chloroform, room temperature, 50 min, then 2,3-dichloro-5,6-dicyano-1,4-benzoquinone (DDQ), room temperature, 1 h, 14 %.

This variation of the synthesis of a porphyrin starts without synthesizing a dipyrromethane. In this case we used 4-iodobenzaldehyde (**50**) with pyrrole (**43**) under highly dilute conditions to obtain the desired *meso*-tetrakis(4-iodophenyl)porphyrin (**48**) in 14 % yield after purification by column chromatography as a dark purple solid.

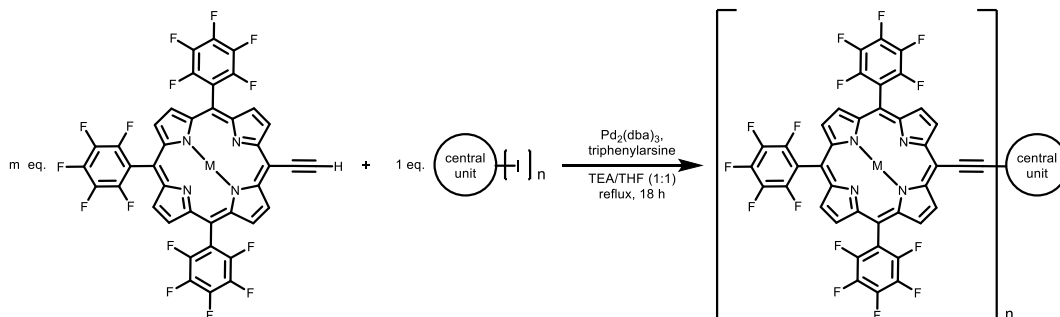


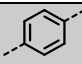
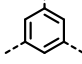
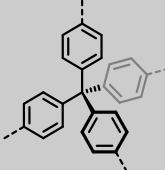
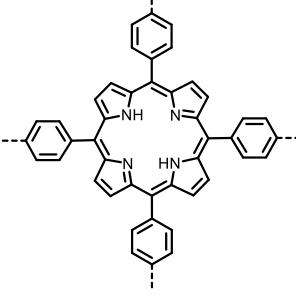
Scheme 23. Synthesis of the two porphyrin building blocks **41** and **36**. (a) TBAF (1 M in THF), dichloromethane, 1 h, then MeOH, 98 %; (b) zinc(II) acetate, MeOH, dichloromethane, RT, 24 h, quant.; (c) TBAF (1 M in THF), dichloromethane, 1 h, then MeOH, quant.

As shown in Scheme 23 for the syntheses of the porphyrin-oligomers we synthesized two free acetylene derivatives. A metal-free porphyrin was obtained by deprotection of the trimethylsilyl (TMS) masked porphyrin **37** by the use of tetrabutyl-ammonium-fluoride (TBAF). The free acetylene porphyrin **41** was obtained in 98 % yield without any purification as a violet solid. As described in section 3.3 it is possible to first introduce a zinc(II) atom to the center of the macrocycle and finally deprotect the TMS masked acetylene using TBAF to obtain the free acetylene zinc(II)porphyrin **36** in quantitative yield over two reaction steps.

Having the ethynyl building blocks (**36** and **41**) we investigated the assembly of oligo porphyrin systems using Sonogashira cross-coupling reaction conditions as shown in Table 5.

Table 5. Reaction conditions of the copper-free Sonogashira type cross-coupling reaction.¹⁰⁹



Central unit	M	m (equiv. 5)	Yield [%] ^[a]	Product	n
 45	Zn	2.3	56	10	2
 46	Zn	3.5	35	11	3
 47	Zn	4.25	51	8	4
 48	2H	4.25	60	9	4

[a] all yields are isolated yields

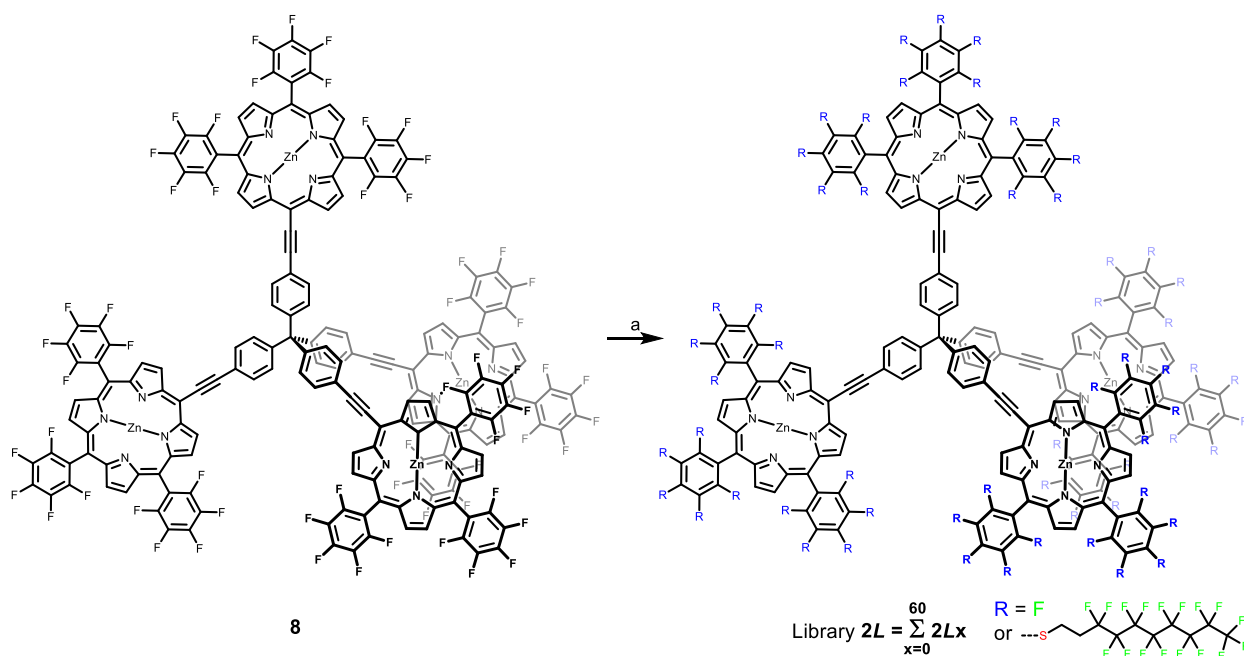
Using classical Sonogashira cross-coupling conditions, with the addition of a catalytic amount of copper iodide, we obtained up to 50 % of the homocoupled diacetylene porphyrin. This not only reduced the yield of the cross-coupling reaction, but also it was extremely

challenging to separate to homocoupled product from the desired products by column chromatography due to similar polarities. Using a protocol developed by Achelle *et al.* we performed the reaction under copper-free cross-coupling conditions and the homocoupled product was no longer observed.¹¹⁷ To investigate the synthesis of oligo porphyrin-systems **10** to **8** the zinc precursor **36** was used. Interestingly the more planar penta-porphyrin system **9** was more stable under strong basic conditions as later described for the nucleophilic aromatic substitution reaction and therefore used as the zinc-free porphyrin system. The oligo-porphyrin systems were obtained in yields between 35 and 60 % after purification by column chromatography. The purity and structure of the obtained oligo-porphyrin systems was proven using ¹H- and ¹⁹F-NMR spectroscopy and high-resolution mass spectrometry. The obtained compounds expose between 30 and 60 fluorine atoms as possible binding positions in nucleophilic aromatic substitution reactions. Therefore these are ideal compounds for synthesis of molecular libraries bearing a various number of fluoroalkylsulfanyl side-chains. These libraries are no longer monodisperse compounds and therefore the molecular structures described in Table 5 are the last well-defined and characterized compounds.

For further investigations and the synthesis of molecular libraries, we focused on the porphyrin-tetramer **8** and the porphyrin-pentamer **9** exposing a number of 60 fluorine atoms at the peripheral pentafluorophenyl-rings. Introduction of the fluoroalkylsulfanyl side-chains was done using commercially available *1H,1H,2H,2H*-perfluorodecanethiol as the nucleophile under basic conditions. Substitution at porphyrin-tetramer **8** was done using 120 equivalents of the thiol and 120 equivalents of potassium carbonate as base. The reaction was heated to 90 °C for 18 h in dimethylformamide (DMF). After aqueous workup and extraction, using *tert*-butyl methyl ether (TBME), the solution was filtered through a short silica plug. The introduction of the fluoroalkylsulfanyl side-chains not only increases the molecular mass of the obtained library but also decreases the Van der Waals interactions between the molecules within the library. The first library **2L_x** obtained from porphyrin-tetramer **8** was analyzed using MALDI-TOF mass spectrometry. As detailed in Table 6, the most abundant number *x* is found to be 18 with a molecular mass 12'230 g/mol. The individual members of the library ranged from *x* equals 15 to 22 and corresponding masses of 10'895 to 14'073 g/mol. The library **2L_x** is composed as expected only with well-defined individual members having a mass difference $\Delta_m = m(\text{C}_{10}\text{H}_6\text{F}_{17}\text{S}) - m(\text{F}) = 479 - 19 = 460$. Within the signal, an exact number *x* of fluorine atoms is substituted by a fluoroalkylsulfanyl side-chain. The introduction of the fluoroalkylsulfanyl

side-chains is to some extent random since within the same mass signal several structural isomers can be obtained. In earlier studies, we found that the *para*-position of the peripheral pentafluorophenyl rings is substituted first. Already the smallest member of library **2Lx** all twelve *para*-positions are substituted. This behavior was proven using ^{19}F -NMR spectroscopy.

Table 6. Nucleophilic aromatic substitution reaction at porphyrin-tetramer **8** to obtain porphyrin library **2Lx** with x being the number of alkylthiol substituents which have replaced a fluorine atom.^{[a]109}



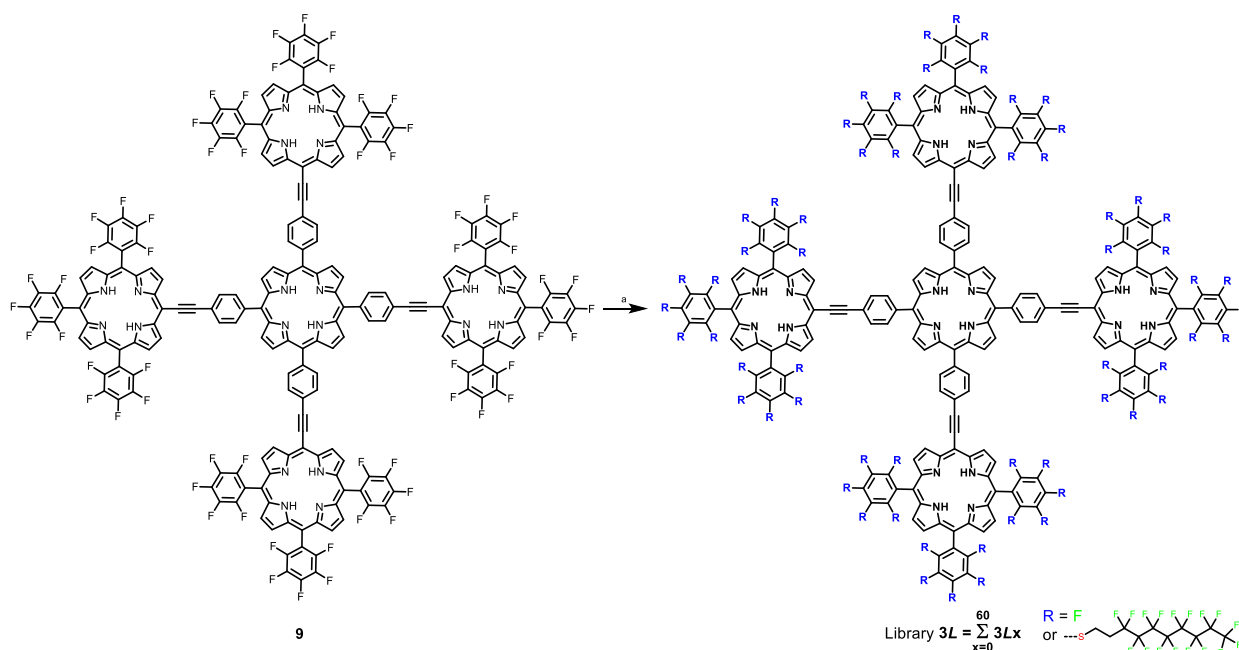
2Lx	x (number of $-\text{S}(\text{CH}_2)_2\text{C}_8\text{F}_{17}$)	Number of F-atoms (= 60-x)	Mass [g/mol]	Calc. Mass [g/mol]	Rel. intensity [%]
2L₁₅	15	45	10'895	10'790	8
2L₁₆	16	44	11'288	11'250	54
2L₁₇	17	43	11'785	11'711	94
2L₁₈	18	42	12'230	12'171	100
2L₁₉	19	41	12'668	12'631	68
2L₂₀	20	40	13'153	13'091	38
2L₂₁	21	39	13'620	13'551	17
2L₂₂	22	38	14'073	14'012	5

[a] The members of the library have the elemental formula $\text{C}_{185}\text{H}_{48}\text{F}_{20-x}\text{N}_{16}\text{Zn}_4(\text{S}(\text{CH}_2)_2\text{C}_8\text{F}_{17})_x$ with $x = 15$ to 22 and the most abundant member (**2L₁₈**) has $x = 18$ (12'230 g/mol). Reagents and conditions: (a) 120 equiv. *1H,1H,2H,2H*-perfluorodecanethiol, 120 equiv. K_2CO_3 , DMF, 90 °C, 18 h.

Introduction of the fluoroalkylsulfanyl side-chains to porphyrin-pentamer **9** was performed under similar conditions as described above for library **2Lx**. Using of 300 equivalents of

1H,1H,2H,2H-perfluorodecanethiol as nucleophile and 300 equivalents of potassium carbonate as base. After the same workup procedure as previously described library **3Lx** was obtained with *x* (number fluoroalkylsulfanyl side-chains) varying between 35 and 43. The largest intensity was obtained for an *x* being 40 and a mass of 22'454 g/mol. As described before the introduction of the side-chains is to some extent random and only the substitution of the *para*-position can be proven by ¹⁹F-NMR spectrometry.

Table 7. Nucleophilic aromatic substitution reaction at porphyrin-pentamer **9** to obtain porphyrin library **3Lx** with *x* being the number of alkylthiol substituents which have replaced a fluorine atom.^{[a]109}



3Lx	x (number of -S(CH ₂) ₂ C ₈ F ₁₇)	Number of F-atoms (= 60-x)	Mass [g/mol]	Calc. Mass [g/mol]	Rel. intensity [%]
3L₃₅	35	25	20'121	20'041	6
3L₃₆	36	24	20'588	20'501	26
3L₃₇	37	23	21'061	20'961	50
3L₃₈	38	22	21'514	21'421	78
3L₃₉	39	21	21'983	21'881	89
3L₄₀	40	20	22'454	22'341	100
3L₄₁	41	19	22'931	22'801	62
3L₄₂	42	18	23'404	23'261	24
3L₄₃	43	17	23'878	23'722	5

[a] The members of the library have the elemental formula C₂₀₄H₆₆F_{60-x}N₂₀(S(CH₂)₂C₈F₁₇)_x with *x* = 35 to 43 and the most abundant member (**3L₄₀**) has *x* = 40 (22'454 g/mol). Reagents and conditions: (a) a) 300 equiv. *1H,1H,2H,2H*-perfluorodecanethiol, 300 equiv. K₂CO₃, DMF, 90 °C, 24 h.

The larger number of substituents in library **3Lx** compared with the library **2Lx** is mostly because a larger amount of thiol (300 equivalents compared to 120 equivalents) has been used. Another important impact can be attributed to higher planarity and conjugation of porphyrin-pentamer library **3Lx**, this should move the pentafluorophenyl rings and with them the fluorine atoms further away from each other.

Both libraries have been investigated using MALDI-TOF mass spectrometry; the results are detailed in Table 6 and Table 7. The entire spectra of porphyrin-tetramer library **2Lx** shown in Figure 40 show the perfect separation of the individual members within the library and masses between 10'000 and 15'000 g/mol. The mass difference between two peaks fits exactly the mass added when one fluoroalkylsulfanyl side-chains substitutes one fluorine atom (460 ± 10 g/mol).

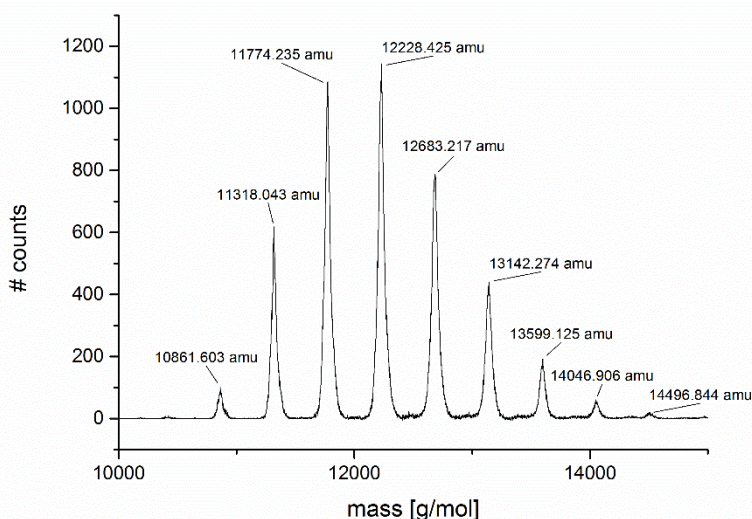


Figure 40. MALDI-ToF analysis of library **2Lx** bearing 15 to 22 perfluoroalkyl side-chains ($x = 15$ to 22). The masses range between 10'000 and 15'000 g/mol and a maximum of $x = 18$ (12'228 g/mol) was obtained. The spectrum was calibrated using CsI_3 clusters.¹¹⁸ DCTB (trans-2-[3-(4-tert-Butylphenyl)-2-methyl-2-propenylidene]malononitrile) was used as a matrix.¹¹⁹ The spectrum was integrated over 2000 shots.¹⁰⁹

In both spectra (Figure 40 and Figure 41), the strongest signal has been labeled. The broadening of the peak is attributed to the presence of a large number of isotopes within both libraries. Furthermore signals of the individual members within the libraries are broadened by the presence of $[\text{M}]^+$ and $[\text{M}+\text{H}]^+$ species. It was very interesting to see that molecular library **3Lx** shown in Figure 41 has better ionization properties compared to molecular library **2Lx**. We attribute this fact to the absence of the zinc atom in the porphyrin macrocycles in library **3Lx**. We observed already good ionization properties of metal free porphyrin-monomers within

preliminary experiments. The MALDI-TOF mass spectrum of library **3Lx** shown in Figure 41 shows the well-separated signals of the individual members within the molecular library. The largest intensity signal was obtained for **3L40** as detailed in Table 7.

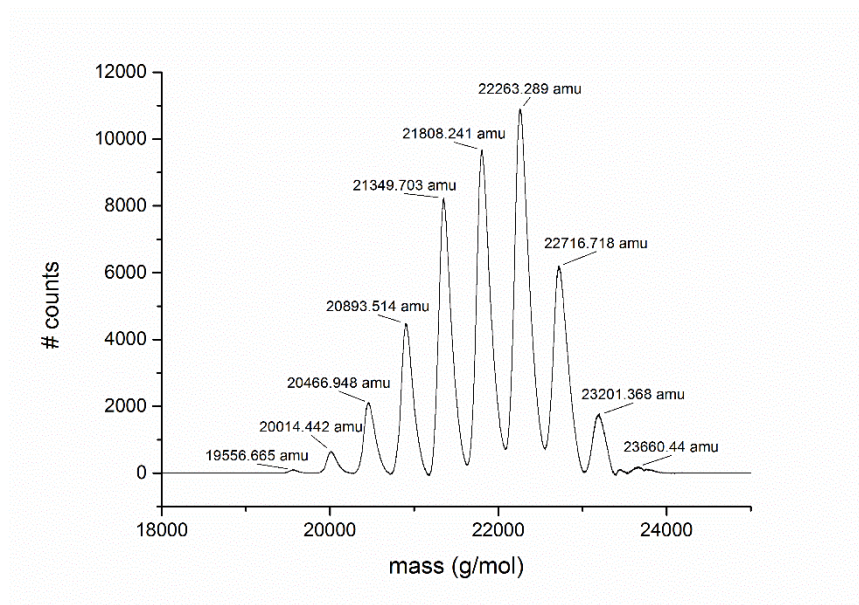
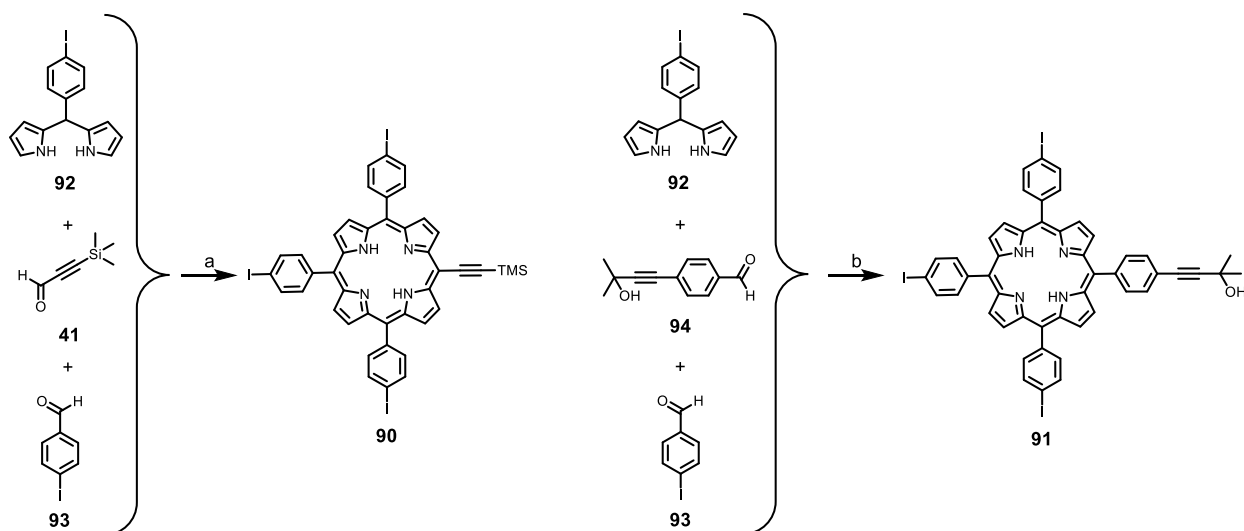


Figure 41. MALDI-ToF analysis library **3Lx** bearing 35 to 43 perfluoroalkyl side-chains ($x = 35$ to 43). The mass range is between 19'000 and 24'000 g/mol and maximum of $x = 40$ (22'263 g/mol) was obtained. Spectra was calibrated using CsI_3 cluster.¹¹⁸ DCTB was used as matrix.¹¹⁹ The number of counts was obtained by integration over 2000 shots.¹⁰⁹

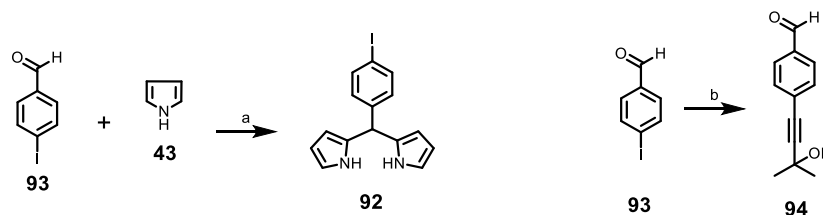
With both molecular libraries in hand, we investigated the possibilities to produce a sufficiently strong molecular beam. These investigations are shown and described in section 4.3.

To further increase the mass and size of particles that produce slow and neutral molecular beams, we wanted to investigate even larger porphyrin-systems. We planned to use a modification of the approach described above. First attempts in this direction started using novel designed unsymmetrical porphyrin monomers as shown in Scheme 24. Central unit **90** was obtained in only 2 % yield using similar conditions as described in section 3.3.



Scheme 24. Synthesis of unsymmetrical porphyrin-systems **90** and **91**. Reagents and conditions: (a) borontrifluoride diethyletherate, chloroform, room temperature, 18 h, then DDQ, room temperature, 2 h. 2 %; (b) borontrifluoride diethyletherate, chloroform, room temperature, 18 h, then DDQ, room temperature, 2 h. 3 %.

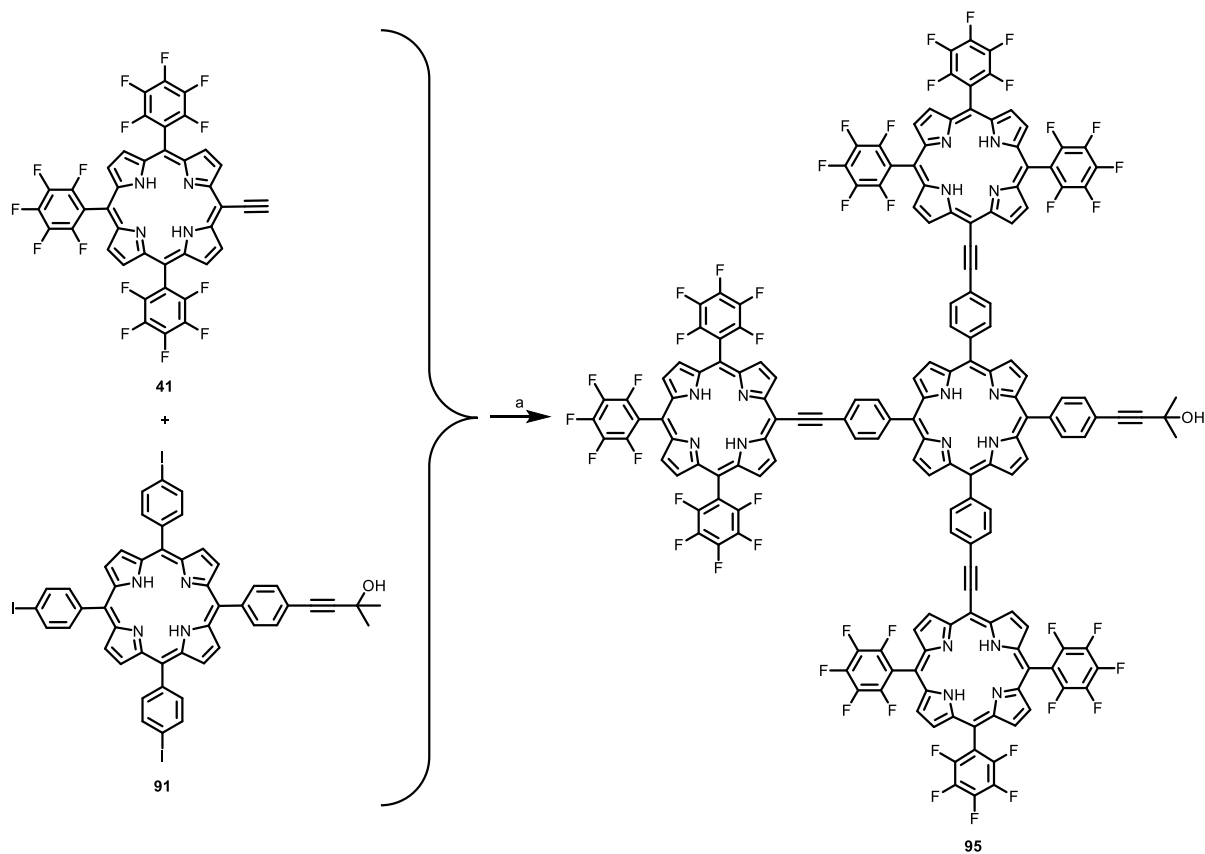
The building-block **91** shown in Scheme 24 was obtained under similar conditions in only 3 % yield. These conditions need to be improved in order to make such model compounds available for QIEs. Dipyrromethane **92** can be obtained from pyrrole (**43**) and the corresponding 4-iodobenzaldehyde (**93**) under acidic conditions following a synthetic pathway developed by Lindsey *et al.* in 65 % yield as a colorless solid.⁸⁴ The synthesis of dipyrromethane **92** is schematically represented in Scheme 25 as well as the synthesis of 4-(3-hydroxy-3-methylbut-1-yn-1-yl)benzaldehyde (**94**). The masked acetylene **94** can be obtained in a Sonogashira cross-coupling reaction using 2-methyl-3-buten-2-ol to introduce the protecting group to 4-iodobenzaldehyde (**93**) in 98 % yield.



Scheme 25. Schematic representation of the synthesis of iododipyrromethane **92** and 4-(3-hydroxy-3-methylbut-1-yn-1-yl)benzaldehyde (**94**). Reagents and conditions: (a) trifluoroacetic acid, room temperature, 30 min, 65 %; (b) 2-methyl-3-buten-2-ol, Pd(PPh₃)₄, CuI, TEA, room temperature, 30 min, 98 %.

The following copper-free Sonogashira cross-coupling reaction of building block **91** and unsymmetrical porphyrin-monomer **41** was performed under conditions described in section 4.2.

We were able to obtain porphyrin tetramer **95** in 40 % yield after purification by column chromatography on silica and size exclusion chromatography.



Scheme 26. Synthesis of porphyrin-tetramer **95**. Reagents and conditions: (a) $\text{Pd}_2(\text{dba})_3$, triphenylarsine, TEA/THF, reflux, 18 h, 40 %.

In further steps we will try to deprotect the porphyrin tetramer **95** and bind four of the deprotected porphyrin tetramers **95** to a central *meso*-tetrakis(4-iodophenyl)porphyrin (**48**) under copper-free cross-coupling conditions. The progress in the synthesis of large porphyrin-systems would finally allow us to build up a system with 17 individual porphyrins having 180 possible binding positions for fluoroalkylsulfanyl side-chains. This would allow us to access even heavier oligo-porphyrins that can be used in QIE.

4.3 Desorption Experiments

The production of sufficiently strong molecular beams is crucial for QIE in the near-field regime. It is very important not only to obtain strong molecular beams, but also the beams have to be slow and neutral. To launch massive particles several methods have been developed for mass spectrometry, such as electrospray ionization (ESI) and matrix-assisted laser desorption ionization (MALDI).^{94,120} These techniques have been used to launch high molecular mass particles using MALDI.¹²¹ The use of ESI to launch neutral particles is not possible, since ESI usually produces highly charged ions. MALDI has the advantage that the experiment operates under high vacuum, and a molecular beam carrying none or only a few charges is produced.¹²² Matrix molecules, such as dihydroxybenzoic acid, are mostly used to in MALDI experiments to enhance the absorption of the desorption UV-laser. This helps to produce a molecular beam and to charge the analytes. The specially designed molecular libraries **2Lx** and **3Lx** can act as their own matrix, since the libraries are sufficiently absorptive and photostable. The main feature apart from the launch of uncharged particles, the particles are by one order of magnitude slower compared to the used of matrix.^{123,124} In the experimental setup designed by the Arndt group represented in Figure 42 a stainless steel sample plate was used, where the analyte was deposited, using droplets of analyte in solution. No matrix was used to launch the particles by a pulsed N₂ laser beam.

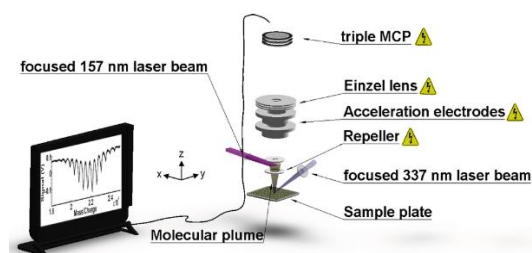


Figure 42. Experimental setup of the short-pulse laser desorption and post-ionization. We used a focused 337 nm short-pulsed laser beam to launch the particles. The post-ionization is done using a 157 nm laser. The produced cations are finally detected by a time of flight mass spectrometer (TOF-MS).¹²⁵

The launched particles were then post-ionized in a distance of 39 mm from the sample plate using a vacuum ultra violet (VUV) light of an F₂ excimer laser beam. Up to now, photoionization was limited to particles below 2000 g/mol and known for clusters of biomolecules up to 7000 g/mol.^{126–130} Detection of the particles after photoionization was done using a time of flight mass spectrometer (TOF-MS).

The post-ionization mass spectra of both libraries are shown in Figure 43. The spectrum of molecular library **2Lx** shown in Figure 43a consists of members varying from $x = 14$ to 21. These signals are well defined with a periodicity of 460 ± 10 g/mol (distance to the neighboring peak). A mean signal was found for $x = 17$ and a mass of 13'492 g/mol. The mass varies between 10'000 and 14'000 g/mol. The post-ionization mass spectrum found for library **2Lx** agrees well with the MALDI spectrum shown in Figure 40 and detailed in Table 6.

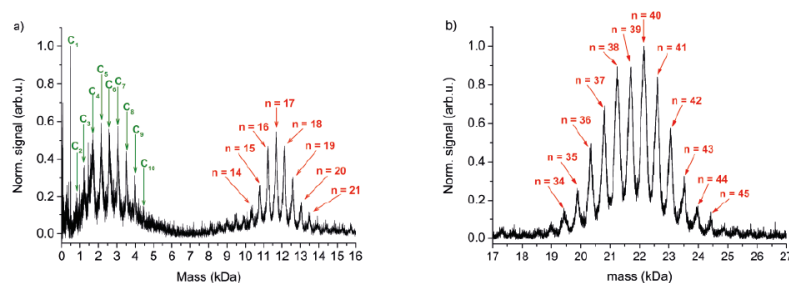


Figure 43. Mass spectra of libraries **2Lx** (a) and **3Lx** (b) after post-ionization. (a) The most abundant peak was found at $x = 17$ and a mass of 11'676 g/mol. (b) The highest intensity signals was found at $x = 40$ and a mass of 22'152 g/mol. In this molecular library, we observed library members having masses beyond 25'000 g/mol.¹²⁵

The post-ionization mass spectrum found for library **3Lx** shown in Figure 43b consists of peaks with similar periodicity as described above for library **2Lx**. The detected post-ionization mass spectrum showed signals for individual members of the library between $x = 34$ and 45 with small peaks up to $x = 50$. Masses varied between 19'000 g/mol and 24'000 g/mol. In addition, it was possible to resolve weak peaks up to 25'000 g/mol. The most intense peak was found for $x = 40$ and a mass of 22'152 g/mol.

To investigate the velocities of the particles launched we varied the time delay between desorption laser and VUV post-ionization laser. Figure 44 shows the time delay versus the counted number of molecules, which have been detected by the post-ionization laser.

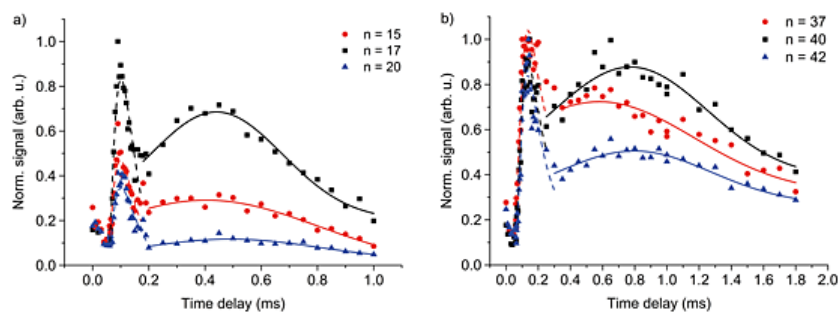


Figure 44. Time delay between desorption laser and VUV post-ionization laser for prominent members of library **2Lx** (a) and **3Lx** (b). The molecules counted with the TOF-MS are shown with respect to the delay time. A delay time of 1.00 ms equals to 39 m/s.¹²⁵

In order to be able to investigate the molecular libraries in QIE, we need to obtain particle beams with a velocity of less than 40 m/s (this equals a delay time of 1.00 ms). In both Figure 44a and Figure 44b the fast part of the velocity distribution best fitted a Maxwell-Boltzmann distribution (dashed lines). This part is attributed to ions that are created in the source. The neutral part of the distribution fitted best a Gaussian distribution (continuous lines). For library **2Lx** we found the center of the distribution around 90 m/s but still substantial signal can be found for particles with velocities around 40 m/s (delay time around 0.50 m/s). In the higher mass library **3Lx** (Figure 44b) we found a similar distribution centered at slightly lower velocities. The center of the distribution can be found at 45 m/s and 20 m/s, where still substantial signals can be found.

Finally, we wanted to prove the ionization properties of the molecular beams produced by the desorption laser. Figure 45 shows the ionization laser energy applied to the particle beam of library **2Lx** (a) and library **3Lx** (b) versus the signal detected by the TOF-MS.

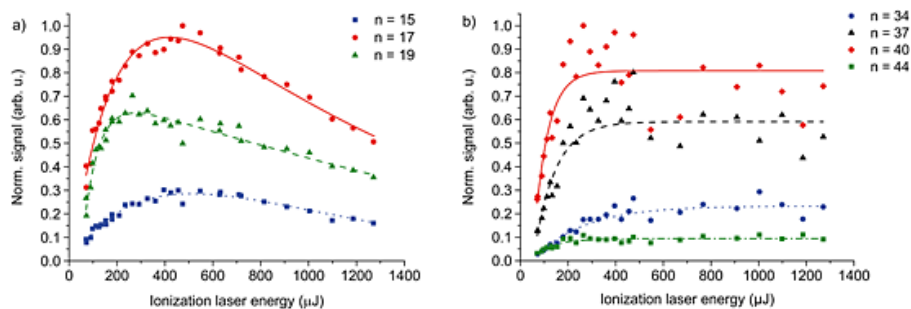


Figure 45. The ionization laser energy is shown versus the photoionization signal detected by the TOF-MS for library **2Lx** (a) and **3Lx** (b). The different colored points indicate a different number of fluoroalkylsulfanyl side-chains attached to the tetra-porphyrin- and penta-porphyrin-core. The lines with the same colors are represented to guide the eye. The signals were taken after delay times of 0.4 ms (library **2Lx**) and 0.8 ms (library **3Lx**) between desorption laser pulse and post-ionization.¹²⁵

As shown in Figure 45, we used for both libraries selected members to vary the ionization energy and detected their signal with a TOF-MS. As expected, an augmented ion yield up to the saturation point was obtained using the ionization laser energy. We found it very interesting that the signal decreases with higher energy for library **2Lx** (a) but stays constant for library **3Lx** (b). We attribute the signal decrease (a) to photoinduced fragmentation and the constant signal (b) to higher stability of the molecules. The molecular beam of library **3Lx** gives the impression to be very stable due to a larger number of fluoroalkylsulfanyl side-chains attached to the periphery of the penta-porphyrin system.

4.4 Conclusion

Within section 4 we present the synthesis of four different oligo-porphyrin systems. The dimer **10** and the trimer **11** have been synthesized to prove the modularity and to optimize the conditions of the copper-free cross-coupling reaction using commercially available central units and the ethynyl porphyrin **36**. We were able to synthesize the dimer **10** in 56 % yield and the trimer in 35 % yield. To be able to access larger molecular libraries then described for the 1st generation porphyrin-systems in section 3 we synthesized a porphyrin-tetramer **8** using a tetrahedral central unit in 51 % yield. Using similar conditions, we were also able to synthesize a porphyrin-pentamer **9** in an excellent yield of 60 % from a tetraiodo-porphyrin **48**. Attaching fluoroalkylsulfanyl side-chains to the tetramer **8** we obtained a molecular library **2Lx** with well-defined mass signals for the individual members between 10'895 and 14'073 g/mol whereby the number of side-chains varied between $x = 15$ and $x = 22$. In this molecular library **2Lx**, 38 to 45 fluorine atoms as potential positions for nucleophilic aromatic substitution reactions remained unsubstituted. The most intense signal was obtained for **2L18** having a mass of 12'230 g/mol and a number of 18 fluoroalkylsulfanyl side-chains. Using porphyrin-pentamer **9** in a nucleophilic aromatic substitution reaction to introduce fluoroalkylsulfanyl side-chains to the peripheral pentafluorophenyl rings, we were able to obtain a molecular library **3Lx** with masses between 20'121 and 23'878 g/mol whereby the number of side-chains varied between $x = 35$ and $x = 43$. The most intense signal was obtained for **3L40** having a mass of 22'454 g/mol and a number of 40 fluoroalkylsulfanyl side-chains. It might be possible to synthesize larger oligo-porphyrin systems but remains synthetically very challenging.

Desorption experiments with both libraries have been performed showing that we are able to produce slow, neutral and mass-selected molecular beams. Both molecular libraries are sufficiently stable to remain intact during laser heating photoionization that is followed by mass spectrometry. The large molecular library **3Lx** containing individual members with masses up to nearly 25'000 g/mol can be neutrally desorbed with velocities as low as 20 m/s. This is one of the main facts that both libraries are potential candidates for new mass records in QIE. Comparing the two libraries, more planar and stronger conjugated library **3Lx** showed better beam and detection properties compared to library **2Lx**. We hypothetically attribute this future to the better ionization properties of conjugated library **3Lx**. In section 6, further experiments and applications are described.

5 Photocleavable Tags

In the previous chapters, the focus was mainly set on the production of sufficiently strong molecular beams. In this chapter, we want to focus on a novel detection method. When going to larger and larger particles it will be more and more difficult to distinguish between the molecules that hit a laser grating and the molecules that interfered in QIE. One of the newly designed experimental quantum interference setups is an optical time-domain ionizing matter-wave (OTIMA) interferometer.^{131–133} The molecular beam is diffracted at three pulsed laser gratings. If photocleavable tags are attached to large molecules, nanoparticles, biomolecules, or proteins it might be possible to cleave them when they are hit by the pulsed laser gratings. The intact molecules passing the interferometer would interfere at the pulsed laser grating and can be detected using a time of flight (TOF) mass spectrometer.

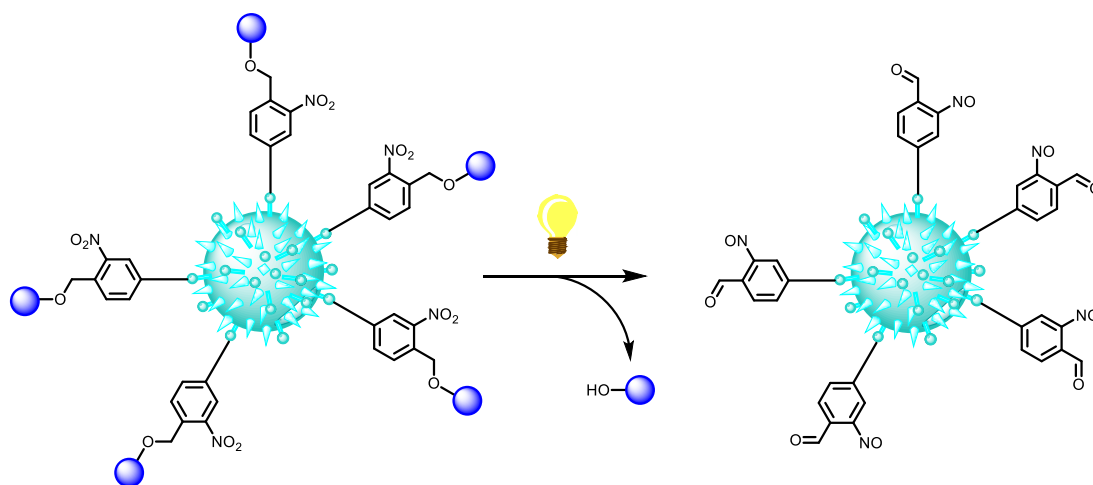


Figure 46. Schematic representation of the cleaving process of a photocleavable tag (dark blue) attached to a virus (light blue).

Cleavage of the tags in the interferometer allows detection of the particles that have been interfering at the three pulsed laser gratings only. The molecules arriving at the detector level without the photocleavable tags can be sorted out by mass spectrometry. This would make it possible to select to detect only the desired molecules of a certain molecular mass.

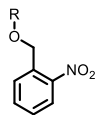


Figure 47. 2-Nitrobenzyl-group. Cleavage is done between the benzylic carbon and the oxygen originating from an alcohol.

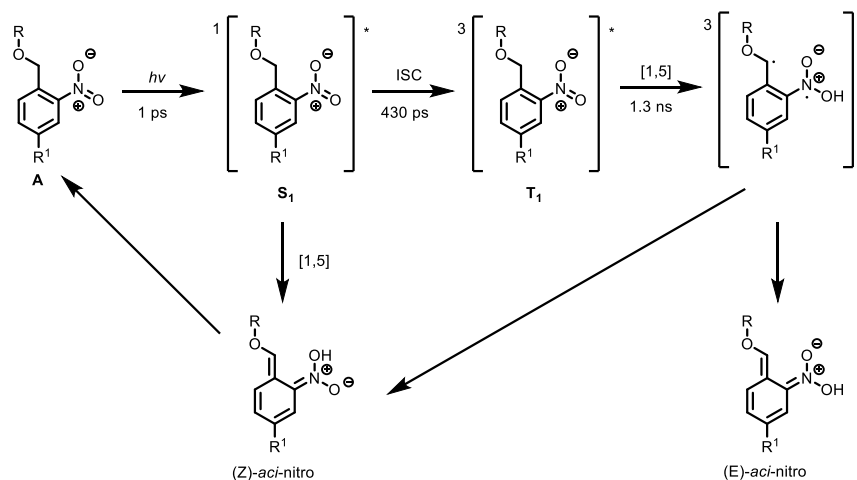
A large number of photocleavable groups is known in literature. Klán *et al.* give a nice overview of all the possibilities in their review.¹³⁴ As schematically represented in Figure 46 and Figure 47 a 2-nitrobenzyl group is proposed to fit all the requirements. The 2-nitrobenzyl group can easily be handled within the synthetic approach. Cleavage is possible under very mild conditions.^{135,136} The process and mechanism of the photocleavage is outlined in section 5.1.

5.1 Photocleavable Protection Groups

In order to explore higher masses in interference experiments a main requirement is the production of new tailor-made molecules or particles as first test systems for photocleavable experiments. A future aim is to investigate even large molecular clusters or biomolecules. In the interferometer, one would need a softer source, keeping the particles intact while launching them, and a different way of detection. The suggestion is to use photocleavable groups, which can be split off by a laser in the interferometer, and only the intact molecules are ionized and detected. This would facilitate the mass selection enormously.

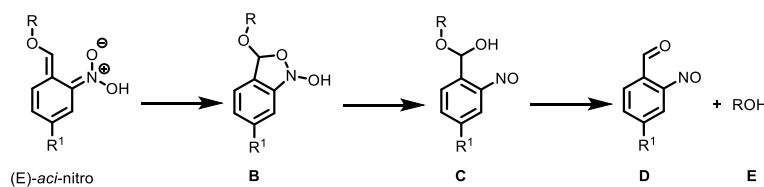
In literature, a large number of photocleavable groups is described. A nice overview can be found in a review by Klán *et al.*¹³⁴ The photocleavable protection groups were invented as a substitute to classical protection groups, since the photocleavage can be done very efficiently under mild conditions. Tracking of the cleavage was done by the split of fluorescent quenching tags, the changes in UV/Vis absorbance and by the variation of retention times in HPLC.^{137–139} In addition, photoremovable protection groups were used in combination with RNA.¹⁴⁰ Within this work only nitro-aryl groups protecting alcohols are discussed, since they are easily accessible.¹⁴¹

The use of nitro-aryl protection groups for alcohols are widely used and are known since 1970.^{142,143} In our specific case, we need to break the bond between the tag and the cluster or biomolecule that we want to investigate with quantum interference. Therefore, in Scheme 27 two different residuals (R and R¹) are mentioned. The cleaving is done at the bridging element between the tag and the investigated particle.



Scheme 27. Photocleavage pathway of benzyl-ester **A** towards the (E)-*aci*-nitro derivative. R being the cleavable tag and R¹ being the particle investigated by QIE. The scheme is adapted from reference¹³⁴.

Upon exposing photocleavable bridge **A** to UV-light, cleavage of the bond is obtained mainly due to the production of (E)-*aci*-nitro compound shown in Scheme 27.¹⁴⁴ Upon irradiation, the first excited singlet state (**S**₁) is obtained. Via intersystem crossing (ISC) the triplet state (**T**₁) is produced, which can undergo a [1,5] proton exchange to finally form the (E)-*aci*-nitro or the (Z)-*aci*-nitro. Fortunately, the decay of (E)-*aci*-nitro (shown in Scheme 28) is much faster than the production and back-reaction of (Z)-*aci*-nitro to the starting molecule.¹³⁶ This pushes the equilibrium towards the desired decay shown in Scheme 28 and reduces the back-reaction towards **A**.



Scheme 28. Decay of the (E)-*aci*-nitro to the nitroso-aldehyde **D** and the corresponding alcohol **E**.¹³⁵

In the decay of (E)-*aci*-nitro shown in Scheme 28 first a ring closing occurs, this is the irreversible step in this pathway. The rate-determining step of the reaction pathway is the ring opening from **B** towards the nitroso-compound **C**. In the last step of the decay the alcohol **E** is released and the corresponding nitroso-aldehyde **D** is formed. The formation of stable alcohols would also enhance the reaction-speed. Cleavage of this protection group can be done at wavelengths ≥ 370 nm and can be followed using time resolved UV/Vis-spectroscopy.¹⁴¹ This

specific cleavage is pH dependent. In the interferometer, cleavage is performed in gas-phase, and the pH cannot be controlled.

To the best of our knowledge, protecting groups that can be photo-cleaved in the gas-phase have not been reported yet. Therefore, it would be extraordinarily interesting to attach these bridging units first to test-systems and further on to biomolecules or clusters.

5.2 Molecular Design

As shortly described in the introduction of this chapter we are interested in the introduction of a 2-nitrobenzyl group as the cleavable part within a photocleavable tag. In Figure 48, we schematically represent the design of the molecule. The green part represents the photocleavable part, red is the tag that can be split off and the blue part is the molecule of interest for QIE.

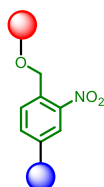


Figure 48. Representation of the photocleavable part (green) merged between the cleavable part (red) and the molecule of interest (blue).

The red part of schematically representation of the molecular design in Figure 48 is proposed to be cleaved off during the QIE if one of the three pulsed laser gratings hits the molecule. If the molecule is interfering and therefore not hit by the laser, it should finally be ionized. Due to these facts, we planned to introduce fluorinated groups as the cleavable part. According to our knowledge from other QIE, fluorinated groups would allow to produce a sufficiently strong molecular beam. In addition, it would be possible to attach molecules that enable the detection of the intact molecules by photo-ionization or two photon absorbance and mass spectrometry. In a first step, we want to prove the concept of cleavage of the red tag in gas phase. As represented in Figure 49 our first target molecule **12** contains a tetraphenylmethane center (blue) to which four cleavable groups (green) and four fluorinated tags (red) can be attached. The basis of this idea is that it might be possible to cleave the tags of the molecule more rapidly with four groups.

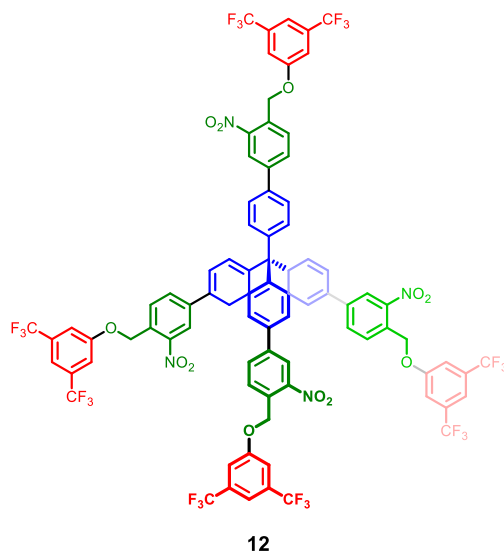
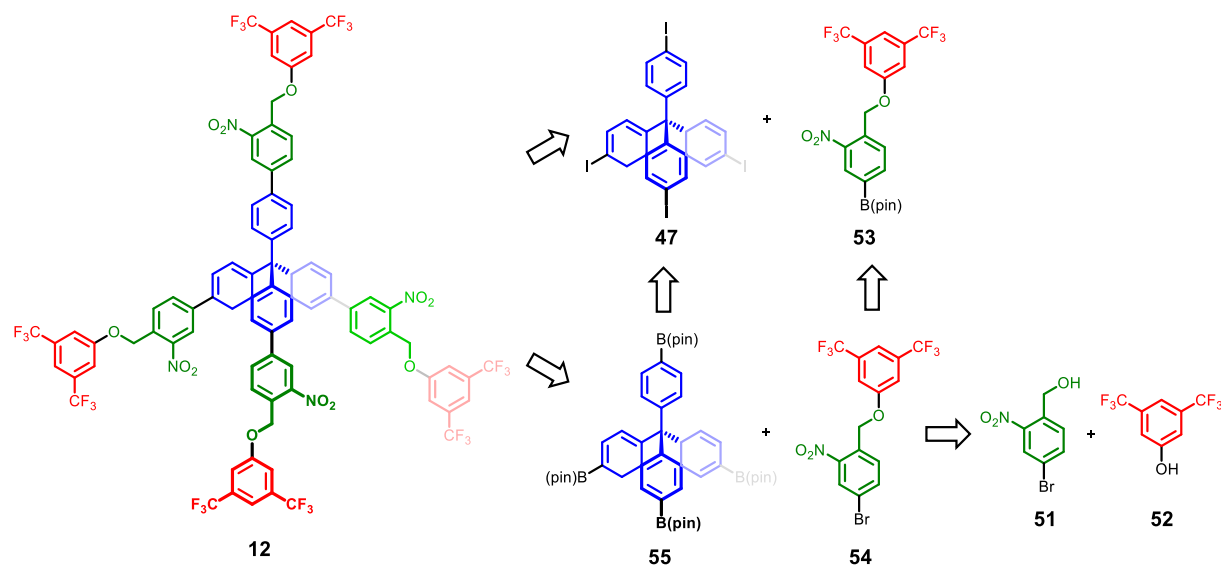


Figure 49. First target molecule **12** having a tetrahedral arrangement of the cleavable parts (green) and the tags (red) around a tetraphenylmethane central unit (blue).

Retrosynthetically it will be possible to synthesize this target molecule in two different ways. Both ways are shown in Scheme 29.



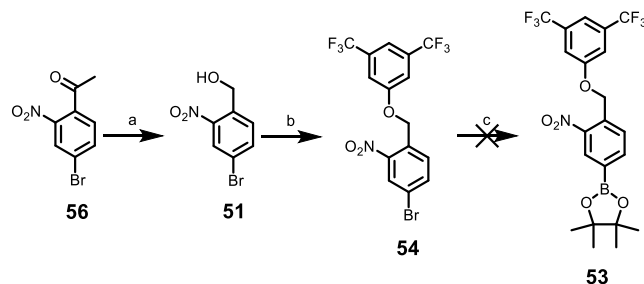
Scheme 29. Retrosynthetic analysis of target molecule **12** in a Suzuki cross-coupling reaction and a Mitsunobu reaction from (4-bromo-2-nitrophenyl)methanol (**51**) and 3,5-bis(trifluoromethyl)phenol (**52**).

The first approach in the upper part of Scheme 29 is the Suzuki cross-coupling reaction between tetrakis(4-iodophenyl)methane (**47**), which synthesis is described in section 4.2, and boronate **53**.^{145–147} This pinacol ester **53** can be obtained in a Myaura cross-coupling reaction using bis(pinacolato)diboron from bromine derivative **54**.¹⁴⁸ The second approach is the Suzuki

cross-coupling reaction between the pinacol ester compound **55** directly with bromine derivative **54**. Boronate **55** can be obtained in a Miyaura borylation from tetrakis(4-iodophenyl)methane (**47**). The photocleavable link between the green and the red part within compound **54** can be build up in a Mitsunobu reaction starting from (4-bromo-2-nitrophenyl)methanol (**51**) and 3,5-bis(trifluoromethyl)phenol (**52**).^{149–151} We suggested the 3,5-bis(trifluoromethyl)phenol (**52**) bearing two CF₃-groups being an ideal test system for first investigations. Using the above-described Mitsunobu conditions, it should be possible to attach other fluorinated phenol systems to the benzylic alcohol **51**. (4-Bromo-2-nitrophenyl)methanol (**51**) can be synthesized from the corresponding aldehyde **56** as described by Lemasson *et al.*¹⁴⁹

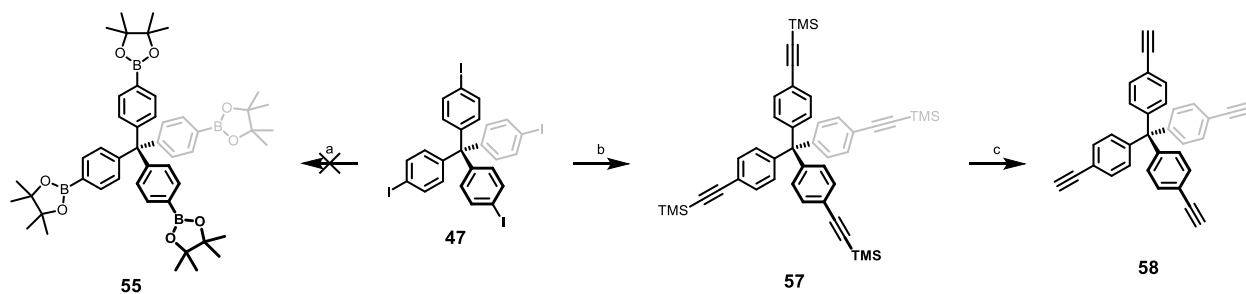
5.3 Syntheses and Characterization

Starting the syntheses towards target photocleavable compound **12** bearing four peripheral tags that can be cleaved using UV-light, we used commercially available 1-(4-bromo-2-nitrophenyl)ethan-1-one (**56**). Reduction of the aldehyde **56** to the benzylic alcohol **51** was done using sodium borohydride at room temperature. After purification by column chromatography the desired product **51** was obtained in quantitative yield as a colorless solid. The next step shown in Scheme 29 is the Mitsunobu reaction introducing 3,5-bis(trifluoromethyl)phenol (**52**) to the benzylic alcohol **51**. Dissolving the benzylic alcohol **51**, the aryl alcohol **52** and triphenylphosphine in THF. We used an ice bath the reaction to cool the reaction mixture to 0 °C and diisopropyl azodicarboxylate (DIAD) was added dropwise. After stirring the reaction for 12 h in the absence of light, we obtained the desired ether bridged molecule **54** in 96 % yield.



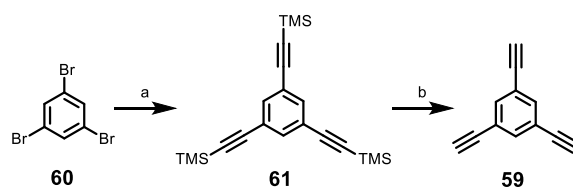
Scheme 30. Synthetic pathway towards pinacol ester **53**. Reagents and conditions: (a) NaBH₄, THF, 30 min, room temperature, quant.; (b) 3,5-bis(trifluoromethyl)phenol (**52**), DIAD, triphenylphosphine, THF, 12 h, room temperature, 96 %; (c) bis(pinacolato)diboron, Pd(dppf)Cl₂, KOAc, toluene, 18 h.

Since we already had tetrakis(4-iodophenyl)methane (**47**) in hand we decided first to try to introduce the pinacol ester to the bromine derivative **54**. This was proposed to be done in a Miyaura reaction using Pd(dppf)Cl₂ catalyst, bis(pinacolato)diboron as the source of boron and potassium acetate as the base. The reaction was performed at different temperatures and reaction times but the desired pinacol ester **53** could not be isolated. We attribute this mainly to purification problems. To overcome the problem we tried to modify the central unit **47** as shown in Scheme 31 towards a higher reactivity with bromine derivative **54**.



Scheme 31. Modification of the tetrahedral central unit **47**. Reagents and conditions: (a) bis(pinacolato)diboron, Pd(dppf)Cl₂, KOAc, toluene, 18 h; (b) TMS-acetylene, Pd(PPh₃)₄, CuI, TEA/THF, room temperature, 12 h, 95 %; (c) TBAF (1 M in THF), dichloromethane, room temperature, 30 min, 97 %.

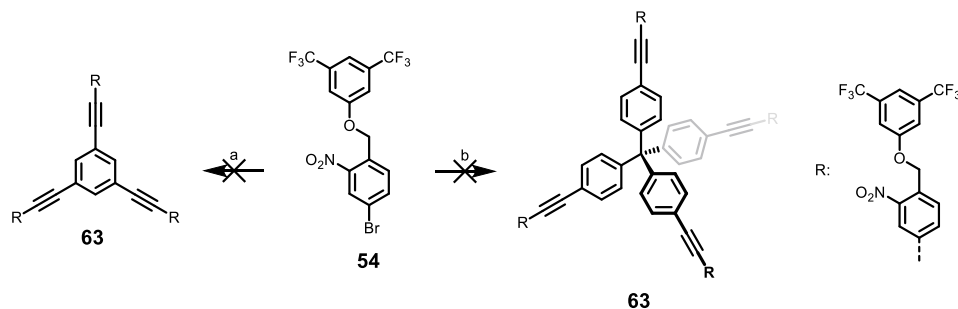
The first modification shown in Scheme 31 was the introduction of pinacol esters in a Miyaura borilation as described above. Unfortunately it was not possible to introduce the pinacol esters to tetrakis(4-iodophenyl)methane (**47**). The central unit **47** was further modified by the introduction of TMS-acetylene in a Sonogashira cross-coupling reaction that we expect to work a lot cleaner at the iodo-compound **47** than the Miyaura borilation. The introduction of the masked acetylene was done using tetrakis(triphenylphosphine) palladium catalyst under the support of copper iodide in a solvent mixture of trimethylamine (also acting as base) and THF at room temperature. The desired product **57** was obtained in 95 % yield. We performed the subsequent deprotection using tetra-butyl-ammonium-fluoride (TBAF) obtaining the free ethynyl tetraeder **58** in 97 % yield as a colorless solid.



Scheme 32. Synthesis of the trimeric central unit **59**. Reagents and conditions: (a) TMS-acetylene, Pd(PPh₃)₄, CuI, TEA, 65 °C, 2 h, quant.; (b) K₂CO₃, THF, MeOH, water, room temperature, 6 h, quant..

Furthermore, we synthesized in a similar pathway the other central unit **59**. The reaction was performed starting from 1,3,5-tribromobenzene (**60**) that was treated with TMS-acetylene in a Sonogashira cross-coupling reaction to obtain the desired product **61**. The subsequent deprotection of the TMS masked acetylene was done using potassium carbonate in methanol, THF and water. The desired triangular free ethynyl benzene central unit **59** was obtained in quantitative yield over the two reaction steps as a colorless solid.

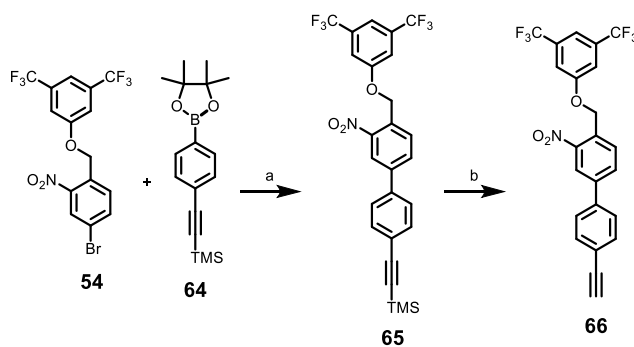
In a next step, we tried to introduce the ether-bridged molecule **54** four and three times to the previously synthesized central units.



Scheme 33. Introduction of the cleavable **54** to the two central units **59** and **58**. Reagents and conditions: (a) **59**, Pd(PPh₃)₄, CuI, TEA, 65 °C; (b) **58**, Pd(PPh₃)₄, CuI, TEA, 65 °C.

Using Sonogashira cross-coupling reaction conditions as shown in Scheme 33 we were not able to obtain the desired molecules having three **62** respectively four **63** photocleavable parts. We could not detect the desired compounds in both cases and the starting material **54** nearly completely recovered.

Facing these problems within the synthetic pathway, we returned to the preliminary idea of modification directly at the benzylic ether derivative **54**. A first attempt was a Suzuki cross-coupling reaction introducing a TMS masked acetylene increasing the distance between the photocleavable tag and the central unit. The desired pinacol ester **64** is commercially available and was used as obtained.



Scheme 34. Suzuki cross-coupling reaction followed by the deprotection of the TMS masked acetylene. Reagents and conditions: (a) Pd(OAc)₂, RuPhos, K₃PO₄, toluene/water (5:1), 50 °C, 12 h, quant.; (b) TBAF (1 M in THF), dichloromethane, room temperature, 30 min, quant..

The reaction conditions of the first Suzuki cross-coupling reaction between bromine compound **54** and boronic ester **64** have been optimized. The optimization steps are detailed in Table 8.

Table 8. Optimization of the Suzuki cross-coupling reaction being the first step of the reactions described in Scheme 34. In all entries one equivalent of bromine derivative **54** and 1.25 equivalents of pinacol ester **64** are used.

Catalyst ^[a]	Base	Solvent	Time [h]	Temp. [°C]	Yield ^[b] [%]
Pd(PPh ₃) ₄	K ₃ PO ₄ (5 equiv.)	toluene/ethanol/water (20:5:1)	12	65	0
Pd(amphos)Cl ₂	K ₂ CO ₃ (5 equiv.)	toluene/water (20:1)	12	100	12
Pd(dppf)Cl ₂	K ₃ PO ₄ (6 equiv.)	THF/ethanol/water (5:10:5)	12	60	traces
Pd(PCy ₃) ₃ Cl ₂	K ₃ PO ₄ (6 equiv.)	toluene/water (5:1)	8	50	72
Pd(OAc) ₂ , XPhos	K ₃ PO ₄ (6 equiv.)	toluene/water (5:1)	8	50	83
Pd(OAc)₂, RuPhos	K₃PO₄ (6 equiv.)	toluene/water (5:1)	8	50	quant.
Pd(OAc) ₂ , SPhos	K ₃ PO ₄ (6 equiv.)	toluene/water (5:1)	8	50	98

[a] 5 mol% of catalyst and 2 mol% of ligand have been used; [b] yields are isolated yields

As described above in Table 8 we started by the use of tetrakis(triphenylphosphine) palladium catalyst and potassium phosphate as base in a solvent mixture of toluene, ethanol and water. We stirred the reaction for twelve hours at 65 °C. Unfortunately, not even traces of product were observed and the starting material was completely recovered. Changing the catalyst to palladium(amphos) or palladium(dppf) only led to 12 % yield or to traces of product respectively. Mostly the starting material could have been recovered. Using of old fashioned tris(cyclohexane)phosphine palladium dichloride catalyst led to a yields of 72 % if the reaction was performed in a solvent mixture of toluene and water using potassium phosphate as base. The structure of the ligand used is shown in Figure 50.

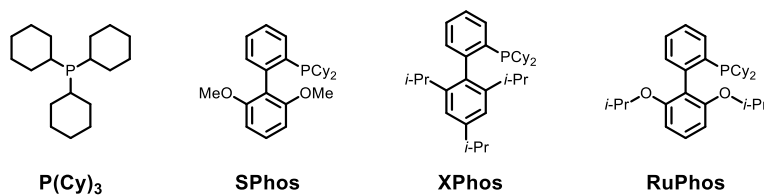
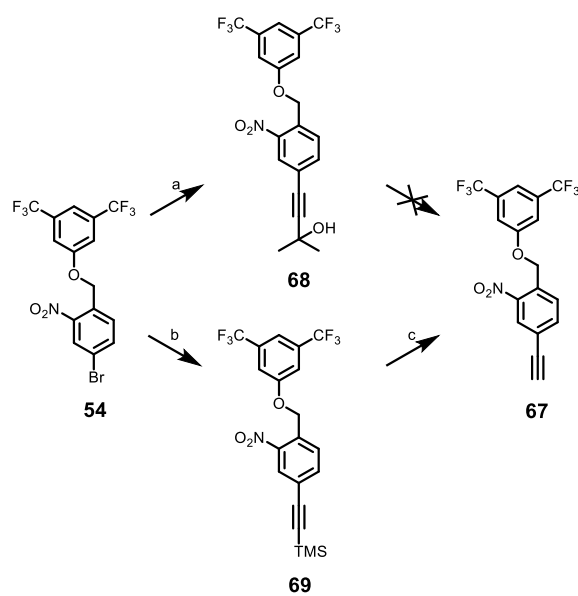


Figure 50. Structures of ligands used to optimize the reaction conditions. One old fashioned phosphine cyclohexane and three new Buchwald ligands have been used.¹⁵²

The other ligands shown in Figure 50 show the ligands developed by Buchwald.¹⁵² These ligands perfectly support the Suzuki cross-coupling reaction obtaining 83 % up to quantitative yields. As described in Scheme 34 we used palladium(II) acetate as the source of palladium, the RuPhos ligand and potassium phosphate as base in a solvent mixture of toluene and water. The reaction was stirred in a pressure tube for eight hours at 50 °C in the absence of oxygen to obtain the TMS masked acetylene derivative **65** after purification by column chromatography in quantitative yield as a colorless solid. Subsequently the TMS protecting group was removed using TBAF to obtain the ethynyl derivative **66** in different quantitative yield. Before we used the ethynyl position in molecule **66** as reagent in Sonogashira cross-coupling reactions we tried to perform other cross-coupling reaction at the bromine in **54**.

As the next attempt, we used Sonogashira cross-coupling reactions to introduce 2-methyl-3-butyn-2-ol and TMS-acetylene. Both reactions are shown in Scheme 35.

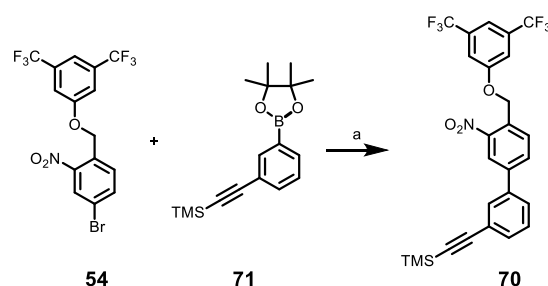


Scheme 35. Sonogashira cross-coupling reactions and deprotections towards free ethynyl derivative **67**. Reagents and conditions: (a) 2-methyl-3-butyn-2-ol, Pd(PPh₃)₄, CuI, TEA, 90 °C (reflux), 12 h, 65 %; (b) TMS-acetylene, Pd(PPh₃)₄, CuI, TEA, 90 °C (reflux), 12 h, 99 %; (c) TBAF (1 M in THF), dichloromethane, room temperature, 30 min, quant.

We introduced the 2-methyl-3-butyn-2-ol protecting group using tetrakis(triphenylphosphine) palladium catalyst, CuI to activate the acetylene species and trimethylamine (TEA) as base. The reaction was refluxed without the addition of solvent in TEA for twelve hours to obtain the masked acetylene derivative **68** in 65 % yield as a colorless solid. Due to the low yield, which we attribute to solubility problems, we did not follow up this reaction

pathway. Deprotection could be done by the use of tetra-butyl-ammonium-hydroxide (TBOH).¹⁵³ The second reaction pathway was to introduce a TMS masked acetylene to the bromine derivative **54** under similar conditions as described to obtain molecule **68**. Under these conditions, we obtained TMS masked acetylene derivative **69** in 99 % yield after purification by column chromatography as a colorless solid. Subsequent deprotection of the acetylene using TBAF we obtained the free ethynyl compound **67** in quantitative yield.

In a last attempt of a cross-coupling reaction at the bromine atom in **54** we introduced a phenyl ring having the TMS masked acetylene in *meta* position as shown in Scheme 36. Having the free acetylene in another position would support the subsequent Sonogashira cross-coupling reaction to a certain central unit.



Scheme 36. Synthesis of the *meta* substituted photo-tag **70** in a Suzuki cross-coupling reaction. Reagents and conditions: (a) Pd(OAc)₂, RuPhos, K₃PO₄, toluene/water (5:1), 50 °C, 12 h, 41 %.

Using the previously described Suzuki cross-coupling reaction protocol of pinacol ether **71** and bromine derivative **54** we were able to obtain *meta* TMS masked acetylene derivative **70** in a yield of 41 %. Due to the low yield we did not follow this reaction pathway.

The two previously described photocleavable tags shown in Figure 51 both have a free acetylene binding position opening a broad variety of possibilities.

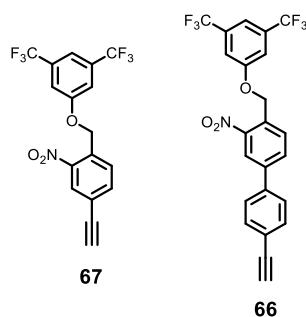
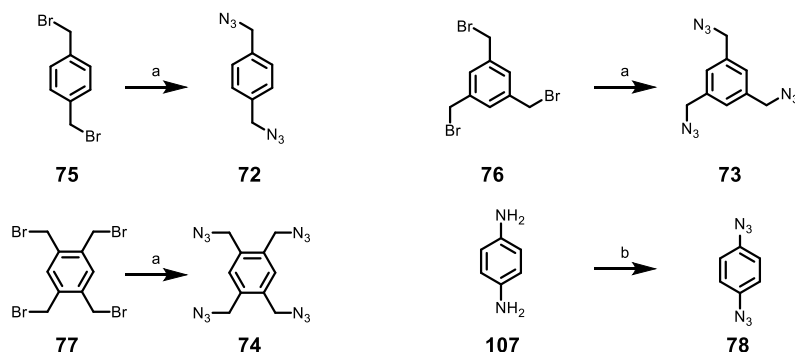


Figure 51. Photocleavable tags **67** and **66**.

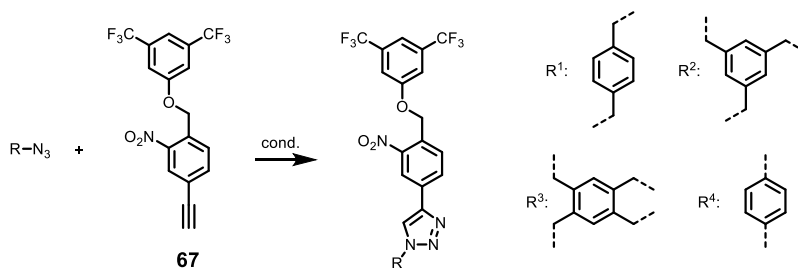
With regard to the attachment to bio-molecules of these tags, it would be very interesting to use click chemistry to attach the tags to the central unit. In a first step, we synthesized four different central units bearing two to four azides to enable click reaction with the free acetylenes.



Scheme 37. Synthesis of the four azide derivatives. Reagents and conditions: (a) NaN₃ (1 M in DMSO), room temperature, 18 h, quant.; (b) tert-butyl nitrite, azidotrimethylsilane, acetonitrile, room temperature, 14 h, dark, 70 %.

The three benzylic azides (**72**, **73** and **74**) were synthesized from the corresponding benzylic bromides (**75**, **76** and **77**) in a S_N2-reaction using a solution of sodium azide in dimethylsulfoxide (DMSO) and all obtained in quantitative yield as colorless oils. The aryl diazide **78** was obtained using tert-butyl nitrite and azidotrimethylsilane in acetonitrile. The diazide **78** was obtained in 70 % yield after purification by column chromatography as a colorless solid. Starting from this azide central units, we performed click reactions using photocleavable-tag **67**. The less reactive benzylic azides were investigated in a first part. The results of the investigated azides and acetylenes are summarized in Table 9.

Table 9. Summary of the conditions in the click reaction of benzylic azides, **72**, **73** and **74** and the aryl azide **78**, with the free acetylene photocleavable tag **67**.



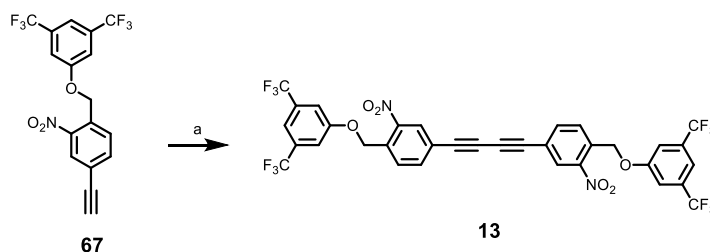
azide	copper-source	addition	solvent	Time [min]	Temp. ^[a] [°C]	Yield ^[b] [%]
72 (R ¹)	Cu(II)SO ₄	L-ascorbic acid	acetone/water (1:1)	30	RT	starting material
72 (R ¹)	Cu(II)SO ₄	L-ascorbic acid	THF/water (1:1)	30	RT	starting material
72 (R ¹)	Cu(II)SO ₄	L-ascorbic acid	MeOH/water (1:1)	30	RT	starting material
72 (R ¹)	Cu(II)SO ₄	L-ascorbic acid	DMF/water (1:1)	30	RT	starting material
72 (R ¹)	Cu(I)I	-	THF/TEA (10:1)	180	70	traces in ESI
72 (R ¹)	Cu(I)PF ₆ (CH ₃ CN) ₄	TBTA ^[c]	THF/acetone(1:1) ^[d]	60	RT	traces in ESI
73 (R ²)	Cu(I)PF ₆ (CH ₃ CN) ₄	TBTA ^[c]	THF/acetone(1:1) ^[d]	60	RT	starting material
74 (R ³)	Cu(I)PF ₆ (CH ₃ CN) ₄	TBTA ^[c]	THF/acetone(1:1) ^[d]	60	RT	starting material
78 (R ⁴)	Cu(II)SO ₄	-	THF/water (1:1)	30	RT	starting material
78 (R ⁴)	Cu(I)I	-	THF/TEA (10:1)	180	70	starting material
78 (R ⁴)	Cu(I)PF ₆ (CH ₃ CN) ₄	TBTA ^[c]	THF/acetone (1:1) ^[d]	60	RT	traces in ESI

[a] room temperature (RT); [b] starting material: photocleavable tag **67** was completely recovered; traces in ESI: traces of product-masses have been found in ESI/MS spectra; [c] TBTA: tris(benzyltriazolylmethyl)amine was used to support the reaction; [d] some drops of TEA have to be added to dissolve the copper compound.

Table 9 summarizes the conditions of the click reaction step. Firstly, we investigated the benzylic diazide **72** in the click reaction with the photocleavable tag **67**. The first attempts using Cu(II)SO₄ as the copper source, which is reduced to the active Cu(I) species using L-ascorbic acid, in a various number of solvent mixtures. The advantage of the use of Cu(II)SO₄ reducing it *in situ* with L-ascorbic acid is that the reaction can be performed in water, this solubility feature would enable the reaction at biomolecules. Unfortunately, it was not possible to obtain the triazole product using acetone, THF, methanol, or DMF in a solvent mixture with water. In all the cases only starting material has been recovered. In a second step we tried to use Cu(I) iodide as a direct source of Cu(I). This reaction has to be performed in triethylamine (TEA) to solubilize the Cu(I) salt. Nevertheless, some traces of the desired product could be observed in ESI mass spectrometry. Mainly starting material could be recovered. The last attempt using benzylic diazide **72** and photocleavable tag **67** was to follow a procedure developed by Schweinfurth *et*

*al.*¹⁵⁴ Cu(I)PF₆(CH₃CN)₄ is used as the direct source of Cu(I) and tris(benzyltriazolylmethyl)-amine (TBTA) was used to support the catalyst. It was found that these reaction conditions enable click reaction under strongly unfavored conditions. Unfortunately, also these optimized conditions did not provide the desired product. Using the benzylic azides (**72**, **73** and **74**) we could only detect traces of the triazol compound **R**¹. Reactions with allylic azides were assumed to be more efficient. Therefore, we tested the reaction of photocleavable tag **67** and the allylic diazide **78**. Unfortunately, the reaction towards the clicked product did not work using all the described procedures. We have to conclude that due to solubility problems and low reactivity of the free acetylene in photocleavable tag **67** it was not possible to obtain clicked products using the previously described procedures.

Simplifying the coupling of two or more photocleavable tags **67** together, we decided to perform a Glaser-Hay coupling to obtain the homocoupled product as shown in Scheme 38.



Scheme 38. Glaser-Hay homocoupling of photocleavable-tag **67**. Reagents and conditions: (a) TMEDA, Cu(I)Cl, air, dichloromethane, room temperature, 1 h, 60 %.

The homocoupling of photocleavable-tag **67** was done using tetramethylethylenediamine (TMEDA) to solubilize copper (I) in dichloromethane. The reaction was stirred vigorously in an open Erlenmeyer flask to aerate the solution. After stirring the reaction mixture for 1 h the desired product **13** was obtained in 60 % yield as a colorless solid. The purification was done using column chromatography eluting the product as the last fraction in pure ethyl acetate. Finally, the crude was recrystallized from chloroform. The product is only poorly soluble in a broad spectrum of organic solvents. Tetrahydrofuran (THF) is the best solvent to solubilize these compounds. The purity and the structural properties of the product **13** was proven by high-resolution mass spectrometry (HRMS), ¹H-, ¹⁹F- and ¹³C-NMR spectrometry. A representative ¹H-NMR spectrum measured in THF-*d*₈ is shown in Figure 52.

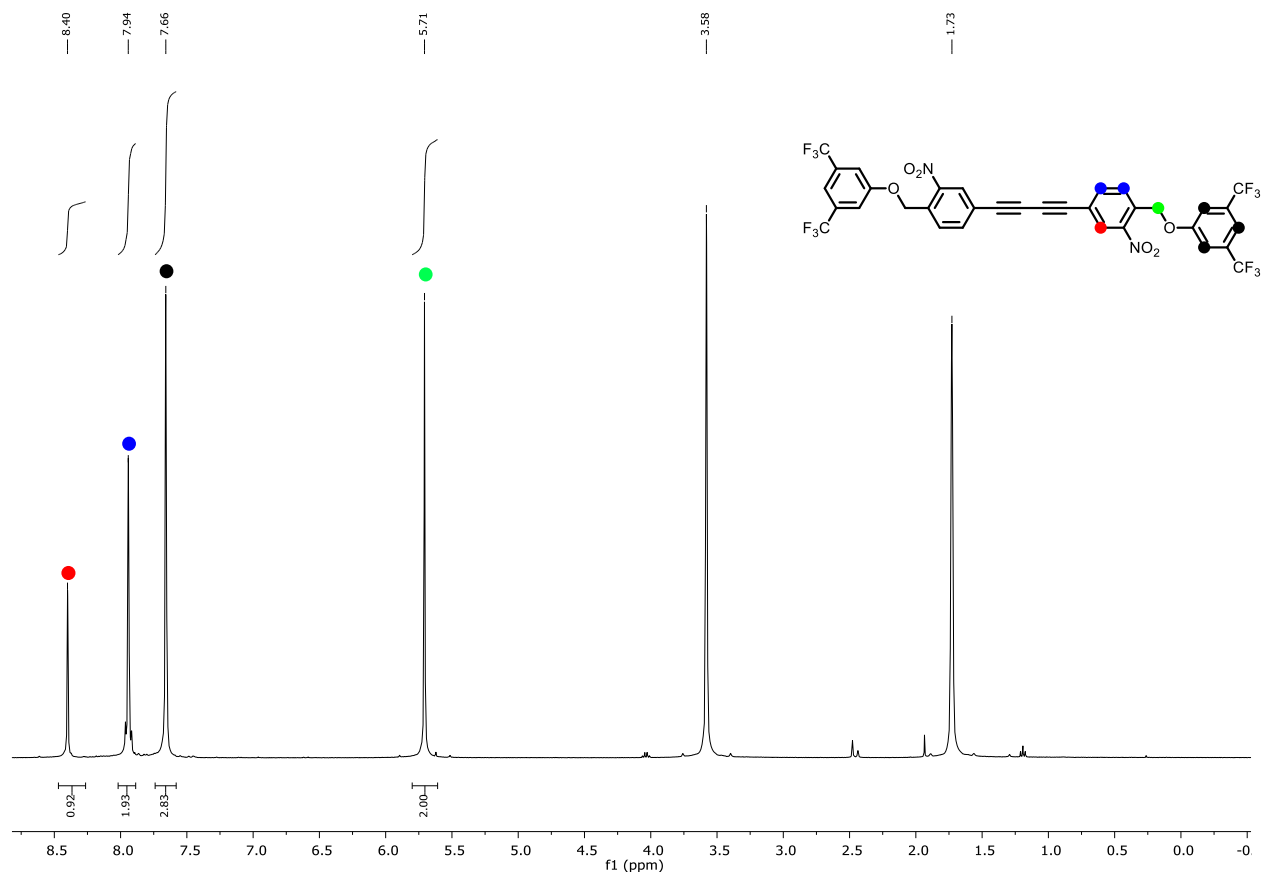


Figure 52. $^1\text{H-NMR}$ in $\text{THF-}d_8$ of photo-dimer **13**. Signals at 1.73 and 3.58 ppm are solvent residue signals of $\text{THF-}d_8$.

In this spectrum (Figure 52) and the following spectra (Figure 54 and Figure 55) of the benzylic protons (green) can be found at chemical shifts around 5.5 ppm. All the integrals are referenced on this signal. The signal at 7.66 ppm is attributed to the combined signal (black) of the fluorinated phenol-ring. Combination of the protons at the nitro-phenyl ring (blue) led to a multiplet signal at 7.94 ppm. The singlet at 8.40 ppm (red) is attributed to hydrogen atom next to the nitro-group. All the expected signals can be found in the representative $^1\text{H-NMR}$ spectrum and the integrals fit the amount of protons in the molecule.

Facing the problems in the click-reactions to build up larger photocleavable systems, we decided to use Sonogashira cross-coupling reactions to bind the free acetylenes of photocleavable tag **67** and **66** to the above described central units **47** and **46** as shown in Figure 53.

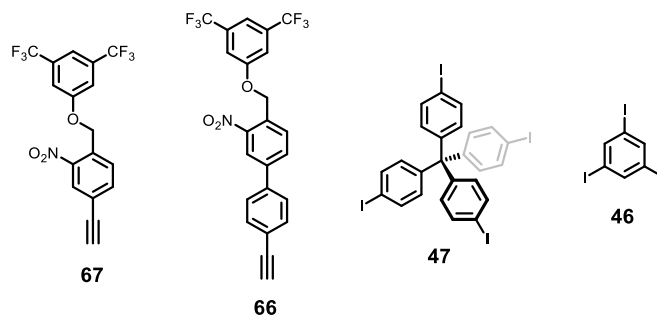
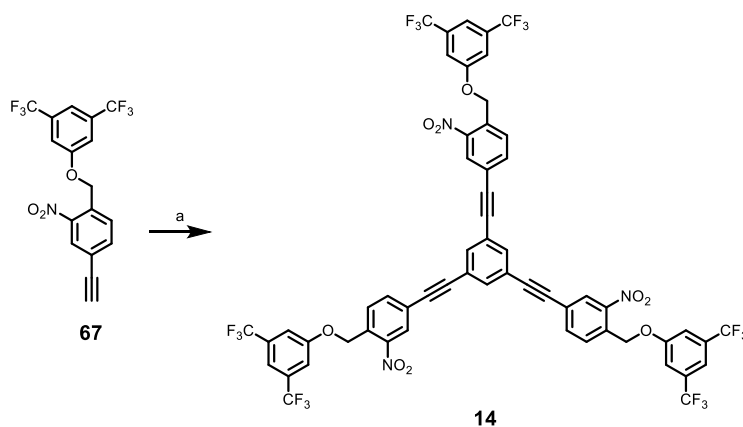


Figure 53. Photocleavable tags **67** and **66**, and the central units **47** and **46** proposed for Sonogashira cross-coupling reactions.

The first Sonogashira cross-coupling reaction was performed using triiodobenzene (**46**) as the central unit the shorter photocleavable tag **67** as shown in Scheme 39.



Scheme 39. Sonogashira cross-coupling reaction of photocleavable tag **67** to the triiodobenzene (**46**) central unit to obtain photo-trimer **14**. Reagents and conditions: (a) 1,3,5-triiodobenzene (**46**), Pd(PPh₃)₄, CuI, THF/TEA (3:1), 12 h, 50 °C, 80 %.

The reactions as shown in Scheme 39 was performed using palladium tetrakis-triphenylphosphine catalyst and copper iodide to activate the binding of the catalyst to the acetylene of photocleavable tag **67**. The reaction was performed in a solvent mixture of THF and triethylamine, the addition of THF is crucial to obtain the desired product since it is poorly soluble in a broad spectrum of organic solvents. The poor solubility does not allow purification by column chromatography. The crude product was recrystallized from chloroform three times to obtain the photo-trimer **14** in 80 % yield as a colorless solid. The purity and the structural properties of the product **14** were proven by high-resolution mass spectrometry (HRMS), ¹H-, ¹⁹F- and ¹³C-NMR spectrometry. A representative ¹H-spectrum is shown in Figure 54.

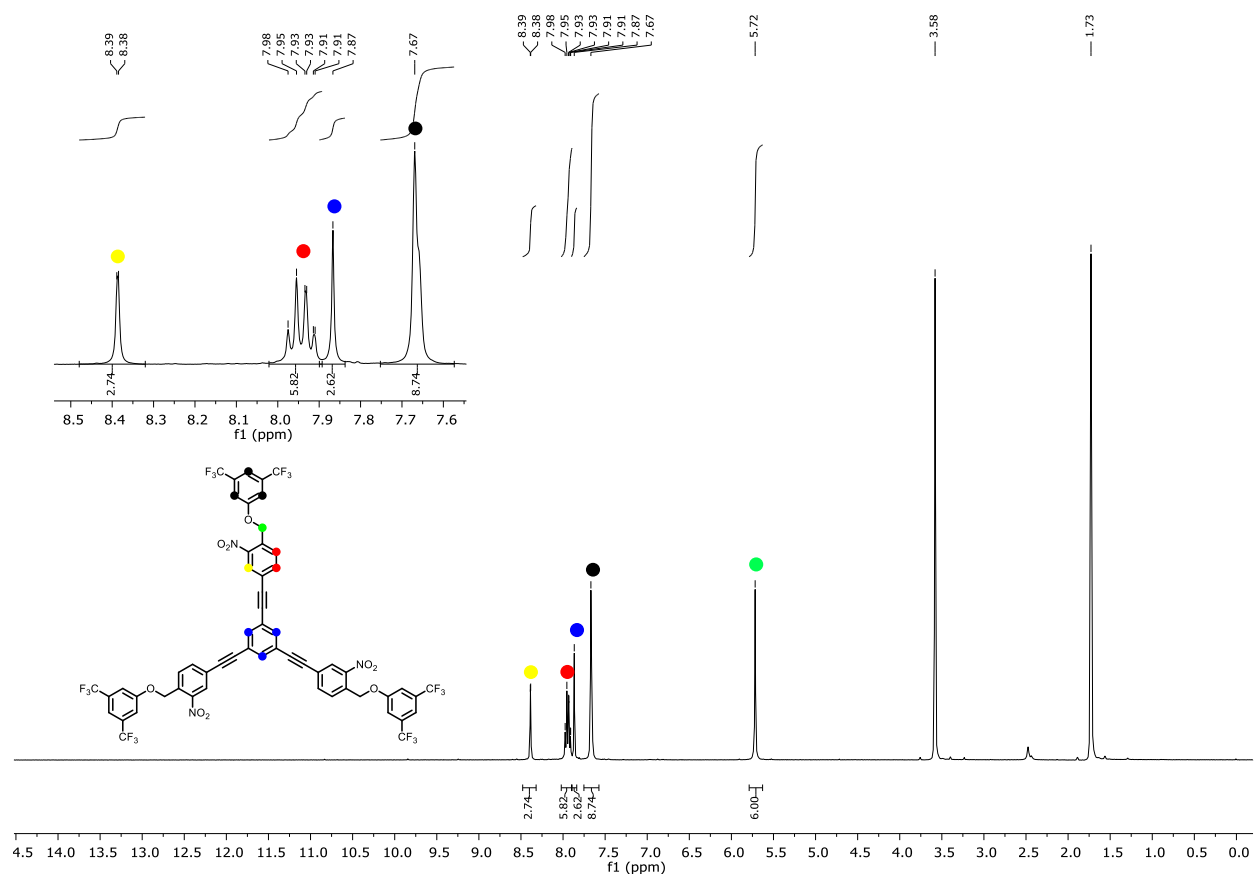
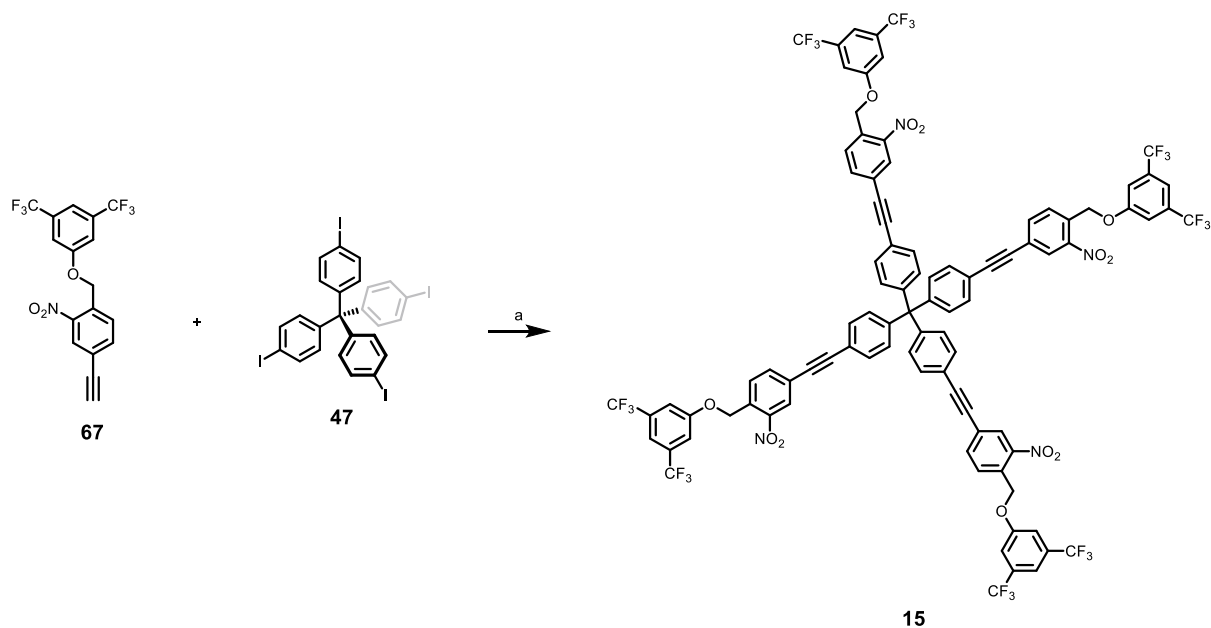


Figure 54. ¹H-NMR in THF-*d*₈ of photo-trimer **14**. Signals at 1.73 and 3.58 ppm are solvent residue signals of THF-*d*₈.

As described above for photo-dimer **13** the photo-trimer **14** shows a signal originating from benzylic protons at 5.72 ppm (green). The hydrogen atoms at the fluorinated phenyl-ring are observed at 7.67 ppm (black) being a combination of all the signals. The protons of the central unit (blue) are attributed to the singlet at 7.87 ppm. The multiplet signal looking like two doublets are assigned to the AB-system (red) in the nitro-phenyl ring. Moreover, as described above the strongest low field shifted signal (yellow) occurs from the proton neighboring the nitro-group at 8.38 ppm. The signals within the ¹H-NMR spectrum and the integrals fit the amount of protons in the molecule.

Using tetrakis (4-iodophenyl) methane (**47**) as the central unit, we obtained the photo-tetramer **15**. The reaction was performed under similar Sonogashira cross-coupling reaction conditions as described above. A schematic representation of the reaction is shown in Scheme 40.



Scheme 40. Sonogashira cross-coupling reaction of photocleavable tag **67** to the tetrakis(4-iodophenyl)methane (**47**) central unit to obtain photo-tetramer **15**. Reagents and conditions: (a) Pd(PPh₃)₄, CuI, THF/TEA (3:1), 12 h, 90 °C, 62 %.

The reaction conditions described in Scheme 40 are similar to the conditions described for photo-trimer **14**. The higher solubility of tetramer **15** versus the trimer **14** allowed the purification by column chromatography. The last eluted band being the product was further purified by recrystallization from chloroform. The pure photo-tetramer **15** was obtained in 62 % yield as a colorless solid. The purity and the structural properties of the obtained product **15** was proved by HRMS and ¹H- and ¹⁹F-NMR spectrometry. A representative ¹H-spectrum is shown in Figure 55. As in the above-described examples, we referenced the integrals on the benzylic protons (green). The AB-system of the central unit (black) can be attributed to the signals at 7.33 and 7.55 ppm. The signals of the fluorinated phenol ring are combined in one multiplet found at 7.65 ppm. The AB-system of the nitro-phenyl-ring is obtained as a multiplet between 7.85 and 7.94 ppm. Finally, the signal of the proton next to the nitro-group is found as a singlet at 8.31 ppm.

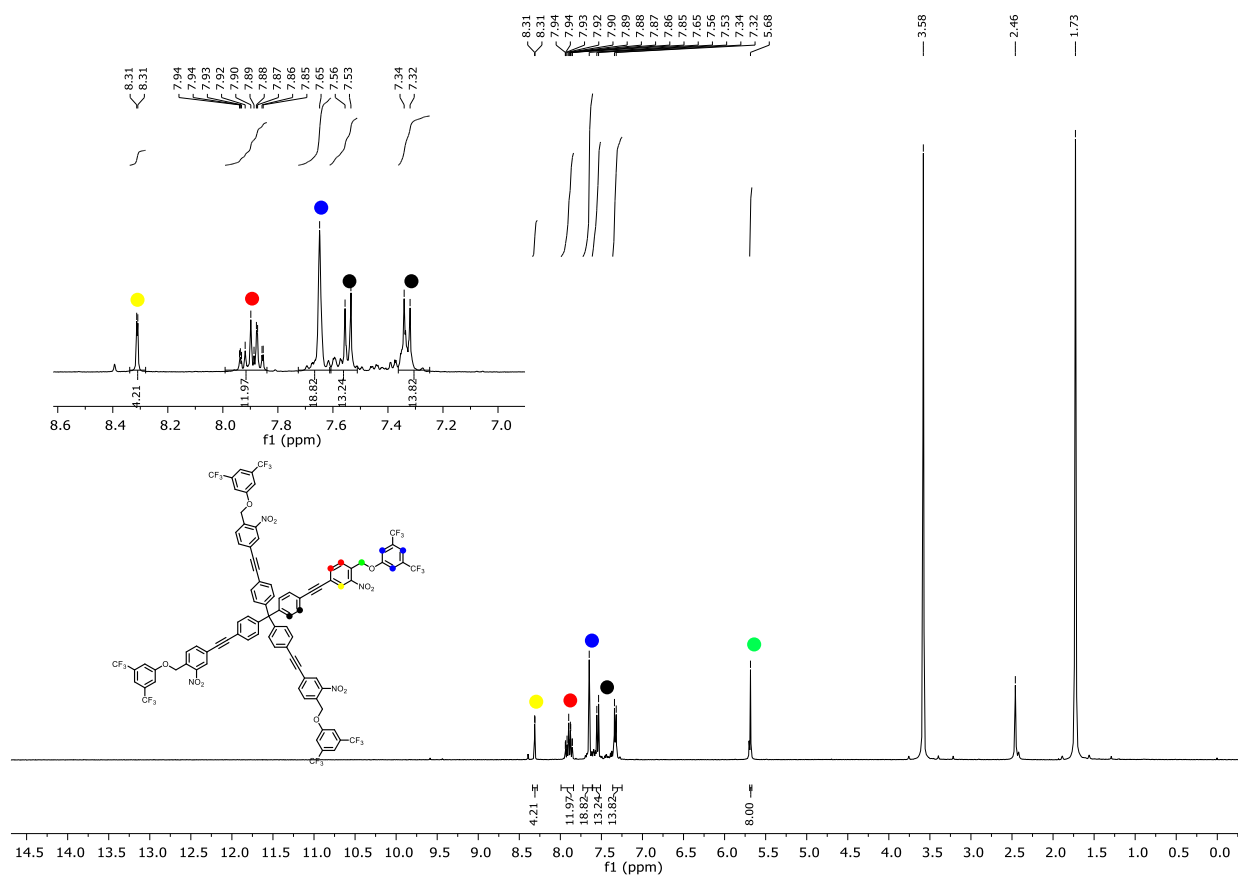
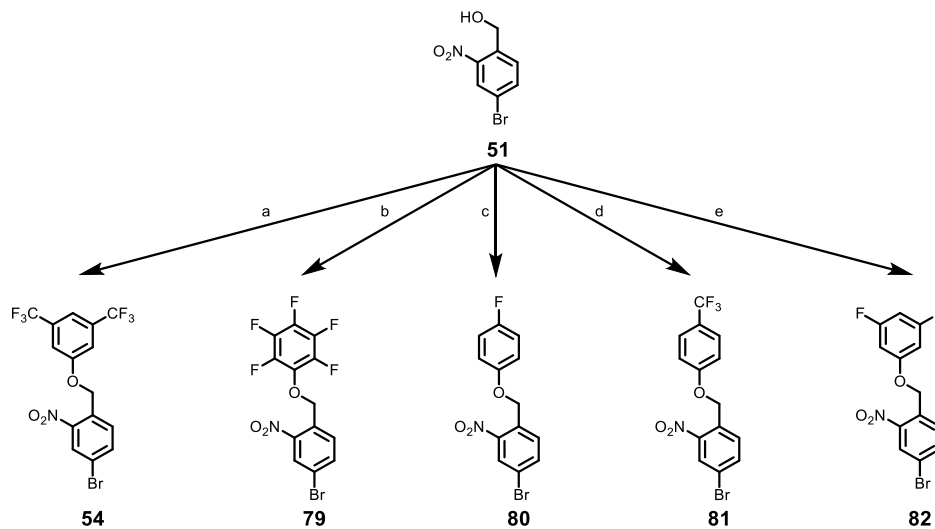


Figure 55. $^1\text{H-NMR}$ in $\text{THF-}d_8$ of photo-tetramer **15**. Signals at 1.73 and 3.58 ppm are solvent residue signals of $\text{THF-}d_8$.

All the signals of the $^1\text{H-NMR}$ spectrum shown in Figure 55 of photo-tetramer **15** can be attributed to the protons found within the structure.

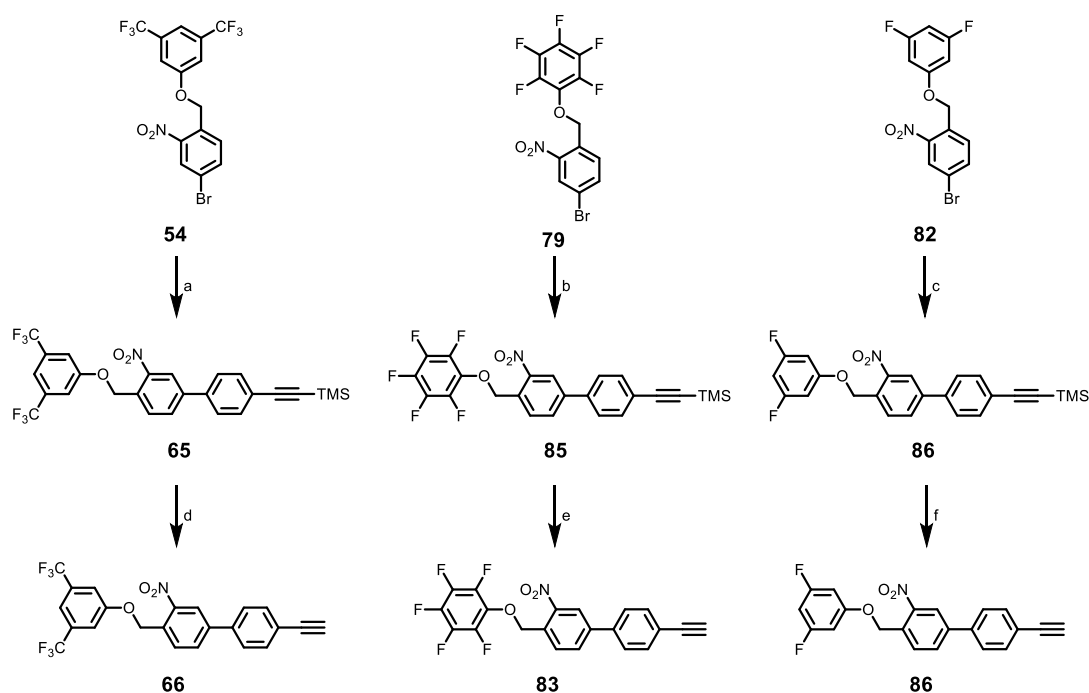
In order to vary the photocleavable-tag we varied the phenol moiety that we introduce in the Mitsunobu reaction. As shown in Scheme 41 five different products can be obtained using similar conditions for the Mitsunobu reaction with five different fluorinated phenols. In addition to above described introduction of a 3,5-bis(trifluoromethyl)phenol (**52**) to the benzylic alcohol **51** we introduced pentafluorophenol, 4-fluorophenol, 4-(trifluoromethyl)phenol, and 3,5-difluorophenol in the Mitsunobu reaction. All the reaction were performed dissolving the benzylic alcohol **51**, the corresponding allylic alcohol and triphenylphosphine in THF. We used an ice bath the reaction to cool the reaction mixture to $0\text{ }^\circ\text{C}$ and diisopropyl azodicarboxylate (DIAD) was added dropwise. After stirring the reaction for 12 h in the absence of light, we obtained the desired ether bridged molecules **54** in 96 %, **79** in 98 %, **80** in 90 %, **81** in 76 %, and **82** in 89 % yield. All the

pure products were obtained after purification by column chromatography as colorless solids. The purity and structures were proven by HRMS and ^1H -, ^{19}F - and ^{13}C -NMR spectrometry.



Scheme 41. Variation of the Mitsunobu reaction conditions found for **54** to obtain the varied photocleavable-tags **79-82**. Reagents and conditions: (a) described in Scheme 30, 3,5-bis(trifluoromethyl)phenol (**52**), DIAD, triphenylphosphine, THF, 12 h, room temperature, 96 %; (b) pentafluorophenol, DIAD, triphenylphosphine, THF, 12 h, room temperature, 98 %; (c) 4-fluorophenol, DIAD, triphenylphosphine, THF, 12 h, room temperature, 90 %; (d) 4-(trifluoromethyl)phenol, DIAD, triphenylphosphine, THF, 12 h, room temperature, 76 %; (e) 3,5-difluorophenol, DIAD, triphenylphosphine, THF, 12 h, room temperature, 89 %.

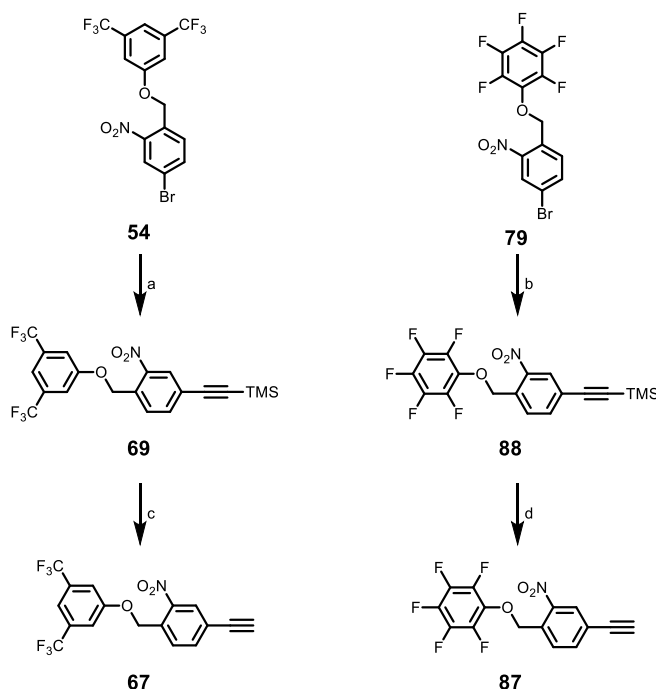
Having these tags, we investigated further functionalization as described above for the test-system bearing two trifluoromethyl groups **54**. We used Suzuki and Sonogashira cross-coupling reactions to introduce a TMS masked ethynyl group to the bromine. We did not use the two photo-tags **81** and **82** since they both do not offer a broad spectrum of possible functionalization at the fluorinated phenyl ring. All the bromine derivatives shown in Scheme 41 are synthesized to investigate the variety of possible tags for photocleavage experiments. Firstly, we performed Suzuki cross-coupling reactions using the optimized conditions described in Table 8. The reaction pathway is shown in Scheme 42.



Scheme 42. Suzuki cross-coupling reactions introducing a phenyl ring bearing a TMS masked ethynyl group and subsequent deprotection of the ethynyl group. Reagents and conditions: (a) Pd(OAc)₂, RuPhos, K₃PO₄, toluene/water (5:1), 50 °C, 12 h, quant.; (b) Pd(OAc)₂, RuPhos, K₃PO₄, toluene/water (5:1), 50 °C, 12 h, 90 %; (c) Pd(OAc)₂, RuPhos, K₃PO₄, toluene/water (5:1), 50 °C, 12 h, 89 %; (d) TBAF (1 M in THF), dichloromethane, room temperature, 30 min, quant.; (e) TBAF (1 M in THF), dichloromethane, room temperature, 30 min, quant.; (f) TBAF (1 M in THF), dichloromethane, room temperature, 30 min, 89 %.

Optimized Suzuki cross-coupling reaction conditions and subsequent deprotection of the TMS masked acetylene we obtained the photocleavable-tags **66** in quantitative, **83** in 90 % and **84** in 79 % yield over two reaction steps as colorless solids. The purity and structure of the free-acetylene tags has been proven by HRMS and ¹H-, ¹⁹F- and ¹³C-NMR spectrometry.

In a second attempt to vary the photocleavable-tags, we used the easier accessible Sonogashira cross-coupling attempt described in Scheme 35. Both reaction steps work also in large scale and without difficult purification steps.



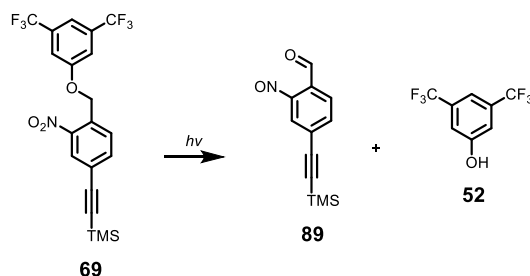
Scheme 43. Sonogashira cross-coupling reactions introducing a TMS masked ethynyl group and subsequent deprotection of the ethynyl group. Reagents and conditions: (a) TMS-acetylene, Pd(PPh₃)₄, CuI, TEA, 90 °C (reflux), 12 h, 99 %; (b) TMS-acetylene, Pd(PPh₃)₄, CuI, TEA, 90 °C (reflux), 12 h, 92 %; (c) TBAF (1 M in THF), dichloromethane, room temperature, 30 min, quant.; (d) TBAF (1 M in THF), dichloromethane, room temperature, 30 min, quant.

The reactions were performed under similar conditions as above described in Scheme 35. The Sonogashira cross-coupling reaction introducing a TMS masked acetylene and subsequent deprotection lead to **67** in 99 % yield and **87** in 92 % yield over two reaction steps.

Having three photocleavable systems and the modified tags in hand, we are now ready to prove our concept. This procedure is described in the next part.

5.4 Cleavage Experiments

As described in section 5.1 the cleavage of the photocleavable tag can be done using UV or visible light. The process of cleavage and the products obtained are described in section 5.1 and schematically represented in Scheme 44 for all the cleavage processes for the photocleavable tag **69**.



Scheme 44. Schematic representation of the photocleavage irradiated on photocleavable tag **69** obtaining the corresponding nitroso-aldehyde **89** and phenol **52** derivatives.

By irradiation on the photocleavable-tag **69** we expect two new compounds, the nitroso-aldehyde compound **89** and the phenol **52** that we used within the Mitsunobu reaction. The obtained nitroso-aldehyde **89** is very interesting for $^1\text{H-NMR}$ investigations. It is possible to irradiate directly to a solution of **69** using a monochromator and track the appearance of an aldehyde-signal in the ^1H -spectrum. The results of this experiment are shown in Figure 56. A NMR-spectrum was taken before the irradiation with 355 nm light, after 10 min, 30 min, 1 h, 3 h, and 5 h. We decided to investigate in a first part only the photocleavable-tag **69** as a test system for the larger photo-dimer **13**, -trimer **14** and -tetramer **15**, since this tag can easily be synthesized in large quantities.

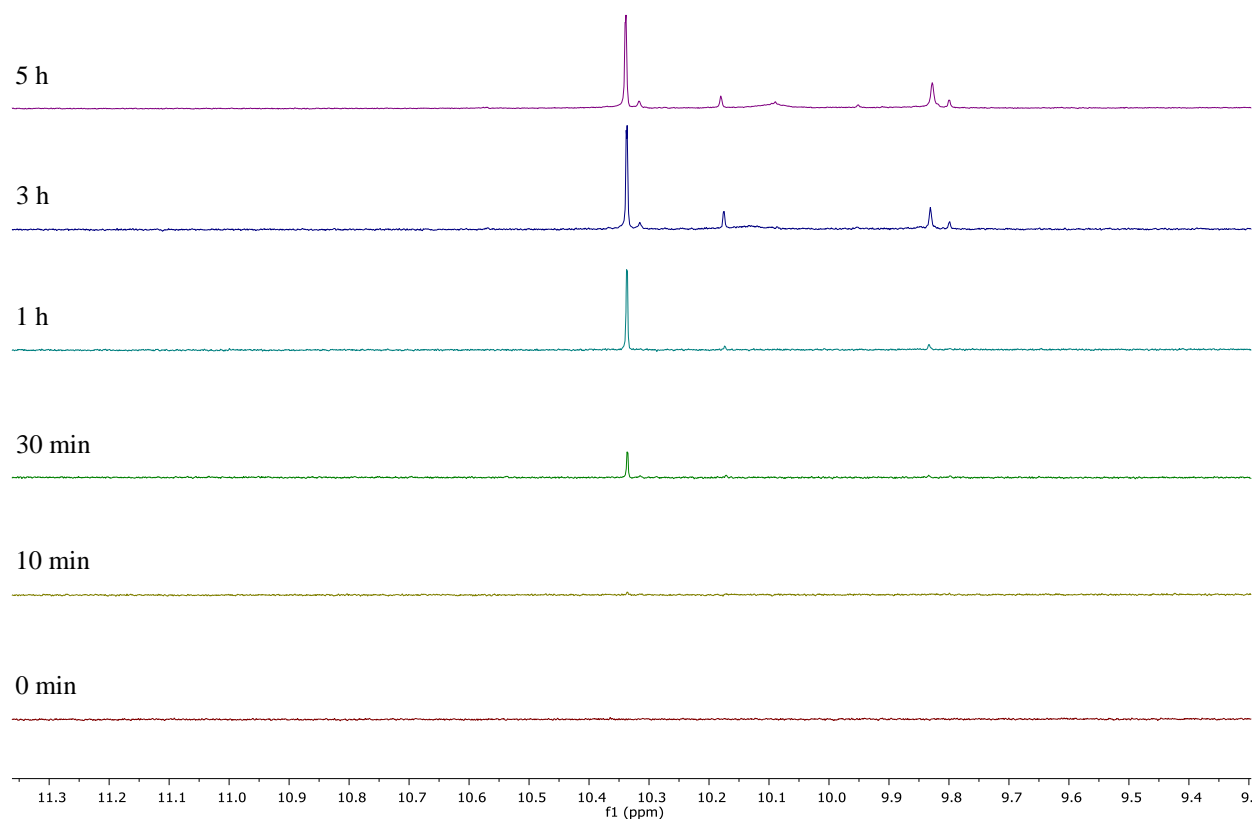


Figure 56. ¹H-NMR spectra of TMS masked photocleavable tag **69** after irradiation with UV-light (355 nm) in a NMR-tube showing the region of the chemical shift of the appearing aldehyde signal.

The results of the irradiation using monochromatic light in a NMR-tube are shown in Figure 56. Already after 10 min, a small signal at 10.35 ppm can be observed. After 30 min and further on after 5 hours we observed a clear and well-defined signal in the aldehyde region of the ¹H-NMR spectrum. Using the photocleavable-tag **69** as a test system for the larger photocleavable systems, we can conclude at this point, that it is possible to track the cleavage-process using ¹H-NMR spectroscopy. Enhancing this measurement to investigate on the three photosystems photo-dimer **13**, -trimer **14** and -tetramer **15** we found limitations in the above described NMR-investigations. The three photosystems photo-dimer **13**, -trimer **14** and -tetramer **15** are only soluble enough in THF to perform NMR-experiments. In all other NMR-solvents (such as dichloromethane, chloroform, acetone, and methanol), the product precipitates after the first experiment. Due to this fact we investigated the three photosystems photo-dimer **13**, -trimer **14** and -tetramer **15** using UV/Vis spectroscopy, since smaller amounts of the substrate can be investigated.

Firstly, we investigated the decay upon irradiation by UV light to the photo-dimer **13**. To perform all the described experiments we irradiated commercially available UV cuvettes by UV-light (254 and 365 nm) of an UV-lamp (8 W, 230 V, ~50 Hz). The distance between the cuvette and the UV-lamp was kept constant at 1.5 cm and also the concentrations of all the probes was kept constant in order to avoid any concentration dependent errors. All the measurements were performed three times using freshly prepared solutions and the mean value was taken for the presented graphs. Errors were calculated according to a Student's t-distribution with a 95% confidence interval.

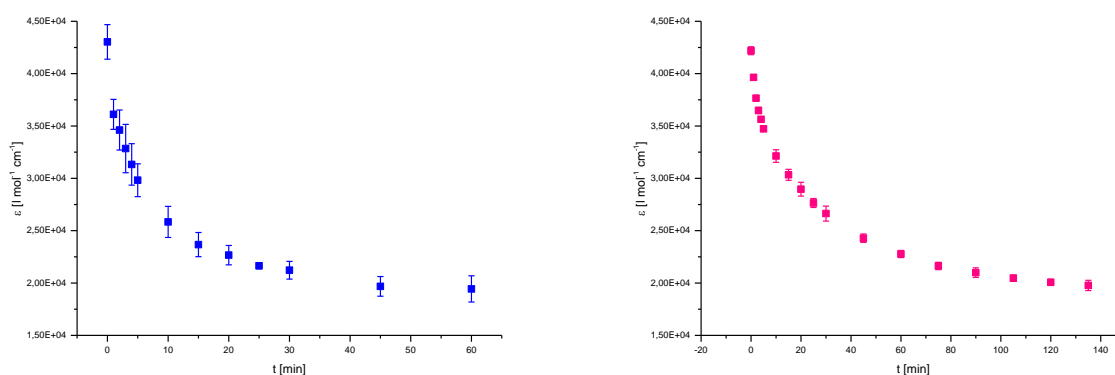


Figure 57. Irradiation of UV-light to photo-dimer **13** with 254 nm (blue) and 365 nm (pink).

The irradiation by UV-light to photo-dimer **13** shown in Figure 57 showed relatively rapid decay of the starting substrate **13** into the aldehyde and the nitroso compound. Irradiation by light with a wavelength of 254 nm (blue) led to an almost complete decay in 60 min, and the irradiation with light having a wavelength of 365 nm (pink) led to an almost complete decay in 120 min. These values, especially the doubled decay time upon irradiation with 365 nm light, have been expected due to the higher energy of the 254 nm light. Both decays reached extinction coefficients of around $20'000 \text{ l mol}^{-1} \text{ cm}^{-1}$ in different timespans.

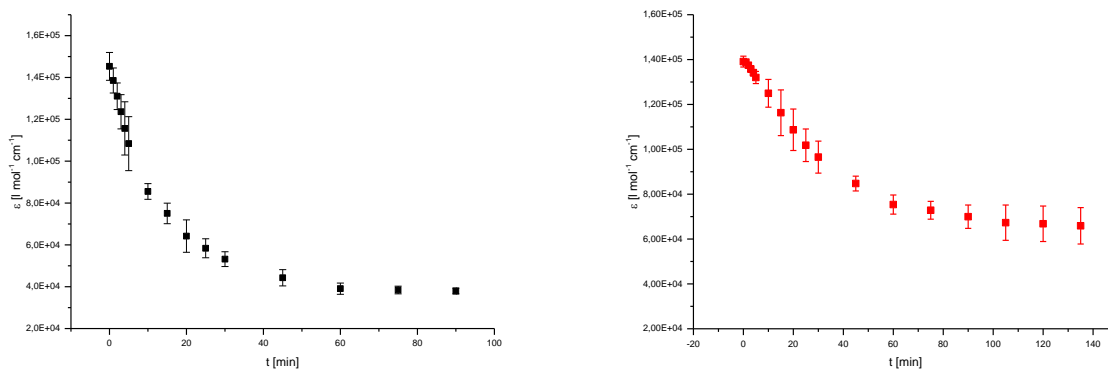


Figure 58. Irradiation of UV-light to photo-trimer **14** with 254 nm (black) and 365 nm (red).

The decay of photo-trimer **14** shown in Figure 58 showed comparable results to photo-dimer shown in Figure 57. The decay to the nitroso and aldehyde compound upon irradiation with 254 nm (black) light was almost complete in 60 min, while the decay with irradiation of 365 nm (red) light was almost complete after 120 min. The photo-trimer **14** showed a lot stronger absorbance compared to photo-dimer **13**. We found it very interesting that after irradiation of 254 nm (black) and 365 nm (red) light the extinction coefficients are not similar. The absorbance after irradiation was a lot stronger, we attributed this feature to the products of the photo-decay. This would lead to a strongly conjugated system in the case of photo-trimer **14**. In addition, the decay upon irradiation of 365 nm (red) light was a lot slower than upon irradiation of 254 nm (black) light. This cleavage process was not found to be very efficient.

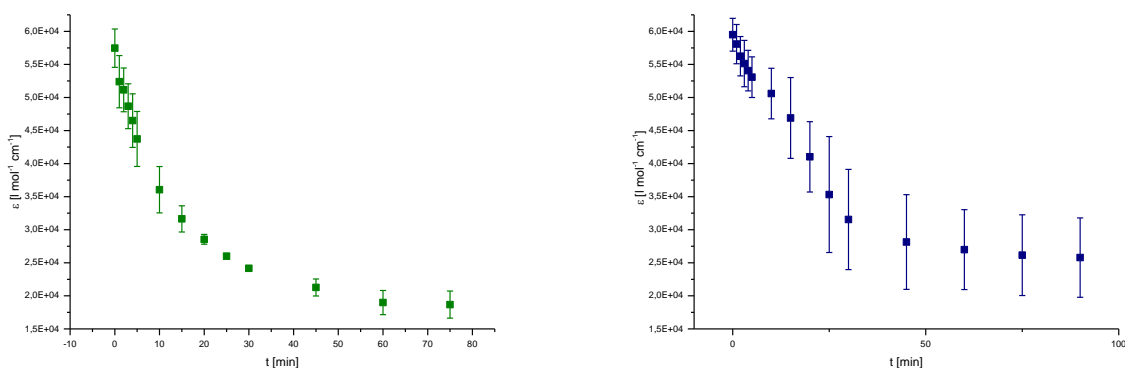


Figure 59. Irradiation of UV-light to photo-tetramer **15** with 254 nm (green) and 365 nm (dark blue).

In contrast to the photo-trimer **14**, the photo-decay of photo-tetramer **15** shows was found to be very similar to the decay of photo-dimer **13**. We found the decay upon irradiation of 254 nm

(green) light shown in Figure 59 being as fast as described before for photo-dimer **13** and photo-trimer **14** but reaching comparable extinction coefficients upon complete decay. The decay was almost complete after 60 min. In this case, the decay of photo-tetramer **15** by irradiation of 364 nm (dark blue) light was considerably faster than in the previously described examples. In the following part, the results are compared in detail.

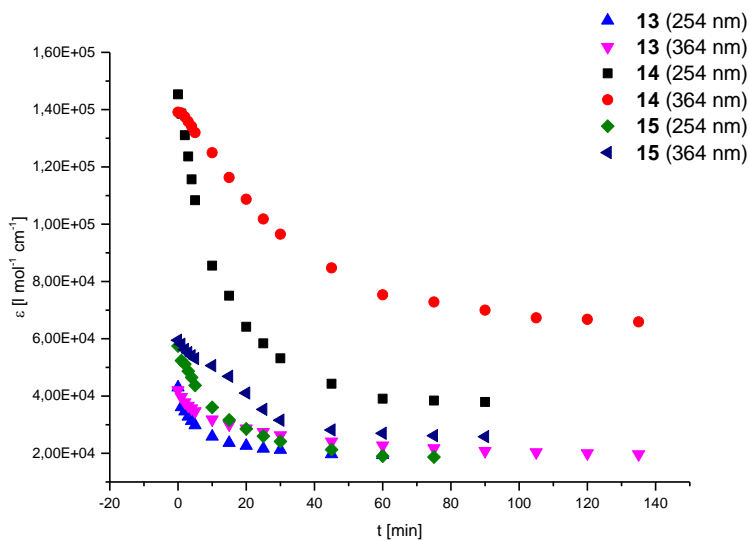


Figure 60. Comparison of the decays to all the photocleavable molecules.

Figure 60 shows all the above-described decays in one schematic representation. This shows the considerably stronger absorbance of photo-trimer **14** (black and red) compared to the two other investigated compounds. The absorbance of photo-dimer **13** and photo-tetramer **15** is nearly similarly strong and reaches comparable values after the cleavage process. Normalizing the graphs represented in Figure 60 allows the comparison of the rate of the decay. A normalized graph is shown in Figure 61.

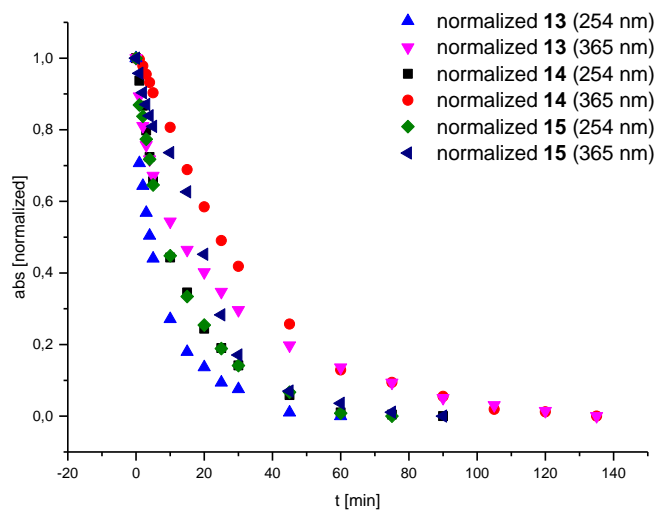


Figure 61. Normalization of the graphs shown in Figure 60 between 0 and 1.

Comparing the rates of decay as shown in Figure 61 we observed that an irradiation with 254 nm light (blue, black and green) leads to a similarly fast decay in approximately 60 min. A similar decay-rate was found for irradiation with 364 nm light to the photo-tetramer **15** (dark blue). Considerably lower decay-rates have been found for irradiation with 365 nm light to photo-dimer **13** (pink) and photo-trimer **14** (red).

5.5 Conclusion

We were able to synthesized three different photocleavable systems. Photo-dimer **13**, photo-trimer **14** and photo-tetramer **15** are represented in Figure 62. All the three test systems are proposed to be very interesting for future QIE using a standing optical wave grid for cleavage in gas-phase, since QIE are done in gas-phase. The herein presented photocleavable systems offer two to four cleavable sites within one molecule.

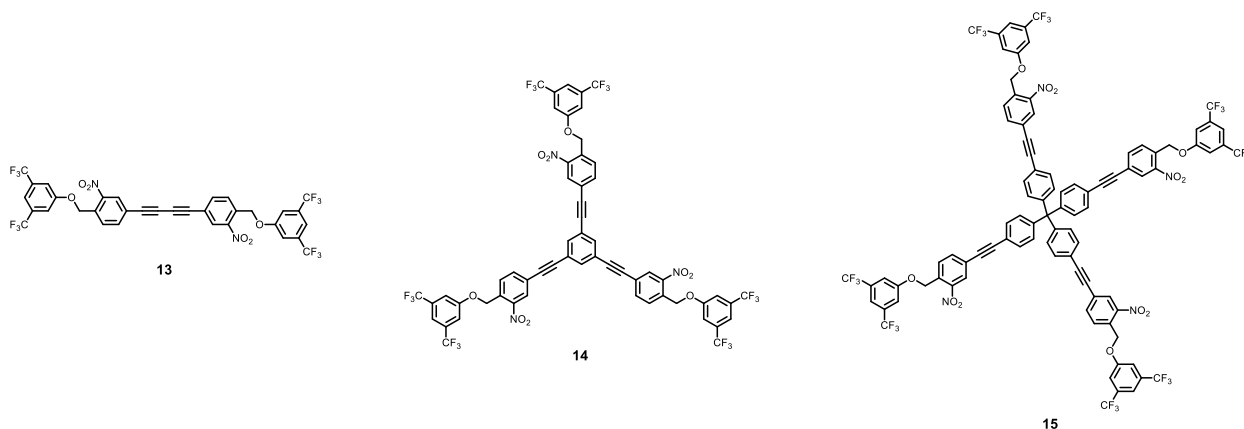


Figure 62. Structures of photo-dimer **13**, photo-trimer **14** and photo-tetramer **15**.

Cleavage experiments have been performed using the three compounds shown in Figure 62. All the shown molecules showed very reliable cleaving properties upon irradiation with light in solution. In conclusion, all the three described molecules showed similar cleavage properties by irradiation with 254 nm light. Using lower energy light at 365 nm only the photo-tetramer **15** showed good results in the photo-decay.

In order to be able to vary the structure of photocleavable systems a broad variation of tags has been synthesized and is represented in Figure 63.

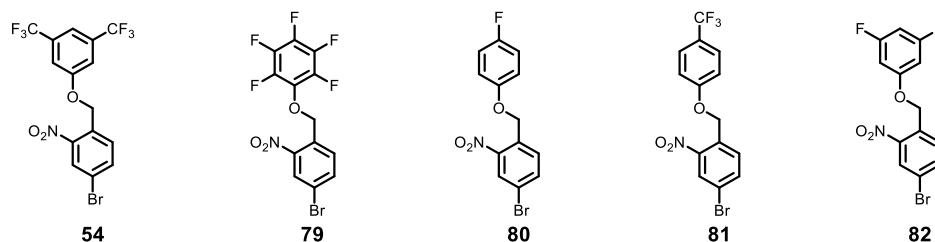


Figure 63. Photo-tags that can be attached to larger molecules.

The broad variety of photo-tags allows the introduction of longer chains to the tag to enhance the mass difference between the tag and the investigated molecule and to tune to some extent the

sublimation properties. Mainly photo-tag **79** would be very interesting for the attachment of sulfur side-chains via nucleophilic aromatic substitution reactions.

Unfortunately, it was not possible to attach the described tags to central units by click reactions. This would be a very interesting feature to introduce the tags to bio-molecules. May the introduction of longer side-chains to the photo-tags will help to optimize the solubility of the tags and therefore make click reactions possible.

6 Summary and Outlook

The approach of the borderline between classical and quantum physics was the main goal of this doctoral thesis. To reach this goal, the ambition of the work of the author in the group of Prof. Dr. Marcel Mayor at the University of Basel was to synthesize tailor made molecules for QIE. The ambition regarding these experiments in the group of Prof. Dr. Markus Arndt at the University of Vienna was to optimize the experimental setup towards optimal beam, interference and detection properties.

The introduction is a summary of previous work done in the field of QIE. The experiments are described with regard to the historical findings, going back to the observations of Thomas Young performing his famous double slit experiments. Based on the previous experiments with tailor made porphyrin molecules, nucleophilic aromatic substitution reactions and the possibility of multi-substitution reactions are introduced. This was found to be a very important reaction to build up large organic libraries. Furthermore, we introduced photocleavable protection groups in a proof of concept as a possible tag on biomolecules in QIE.

6.1 Far-Field Interferometry

The first part focusses on the investigation towards novel tailor made molecules for QIE in the far-field regime. The synthesis of heavier molecules was the aim within this part of the doctoral thesis. Using the knowledge from previous experiments in the far-field regime, we synthesized free base phthalocyanine molecules. The molecule as shown in Figure 64 was the only molecule that allowed investigations by fluorescence, since we were able to obtain the free base phthalocyanine.

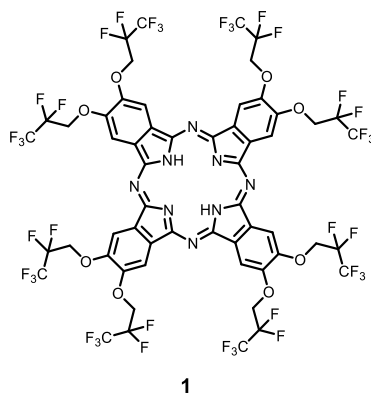


Figure 64. Phthalocyanine molecule **1** bearing eight fluoroalkoxy side-chains.

To our delight, it was possible to produce a sufficiently strong molecular beam using the above shown molecule **1** and in addition, we were able to detect the molecule by fluorescence. Unfortunately, it was not possible to observe any interference of the particles in the interferometer. We observed interference pattern that are comparable with molecules having a strong dipole moment. The quantum interference experimental setup in the far-field regime to investigate larger particles needs to be optimized.

6.2 Near-field Interferometry

The main advantage of experiments in the near-field is based on the findings of Talbot and Lau. Using the Talbot-distance between interference grating and detection grating, the grating distance does not need to be reduced that strongly if the particle size is increased. Lau described the use of an additional grating to delimit the molecular beam. This allows the use of alternative more efficient sources.

This part of the doctoral thesis was focused on the synthesis of novel tailor made molecular libraries to be investigated in near-field interferometry. Libraries can be used, since it is possible to select within the interferometer individual member by mass and finally describe the selected particles by mass spectrometry. Experimental optimization towards molecular interferometry using larger particles, are the investigations in beam and ionization properties. To optimize these properties, we successfully synthesized three different molecular libraries represented in Figure 65.

of this size should be around 40 m/s, and at the same time, the intensity of the molecular beam should be high enough with these velocities. We were able to fulfill these properties with both libraries **2Lx** and **3Lx**. Interestingly, library **3Lx** showed slow beams at very high intensity and was found to be thermally more stable than library **2Lx**. Especially library **3Lx** is of great interest for future QIE. In first test syntheses, we showed the synthetically very challenging approach towards even larger oligo-porphyrin systems.

In order to investigate the beam properties by tuning the chemical properties of the particles, we varied the metal-atom in the porphyrin macrocycle as shown in Figure 66 and investigated the optical properties of the particles.

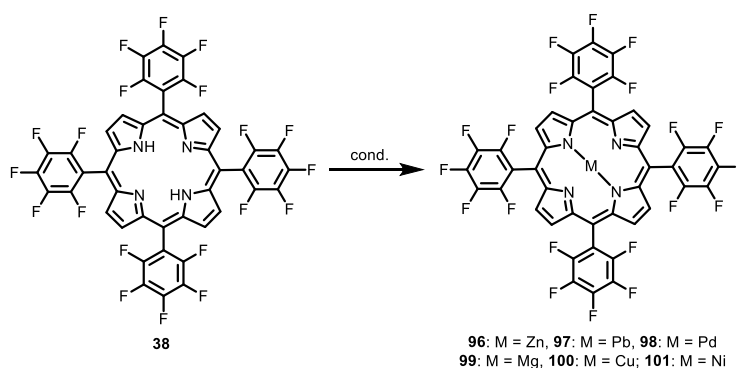


Figure 66. Variation of the metal-atom in the porphyrin macrocycle. Reagents and conditions: **96**: zinc(II) acetate in methanol, dichloromethane, room temperature, 24 h, quant.; **80**: lead(II) acetate, methanol, THF, 80 °C, 4 h, 90 %; **98**: palladium(II) acetate, chloroform, methanol, 40 °C, 48 h, quant.; **99**: magnesium(II) iodide, DIPEA, dichloromethane, room temperature, 3 h, 92 %; **100**: copper(II) acetate, chloroform, methanol, reflux, 3 h, dark, 96 %; **101**: nickel(II)(acac)₂, toluene, reflux, 24 h, 71 %.

We successfully synthesized six different porphyrin systems having different metals in the center of the macrocycle.¹⁵⁵ Having these porphyrins, it is possible quench the fluorescence emission to some extent. The energy is then proposed to be dissipated as thermal emission.^{156–158} In a first experiment we compared the absorption spectra of the metallated porphyrins. All the spectra are represented in Figure 67. Binding a metal to the center of the macrocycle shifts the absorption spectrum considerably in some cases.

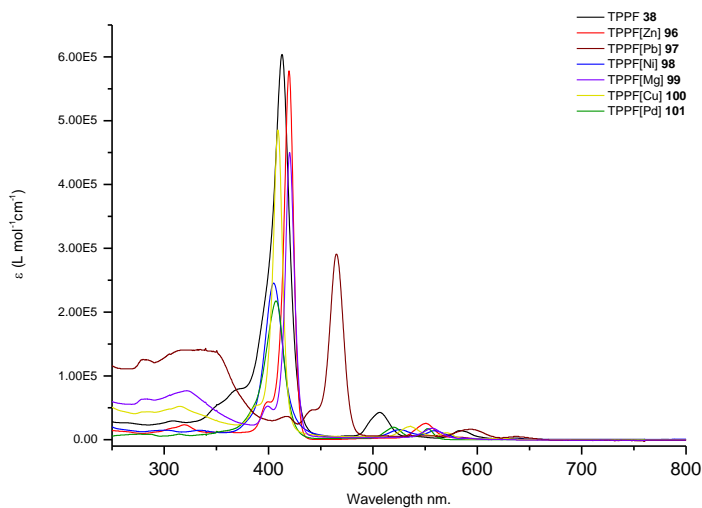


Figure 67. UV-Vis absorbance spectra of metallated porphyrins.

Comparing the emission spectrum of unmetallated porphyrin **38** (Figure 68) with palladium porphyrin **98** (Figure 69) showed enormous differences.

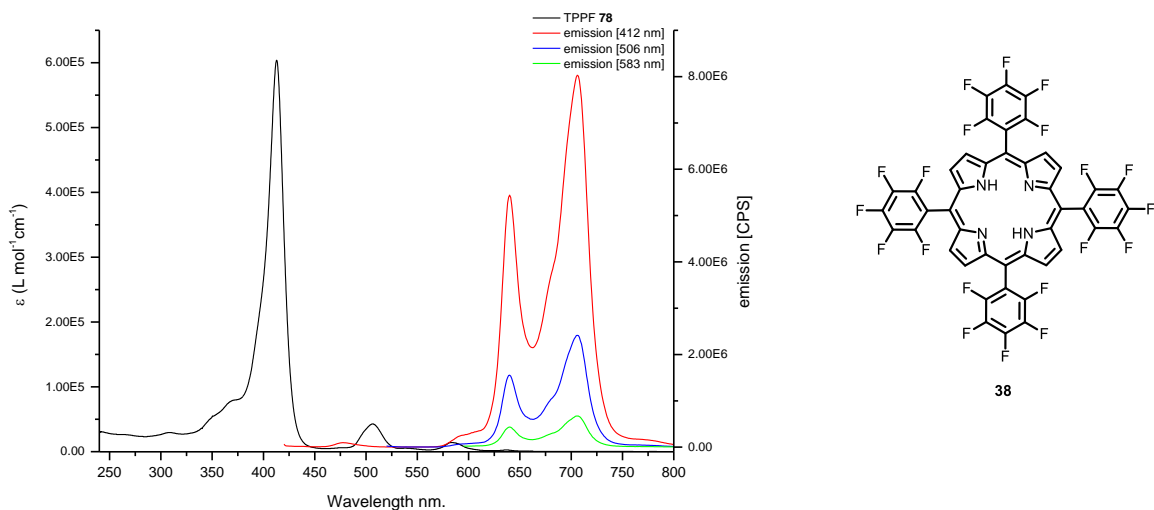


Figure 68. Absorption and emission spectra of *meso*-tetrakis(pentafluorophenyl)porphyrin (**38**).

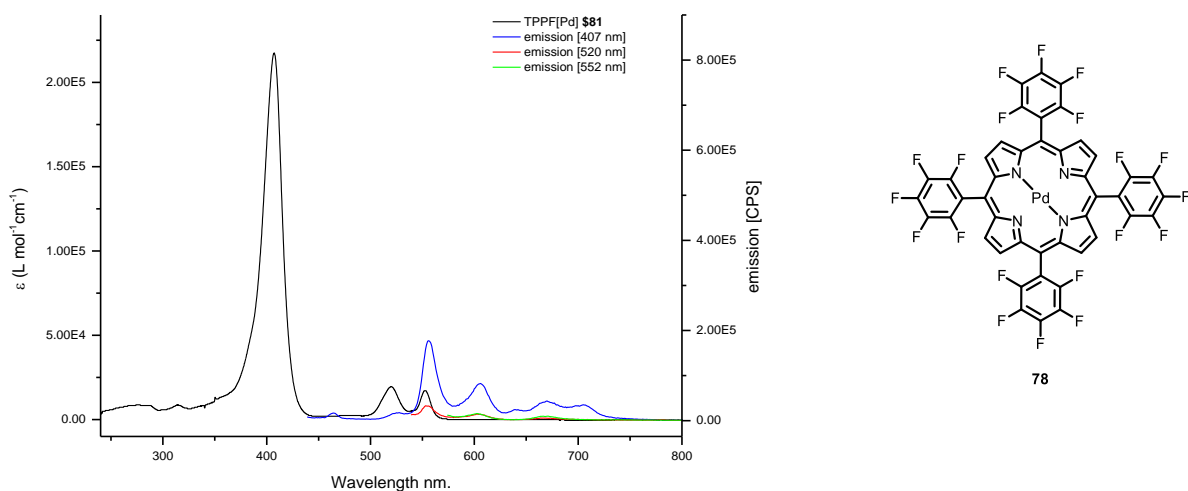


Figure 69. Absorption and emission spectra of *meso*-tetrakis(pentafluorophenyl)porphyrin palladium (**98**).

Irradiation at the B(Soret)-band (412 nm) of metal-free porphyrin **38** did lead to a reliable emission at around 625 and 710 nm. Irradiation on the lower energy Q-bands (506 and 583 nm) did also lead to emission. Comparing the palladium-porphyrin **98** with the metal-free porphyrin **38** the emission has nearly been quenched. We attributed this phenomenon to a heavy metal effect.

Even though we compared only free-base and zinc porphyrins in beam technology studies mentioned above, this feature could be used in future to tune to beam properties in QIE, since the thermal emission energy can be used to launch the particles in a softer way. In a next step, the quantum yields have to be investigated to quantify the quenching effect of the metals in the porphyrin macrocycle.

6.3 Photocleavable Tags

In the last part of this doctoral thesis, we describe the synthesis of photocleavable tags. These tags are attached to central units to obtain model compounds for a general proof of concept. Using a standing light wave the cleavable part should be split of in gas-phase.

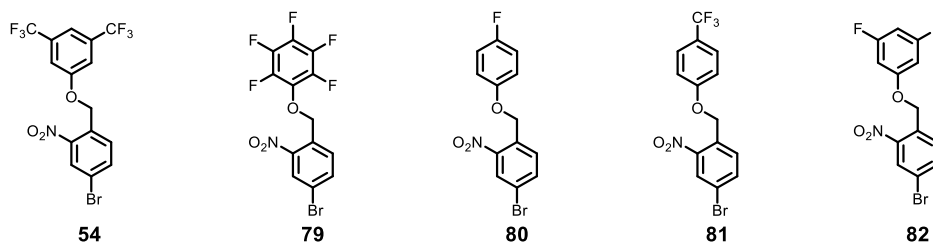


Figure 70. Photocleavable tags synthesized within this work. Further functionalization at peripheral fluorine atoms should be possible.

Unfortunately, first attempts to use click reactions to introduce the tags two, three and four times to a central unit have not been successful yet. We attribute this to the poor solubility of the fluorinated structures in common organic solvents. We found reaction conditions that allow Glaser-Hay couplings to obtain dimer, and Sonogashira cross-coupling reactions to obtain trimers and tetramers of the tags, even though the solubility of the obtained products was very poor. The structures shown in Figure 71 were further investigated in photocleavable experiments.

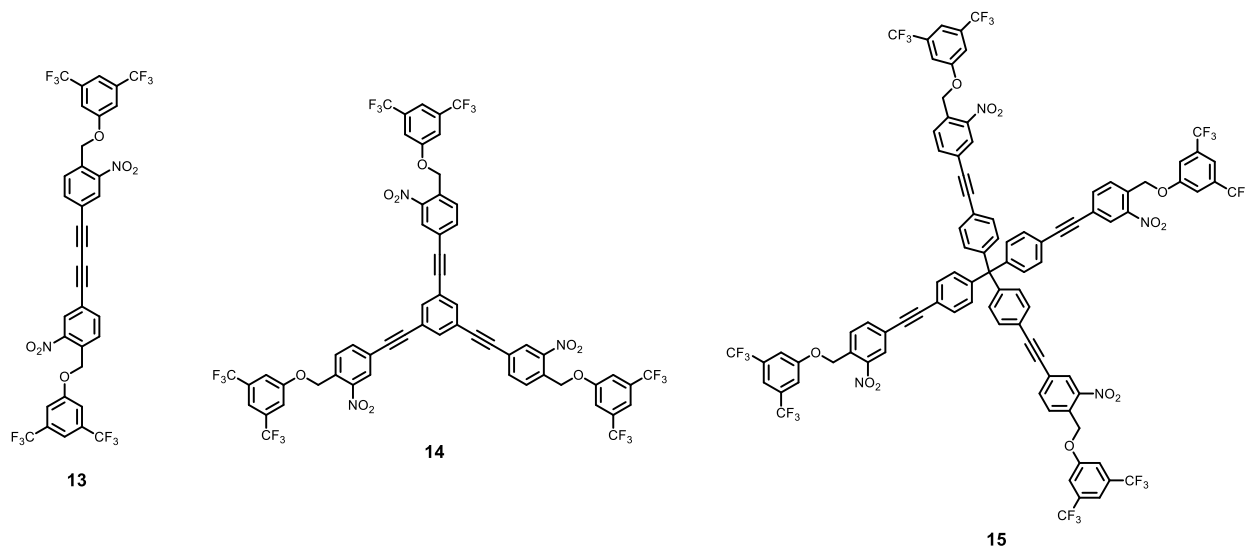


Figure 71. Photocleavable systems synthesized within this work. Photo-dimer **13**, photo-trimer **14** and photo-tetramer **15**.

The three photocleavable systems were obtained for the cleavage experiments. We used a standard laboratory UV-lamp to irradiate on a solution of the photocleavable systems. Light with 254 and 365 nm wavelength was used.

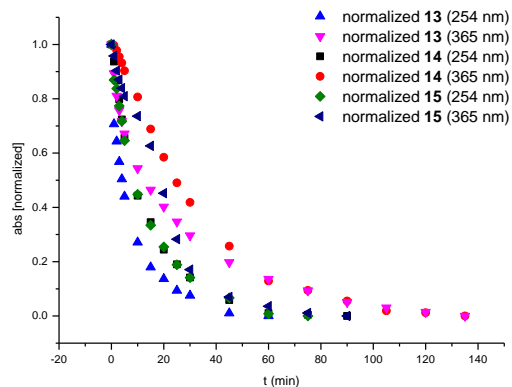


Figure 72. Photocleavable experiment using irradiation of 254 and 365 nm light to cleave the tag at photo-dimer **13**, photo-trimer **14** and photo-tetramer **15**.

The experiment showed decays of all the photocleavable-systems within 60 min when irradiated with 254 nm light and around 120 min when irradiated with 365 nm light (Figure 72). In summary it seems that irradiation at the photo-tetramer **15** is to some extent more efficient than irradiation at the other systems. We have to prove concept using these model compounds for cleavage experiments in gas-phase. With the knowledge of these preliminary experiments, it might be possible to attach the tags to larger biomolecules.

6.4 General Summary and Outlook

Overall, the synthetic approaches described within this doctoral thesis have been very successful. Further improvements in the molecular design could lead to even better beam or detection properties as well as to larger and more massive particles. Furthermore, we described the efficient production of molecular beams using LIAD and desorption experiments. In future QIE in the Arndt group it might be possible to observe interference for the massive particles above 20'000 g/mol.

Nevertheless, the exploration of the borderline of quantum physics and classical physics is mostly limited by the synthetic approach in molecular interference. It is only possible to synthesize small amounts of the oligo-porphyrin systems. We hypothesize that we reached the mass limit of molecules in QIEs.

Newly synthesized tailor made nanoparticles, clusters or proteins are very promising to push the mass limit of interfering particles to even higher masses. It might be possible to use an adapted library-approach to obtain well-separated masses within the synthesis of nanoparticles, clusters or proteins. Another very promising tool is the attachment of photocleavable tags to large bio-molecules or nanoparticles. This would allow the detection of those under mild conditions.

7 Experimental Part

7.1 General Remarks

Reagents and Solvents

All commercially available starting materials were of reagent grade and used as received from Fluka AG (Buchs, Switzerland), Acros AG (Basel, Switzerland), Merck (Darmstadt, Germany), Alfa Aesar (Karlsruhe, Germany), ABCR (Karlsruhe, Germany), Aldrich (Buchs, Switzerland), Fluorochem (Hadfield, United Kingdom) and Porphyrin Systems GbR (Norderstedt, Germany). The solvents for chromatography, crystallization and for extraction were used in technical grade. The solvents for HPLC analyses and GPC were of HPLC grade. Dry THF, dry DMF and dry CH₂Cl₂ were purchased from Acros, stored over 4 Å molecular sieves and handled under argon. For an inert atmosphere, Argon 4.8 from PanGas AG (Dagmersellen, Switzerland) was used.

Syntheses

All reactions with reagents that are sensitive to air or moisture were performed under an argon atmosphere using Schlenk technique, only dry solvents were used and the glassware was heated out before use. In reactions where highly fluorinated compounds were involved the use of glass coated magnetic stirring bars was favored over PTFE (Teflon) bars.

¹H-Nuclear Magnetic Resonance (¹H-NMR)

Bruker DRX-NMR (600 MHz or 500 MHz), Bruker DPX-NMR (400 MHz) and Bruker BZH-NMR (250 MHz) instruments were used to record the spectra. Chemical shifts (δ) are reported in parts per million (ppm) relative to residual solvent peaks (CDCl₃: 7.26 ppm) or trimethylsilane (TMS: 0.00 ppm), and coupling constants (J) are reported in Hertz (Hz). The bond distance of the coupling constant is stated with a superscript number (^{*n*} J). NMR solvents were obtained from Cambridge Isotope Laboratories, Inc. (Andover, MA, USA). The measurements were done at room temperature. The multiplicities are written as s = singlet, d = doublet, t = triplet, q = quartet, quin. = quintet, m = multiplet and brs = broad.

¹³C-Nuclear Magnetic Resonance (¹³C-NMR)

Bruker DRX-NMR (126 MHz) and Bruker DPX-NMR (101 MHz) instruments were used to record the spectra. Chemical shifts (δ) are reported in parts per million (ppm) relative to residual solvent peaks (CDCl₃: 77.0 ppm or TMS: 0.0 ppm). The measurements were performed at room temperature. The multiplicities are written as s = singlet, d = doublet, t = triplet, q = quartet, quin. = quintet and m = multiplet. The coupling constants (*J*) are reported in Hertz (Hz) and are just stated in fluorine containing molecules. The signals of fluoroalkylsulfanyl segments were not assigned due to the coupling to fluorine.

¹⁹F-Nuclear Magnetic Resonance (¹⁹F-NMR)

A Bruker DPX-NMR (377 MHz) instrument was used to record the spectra. Chemical shifts (δ) are reported in parts per million (ppm), uncorrected. The measurements were performed at room temperature. Coupling constants (*J*) are reported in Hertz (Hz). The multiplicities are written as: s = singlet, d = doublet, t = triplet, q = quartet, quin. = quintet, m = multiplet.

Mass Spectrometry (MS)

Matrix-Assisted Laser Desorption Ionization Time of Flight (MALDI-TOF) mass spectra were performed with a Bruker Microflex LRF. MALDI-TOF spectra were calibrated using CsI₃ cluster.¹¹⁸ DCTB (trans-2-[3-(4-tert-Butylphenyl)-2-methyl-2-propenylidene]malononitrile) was used as matrix if needed.¹¹⁹ High-resolution mass spectra were taken on a Bruker solariX (ESI/MALDI-FTICR-MS), Bruker maXis 4G (QTOF-ESI) and a Waters AutoSpec Ultima (EI-triSector-MS). Electron impact (EI) mass spectra were recorded with a Finnigan MAT 95Q. Electron spray ionization (ESI) spectra were taken on a Bruker amaZon X. Electron-impact quadrupole mass spectra (EI-QMS) were recorded on a GCMS-QP2010 SE from Shimadzu.

Elemental Analysis (EA)

Elemental analyses were measured on a Perkin-Elmer Analysator 240. The values are given in mass percent.

Ultraviolet Spectroscopy (UV)

UV/Vis-spectra were recorded on a UV-1800 spectrophotometer from Shimadzu using optical 114-QS Hellma cuvettes (10 mm light path) at room temperature and ambient conditions.

Fluorescence Spectroscopy

Emission spectra were recorded on a Horiba FluoroMax-4 spectrofluorophotometer under ambient conditions.

Gel Permeation Chromatography (GPC)

Gel Permeation Chromatography (GPC) was performed on a Shimadzu Prominence System with PSS SDV preparative columns from PSS (2 columns in series: 600 mm x 20.0 mm, 5 μ m particles, linear porosity "S", operating ranges: 100 – 100 000 g/mol) using chloroform as eluent.

Column Chromatography (CC)

For CC silica gel 60 (particle size 40-63 μ m) from SiliCycle or silica gel 60 (particle size 40-63 μ m) from Fluka was used.

Thin Layer Chromatography (TLC)

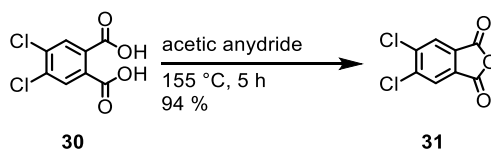
Silica gel 60 F254 glass plates with a thickness of 0.25 mm from Merck were used. For detection, a UV lamp with 254 nm or 366 nm was used.

Microwave Reactions

Microwave reactions were carried out in an Initiator 8 (400 W) from Biotage[®].

7.2 Synthetic Procedures

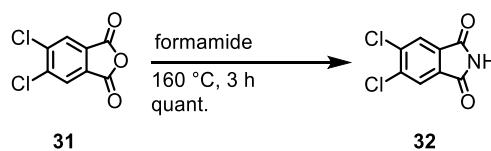
5,6-Dichloroisobenzofuran-1,3-dione (**31**)⁷¹



4,5-Dichlorophthalic acid (**30**, 30 g, 128 mmol, 1.0 equiv.) and acetic anhydride (50 ml) were heated to reflux for 5 h with slow distilling off of acetic acid. The suspension was allowed to cool to room temperature and then filtered. The solid residue was washed excessively with n-hexane and pentane and dried under high vacuum to obtain 5,6-dichloroisobenzofuran-1,3-dione (**31**) in 94 % yield as a colorless solid (25.3 g, 117 mmol, 215.94 g/mol).

¹H-NMR (400 MHz, *d*-acetone, δ /ppm): 8.33 (s, 2 H, Ar-H).

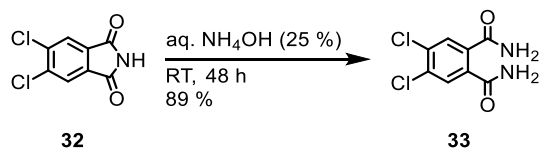
All analytical data were comparable to literature values.

5,6-Dichloroisindoline-1,3-dione (32)⁷¹

5,6-Dichloroisobenzofuran-1,3-dione (**31**, 25.9 g, 117 mmol, 1.0 equiv.) was heated to reflux in formamide (35 ml, 876 mmol, 7.5 equiv.) for 3 h. The suspension was cooled to room temperature and the reaction mixture was filtered. The solid residue was washed with water and dried at high vacuum yielding 5,6-dichloroisindoline-1,3-dione (**32**) as a colorless solid in quantitative yield (25.3 g, 117 mmol, 214.95 g/mol).

¹H-NMR (400 MHz, *d*-acetone, δ /ppm): 2.90 (brs, 1 H, NH), 8.02 (s, 2 H, Ar-H).

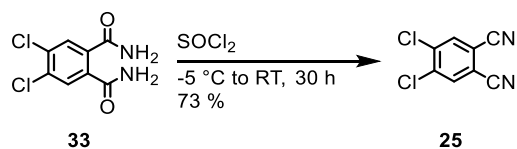
All analytical data were comparable to literature values.

4,5-Dichlorophthalamide (33)⁷¹

5,6-Dichloroisindoline-1,3-dione (**32**, 25.3 g, 117 mmol, 1.0 equiv.) was treated with ammonium hydroxide (300 ml, 25 % in H₂O) and stirred for 24 h. Another portion of ammonium hydroxide (100 ml, 25 % in H₂O) was added and the reaction stirred for additional 24 h. The colorless solid was filtered off and washed with water. The remaining colorless solid was dried under high vacuum for 48 h yielding 4,5-dichlorophthalamide (**33**) in 89 % (24.9 g, 106.83 mmol, 231.98 g/mol).

¹H-NMR (400 MHz, *d*-acetone, δ /ppm): 6.96 (brs, 2 H, NH₂), 7.59 (brs, 2 H, NH₂), 7.80 (s, 2 H, Ar-H).

All analytical data were comparable to literature values.

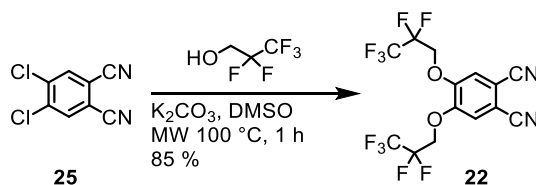
4,5-Dichlorophthalonitrile (25)⁷¹

Thionylchloride (85 ml, 1.17 mol, 11.0 equiv.) was stirred in DMF (85 ml) at 0 °C for 2 h. 4,5-Dichlorophthalamide (**33**, 24.9 g, 107 mmol, 1.0 equiv.) was added and the reaction stirred at 0-5 °C for 4 h. The reaction mixture was stirred for 24 h at RT and poured into ice water. The white precipitate was filtered off and washed with cold water. The crude product was recrystallized from methanol to give the 4,5-dichlorophthalonitrile (**25**) as a colorless solid in 73 % yield (15.4 g, 78.0 mmol, 195.96 g/mol).

¹H-NMR (400 MHz, *d*-acetone, δ /ppm): 7.91 (s, 2 H, Ar-H).

¹³C NMR (126 MHz, *d*-acetone, δ /ppm): δ = 113.63, 115.10, 134.98, 139.09.

MS (EI-QMS): *m/z* (%): 196.0 (100) [M]⁺, 198.0 (64), 200.0 (10).

4,5-Bis(2,2,3,3,3-pentafluoropropoxy)phthalonitrile (22)

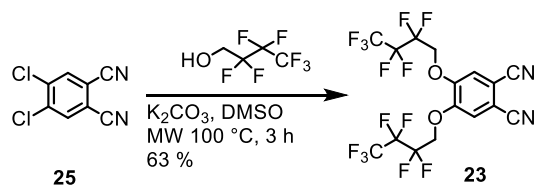
4,5-Dichlorophthalonitrile (**25**, 201 mg, 1.02 mmol, 1.0 equiv.), pentafluoropropan-1-ol (0.92 ml, 6.12 mmol, 6.0 equiv.) and potassium carbonate (854 mg, 6.12 mmol, 6.0 equiv.) were added to dry DMSO (10 ml) in a microwave vial (Biotage[®] microwave vial 10-20 ml). The sealed tube was heated to 100 °C in the microwave apparatus for 3 h. After cooling to room temperature, water was added and the mixture extracted with dichloromethane. The combined organic phases were washed with water and brine. After evaporation of the solvent under reduced pressure the crude product was purified by column chromatography (silica gel, cyclohexane/ethyl acetate, 4:1) yielding 4,5-bis(2,2,3,3,3-pentafluoropropoxy)phthalonitrile (**22**) in 85 % as a colorless solid (367 mg, 0.87 mmol, 424.03 g/mol).

¹H-NMR (400 MHz, CDCl₃, δ/ppm): 4.55 (t, ³J_{HF} = 11.6 Hz, 4 H, CH₂), 7.31 (s, 2 H, Ar-H).

¹⁹F-NMR (376 MHz, CDCl₃, δ/ppm): -83.4 (m, 6 F, CF₃), -123.2 (m, 4 F, CF₂).

¹³C NMR (126 MHz, CDCl₃, δ/ppm): 66.21 (t), 111.50, 114.52, 119.19, 150.69.

MS (EI-QMS): *m/z* (%): 424.0 (100) [M]⁺, 305.0 (20), 172.0 (26).

4,5-Bis(2,2,3,3,4,4,4-heptafluorobutoxy)phthalonitrile (**23**)

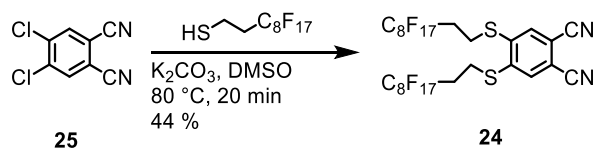
4,5-Dichlorophthalonitrile (**25**, 201 mg, 1.02 mmol, 1.0 equiv.), pentafluorobutan-1-ol (0.77 ml, 6.12 mmol, 6.0 equiv.) and potassium carbonate (854 mg, 6.12 mmol, 6.0 equiv.) were added to dry DMSO (10 ml) in a microwave vial (Biotage[®] microwave vial 10-20 ml). The sealed tube was heated to $100\text{ }^\circ\text{C}$ in the microwave apparatus for 1 h. After cooling to room temperature, water was added and the mixture extracted with dichloromethane. The combined organic phases were washed with water and brine. After evaporation of the solvent under reduced pressure the crude product was purified by column chromatography (silica gel, cyclohexane/ethyl acetate, 6:1) obtaining 4,5-bis(2,2,3,3,4,4,4-heptafluorobutoxy)phthalonitrile (**23**) as colorless solid in 63 % yield (339 mg, 0.65 mmol, 524.02 g/mol).

¹H-NMR (400 MHz, $CDCl_3$, δ /ppm): 4.60 (t, $^3J_{HF} = 12.2$ Hz, 4 H, CH_2), 7.33 (s, 2 H, Ar-H).

¹⁹F-NMR (376 MHz, $CDCl_3$, δ /ppm): -80.7 (m, 6 F, CF_3), -120.4 (m, 4 F, CF_2), -127.4 (m, 4 F, CF_2).

¹³C NMR (126 MHz, $CDCl_3$, δ /ppm): 66.32 (t), 111.49, 114.51, 119.35, 150.73.

MS (EI-QMS): m/z (%): 524.0 (100) $[M]^+$, 172.1 (69), 69.0 (56).

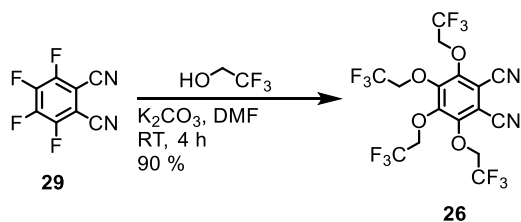
4,5-Bis((3,3,4,4,5,5,6,6,7,7,8,8,9,9,10,10-heptafluorodecyl)thio)phthalonitrile (24)

1H,1H,2H,2H-Perfluorodecanethiol (449 μ l, 1.52 mmol, 3 equiv.) and K₂CO₃ (425 mg, 3.04 mmol, 6 equiv.) were dissolved in dry DMSO (5 ml) under an argon atmosphere and stirred for 15 minutes. The reactant 4,5-dichlorophthalonitrile (**25**, 100 mg, 0.51 mmol, 1.0 equiv.) was added, the reaction mixture heated to 80 °C and there stirred for 20 min. Water was added and the reaction mixture cooled to room temperature, the suspension was filtered and the black residue dissolved in acetone. The solvent was removed under reduced pressure and the resulting solid purified by column chromatography (silica gel, hexane/ ethyl acetate, 6:1) to yield in 44 % 4,5-bis-(*1H,1H,2H,2H*-perfluorodecylthio)-phthalonitrile (**24**) as a colorless solid (242 mg, 0.223 mmol, 1083.97 g/mol).

¹H-NMR (400 MHz, CDCl₃, δ /ppm): 2.50 (m, 4 H, CH₂), 3.26 (m, 4 H, CH₂), 7.55 (s, 2 H, Ar-H).

¹⁹F-NMR (376 MHz, CDCl₃, δ /ppm): 80.7 (m, 6 F, CF₃), -114.0 (m, 4 F, CF₂), -121.6 (m, 4 F, CF₂), -121.9 (m, 8 F, 2 x CF₂), -122.7 (m, 4 F, CF₂), -123.1 (m, 4 F, CF₂), -126.1 (m, 4 F, CF₂).

MS (MALDI-TOF): *m/z* (%): 1083.75 (58) [M]⁺, 1084.76 (100) [M+H]⁺, 1085.75 (48), 1086.76 (46), 1087.77 (22), 1088.78 (23), 1089.77 (18).

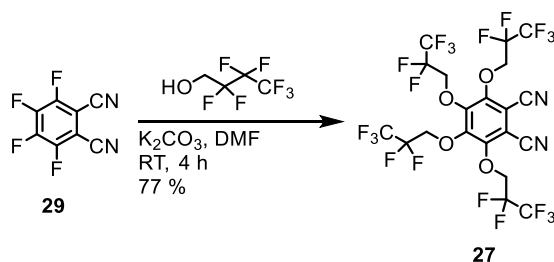
3,4,5,6-Tetrakis(2,2,2-trifluoroethoxy)phthalonitrile (26)¹⁵⁹

3,4,5,6-Tetrafluorophthalonitrile (**29**, 450 mg, 2.14 mmol, 1.0 equiv.), 2,2,2-trifluoroethan-1-ol (1.54 ml, 21.4 mmol, 10 equiv.) and potassium carbonate (2.98 g, 21.4 mmol, 10 equiv.) were dissolved in dry DMF (6 ml) and stirred under an atmosphere of argon for 4 h. The reaction mixture was poured into water (25 ml) and the solid was filtered off. The colorless solid residue was washed with water and dried under high vacuum to yield 3,4,5,6-tetrakis(2,2,2-trifluoroethoxy)phthalonitrile (**26**) as a colorless solid in 90 % yield (1.0 g, 1.92 mmol, 520.03 g/mol).

¹H-NMR (400 MHz, CDCl₃, δ/ppm): 4.88-4.95 (q, ³J_{HF} = 8.5 Hz, 4 H, CH₂), 4.91-4.97 (m, 4 H, ³J_{HF} = 8.5 Hz, CH₂).

¹⁹F-NMR (376 MHz, CDCl₃, δ/ppm): -75.2 (m, 6 F, CF₃), -75.4 (m, 6 F, CF₃).

MS (EI-QMS): *m/z* (%): 520.0 (86) [M]⁺, 437 (100), 409.0 (29), 327.0 (26), 83.0 (24).

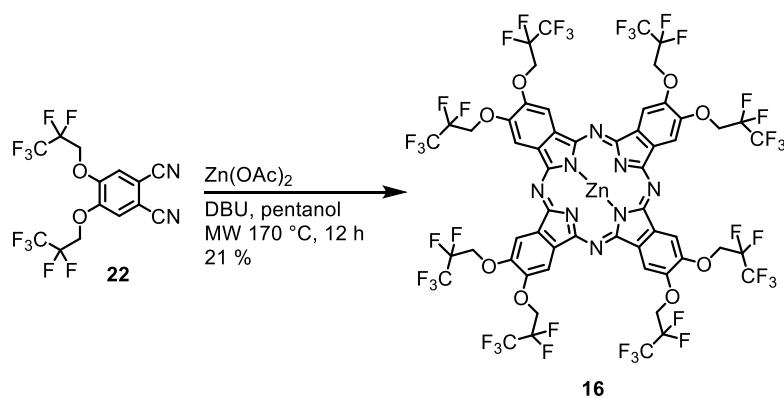
3,4,5,6-Tetrakis(2,2,3,3,3-pentafluoropropoxy)phthalonitrile (27)¹⁵⁹

3,4,5,6-Tetrafluorophthalonitrile (**29**, 450 mg, 2.14 mmol, 1.0 equiv.), *1H,1H*-pentafluoropropan-1-ol (3.21 ml, 21.4 mmol, 10 equiv.) and potassium carbonate (2.98 g, 21.4 mmol, 10 equiv.) were dissolved in dry DMF (6 ml) and stirred under an atmosphere of argon for 4 h. The reaction mixture was poured into water (25 ml) and the solid was filtered off. The colorless solid residue was washed with water and dried under high vacuum to obtain 3,4,5,6-tetrakis(2,2,3,3,3-pentafluoropropoxy)phthalonitrile (**27**) as a colorless solid in 77 % yield (1.18 g, 1.64 mmol, 720.02 g/mol).

¹H-NMR (400 MHz, CDCl₃, δ/ppm): 4.57-4.71 (m, 8 H, CH₂).

¹⁹F-NMR (376 MHz, CDCl₃, δ/ppm): -84.3 (m, 6 F, CF₃), -84.5 (m, 6 F, CF₃), -124.9 (m, 4 F, CF₂), -125.1 (m, 4 F, CF₂).

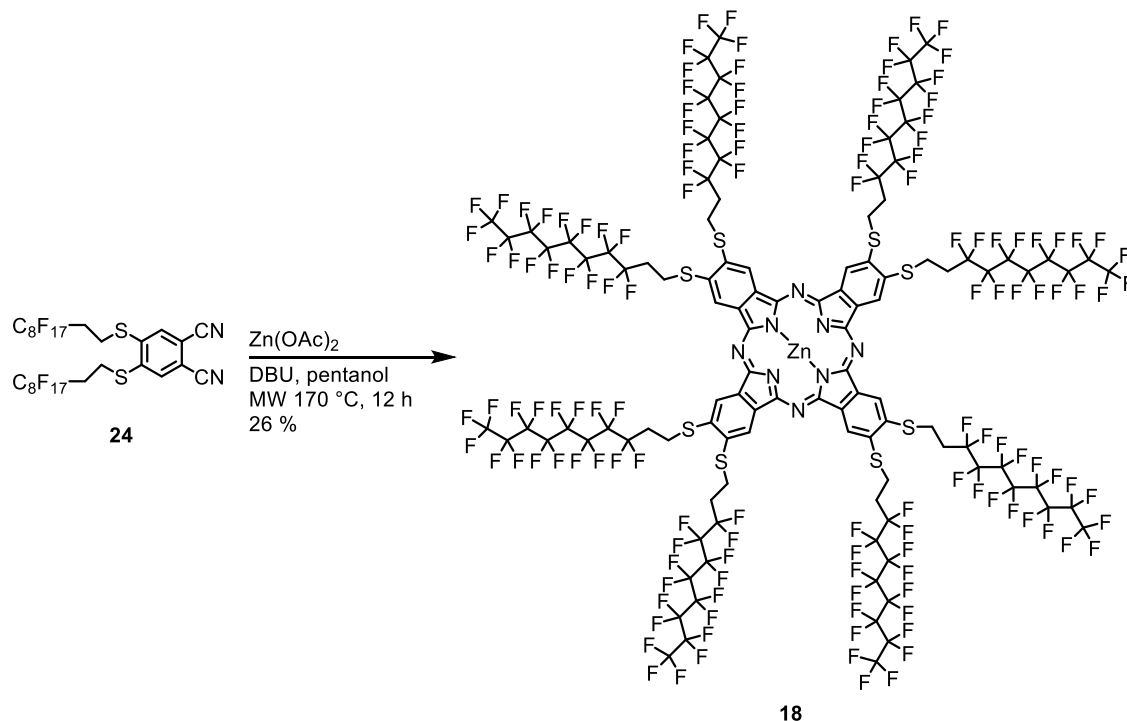
MS (EI-QMS): *m/z* (%): 720.0 (100) [M]⁺, 701.0 (17), 602.0 (53), 587.0 (71), 469.0 (36), 335.0 (13), 133.0 (14), 69.0 (15).

Zinc 2,3,9,10,16,17,23,24-octakis(2,2,3,3,3-pentafluoropropoxy)phthalocyanine (16)

4,5-Bis(2,2,3,3,3-pentafluoropropoxy)phthalonitrile (**22**, 212 mg, 0.5 mmol, 1.0 equiv.), zinc acetate (22.9 mg, 0.125 mmol, 0.25 equiv.) and DBU (76 μ l, 0.5 mmol, 1.0 equiv.) were added to pentanol (5 ml) in a microwave tube (Biotage[®] microwave vial 2-5 ml). The sealed tube was heated in the microwave apparatus to 170 °C for 12 h. After cooling to room temperature the solvent was removed by distillation at ambient pressure. TBME was added and the solution washed excessively with water and brine. The solvent was removed under reduced pressure and the resulting solid was purified by column chromatography (silica gel, diethyl ether/hexane, 8:2) to obtain zinc 2,3,9,10,16,17,23,24-octakis(2,2,3,3,3-pentafluoropropoxy)phthalocyanine (**16**) as a dark blue solid in 21 % yield (21 mg, 0.027 mmol, 1760.04 g/mol). Due to low solubility of the phthalocyanine only MALDI-TOF analysis were performed.

MS (MALDI-TOF): m/z (%): 1759.31 (100) [M]⁺, 1760.30 (73), 1761.33 (76), 1762.32 (58), 1763.31 (62), 1764.33 (40), 1765.28 (22).

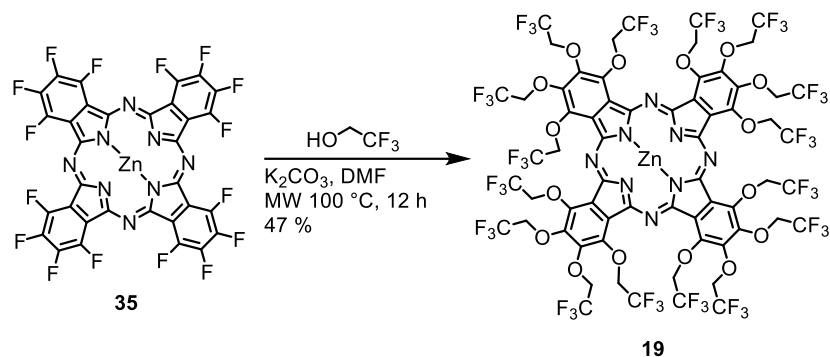
Zinc 2,3,9,10,16,17,23,24-octakis((3,3,4,4,5,5,6,6,7,7,8,8,9,9,10,10,10-heptafluorodecyl)thio)phthalocyanine (18)



4,5-Bis-(1*H*,1*H*,2*H*,2*H*-perfluorodecylthio)-phthalonitrile (**24**, 163 mg, 0.15 mmol, 1.0 equiv.), zinc acetate (7 mg, 0.038 mmol, 0.25 equiv.) and DBU (23 μl , 0.5 mmol, 1.0 equiv.) were added to pentanol (3.5 ml) in a microwave tube (Biotage[®] microwave vial 2-5 ml). The sealed tube was heated in the microwave apparatus to 170 $^\circ\text{C}$ for 12 h. After cooling to room temperature, the solvent was removed by distillation at ambient pressure. TBME was added and the solution washed excessively with water and brine. The solvent was removed under reduced pressure and the resulting solid purified by column chromatography (silica gel, diethyl ether/hexane, 8:2) to obtain zinc 2,3,9,10,16,17,23,24-octakis((3,3,4,4,5,5,6,6,7,7,8,8,9,9,10,10,10)heptafluoro-decyl)thio)phthalocyanine (**18**) as a dark blue solid in 26 % yield (26 mg, 0.006 mmol, 4399.83 g/mol). Due to low solubility of the phthalocyanine only MALDI-TOF analysis were performed.

MS (MALDI-TOF): m/z (%): 4400.88 (100) $[\text{M}+\text{H}]^+$.

Zinc 1,2,3,4,8,9,10,11,15,16,17,18,22,23,24,25-hexadecakis(2,2,2-trifluoroethoxy)-phthalocyanine (19)



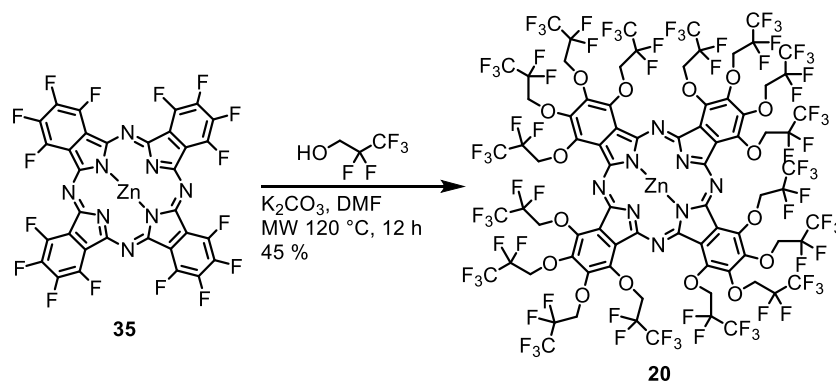
Trifluoroethanol (350 μl , 4.64 mmol, 40 equiv.), Zinc 1,2,3,4,8,9,10,11,15,16,17,18,22,23,24,25-hexadecafluorophthalocyanine (**35**, 100 mg, 0.116 mmol, 1.0 equiv.) and potassium carbonate (650 mg, 4.64 mmol, 40 equiv.) were dissolved in DMF (1.5 ml) in a microwave tube (Biotage microwave vial 1-2 ml). The sealed tube was heated in the microwave apparatus to 100 °C for 12 h. The reaction mixture was extracted with TBME and washed three times with water and brine. After drying over anhydrous Na_2SO_4 , the solvent was removed under reduced pressure. The resulting residue was purified by column chromatography (silica gel, cyclohexane/acetone, 1:1) zinc 1,2,3,4,8,9,10,11,15,16,17,18,22,23,24,25-hexadecakis(2,2,2-trifluoroethoxy) phthalocyanine (**19**) was obtained as a green solid in a yield of 47 % (117 mg, 0.055 mmol, 2144.05 g/mol).

¹H-NMR (400 MHz, CDCl_3 , δ/ppm): 5.16 (q, $^3J_{\text{HF}} = 8.5$ Hz, 16 H, CH_2), 5.77 (q, 16 H, $^3J_{\text{HF}} = 8.7$ Hz, CH_2).

¹⁹F-NMR (376 MHz, CDCl_3 , δ/ppm): -74.8 (m, 24 F, CF_3), -75.3 (m, 24 F, CF_3).

MS (MALDI-TOF): m/z (%): 2143.76 (73) $[\text{M}]^+$, 2144.76 (94) $[\text{M}+\text{H}]^+$, 2145.70 (100), 2146.65 (86), 2147.61 (77), 2148.62 (59), 2149.61 (33), 2150.62 (15).

Zinc 1,2,3,4,8,9,10,11,15,16,17,18,22,23,24,25-hexadecakis(2,2,3,3,3-pentafluoropropoxy)phthalocyanine (20)

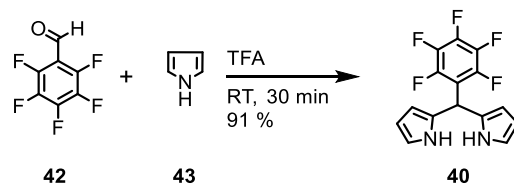


1H,1H-Pentafluoropropanol (460 μ l, 4.64 mmol, 40 equiv.), Zinc 1,2,3,4,8,9,10,11,15,16,17,18,22,23,24,25-hexadecafluorophthalocyanine (**35**, 100 mg, 0.116 mmol, 1.0 equiv.) and potassium carbonate (650 mg, 4.64 mmol, 40 equiv.) were dissolved in DMF (1.5 ml) in a microwave tube (Biotage[®] microwave vial 1-2 ml). The sealed tube was heated in the microwave apparatus to 100 °C for 12 h. The reaction mixture was extracted with TBME and washed three times with water and brine. After drying over anhydrous Na₂SO₄, the solvent was removed under reduced pressure. The resulting residue was purified by column chromatography (silica gel, cyclohexane/acetone, 1:1) zinc phthalocyanine (**20**) was obtained as a green solid in a yield of 45 % (151 mg, 0.052 mmol, 2945.00 g/mol).

¹H-NMR (400 MHz, CDCl₃, δ /ppm): 4.75 (q, ³*J*_{HF} = 8.4 Hz, 16 H, CH₂), 4.91 (q, 16 H, ³*J*_{HF} = 8.7 Hz, CH₂).

¹⁹F-NMR (376 MHz, CDCl₃, δ /ppm): -84.7 (m, 24 F, CF₃), -84.9 (m, 24 F, CF₃), -125.2 (m, 16 F, CF₃), -125.6 (m, 16 F, CF₃).

MS (MALDI-TOF): *m/z* (%): 2943.62 (32), 2944.66 (83) [M]⁺, 2945.53 (99) [M]⁺, 2946.46 (100), 2947.38 (88), 2948.33 (75), 2949.28 (63), 2950.28 (31), 2951.24 (16).

5-(Pentafluorophenyl)-dipyrrolmethane (40)⁷⁵

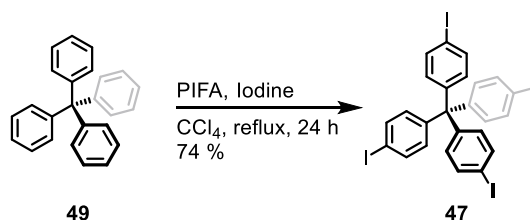
Pentafluorobenzaldehyde (**42**, 6.21 ml, 50.0 mmol, 1.0 equiv.) was dissolved in freshly distilled pyrrole (**43**) (192 ml, 2.75 mol, 55 equiv.) and degassed in an argon stream for 20 min. TFA (372 μ l, 570 mg, 5.00 mmol, 0.1 equiv.) was added and the mixture stirred at room temperature for 30 min. The reaction mixture was extracted with dichloromethane and washed with aq. NaOH (0.1 M), water and brine. Combined organic phases were dried over anhydrous Na_2SO_4 and the solvent removed under reduced pressure. The remaining solid was recrystallized from dichloromethane/cyclohexane (1:1) to obtain 5-(pentafluorophenyl)-dipyrrolmethane (**40**) as a colorless solid in 91 % yield (5.43 g, 312.24 g/mol, 17.4 mmol).

¹H-NMR (400 MHz, CDCl_3 , δ /ppm): 5.89 (s, 1 H, CH), 6.02 (m, 2 H, Ar-H), 6.16 (m, 2 H, Ar-H), 6.72 (m, 2 H, Ar-H), 8.10 (brs, 2 H, NH).

¹⁹F-NMR (376 MHz, CDCl_3 , δ /ppm): -141.5 (m, 1 F Ar-F), -155.7 (m, 2 F, Ar-F), -161.2 (m, 2 F, Ar-F).

¹³C-NMR (101 MHz, CDCl_3 , δ /ppm): 33.1, 107.7, 108.7, 118.2, 128.1, 136.8, 138.8, 144.0, 146.0.

MS (ED): m/z (%) = 312 (100) $[\text{M}]^+$, 246 (35), 226 (7), 145 (41), 67 (12).

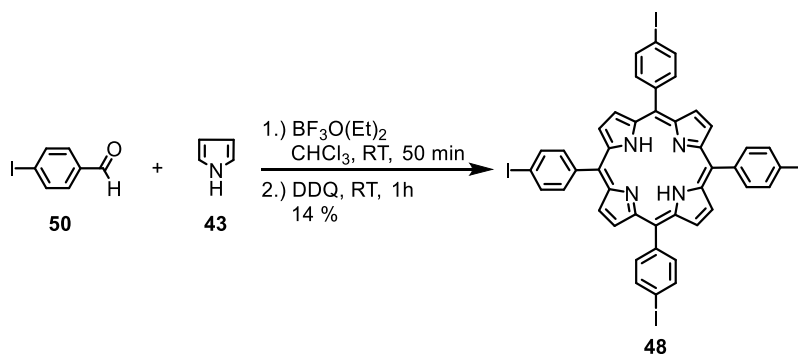
Tetrakis(4-iodophenyl)methane (47)¹¹⁵

A suspension of tetraphenylmethane (**49**, 154 mg, 0.48 mmol, 1.0 equiv.), [bis(trifluoroacetoxy)iodo]benzene (PIFA) (514 mg, 1.20 mmol, 2.5 equiv.) and iodine (366 mg, 1.44 mmol, 3.0 equiv.) in carbon tetrachloride (5 ml) was heated to reflux for 24 h. The suspension was then filtered and the resulting pink residue washed with dichloromethane. The solvent was removed under reduced pressure and the resulting dried at high vacuum to give the tetrakis(4-iodophenyl)methane (**47**) as a pink solid in a yield of 74 % (292 mg, 0.35 mmol, 824.02 g/mol).

¹H-NMR (400 MHz, CDCl₃, δ /ppm): 6.88 (d, $^3J_{\text{HH}} = 8.4$ Hz, 8 H, Ar-H), 7.93 (d, $^3J_{\text{HH}} = 8.4$ Hz, 8 H, Ar-H).

¹³C-NMR (101 MHz, CDCl₃, δ /ppm): 92.5, 100.0, 132.6, 137.1, 145.1.

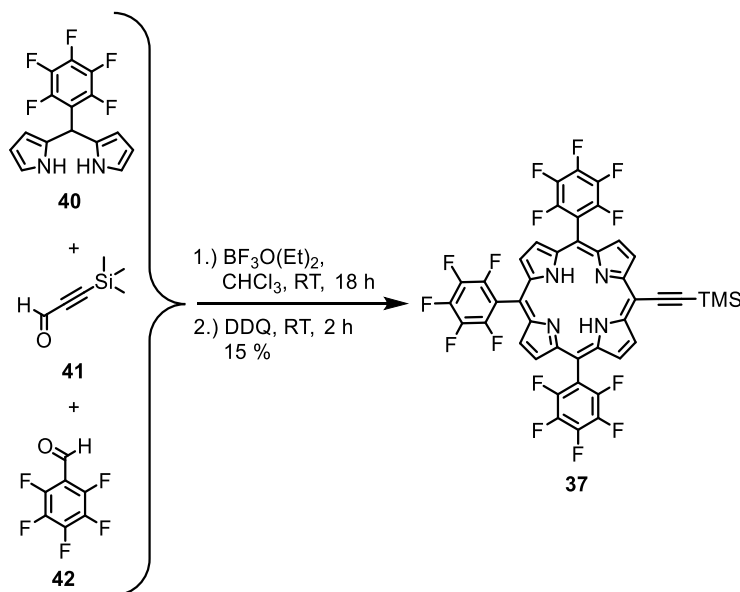
MS (ED): m/z (%): 824 (52) [M]⁺, 696.9 (13), 620.8 (100), 494.9 (10), 367.0 (11), 239.1 (29).

meso-Tetrakis(4-iodophenyl)porphyrin (**48**)⁸⁴

Freshly distilled pyrrole (**43**, 21.5 μl , 0.62 mmol, 1.0 equiv.) and 4-iodobenzaldehyde (**50**, 144 mg, 0.62 mmol, 1.0 equiv.) were dissolved in chloroform (60 ml) and degassed in a constant argon stream for 30 min. A solution of $\text{BF}_3 \cdot \text{O}(\text{Et})_2$ (2.5 M in CHCl_3 , 81 μl , 0.33 equiv.) was added. The reaction was stirred for 50 min at room temperature before DDQ (108 mg, 0.47 mmol, 0.75 equiv.) was added. After stirring for another hour, triethylamine (88 μl , 0.62 mmol, 1.0 equiv.) was added to quench excess acid. The solvent was removed under reduced pressure and the resulting residue purified by column chromatography (silica gel, dichloromethane) to yield *meso*-tetrakis(4-iodophenyl)porphyrin (**48**) in 14 % as a dark purple solid (25 mg, 22.4 μmol , 1118.34 g/mol).

$^1\text{H-NMR}$ (400 MHz, CDCl_3 , δ/ppm): -2.88 (s, 2 H, NH), 7.93 (d, $^3J_{\text{HH}} = 8.2$ Hz, 8 H, Ar-H), 8.11 (d, $^3J_{\text{HH}} = 8.2$ Hz, 8 H, Ar-H), 8.84 (s, 8 H, Ar-H).

MS (MALDI-TOF): m/z (%): 1119.5 (100) $[\text{M}+\text{H}]^+$.

5,10,15-Tris(pentafluorophenyl)-20-(2-trimethylsilyl ethynyl)-porphyrin (**37**)

A solution of pentafluorobenzaldehyde (**42**, 2.74 ml, 22 mmol, 2.0 equiv.), 3-(trimethylsilyl)-2-propynal (**41**, 1.84 ml, 12 mmol, 1.1 equiv.) and 5-(pentafluorophenyl)-dipyrromethane (**40**, 6.9 g, 22 mmol, 2.0 equiv.) in chloroform (2.5 l) was degassed in a constant argon stream for 45 min and then treated with $\text{BF}_3\text{O}(\text{Et})_2$ (2.5 M in CHCl_3 , 2.92 ml, 0.66 equiv.). The reaction was stirred at room temperature for 18 h. DDQ (7.68 g, 1.5 mmol, 3.0 equiv.) was added and the reaction mixture stirred for another 2 h at room temperature. After filtration through silica, the solvent was removed under reduced pressure. The remaining solid was purified three times by column chromatography (silica gel; cyclohexane/dichloromethane, 5:1) to obtain 5,10,15-tris(pentafluorophenyl)-20-(2-trimethylsilyl ethynyl)-porphyrin (**37**) as a dark purple solid in 15 % yield (1.52 g, 11.1 mol, 904.11 g/mol).

$^1\text{H-NMR}$ (400 MHz, CDCl_3 , δ/ppm): -2.55 (brs, 2 H, NH), 0.65 (s, 9 H, TMS), 8.85 (s, 4 H, Ar-H), 8.88 (d, $^3J_{\text{HH}} = 4.8$ Hz, 2 H, Ar-H), 9.80 (d, $^3J_{\text{HH}} = 4.8$ Hz, 2 H, Ar-H).

$^{19}\text{F-NMR}$ (376 MHz, CDCl_3 , δ/ppm): -136.5 (m, 2 F, Ar-F), -136.6 (m, 4 F, Ar-F), -151.5 (m, 3 F, Ar-F), -161.5 (m, 6 F, Ar-F).

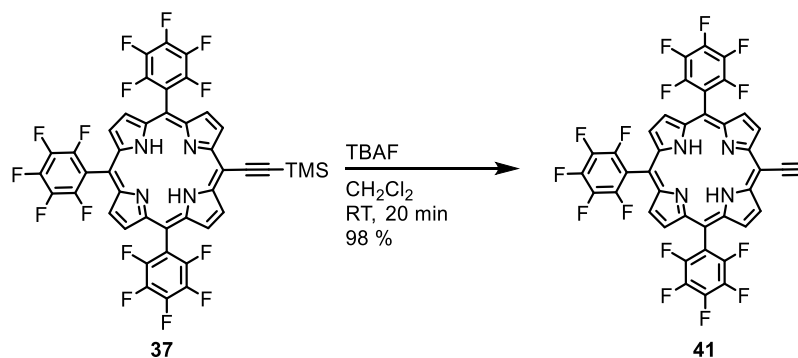
$^{13}\text{C-NMR}$ (126 MHz, CDCl_3 , δ/ppm): 0.68 (s, 3Cs, TMS), 102.65 (s, Cq, 1C), 103.36 (s, Cq, 1C), 103.69 (s, Cq, 2C), 104.55 (s, Cq, 1C), 105.56 (s, Cq, 1C), 115.36 (s, Cq, 1C), 115.59 (s, Cq, 2C), 130.25 (m, Ct, 2C), 130.90 (m, Ct, 2C), 130.94 (m, Ct, 2C), 132.40 (m, Ct, 2C), 137.55 (s, Ct, 2C), 137.57 (s, Ct, 4C), 146.47 (m, Ct, 4C), 146.50 (m, Ct, 2C).

MS (MALDI-TOF): m/z (%): 904.2 (100) $[M]^+$, 905.2 (82), 906.1 (27), 907.1 (10).

UV/Vis (CHCl_3): $\lambda = 415, 508, 536, 584$ nm.

HRMS (MALDI/ESI): m/z calcd for $\text{C}_{43}\text{H}_{19}\text{F}_{15}\text{N}_4\text{Si}$: 904.1134; found 904.1136.

EA $\text{C}_{43}\text{H}_{19}\text{F}_{15}\text{N}_4\text{Si}$ (904.11): calcd C 57.09, H 2.12, N 6.19 ; found C 57.45, H 2.49, N 6.62.

5,10,15-Tris(pentafluorophenyl)-20-(ethynyl)-porphyrin (41)

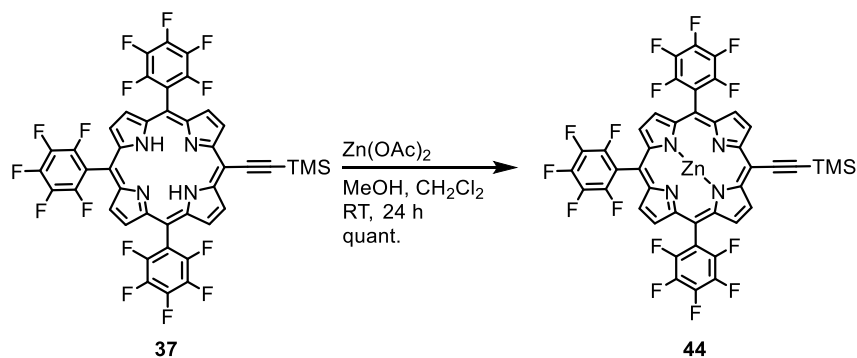
5,10,15-Tris(pentafluorophenyl)-20-(2-trimethylsilyl-ethynyl)-porphyrin (**37**, 100 mg, 0.11 mmol, 1.0 equiv.) was dissolved in dichloromethane (50 ml) and TBAF (1 M in THF, 220 μ l, 0.22 mmol, 2.0 equiv.) was added dropwise. The reaction mixture was stirred for 20 min at room temperature. Then methanol (50 ml) was added and the solvent removed under reduced pressure. The resulting solid was dissolved in dichloromethane (50 ml) and washed with water and brine. The organic layer were dried over anhydrous Na₂SO₄ and the solvent removed under reduced pressure. The resulting solid was purified by column chromatography (silica gel; cyclohexane/acetone, 2:1) to yield 5,10,15-tris(pentafluorophenyl)-20-(ethynyl)-porphyrin (**41**) as a violet solid in 98 % yield (92 mg, 0.11 mmol, 832.5 g/mol).

¹H-NMR (400 MHz, CDCl₃, δ /ppm): -2.65 (brs, 2 H, NH), 4.17 (s, 1 H, CH), 8.85 (s, 4 H, Ar-H), 8.87 (m, 2 H, Ar-H), 9.80 (m, 2 H, Ar-H).

¹⁹F-NMR (376 MHz, CDCl₃, δ /ppm): -136.6 (m, 3 F, Ar-F), -151.4 (m, 6 F, Ar-F), -161.4 (m, 6 F, Ar-F).

MS (MALDI-TOF): m/z (%): 832.2 (100) [M]⁺, 833.2 (94), 834.1 (34), 835.1 (17), 836.1 (6).

HRMS (MALDI/ESI): m/z calcd for C₄₀H₁₁F₁₅N₄: 832.0739; found 832.0736.

5,10,15-Tris(pentafluorophenyl)-20-(2-TMS-ethynyl)-porphyrin-zinc (44)

A solution of zinc acetate (594 mg, 0.13 mmol, 3.2 equiv.) in methanol (25 ml) was added to a solution of 5,10,15-tris(pentafluorophenyl)-20-(2-trimethylsilyl ethynyl)-porphyrin (**37**, 507 mg, 0.56 mmol, 1.0 equiv.) in dichloromethane (110 ml). The reaction mixture was stirred for 24 h at room temperature and then washed with water. The solvent was removed under reduced pressure to obtain 5,10,15-tris(pentafluorophenyl)-20-(2-TMS-ethynyl)-porphyrin-zinc (**44**) quantitatively as a purple solid (542 mg, 0.56 mmol, 966.0 g/mol).

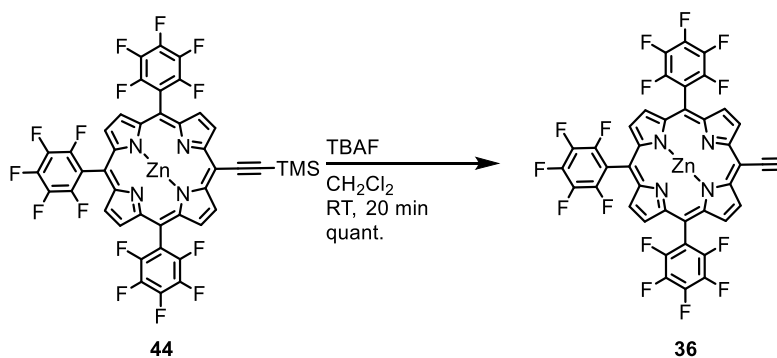
¹H-NMR (400 MHz, CDCl₃, δ/ppm): 0.64 (s, 9 H, TMS), 8.92 (s, 4 H, Ar-H), 8.96 (d, ³J_{HH} = 4.7 Hz, 2 H, Ar-H), 9.88 (d, ³J_{HH} = 4.7 Hz, 2 H, Ar-H).

¹⁹F-NMR (376 MHz, CDCl₃, δ/ppm): -136.9 (m, 3 F, Ar-F), -152.1 (m, 6 F, Ar-F), -161.7 (m, 6 F, Ar-F).

MS (MALDI-TOF): *m/z* (%): 966.8 (100) [M]⁺, 967.8 (89), 968.7 (98), 969.6 (80), 970.6 (82), 971.6 (58), 972.6 (20).

HRMS (MALDI/ESI): *m/z* calcd for C₄₃H₁₇F₁₅N₄SiZn: 966.0269; found 966.0269.

5,10,15-Tris(pentafluorophenyl)-20-(ethynyl)-porphyrin-zinc (36)



5,10,15-Tri-(pentafluorophenyl)-20-(2-TMS-ethynyl)-porphyrin-zinc (**44**, 250 mg, 0.26 mmol, 1.0 equiv.) was dissolved in dichloromethane (100 ml) and TBAF (1 M in THF, 516 ml, 0.52 mmol, 2.0 equiv.) was added dropwise. The reaction mixture was stirred for 20 min at room temperature. Then methanol (100 ml) was added and the solvent removed under reduced pressure. The resulting solid was dissolved in dichloromethane (50 ml) and washed with water. Combined organic layers were dried over anhydrous Na₂SO₄ and the solvent removed under reduced pressure. The resulting solid was purified by column chromatography (silica gel; cyclohexane/acetone, 2:1) to yield 5,10,15-tris(pentafluorophenyl)-20-(ethynyl)-porphyrin-zinc (**36**) as a violet solid in quantitative yield (229 mg, 0.26 mmol, 895.9 g/mol).

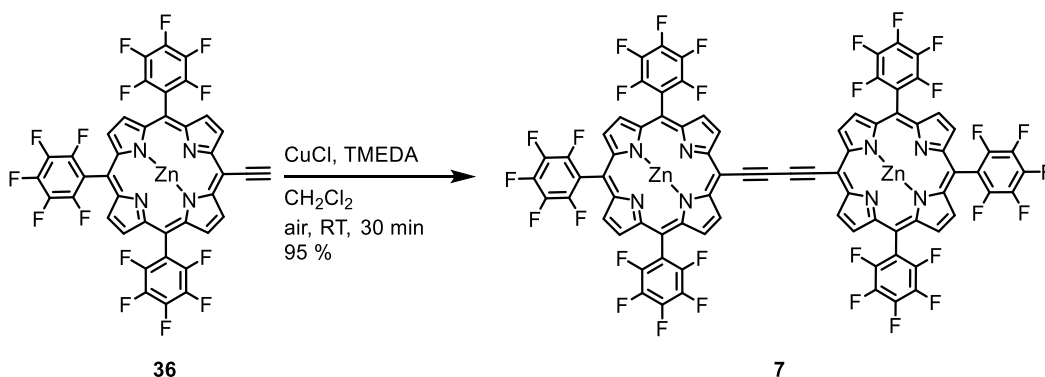
¹H-NMR (400 MHz, CDCl₃, δ/ppm): 3.65 (s, 1 H, CH), 8.88 (d, ³J_{HH} = 4.6 Hz, 2 H, Ar-H), 8.94 (s, 4 H, Ar-H), 9.51 (d, ³J_{HH} = 4.7 Hz, 2 H, Ar-H).

¹⁹F-NMR (376 MHz, CDCl₃, δ/ppm): δ = -136.9 (m, 3 F, Ar-F), -152.0 (m, 6 F, Ar-F), -161.8 (m, 6 F, Ar-F).

MS (MALDI-TOF): *m/z* (%): 893.8 (100) [M]⁺, 894.8 (31), 895.7 (55), 896.7 (22), 897.7 (31), 898.7 (6).

UV/Vis (CHCl₃): λ = 322, 432, 565, 603 nm.

HRMS (MALDI/ESI): *m/z* calcd for C₄₀H₉F₁₅N₄Zn: 893.9874; found 893.9874.

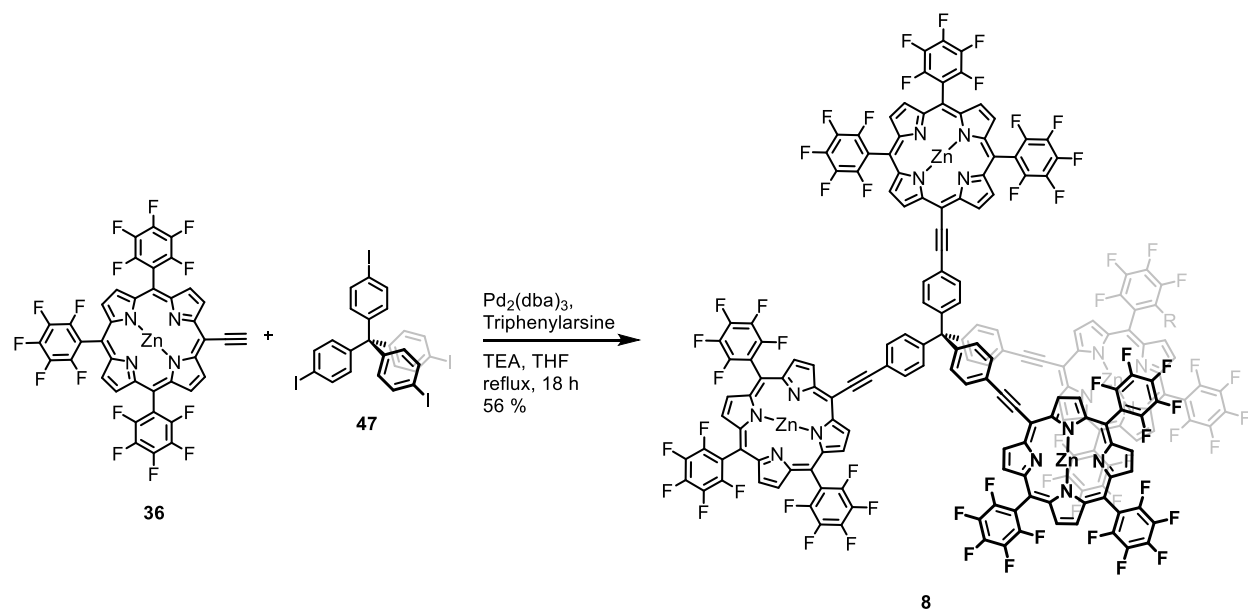
5,10,15-Tris(pentafluorophenyl)-20-(ethynyl)-porphyrin-zinc dimer (**7**)

5,10,15-Tri(pentafluorophenyl)-20-(ethynyl)-porphyrin-zinc (**36**, 312 mg, 0.35 mmol, 1.0 equiv.) was dissolved in dichloromethane (200 ml) and stirred vigorously for 15 min to aerate the solution. Cu(I)Cl (1.03 g, 10.4 mmol, 30 equiv.) was added and the solution stirred for another 3 min. Tetramethyl-ethylenediamine (TMEDA) (1.59 ml, 10.4 mmol, 30 equiv.) was added and the solution was stirred for 30 min at room temperature in an atmosphere of air. The solvent was removed under reduced pressure and the resulting solid purified by column chromatography (silica gel; hexane/acetone, 1:1) to obtain 5,10,15-tri(pentafluorophenyl)-20-(ethynyl)-porphyrin dimer (**7**) as a green solid in 95 % yield (295 mg, 0.17 mmol, 1785.95 g/mol).

¹H-NMR (400 MHz, CDCl₃, δ/ppm): 8.94 (m, 8 H, ArH), 9.08 (m, 4 H, ArH), 10.13 (m, 4 H, ArH).

¹⁹F-NMR (376 MHz, CDCl₃, δ/ppm): -136.9 (m, 6 F, ArF), -151.9 (m, 12 F, ArF), -161.8 (m, 12 F, ArF).

MS (MALDI-TOF, m/z): 1789.33 (100 %), 1801.45 (28 %).

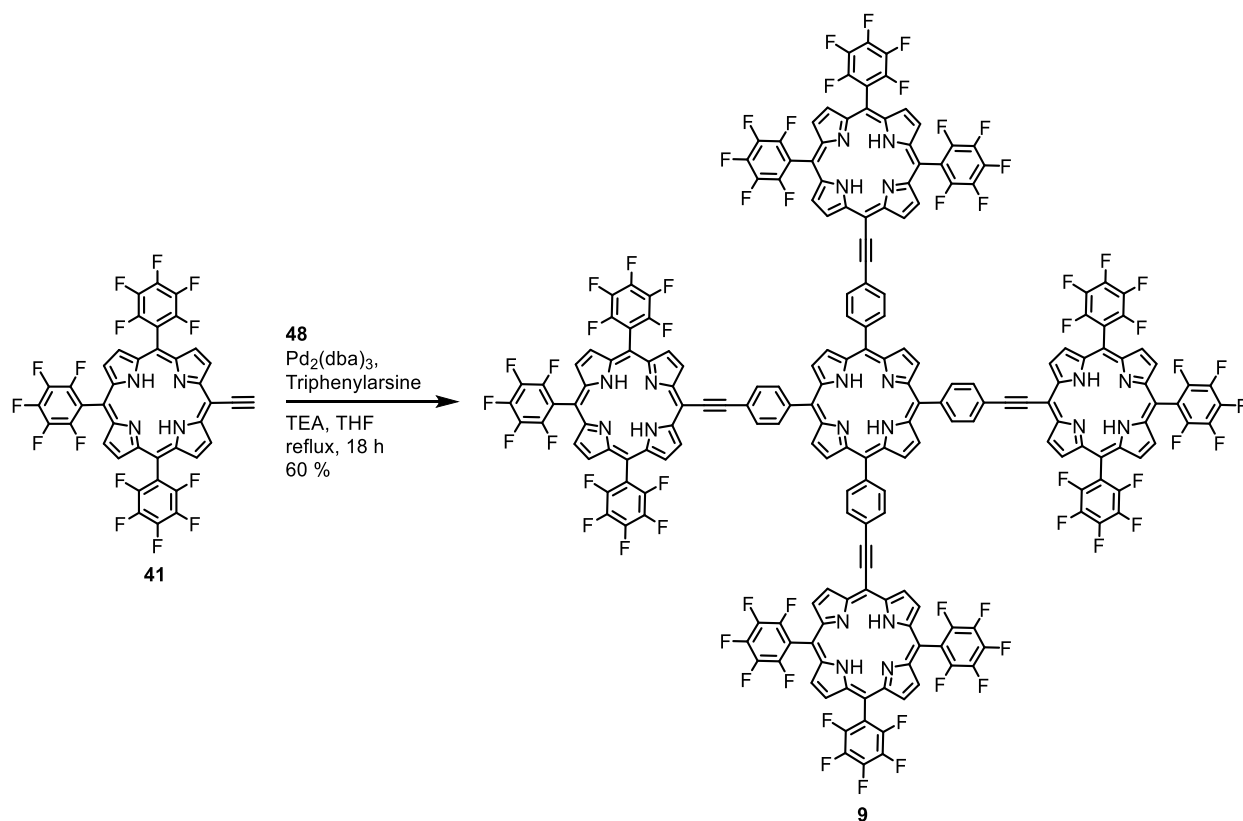
5,10,15-Tris(pentafluorophenyl)-20-(ethynylphenyl)porphyrin-zinc tetramer (**8**)

5,10,15-Tris(pentafluorophenyl)-20-(ethynyl)porphyrin-zinc (**36**, 100 mg, 112 μmol , 1.0 equiv.) and tetrakis(4-iodophenyl)methane (**47**, 19 mg, 22 μmol , 0.20 equiv.) were dissolved in THF (6 ml) using an oven dried two neck flask. The solution was degassed in a constant argon stream for 20 min. Then tris(dibenzylideneacetone)-dipalladium(0) (61 mg, 67 μmol , 0.60 equiv.) and triphenylarsine (106 mg, 0.34 mmol, 3.0 equiv.) were added and the reaction started by the addition of triethylamine (TEA) (6 ml). The reaction mixture was heated to reflux for 18 h, when TLC showed full conversion of the starting materials. After cooling to room temperature TBME was added and the organic phase washed with aq. sat. Na_2HCO_3 , water and brine. Combined organic phases were dried over anhydrous Na_2SO_4 and the solvent removed under reduced pressure. After purification by column chromatography (silica gel, cyclohexane/ acetone, 3:1) 5,10,15-tris(pentafluorophenyl)-20-(ethynylphenyl)porphyrin-zinc tetramer (**8**) was obtained as a dark green solid in 56 % yield (56 mg, 14 μmol , 3895.99 g/mol).

$^1\text{H-NMR}$ (400 MHz, CDCl_3 , δ/ppm): -2.55 (brs, 2 H, NH), 0.65 (s, 9 H, TMS), 8.85 (s, 4 H, Ar-H), 8.88 (d, $^3J_{\text{HH}} = 4.8$ Hz, 2 H, Ar-H), 9.80 (d, $^3J_{\text{HH}} = 4.8$ Hz, 2 H, Ar-H).

$^{19}\text{F-NMR}$ (376 MHz, CDCl_3 , δ/ppm): -136.6 (m, 12 F, Ar-F), -151.2 (m, 24 F, Ar-F), -161.5 (m, 24 F, Ar-F).

HRMS (MALDI/ESI): m/z calcd for $\text{C}_{185}\text{H}_{48}\text{F}_{60}\text{N}_{16}\text{Zn}_4$: 3889.0528; found 3889.0523.

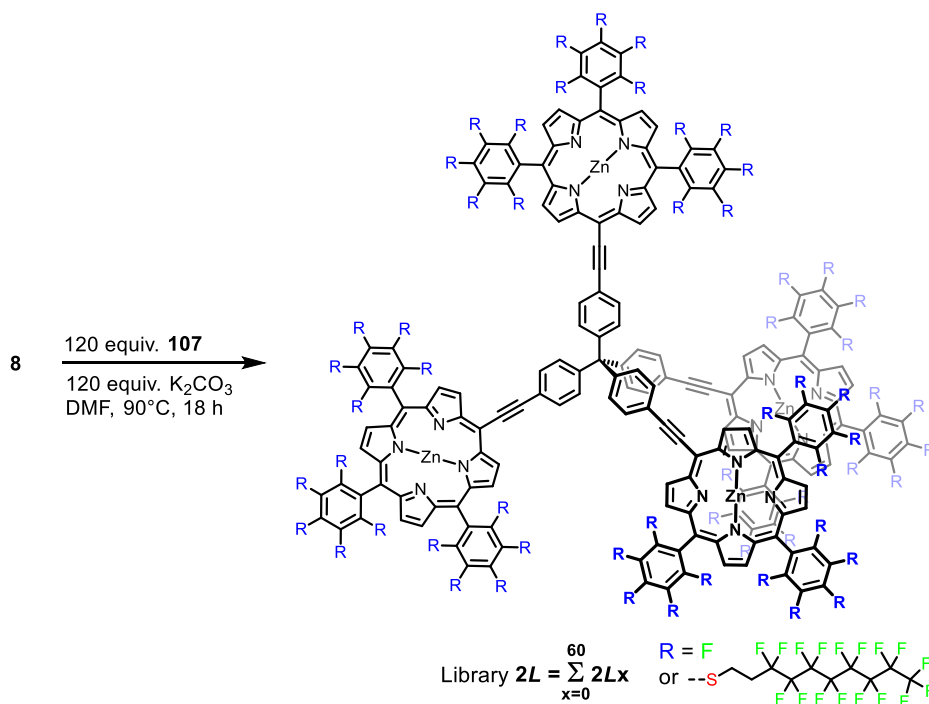
5,10,15-Tris(pentafluorophenyl)-20-(ethynyl)porphyrin pentamer (**9**)

5,10,15-Tris(pentafluorophenyl)-20-(ethynyl)porphyrin (**41**, 164 mg, 197 μmol , 1 equiv.) and *meso*-tetrakis(4-iodophenyl)porphyrin (**48**, 44 mg, 39.3 μmol , 0.2 equiv.) were dissolved in THF (6 ml) using an oven dried two neck flask. The solution was degassed in a constant argon stream for 20 min. Then tris(dibenzylideneacetone)-dipalladium(0) (122 mg, 67 μmol , 0.6 equiv.) and triphenylarsine (212 mg, 0.34 mmol, 3 equiv.) were added and the reaction started by the addition of triethylamine (6 ml). The reaction mixture was heated to reflux for 18 h, when TLC showed full conversion of the starting materials. After cooling to room temperature TBME was added and combined organic phases washed with aq. sat. Na_2HCO_3 , water and brine. Combined organic phases were dried over anhydrous Na_2SO_4 and the solvent removed under reduced pressure. The resulting residue was purified by column chromatography (silica gel, cyclohexane/acetone, 3:1) to obtain 5,10,15-tris(pentafluorophenyl)-20-(ethynylphenyl)porphyrin pentamer (**9**) as a dark green solid in a yield of 60 % (93 mg, 39 μmol , 3936.81 g/mol).

¹H-NMR (400 MHz, CDCl₃, δ/ppm): -2.47 (brs, 2 H, NH), -2.35 (brs, 8 H, NH), 8.55 (d, ³J_{HH} = 7.8 Hz, 8 H, Ar-H), 8.61 (d, ³J_{HH} = 7.8 Hz, 8 H, Ar-H), 8.85 (m, 16 H, Ar-H), 8.98 (m, 8 H, Ar-H), 9.21 (m, 8 H, Ar-H), 10.08 (m, 8 H, Ar-H).

¹⁹F-NMR (376 MHz, CDCl₃, δ/ppm): -136.6 (m, 12 F, Ar-F), -151.4 (m, 24 F, Ar-F), -161.4 (m, 24 F, Ar-F).

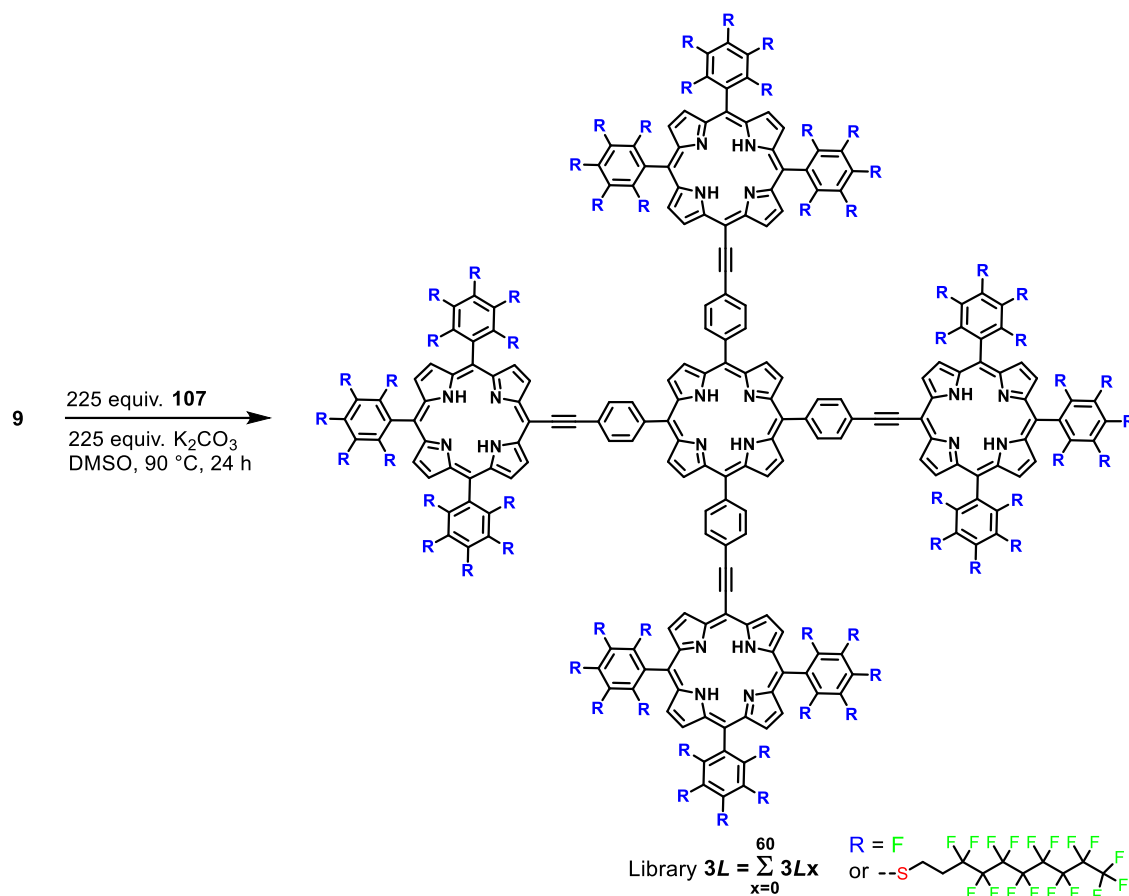
HRMS (MALDI/ESI): *m/z* calcd for C₂₀₄H₆₆F₆₀N₂₀: 3934.4816; found 3934.4847.

Porphyrin-tetramer library **2Lx**

Porphyrin tetramer (**8**, 25 mg, 6.42 μmol , 1.0 equiv.) was dissolved in DMF (10 mL) and *1H,1H,2H,2H*-perfluorodecanethiol (**107**, 220 μL , 770 μmol , 120 equiv.) was added. After the addition of potassium carbonate (106 mg, 770 μmol , 120 equiv.) in two portions the reaction mixture was heated to 90 $^\circ\text{C}$ for 18 h. Water was added to the hot reaction mixture and the aqueous phase separated. Aqueous phases were extracted with TBME. Combined organic phases were washed three times with water and brine and dried over anhydrous sodium sulfate. The solvent was removed under reduced pressure. The resulting brown residue was dissolved again in TBME (10 ml) and filtered through silica gel to remove dithiol residues. The solvent was removed under reduced pressure and the resulting library **2Lx** (258 mg) analyzed by MALDI-TOF mass spectrometry.

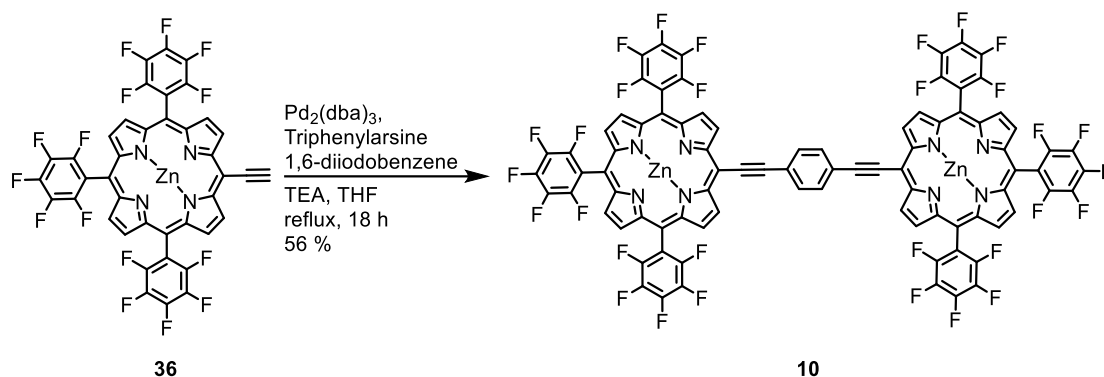
MS (MALDI-TOF, m/z): 14 073 (5%), 13 620 (17%), 13 153 (38%), 12 668 (68%), 12 230 (100%), 11 785 (94%), 11 288 (54%), 10 895 (8%).

Porphyrin-pentamer library 3Lx



Porphyrin-pentamer (**9**, 21 mg, 5.33 μ mol, 1 equiv.) was dissolved in DMSO (10 mL) and *1H,1H,2H,2H*-perfluorodecanethiol (**107**, 345 μ L, 1.20 mmol, 225 equiv.) was added. After the addition of potassium carbonate (170 mg, 1.20 mmol, 225 equiv.) in two portions the reaction mixture was heated to 90 $^\circ$ C for 18 h. Water was added to the hot reaction mixture and the aqueous phase separated. Aqueous phases were extracted with TBME. Combined organic phases were washed three times with water and brine and dried over anhydrous sodium sulfate. The solvent was removed under reduced pressure. The resulting brown residue was dissolved again in TBME (10 ml) and filtered through a plug of silica to remove dithiol residues. The solvent was removed under reduced pressure and the resulting library **3Lx** (198 mg) analyzed by MALDI-TOF mass spectrometry.

MS (MALDI-TOF, *m/z*): 23 878 (5%), 23 404 (24%), 22 931 (62%), 22 454 (100%), 21 983 (89%), 21 514 (78%), 21 061 (50%), 20 588 (26%), 20 121 (6%).

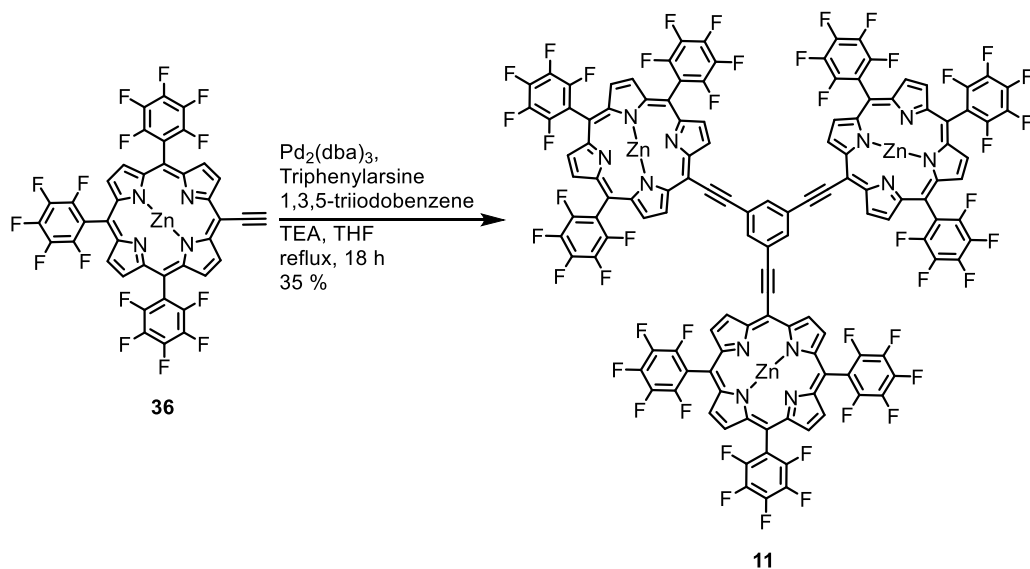
5,10,15-Tris(pentafluorophenyl)-20-(ethynyl)porphyrin-zinc dimer (**10**)

5,10,15-Tris(pentafluorophenyl)-20-(ethynyl)porphyrin-zinc (**36**, 30 mg, 33.5 μmol , 1.0 equiv.) and 1,4-diiodobenzene (3.32 mg, 10 μmol , 0.30 equiv.) were dissolved in THF (2 ml) using an oven dried two neck flask. The solution was degassed in a constant argon stream for 20 min. Then tris(dibenzylideneacetone)-dipalladium(0) (9.2 mg, 10 μmol , 0.30 equiv.) and triphenylarsine (16 mg, 0.05 mmol, 1.5 equiv.) were added and the reaction started by the addition of triethylamine (2 ml). The reaction mixture was heated to reflux for 18 h. When TLC showed full conversion of the starting materials, the reaction was allowed to cool to room temperature. TBME was added and combined organic phases were washed with aq. sat. Na_2HCO_3 , water and brine. Combined organic phases were dried over anhydrous Na_2SO_4 and the solvent removed under reduced pressure. The resulting residue was purified by column chromatography (silica gel; cyclohexane/acetone, 3:1) to obtain 5,10,15-tris(pentafluorophenyl)-20-(ethynylphenyl)-porphyrin-zinc dimer (**10**) as a dark green solid in 56 % yield (35 mg, 18.8 μmol , 1865.87 g/mol).

$^1\text{H-NMR}$ (400 MHz, CDCl_3 , δ/ppm): 38.55 (s, 4 H, Ar-H), 9.19 (m, 8 H, Ar-H), 9.31 (d, $^3J_{\text{HH}} = 4.6$ Hz, 4 H, Ar-H), 10.10 (d, $^3J_{\text{HH}} = 4.6$ Hz, 4 H, Ar-H).

$^{19}\text{F-NMR}$ (376 MHz, CDCl_3 , δ/ppm): -140.0 (m, 6 F, Ar-F), -156.3 (m, 12 F, Ar-F), -165.1 (m, 12 F, Ar-F).

HRMS (MALDI/ESI): m/z calcd for $\text{C}_{86}\text{H}_{20}\text{F}_{30}\text{N}_8\text{Zn}_2$: 1861.9909; found 1861.9919.

5,10,15-Tris(pentafluorophenyl)-20-(ethynylphenyl)porphyrin-zinc trimer (**11**)

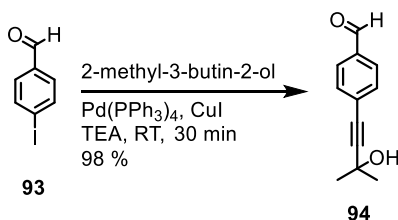
5,10,15-Tris(pentafluorophenyl)-20-(ethynyl)porphyrin-zinc (**36**, 50 mg, 51.6 μmol , 1.0 equiv.) and 1,3,5-triiodobenzene (3.32 mg, 10 μmol , 0.3 equiv.) were dissolved in THF (5 ml) using an oven dried two neck flask. The solution was degassed in a constant argon stream for 20 min. Then tris(dibenzylideneacetone)-dipalladium(0) (21 mg, 23.2 μmol , 0.45 equiv.) and triphenylarsine (48 mg, 0.15 mmol, 3.0 equiv.) were added and the reaction started by the addition of triethylamine (5 ml). The reaction mixture was heated to reflux for 18 h, when TLC showed full conversion of the starting materials. After cooling to room temperature TBME was added and combined organic phases washed with aq. sat. Na_2HCO_3 , water and brine. Combined organic phases were dried over anhydrous Na_2SO_4 and the solvent removed under reduced pressure. Purification of the crude was performed using column chromatography (silica gel; cyclohexane/ethyl acetate, 4:1) to obtain 5,10,15-tris(pentafluorophenyl)-20-(ethynylphenyl)porphyrin-zinc trimer (**11**) as a dark green solid in 35 % yield (17 mg, 6 μmol , 2753.96 g/mol).

$^1\text{H-NMR}$ (400 MHz, CDCl_3 , δ/ppm): 9.15 (m, 3 H, Ar-H), 9.22 (m, 12 H, Ar-H), 9.38 (m, 6 H, Ar-H), 10.31 (m, 6 H, Ar-H).

$^{19}\text{F-NMR}$ (376 MHz, CDCl_3 , δ/ppm): -139.9 (m, 9 F, Ar-F), -156.3 (m, 18 F, Ar-F), -165.0 (m, 18 F, Ar-F).

MS (MALDI-TOF): m/z (%): 2753.61 (100) $[\text{M}]^+$, 2775.18 (30), 2781.79 (32), 2783.93 (35).

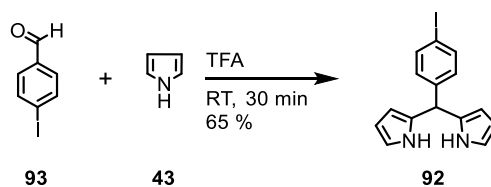
HRMS (MALDI/ESI): m/z calcd for $\text{C}_{126}\text{H}_{27}\text{F}_{45}\text{N}_{12}\text{Zn}_3$: 2753.9637; found 2754.9710.

4-(3-Hydroxy-3-methylbut-1-yn-1-yl)benzaldehyde (**94**)

4-Iodobenzaldehyde (**93**, 4.64 g, 20.0 mmol, 1.0 equiv.), tetrakis(triphenylphosphine)-palladium (231 mg, 10 mol%), and copper(I) iodide (19 mg, 5 mol%) were dissolved in TEA (150 ml). The reaction mixture was degassed for 20 min in a constant argon stream. 2-Methyl-3-buten-2-ol (2.93 ml, 30.0 mmol, 1.5 equiv.) was added and the reaction stirred for 30 min at RT. When TLC showed full conversion, water was added. After filtration through Celite[®] combined organic phases were washed with water and brine. After drying over anhydrous Na₂SO₄ the solvent was removed under reduced pressure. The crude was purified by column chromatography (silica gel, cyclohexane/ ethyl acetate, 2:1) to obtain 4-(3-hydroxy-3-methylbut-1-yn-1-yl)benzaldehyde (**94**) as a colorless oil in 98 % yield (3.68 g, 19.6 mmol, 188.08 g/mol).

¹H-NMR (400 MHz, CDCl₃, δ/ppm): 1.64 (s, 6 H, CH₃), 2.32 (s, 1 H, CH), 7.55 (d, ³J_{HH} = 8.2 Hz, 2 H, ArH), 7.82 (td, ³J_{HH} = 8.5 Hz, 2 H, ArH), 10.00 (s, 1 H, CHO).

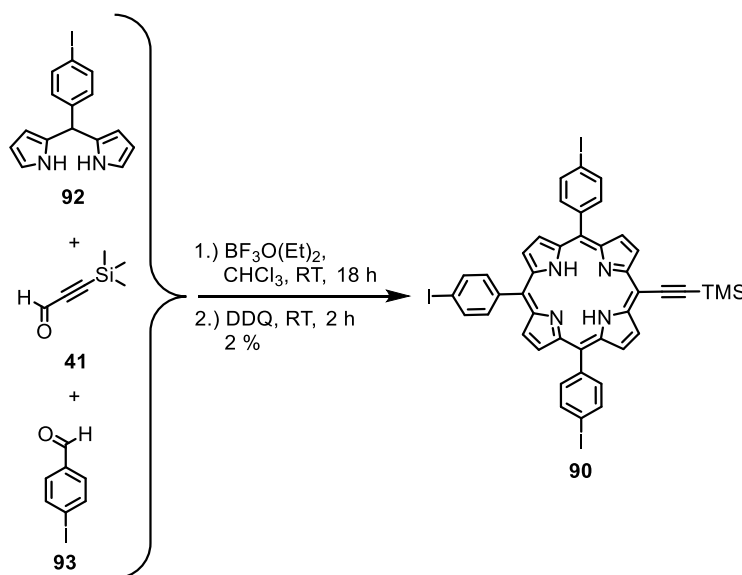
¹³C-NMR (101 MHz, CDCl₃, δ/ppm): 31.33, 65.64, 81.34, 97.84, 129.09, 129.48, 132.17, 135.47, 191.47.

2,2'-((4-Iodophenyl)methylene)bis(1*H*-pyrrole) (**92**)⁷⁵

4-Iodobenzaldehyde (**93**, 10.5 g, 45.3 mmol, 1.0 equiv.) was dissolved in freshly distilled pyrrole (**43**, 174 ml, 2.49 mol, 55 equiv.) and degassed for 20 min. Then TFA (0.335 ml, 4.53 mmol, 0.1 equiv.) was added and the reaction stirred for 30 min. The reaction was diluted in dichloromethane (500 ml) and washed with aq. NaOH (0.1 M, 500 ml). The combined organic phases were dried over anhydrous Na₂SO₄ and the solvent removed under reduced pressure. The brown oil was purified by column chromatography (silica gel, cyclohexane/ethyl acetate/triethylamine, 80:20:1) to obtain 2,2'-((4-iodophenyl)methylene)bis(1*H*-pyrrole) (**92**) as a colorless solid in 65 % yield (10.3 g, 29.6 mmol, 348.01 g/mol).

¹H-NMR (400 MHz, CD₂Cl₂, δ/ppm): 5.46 (s, 1 H, CH), 5.88 (m, 2 H, ArH), 6.15 (dt, ³J_{HH} = 3.4 Hz, ⁴J_{HH} = 2.7 Hz, 2 H, ArH), 6.74 (td, ⁴J_{HH} = 2.7 Hz, ⁴J_{HH} = 1.6 Hz, 2 H, ArH), 7.01 (m, 2 H, ArH), 7.69 (m, 2 H, ArH), 8.06 (brs, 2 H, NH).

¹³C-NMR (101 MHz, CD₂Cl₂, δ/ppm): 44.08, 92.58, 107.71, 108.91, 117.92, 130.94, 132.44, 138.17, 142.29.

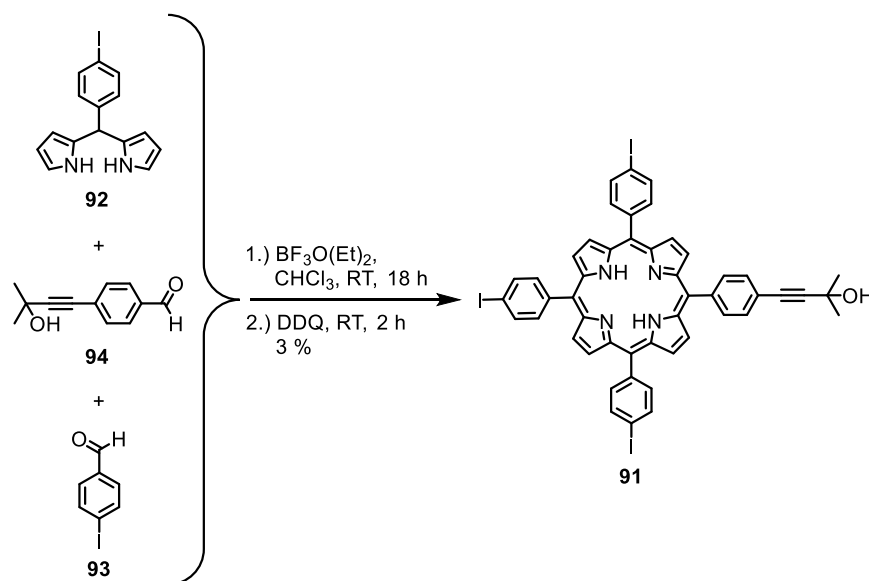
5,10,15-Tris(4-iodophenyl)-20-((trimethylsilyl)ethynyl)porphyrin (**90**)

3-(Trimethylsilyl)-2-propynal (**41**, 0.42 ml, 2.87 mmol, 1.0 equiv.), 4-iodobenzaldehyde (**93**, 666 mg, 2.87 mmol, 1.0 equiv.), and 2,2'-((4-iodophenyl)methylene)bis(1*H*-pyrrole) (**92**, 2.0 g, 5.74 mmol, 2.0 equiv.) were dissolved in chloroform (290 ml). The solution was degassed in a constant argon stream for 30 min. Then boron-trifluoride-diethyletherate (0.12 ml, 0.947 mmol, 0.33 equiv.) was added to start the reaction. After stirring the reaction for 18 h at room temperature DDQ (1.99 g, 8.61 mmol, 3.0 equiv.) was added and the reaction stirred for another 2 hours at room temperature. The dark black reaction mixture was directly filtered three times through a plug of silica. The solvent was removed under reduced pressure and the crude purified by column chromatography (silica gel, cyclohexane/dichloromethane, 3:1) to obtain 5,10,15-tris(4-iodophenyl)-20-((trimethylsilyl)ethynyl)porphyrin (**90**) as a violet solid in 2 % yield (62 mg, 0.061 mmol, 1011.94 g/mol).

$^1\text{H-NMR}$ (400 MHz, CDCl_3 , δ/ppm): -2.52 (s, 2 H, NH), 0.62 (s, 9 H, TMS), 7.90 (m, 6 H, ArH), 8.10 (m, 6 H, ArH), 8.76 (s, 4 H, ArH), 8.87 (m, 2 H, ArH), 9.67 (m, 2 H, ArH).

MS (MALDI-TOF): m/z (%): 1010.6 (100) $[\text{M}]^+$.

HRMS (ESI/MALDI): m/z calcd for $\text{C}_{43}\text{H}_{31}\text{I}_3\text{N}_4\text{Si}$: 1011.9447 found 1011.9445.

2-Methyl-4-(4-(10,15,20-tris(4-iodophenyl)porphyrin-5-yl)phenyl)but-3-yn-2-ol (**91**)

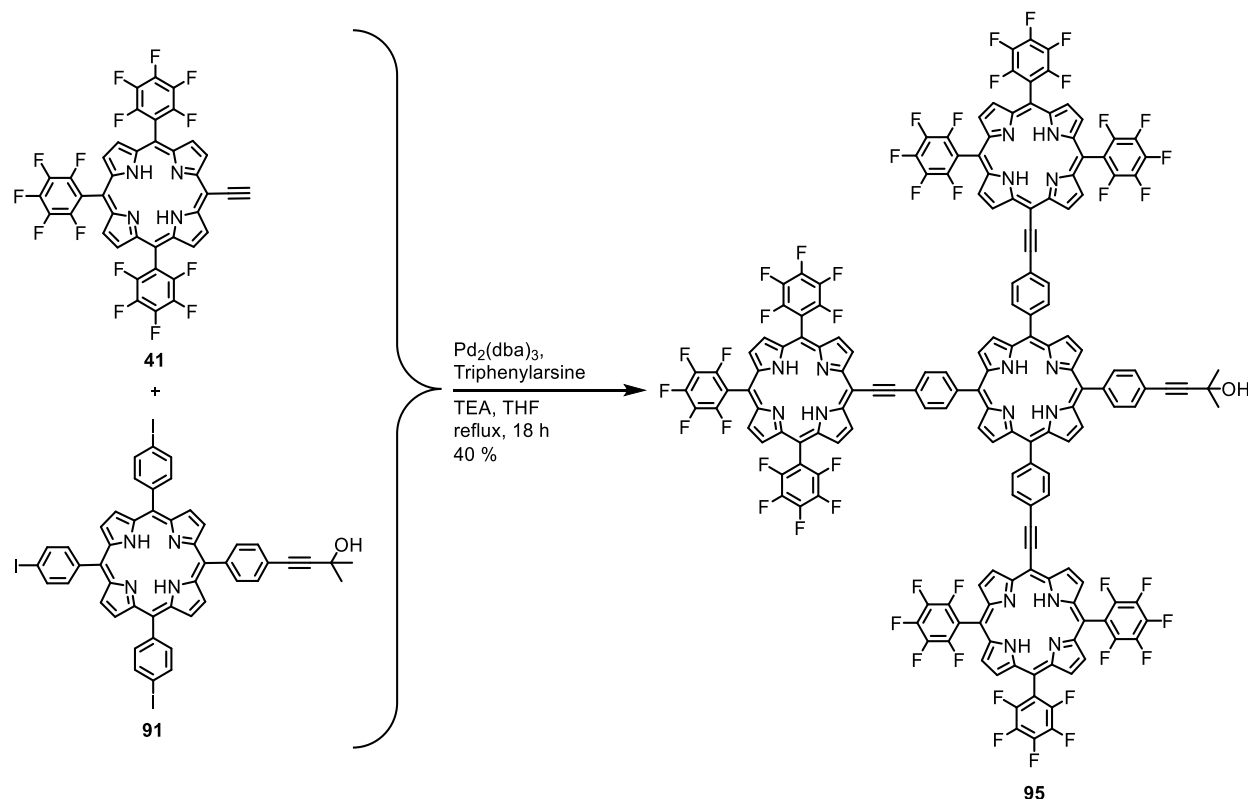
4-(3-Hydroxy-3-methylbut-1-yn-1-yl)benzaldehyde (**94**, 954 mg, 5.07 mmol, 1.0 equiv.), 4-iodobenzaldehyde (**93**, 2 g, 8.62 mmol, 1.7 equiv.), and 2,2'-((4-iodophenyl)methylene)-bis(1H-pyrrole) (**92**, 3.52 g, 10.1 mmol, 2.0 equiv.) were dissolved in chloroform (450 ml). The solution was degassed in a constant argon stream for 30 min. Then boron-trifluoride-diethyletherate (0.21 ml, 1.67 mmol, 0.33 equiv.) was added to start the reaction. After stirring the reaction for 18 h DDQ (3.52 g, 15.2 mmol, 3.0 equiv.) was added and the reaction stirred for another 2 hours. The dark black reaction mixture was directly filtered three times through a plug of silica. The solvent was removed under reduced pressure and the crude purified by column chromatography (silica gel, cyclohexane/dichloromethane, 3:1) to obtain 2-methyl-4-(4-(10,15,20-tris(4-iodophenyl)porphyrin-5-yl)phenyl)but-3-yn-2-ol (**91**) as a violet solid in 3 % yield (153 mg, 0.142 mmol, 1073.98 g/mol).

¹H-NMR (400 MHz, CDCl₃, δ/ppm): -2.88 (s, 2 H, NH), 1.77 (s, 6 H, CH₃), 2.16 (s, 1 H, OH), 7.91 (m, 8 H, ArH), 8.08 (m, 8 H, ArH), 8.82 (s, 8 H, ArH).

MS (MALDI-TOF): *m/z* (%): 1074.4 (100) [M]⁺.

HRMS (ESI/MALDI): *m/z* calcd for C₄₉H₃₃I₃N₄O: 1074.9861 found 1074.9863.

2-Methyl-4-(10,15,20-tris(5,10,15-tris(pentafluorophenyl)-20-(ethynyl)-porphyrin)porphyrin-5-yl)but-3-yn-2-ol (95**)**



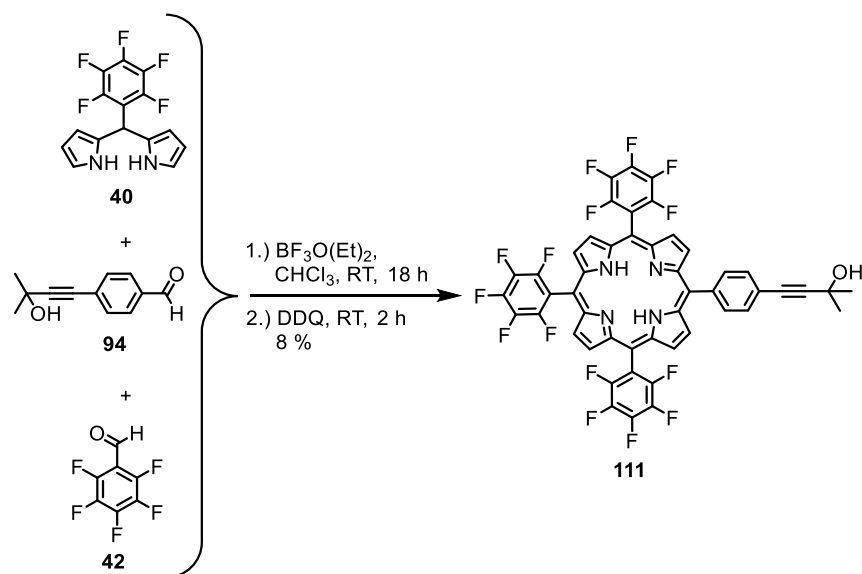
5,10,15-Tri(pentafluorophenyl)-20-(ethynyl)-porphyrin (**41**, 332 mg, 0.34 mmol, 3.5 equiv.) and 2-methyl-4-(10,15,20-tris(4-iodophenyl)porphyrin-5-yl)but-3-yn-2-ol (**91**, 123 mg, 0.11 mmol, 1.0 equiv.) were dissolved in dry THF (5 ml) and the solution degassed in a constant argon stream for 30 min. Then tris(dibenzylideneacetone)dipalladium (0) (10 mg, 10 mol%) and triphenylarsine (1.75 mg, 1 mol%) were added, followed by the addition of TEA (5 ml). The reaction mixture was heated to reflux for 18 h. TBME was added and the organic phase washed with water and brine. Combined organic phases were dried over anhydrous Na_2SO_4 and the solvent removed under reduced pressure. The resulting solid was purified by column chromatography (Silica gel, cyclohexane/acetone, 2:1) followed by a purification on BioBeads[®] SX1. 2-methyl-4-(10,15,20-tris(5,10,15-tris(pentafluorophenyl)-20-(ethynyl)-porphyrin)porphyrin-5-yl)but-3-yn-2-ol (**95**) was obtained as a dark violet solid in 40% yield (219 mg, 0.069 mmol, 3186.47 g/mol).

¹H-NMR (400 MHz, CDCl_3 , δ /ppm): -2.55 (s, 2 H, NH), -2.37 (s, 6 H, NH), 1.72 (s, 6 H, CH_3), 2.34 (s, 1 H, OH), 7.93 (d, $^3J_{\text{HH}} = 8.2$ Hz, 2 H, ArH), 8.29 (d, $^3J_{\text{HH}} = 8.2$ Hz, 2 H, ArH), 8.54 (m,

12 H, ArH), 8.86 (m, 12 H, ArH), 8.98 (m, 6 H, ArH), 9.02 (d, $^3J_{\text{HH}} = 4.8$ Hz, 2 H, ArH), 9.12 (d, $^3J_{\text{HH}} = 4.8$ Hz, 2 H, ArH), 9.18 (s, 4 H, ArH), 10.07 (d, $^3J_{\text{HH}} = 4.9$ Hz, 2 H, ArH).

$^{19}\text{F-NMR}$ (376 MHz, CDCl_3 , δ/ppm): -136.6 (m, 9 F, Ar-F), -151.4 (m, 18 F, Ar-F), -161.4 (m, 18 F, Ar-F).

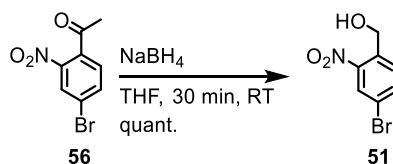
MS (MALDI-TOF): m/z (%): 3186.6 (100) $[\text{M}]^+$.

2-Methyl-4-(4-(10,15,20-tris(perfluorophenyl)porphyrin-5-yl)phenyl)but-3-yn-2-ol (**111**)

A solution of pentafluorobenzaldehyde (**42**) (0.60 ml, 4.80 mmol, 1.0 equiv.), 4-(3-hydroxy-3-methylbut-1-yn-1-yl)benzaldehyde (**94**) (904 mg, 4.80 mmol, 1.0 equiv.) and 5-(perfluorophenyl)-dipyrromethane (**40**) (3.00 g, 9.60 mmol, 2.0 equiv.) in chloroform (1.0 l) was degassed in a constant argon stream for 45 min and then treated with $\text{BF}_3\text{O}(\text{Et})_2$ (0.40 ml, 3.16 mmol, 0.66 equiv.). The reaction was stirred at room temperature for 18 h. DDQ (1.63 g, 7.20 mmol, 1.5 equiv.) was added and the reaction mixture stirred for another 2 h at room temperature. After filtration through silica, the solvent was removed under reduced pressure. The remaining solid was purified three times by column chromatography (silica gel; cyclohexane/dichloromethane, 5:1) to obtain 2-methyl-4-(4-(10,15,20-tris(perfluorophenyl)porphyrin-5-yl)phenyl)but-3-yn-2-ol (**111**) as a dark purple solid in a yield of 8% (368 mg, 0.38 mmol, 966.15 g/mol).

$^1\text{H-NMR}$ (400 MHz, CDCl_3 , δ /ppm): -2.85 (s, 2 H, NH), 1.69 (s, 6 H, CH_3), 2.31 (s, 1 H, OH), 7.89 (d, $^3J_{\text{HF}} = 8.1$ Hz, $^4J_{\text{HF}} = 1.0$ Hz, 2 H, ArH), 8.30 (d, $^3J_{\text{HF}} = 8.1$ Hz, $^4J_{\text{HF}} = 1.0$ Hz, 2 H, ArH), 9.06 (m, 2 H, ArH), 9.26 (m, 2 H, ArH), 9.34 (m, 4 H, ArH).

MS (MALDI-TOF): m/z (%): 967.2 (100) $[\text{M}+\text{H}]^+$.

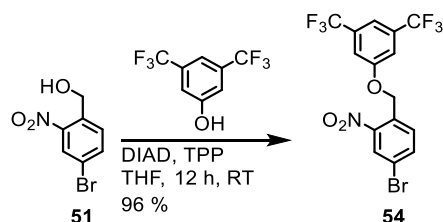
(4-Bromo-2-nitrophenyl)methanol (51)¹⁴⁹

In an oven dried flask 1-(4-bromo-2-nitrophenyl)ethan-1-one (**56**, 10 g, 43.5 mmol, 1.00 equiv.) was dissolved in dry THF (140 ml) and NaBH₄ (3.34 g, 84.7 mmol, 1.95 equiv.) was added in portions. The reaction was stirred for 15 min at room temperature. When TLC showed full conversion the reaction mixture was cooled down to 0 °C and aq. NH₄Cl (20 %, 100 ml) was slowly added. After extraction with TBME combined organic phases were washed with water and brine. After drying over anhydrous MgSO₄ the solvent was removed under reduce pressure. The remaining residue was purified by column chromatography (silica gel, cyclohexane/ethyl acetate; 2:1) to give (4-bromo-2-nitrophenyl)methanol (**51**) as a colorless solid in quantitative yield (10 g, 43.5 mmol, 230.95 g/mol).

¹H-NMR (400 MHz, CDCl₃, δ/ppm): 2.45 (brs, 1 H, OH), 4.96 (s, 2 H, CH₂), 7.67 (d, ³J_{HH} = 8.3 Hz, 1 H, ArH), 7.80 (dd, ³J_{HH} = 8.3 Hz, ⁴J_{HH} = 2.0 Hz, 1 H, ArH), 8.25 (d, ⁴J_{HH} = 2.0 Hz, 1 H, ArH).

¹³C-NMR (101 MHz, CDCl₃, δ/ppm): 62.12 (s, 2 C), 121.65, 128.01, 131.23, 136.03, 137.18, 147.92.

All analytical data were according to literature values.

1-((3,5-Bis(trifluoromethyl)phenoxy)methyl)-4-bromo-2-nitrobenzene (**54**)

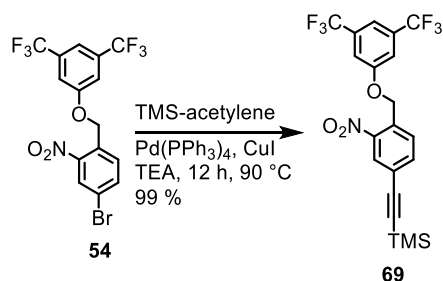
The whole reaction was performed in the absence of light. A solution of 4-bromo-2-nitrophenyl)methanol (**51**, 4 g, 17.24 mmol, 1.0 equiv.), 3,5-bis(trifluoromethyl)phenol (4.88 g, 20.6 mmol, 1.2 equiv.) and triphenylphosphine (5.26 g, 20.6 mmol, 1.2 equiv.) in dry THF (125 ml) was cooled to 0 °C. DIAD (4.3 ml, 20.6 mmol, 1.2 equiv.) was added dropwise within 15 min. The reaction was allowed to warm to room temperature and stirred for 12 h. When TLC showed full conversion of the starting materials the solvent was removed in vacuo and the remaining residue purified by column chromatography (silica gel, cyclohexane/ ethyl acetate; 10:1) yielding 1-((3,5-bis(trifluoromethyl)phenoxy)methyl)-4-bromo-2-nitrobenzene (**54**) as a colorless solid in 96 % yield (7.32 g, 16.48 mmol, 442.96 g/mol).

¹H-NMR (400 MHz, CDCl₃, δ/ppm): 5.51 (s, 2 H, CH₂), 7.24 (s, 2 H, ArH), 7.55 (s, 1 H, ArH), 7.77 (d, ³J_{HH} = 8.4 Hz, 1 H, ArH), 7.86 (dd, ³J_{HH} = 8.4 Hz, ⁴J_{HH} = 2.0 Hz, 1 H, ArH), 8.36 (d, ⁴J_{HH} = 2.0 Hz, 1 H, ArH).

¹⁹F-NMR (376 MHz, CDCl₃, δ/ppm): -63.0 (s, 6 F, 2 x CF₃).

¹³C-NMR (101 MHz, CDCl₃, δ/ppm): 67.12, 115.20 (m), 121.62, 122.40, 124.33, 128.29, 129.97, 131.01, 133.19 (m), 137.21, 147.27, 158.42.

HRMS (ESI): *m/z* calcd for C₁₅H₈BrF₆NO₃: 442.9592; found 441.9591.

((4-((3,5-Bis(trifluoromethyl)phenoxy)methyl)-3-nitrophenyl)ethynyl)trimethylsilane (69)

In an oven dried two neck flask 4-bromo-1-((4-(3,5-bis(trifluoromethyl)phenoxy)methyl)-2-nitrophenyl)ethane (**54**, 100 mg, 0.226 mmol, 1.0 equiv.) was dissolved in triethylamine (6 ml). The solution was degassed for 20 min in an argon stream. Then copper(I) iodide (0.44 mg, 1 mol%), and tetrakis(triphenylphosphine)palladium (1.32 mg, 0.5 mol%) were added, and the resulting solution degassed again for 10 min in an argon stream. Trimethylsilylacetylene (0.05 ml, 0.339 mmol, 1.5 equiv.) was added and the reaction heated to reflux for 12 h. After filtration through Celite[®], the solution was dissolved in TBME, and combined organic phases washed with water and brine. After drying over anhydrous Na₂SO₄, the solvent was removed under reduced pressure. The crude was purified by column chromatography (silica gel, cyclohexane/ethyl acetate; 5:1) to obtain ((4-((3,5-bis(trifluoromethyl)phenoxy)methyl)-3-nitrophenyl)ethynyl)trimethylsilane (**69**) as a colorless solid in 99 % yield (103 mg, 0.223 mmol, 461.09 g/mol).

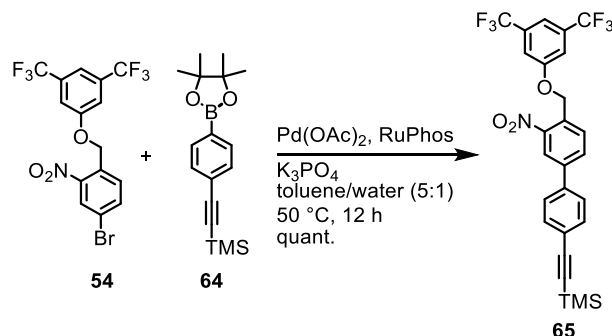
¹H-NMR (400 MHz, CDCl₃, δ/ppm): 0.27 (s, 9 H, TMS), 5.56 (s, 2 H, CH₂), 7.46 (s, 2 H, ArH), 7.56 (s, 1 H, ArH), 7.77 (dd, ³J_{HH} = 8.1 Hz, ⁴J_{HH} = 1.6 Hz, 1 H, ArH), 7.82 (d, ³J_{HH} = 8.1 Hz, 1 H, ArH), 8.26 (d, ⁴J_{HH} = 1.6 Hz, 1 H, ArH).

¹⁹F-NMR (376 MHz, CDCl₃, δ/ppm): -63.3 (s, 6 F, ArF).

¹³C-NMR (101 MHz, CD₂Cl₂, δ/ppm): -0.08 (s, TMS), 68.05 (s), 98.70 (s), 102.08 (s), 115.80 (m), 115.94 (m), 122.38 (s), 125.10 (s), 128.86 (s), 129.24 (s), 132.46 (s), 133.45 (q), 137.49 (s), 147.36 (s), 159.26 (s).

HRMS (ESI): *m/z* calcd for C₂₀H₁₇F₆NO₃Si: 461.0882 found 460.0809.

((4'-((3,5-Bis(trifluoromethyl)phenoxy)methyl)-3'-nitro-[1,1'-biphenyl]-4-yl)ethynyl)trimethylsilane (65)



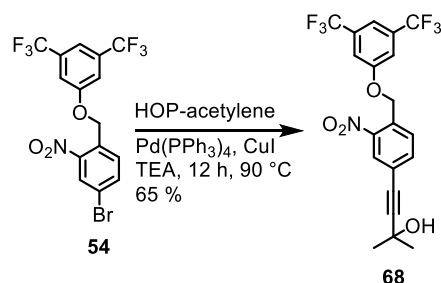
In an oven dried Schlenk tube 4-bromo-1-((4-fluorophenoxy)methyl)-2-nitrobenzene (**54**, 600 mg, 1.35 mmol, 1.0 equiv.), 4-[(trimethylsilyl)ethynyl]phenylboronic acid pinacol ester (**64**, 507 mg, 1.69 mmol, 1.25 equiv.) and potassium phosphate (1.72 g, 8.1 mmol, 6.0 equiv.) were dissolved in toluene/water (5:1, 75 ml), and degassed for 30 min in an argon stream. Pd(OAc)₂ (6.1 mg, 2 mol%) and RuPhos (26.5 mg, 4 mol%) were added, and the reaction mixture degassed for another 10 min. After heating to 50 °C for 12 h the reaction mixture was dissolved in TBME. Combined organic phases were washed with water and brine and dried over anhydrous Na₂SO₄. The solvent was removed under reduced pressure, and the resulting solid purified by column chromatography (silica gel, cyclohexane/ ethyl acetate; 10:1) to obtain ((4'-((3,5-bis(trifluoromethyl)phenoxy)methyl)-3'-nitro-[1,1'-biphenyl]-4-yl)ethynyl)trimethylsilane (**65**) in quantitative yield as a colorless solid (726 mg, 1.35 mmol, 537.12 g/mol).

¹H-NMR (400 MHz, CDCl₃, δ/ppm): 0.28 (s, 9 H, TMS), 5.59 (s, 2 H, CH₂), 7.45 (m, 2 H, ArH), 7.54 (m, 1 H, ArH), 7.59 (m, 4 H, ArH), 7.92 (m, 2 H, ArH), 8.42 (m, 1 H, ArH).

¹⁹F-NMR (376 MHz, CDCl₃, δ/ppm): -63.0 (s, 6 F, ArF).

¹³C-NMR (101 MHz, CDCl₃, δ/ppm): 0.87 (s, TMS), 67.59 (s), 96.38 (s), 104.37 (s), 115.39 (m), 122.09 (s), 123.36 (s), 123.91 (s), 124.26 (s), 126.95 (s), 129.23 (s), 130.95 (s), 132.35 (s), 132.94 (s), 133.32 (q), 137.78 (s), 141.70 (s), 147.50 (s), 158.97 (s).

HRMS (ESI): *m/z* calcd for C₂₆H₂₁F₆NO₃Si: 537.1195 found 536.1122.

4-(4-((3,5-Bis(trifluoromethyl)phenoxy)methyl)-3-nitrophenyl)-2-methylbut-3-yn-2-ol (**68**)

In an oven dried two neck flask 4-bromo-1-((4-fluorophenoxy)methyl)-2-nitrobenzene (**54**, 2.0 g, 4.5 mmol, 1.0 equiv.) was dissolved in triethylamine (120 ml). The solution was degassed for 20 min in an argon stream. Then copper(I) iodide (8.75 mg, 1 mol%), and tetrakis(triphenylphosphine)palladium (26.3 mg, 0.5 mol%) were added, and the resulting solution degassed again for 10 min in an argon stream. 2-Methyl-3-butyn-2-ol (0.67 ml, 6.75 mmol, 1.5 equiv.) was added and the reaction heated to reflux for 12 h. After filtration through Celite[®] the solution was dissolved in TBME, and combined organic phases washed with water and brine. After drying over anhydrous Na₂SO₄ the solvent was removed under reduced pressure. The crude was purified by column chromatography (silica gel, cyclohexane/ethyl acetate; 5:1) to obtain 4-(4-((3,5-bis(trifluoromethyl)phenoxy)methyl)-3-nitrophenyl)-2-methylbut-3-yn-2-ol (**68**) as a colorless solid in 65 % yield (1.3 g, 4.5 mmol, 447.09 g/mol).

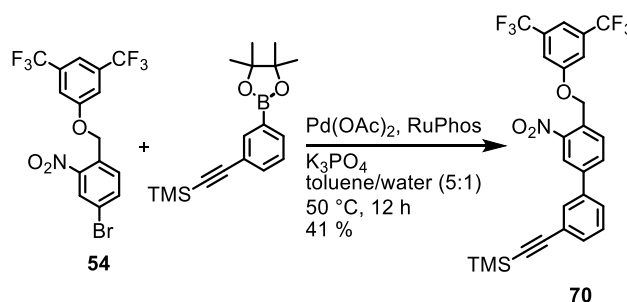
¹H-NMR (400 MHz, CDCl₃, δ/ppm): 1.65 (s, 6 H, CH₃), 2.08 (s, 1 H, OH), 5.55 (s, 2 H, CH₂), 7.24 (s, 2 H, ArH), 7.54 (s, 1 H, ArH), 7.73 (dd, ³J_{HH} = 8.1 Hz, ⁴J_{HH} = 1.7 Hz, 1 H, ArH), 7.82 (d, ³J_{HH} = 8.1 Hz, 1 H, ArH), 8.24 (d, ⁴J_{HH} = 1.7 Hz, 1 H, ArH).

¹⁹F-NMR (376 MHz, CDCl₃, δ/ppm): -63.0 (s, 6 F, ArF).

¹³C-NMR (101 MHz, CDCl₃, δ/ppm): 31.43 (s, CH₃), 65.77 (s), 67.48 (s), 79.53 (s), 91.17 (s), 115.39 (m), 115.51 (m), 121.79 (s), 124.49 (s), 128.32 (s), 128.65 (s), 131.79 (s), 133.39 (q), 136.90 (s), 14683 (s), 158.65 (s).

MS (ESI): *m/z* (%): 663.2 (33), 446.2 (100) [M-H]⁻, 229 (20).

((4'-((3,5-Bis(trifluoromethyl)phenoxy)methyl)-3'-nitro-[1,1'-biphenyl]-3-yl)ethynyl)trimethylsilane (70)



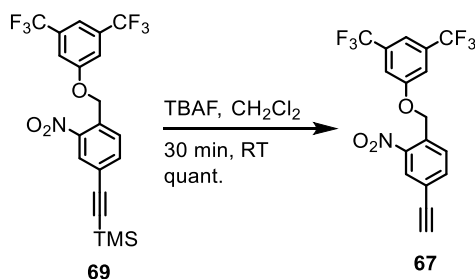
In an oven dried Schlenk tube 4-bromo-1-((4-(3,5-bis(trifluoromethyl)phenoxy)methyl)-2-nitrobenzene (**54**, 1.33 g, 3 mmol, 1.0 equiv.), 3-[(trimethylsilyl)ethynyl]phenylboronic acid pinacol ester (991 mg, 3.3 mmol, 1.1 equiv.) and potassium phosphate (3.82 g, 18 mmol, 6.0 equiv.) were dissolved in toluene/water (5:1, 60 ml), and degassed for 30 min in an argon stream. Pd(OAc)₂ (13.5 mg, 2 mol%) and RuPhos (58.9 mg, 4 mol%) were added, and the reaction mixture degassed for another 10 min. After heating to 50 °C for 12 h the reaction mixture was dissolved in TBME. Combined organic phases were washed with water and brine and dried over anhydrous Na₂SO₄. The solvent was removed under reduced pressure, and the resulting solid purified by column chromatography (silica gel, cyclohexane/ethyl acetate; 10:1) to obtain ((4'-((3,5-bis(trifluoromethyl)phenoxy)methyl)-3'-nitro-[1,1'-biphenyl]-4-yl)ethynyl)trimethylsilane (**70**) in 41 % yield as a colorless solid (660 mg, 1.23 mmol, 537.12 g/mol).

¹H-NMR (400 MHz, CDCl₃, δ/ppm): 0.28 (s, 9 H, TMS), 5.60 (s, 2 H, CH₂), 7.42-7.60 (m, 6 H, ArH), 7.75 (m, 1 H, ArH), 7.92 (m, 2 H, ArH), 8.42 (m, 1 H, ArH).

¹⁹F-NMR (376 MHz, CDCl₃, δ/ppm): -63.0 (s, 6 F, ArF).

¹³C-NMR (101 MHz, CDCl₃, δ/ppm): 0.07 (s, TMS), 67.61 (s), 95.59 (s), 104.36 (s), 115.39 (m), 123.76 (s), 124.44 (s), 127.21 (s), 129.32 (s), 130.70 (s), 130.70 (s), 130.99 (s), 132.28 (s), 132.49 (s), 133.14 (s), 133.47 (s), 134.53 (s), 137.85 (s), 138.15 (s), 141.75 (s), 147.50 (s).

MS (ESI): *m/z* (%): 536.2 (46) [M-H]⁻, 459.1 (100), 229 (48).

1-((3,5Bis(trifluoromethyl)phenoxy)methyl)-4-ethynyl-2-nitrobenzene (67)

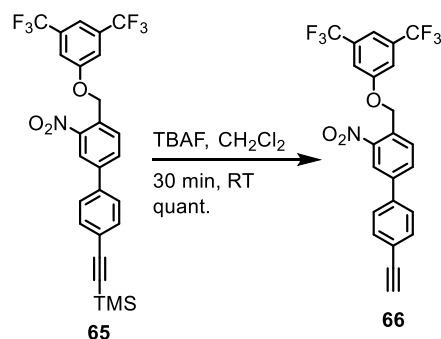
4-Bromo-1-((4-fluorophenoxy)methyl)-2-nitrobenzene (**69**, 100 mg, 4.76 mmol, 1.0 equiv.) was dissolved in dichloromethane (150 ml) under an atmosphere of argon. TBAF (1 M in THF, 11.9 ml, 11.9 mmol, 2.5 equiv.) was added, and the solution stirred for 30 min at room temperature. When TLC showed full conversion of the starting material, methanol (100 ml) was added. After evaporation of the solvents the crude was purified by column chromatography (silica gel, cyclohexane/ethyl acetate; 10:1) to obtain 1-((3,5bis(trifluoromethyl)phenoxy)methyl)-4-ethynyl-2-nitrobenzene (**67**) in quantitative yield (1.85 g, 4.77 mmol, 389.05 g/mol).

¹H-NMR (400 MHz, CDCl₃, δ/ppm): 3.16 (s, 1 H, CH), 5.56 (s, 2 H, CH₂), 7.43 (s, 2 H, ArH), 7.54 (s, 1 H, ArH), 7.81 (dd, ³J_{HH} = 8.1 Hz, ⁴J_{HH} = 1.6 Hz, 1 H, ArH), 7.86 (d, ³J_{HH} = 8.1 Hz, 1 H, ArH), 8.31 (d, ⁴J_{HH} = 1.6 Hz, 1 H, ArH).

¹⁹F-NMR (376 MHz, CDCl₃, δ/ppm): -63.0 (s, 6 F, ArF).

¹³C-NMR (101 MHz, CDCl₃, δ/ppm): 67.43 (s), 80.68 (s), 80.73 (s), 115.38 (m), 115.55 (m), 123.14 (q), 123.76 (s), 128.74 (s), 128.80 (s), 132.50 (s), 133.33 (q), 137.39 (s), 146.38 (s), 158.62 (s).

HRMS (ESI): *m/z* calcd for C₁₇H₉F₆NO₃Si: 389.0487 found 388.0417.

4-((3,5-Bis(trifluoromethyl)phenoxy)methyl)-4'-ethynyl-3-nitro-1,1'-biphenyl (**66**)

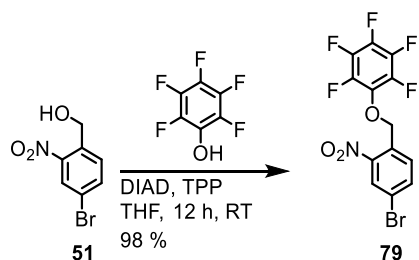
((4'-((3,5-Bis(trifluoromethyl)phenoxy)methyl)-3'-nitro-[1,1'-biphenyl]-4-yl)ethynyl)-trimethylsilane (**65**, 828 mg, 1.54 mmol, 1.0 equiv.) was dissolved in dichloromethane (100 ml) under an atmosphere of argon. TBAF (1 M in THF, 3.0 ml, 3.0 mmol, 1.95 equiv.) was added, and the solution stirred for 30 min at room temperature. When TLC showed full conversion of the starting material methanol (80 ml) was added. After evaporation of the solvents the crude was purified by column chromatography (silica gel, cyclohexane/ethyl acetate; 5:1) to obtain 4-((3,5-bis(trifluoromethyl)phenoxy)methyl)-4'-ethynyl-3-nitro-1,1'-biphenyl (**66**) in quantitative yield (717 mg, 1.54 mmol, 465.08 g/mol).

¹H-NMR (400 MHz, CDCl₃, δ/ppm): 3.19 (s, 1 H, CH), 5.60 (s, 2 H, CH₂), 7.45 (m, 2 H, ArH), 7.55 (m, 1 H, ArH), 7.62 (m, 4 H, ArH), 7.93 (m, 2 H, ArH), 8.42 (m, 1 H, ArH) ppm.

¹⁹F-NMR (376 MHz, CDCl₃, δ/ppm): -63.0 (s, 6 F, ArF).

¹³C-NMR (101 MHz, CDCl₃, δ/ppm): 67.45 (s), 78.85 (s), 82.92 (s), 115.26 (m), 121.68 (s), 122.74 (s), 123.54 (s), 124.39 (s), 126.96 (s), 129.23 (s), 130.94 (s), 132.24 (s), 132.97 (s), 133.32 (s), 138.10 (s), 141.50 (s), 147.38 (s), 158.65 (s).

HRMS (ESI): *m/z* calcd for C₂₃H₁₃F₆NO₃: 465.0800 found 464.0727.

1-((4-Bromo-2-nitrobenzyl)oxy)-2,3,4,5,6-pentafluorobenzene (79)

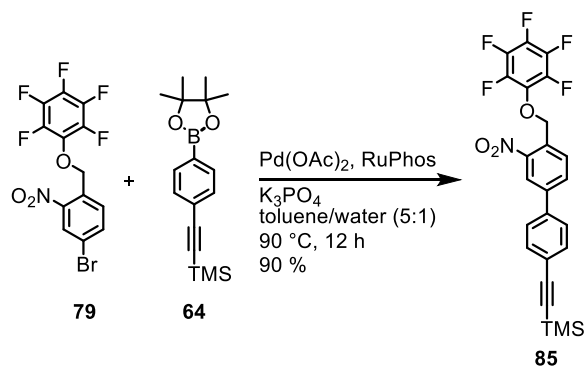
The whole reaction was performed in the absence of light. A solution of 4-bromo-2-nitrophenyl)methanol (**51**, 775 mg, 3.34 mmol, 1.0 equiv.), pentafluorophenol (745 mg, 4.01 mmol, 1.2 equiv.) and triphenylphosphine (1.06 g, 4.01 mmol, 1.2 equiv.) in dry THF (25 ml) was cooled to 0 °C. DIAD (0.84 ml, 4.01 mmol, 1.2 equiv.) was added dropwise within 15 min. The reaction was allowed to warm to room temperature and stirred for 12 h. When TLC showed full conversion of the starting materials the solvent was removed in vacuo and the remaining residue purified by column chromatography (silica gel, cyclohexane/ethyl acetate; 10:1) yielding 1-((4-bromo-2-nitrobenzyl)oxy)-2,3,4,5,6-pentafluorobenzene (**79**) as a colorless solid in 98 % yield (1.30 g, 3.27 mmol, 396.94 g/mol).

¹H-NMR (400 MHz, CDCl₃, δ/ppm): 5.54 (s, 2 H, CH₂), 7.87 (m, 2 H, ArH), 8.33 (s, 1 H, ArH).

¹⁹F-NMR (376 MHz, CDCl₃, δ/ppm): -156.1 (m, 2 F, ArF), -161.7 (m, 1 F, ArF), -162.4 (m, 2 F, ArF).

¹³C-NMR (101 MHz, CDCl₃, δ/ppm): 72.99 (s), 122.42 (s), 128.08 (s), 130.06 (s), 131.40 (s), 136.83 (m), 137.21 (s), 139.21 (m), 140.48 (m), 142.91 (m), 147.06 (s).

HRMS (ESI): *m/z* calcd for C₁₃H₅BrF₅NO₃: 396.9373 found 395.9300.

Trimethyl((3'-nitro-4'-((perfluorophenoxy)methyl)-[1,1'-biphenyl]-4-yl)ethynyl)silane (85)


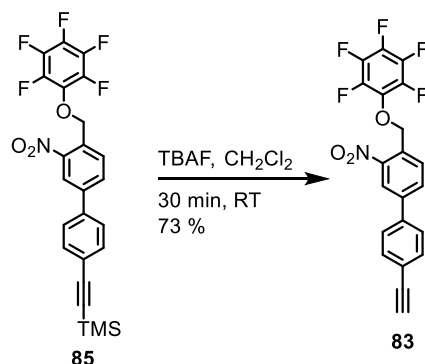
In an oven dried Schlenk tube ((4-bromo-2-nitrobenzyl)oxy)-2,3,4,5,6-pentafluorobenzene (**79**, 1.31 g, 3.29 mmol, 1.0 equiv.), 4-[(trimethylsilyl)ethynyl]phenylboronic acid pinacol ester (**64**, 1.27 g, 4.11 mmol, 1.25 equiv.) and potassium phosphate (4.19 g, 19.7 mmol, 6.0 equiv.) were dissolved in toluene/water (5:1, 120 ml), and degassed for 30 min in an argon stream. Pd(OAc)₂ (14.8 mg, 2 mol%) and RuPhos (64.6 mg, 4 mol%) were added, and the reaction mixture degassed for another 10 min. After heating to 90 °C for 12 h the reaction mixture was dissolved in TBME. Combined organic phases were washed with water and brine, and dried over anhydrous Na₂SO₄. The solvent was removed under reduced pressure, and the resulting solid purified by column chromatography (silica gel, cyclohexane/ethyl acetate; 5:1) to obtain trimethyl((3'-nitro-4'-((perfluorophenoxy)methyl)-[1,1'-biphenyl]-4-yl)ethynyl)silane (**85**) in 90 % yield as a colorless solid (1.45 g, 2.95 mmol, 491.10 g/mol).

¹H-NMR (400 MHz, CDCl₃, δ/ppm): 0.28 (s, 9 H, TMS), 5.64 (s, 2 H, CH₂), 7.59 (m, 4 H, ArH), 7.95 (dd, ³J_{HH} = 8.2 Hz, ⁴J_{HH} = 1.9 Hz, 1 H, ArH), 8.02 (d, ³J_{HH} = 8.1 Hz, 1 H, ArH), 8.39 (d, ⁴J_{HH} = 1.9 Hz, 1 H, ArH).

¹⁹F-NMR (376 MHz, CDCl₃, δ/ppm): -156.0 (m, 2 F, ArF), -162.0 (m, 1 F, ArF), -162.6 (m, 2 F, ArF).

¹³C-NMR (101 MHz, CDCl₃, δ/ppm): 0.08 (s, TMS), 73.49 (s), 96.34 (s), 104.40 (s), 123.42 (s), 123.89 (s), 126.96 (s), 129.46 (s), 131.32 (s), 132.34 (s), 132.92 (s), 137.85 (s), 141.73 (s), 147.33 (s).

HRMS (ESI): *m/z* calcd for C₂₄H₁₈F₅NO₃Si: 491.0976 found 490.0899.

4'-Ethynyl-3-nitro-4-((perfluorophenoxy)methyl)-1,1'-biphenyl (83)

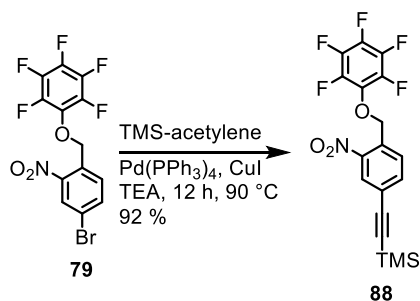
Trimethyl((3'-nitro-4'-((perfluorophenoxy)methyl)-[1,1'-biphenyl]-4-yl)ethynyl)silane (**85**, 1.00 g, 2.03 mmol, 1.0 equiv.) was dissolved in dichloromethane (100 ml) under an atmosphere of argon. TBAF (1 M in THF, 3.97 ml, 3.0 mmol, 1.95 equiv.) was added, and the solution stirred for 30 min at room temperature. When TLC showed full conversion of the starting material, methanol (80 ml) was added. After evaporation of the solvents the crude was purified by column chromatography (silica gel, cyclohexane/ethyl acetate; 5:1) to obtain 4'-ethynyl-3-nitro-4-((perfluorophenoxy)methyl)-1,1'-biphenyl (**83**) in 73 % yield as a colorless solid (625 mg, 1.49 mmol, 419.06 g/mol).

¹H-NMR (400 MHz, CDCl₃, δ/ppm): 3.19 (s, 1 H, CH), 5.64 (s, 2 H, CH₂), 7.61 (m, 4 H, ArH), 7.95 (dd, ³J_{HH} = 8.1 Hz, ⁴J_{HH} = 1.9 Hz, 1 H, ArH), 8.03 (d, ³J_{HH} = 8.1 Hz, 1 H, ArH), 8.39 (d, ⁴J_{HH} = 1.9 Hz, 2 H, ArH).

¹⁹F-NMR (376 MHz, CDCl₃, δ/ppm): -156.0 (m, 2 F, ArF), -162.0 (m, 1 F, ArF), -162.5 (m, 2 F, ArF).

¹³C-NMR (101 MHz, CDCl₃, δ/ppm): 73.33 (s), 78.81 (s), 82.94 (s), 122.69 (s), 123.31 (s), 126.95 (s), 129.33 (s), 131.32 (s), 132.22 (s), 132.95 (s), 138.15 (s), 141.48 (s), 147.17 (s).

HRMS (ESI): *m/z* calcd for C₂₁H₁₀F₅NO₃: 419.0581 found 418.0506.

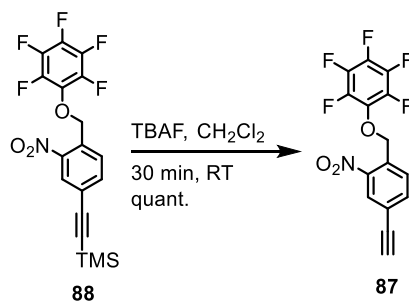
Trimethyl((3-nitro-4-((perfluorophenoxy)methyl)phenyl)ethynyl)silane (88)


In an oven dried two neck flask 4((4-bromo-2-nitrobenzyl)oxy)-2,3,4,5,6-pentafluorobenzene (**79**, 1.00 g, 2.51 mmol, 1.0 equiv.) was dissolved in triethylamine (60 ml). The solution was degassed for 20 min in an argon stream. Then copper(I) iodide (4.88 mg, 1 mol%), and tetrakis(triphenylphosphine)palladium (14.7 mg, 0.5 mol%) were added, and the resulting solution degassed again for 10 min in an argon stream. Trimethylsilylacetylene (0.54 ml, 0.339 mmol, 1.5 equiv.) was added and the reaction heated to reflux for 12 h. After filtration through Celite[®] the solution was dissolved in TBME, and combined organic phases washed with water and brine. After drying over anhydrous Na₂SO₄ the solvent was removed under reduced pressure. The crude was purified by column chromatography (silica gel, cyclohexane/ethyl acetate; 5:1) to obtain trimethyl((3-nitro-4-((perfluorophenoxy)methyl)phenyl)ethynyl)silane (**88**) as a colorless solid in 92 % yield (960 mg, 2.31 mmol, 415.07 g/mol).

¹H-NMR (400 MHz, CDCl₃, δ/ppm): 0.28 (s, 9 H, TMS), 5.58 (s, 2 H, CH₂), 7.78 (dd, ³J_{HH} = 8.1 Hz, ⁴J_{HH} = 1.7 Hz, 1 H, ArH), 7.90 (d, ³J_{HH} = 8.1 Hz, 1 H, ArH), 8.24 (d, ⁴J_{HH} = 1.7 Hz, 1 H, ArH).

¹⁹F-NMR (376 MHz, CDCl₃, δ/ppm): -156.0 (m, 2 F, ArF), -161.9 (m, 1 F, ArF), -162.5 (m, 2 F, ArF).

HRMS (ESI): *m/z* calcd for C₁₈H₁₄F₅NO₃Si: 415.0663 found 414.0590.

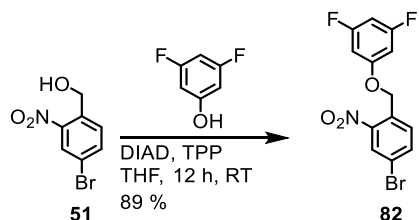
1-((4-Ethynyl-2-nitrobenzyl)oxy)-2,3,4,5,6-pentafluorobenzene (**87**)

Trimethyl((3-nitro-4-((perfluorophenoxy)methyl)phenyl)ethynyl)silane (**88**, 515 mg, 1.24 mmol, 1.0 equiv.) was dissolved in dichloromethane (150 ml) under an atmosphere of argon. TBAF (1 M in THF, 2.42 ml, 2.42 mmol, 2.5 equiv.) was added, and the solution stirred for 15 min at room temperature. When TLC showed full conversion of the starting material methanol (100 ml) was added. After evaporation of the solvents the crude was purified by column chromatography (silica gel, cyclohexane/ethyl acetate; 10:1) to obtain 1-((4-ethynyl-2-nitrobenzyl)oxy)-2,3,4,5,6-pentafluorobenzene (**87**) in quantitative yield (425 mg, 1.24 mmol, 343.03 g/mol).

¹H-NMR (400 MHz, CDCl₃, δ/ppm): 3.25 (s, 1 H, CH), 5.59 (s, 2 H, CH₂), 7.83 (d, ³J_{HH} = 8.1 Hz, 1 H, ArH), 7.95 (d, ³J_{HH} = 8.1 Hz, 1 H, ArH), 8.28 (s, 1 H, ArH).

¹⁹F-NMR (376 MHz, CDCl₃, δ/ppm): -156.0 (m, 2 F, ArF), -161.7 (m, 1 F, ArF), -162.4 (m, 2 F, ArF).

HRMS (ESI): *m/z* calcd for C₁₅H₆F₅NO₃: 343.0268 found 343.0198.

4-Bromo-1-((3,5-difluorophenoxy)methyl)-2-nitrobenzene (82)

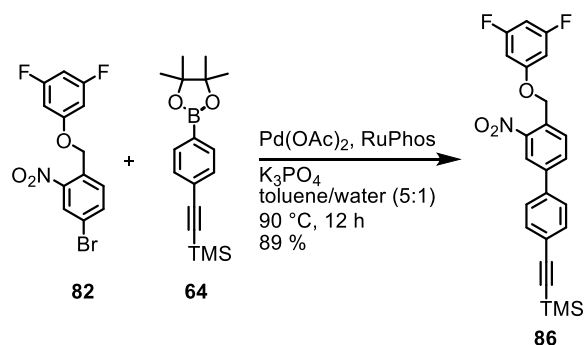
The whole reaction was performed in the absence of light. A solution of 4-bromo-2-nitrophenyl)methanol (**51**, 1 g, 4.31 mmol, 1.0 equiv.), 3,5-difluorophenol (673 mg, 5.17 mmol, 1.2 equiv.) and triphenylphosphine (1.37 g, 5.17 mmol, 1.2 equiv.) in dry THF (40 ml) was cooled to 0 °C. DIAD (1.08 ml, 5.17 mmol, 1.2 equiv.) was added dropwise within 15 min. The reaction was allowed to warm to room temperature and stirred for 12 h. When TLC showed full conversion of the starting materials the solvent was removed under reduced pressure and the remaining residue purified by column chromatography (silica gel, cyclohexane/ ethyl acetate; 10:1) yielding 4-bromo-1-((3,5-difluorophenoxy)methyl)-2-nitrobenzene (**82**) as a colorless solid in 89 % yield (1.32 g, 3.84 mmol, 342.97 g/mol).

¹H-NMR (400 MHz, CDCl₃, δ/ppm): 5.39 (s, 2 H, CH₂), 6.50 (m, 3 H, ArH), 7.72 (d, ³J_{HH} = 8.4 Hz, 1 H, ArH), 7.82 (dd, ³J_{HH} = 8.4 Hz, ⁴J_{HH} = 2.0 Hz, 1 H, ArH), 8.33 (d, ⁴J_{HH} = 2.0 Hz, 1 H, ArH).

¹⁹F-NMR (376 MHz, CDCl₃, δ/ppm): -108.4 (s, 2 F, ArF).

¹³C-NMR (101 MHz, CDCl₃, δ/ppm): 66.91 (s), 97.45 (t), 98.81 (m), 122.02 (s), 128.13 (s), 129.88 (s), 131.73 (s), 137.13 (s), 147.17 (s), 159.64 (t), 163.72 (dd).

HRMS (ESI): *m/z* calcd for C₁₃H₈BrF₂NO₃: 342.9656 found 341.9583.

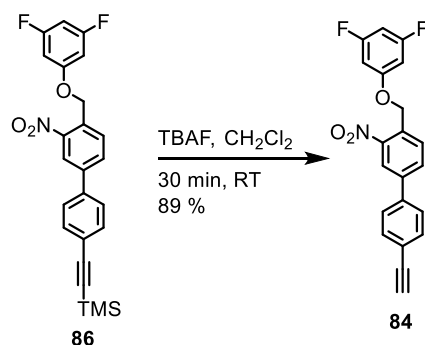
((4'-((3,5-Difluorophenoxy)methyl)-3'-nitro-[1,1'-biphenyl]-4-yl)ethynyl)trimethylsilane (**86**)

In an oven dried Schlenk tube 4-bromo-1-((3,5-difluorophenoxy)methyl)-2-nitrobenzene (**82**, 1.50 g, 4.36 mmol, 1.0 equiv.), 4-[(trimethylsilyl)ethynyl]phenylboronic acid pinacol ester (**64**, 1.69 g, 5.45 mmol, 1.25 equiv.) and potassium phosphate (5.55 g, 26.2 mmol, 6.0 equiv.) were dissolved in toluene/water (5:1, 120 ml), and degassed for 30 min in an argon stream. Pd(OAc)₂ (19.6 mg, 2 mol%) and RuPhos (85.7 mg, 4 mol%) were added, and the reaction mixture degassed for another 10 min. After heating to 90 °C for 12 h the reaction mixture was dissolved in TBME. Combined organic phases were washed with water and brine, and dried over anhydrous Na₂SO₄. The solvent was removed under reduced pressure, and the resulting solid purified by column chromatography (silica gel, cyclohexane/ethyl acetate; 10:1) to obtain ((4'-((3,5-difluorophenoxy)methyl)-3'-nitro-[1,1'-biphenyl]-4-yl)ethynyl)trimethylsilane (**86**) in 89 % yield as a colorless solid (1.70 g, 3.90 mmol, 437.13 g/mol).

¹H-NMR (400 MHz, CDCl₃, δ/ppm): 0.28 (s, 9 H, TMS), 5.50 (s, 2 H, CH₂), 6.48 (m, 1 H, ArH), 6.55 (m, 2 H, ArH), 7.59 (s, 4 H, ArH), 7.89 (m, 2 H, ArH), 8.40 (m, 1 H, ArH).

¹⁹F-NMR (376 MHz, CDCl₃, δ/ppm): -108.6 (s, 2 F, ArF).

HRMS (ESI): *m/z* calcd for C₂₄H₂₁F₂NO₃Si: 437.1259 found 436.1182.

4-((3,5-Difluorophenoxy)methyl)-4'-ethynyl-3-nitro-1,1'-biphenyl (**84**)

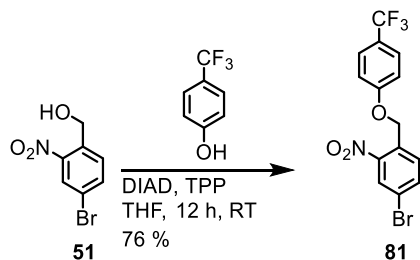
((4'-((3,5-Difluorophenoxy)methyl)-3'-nitro-[1,1'-biphenyl]-4-yl)ethynyl)trimethylsilane (**86**, 166 mg, 0.38 mmol, 1.0 equiv.) was dissolved in dichloromethane (30 ml) under an atmosphere of argon. TBAF (1 M in THF, 0.74 ml, 0.74 mmol, 1.95 equiv.) was added, and the solution stirred for 30 min at room temperature. When TLC showed full conversion of the starting material methanol (80 ml) was added. After evaporation of the solvents the crude was purified by column chromatography (silica gel, cyclohexane/ethyl acetate; 5:1) to obtain 4-((3,5-difluorophenoxy)methyl)-4'-ethynyl-3-nitro-1,1'-biphenyl (**84**) in 89 % yield as a colorless solid (124 mg, 0.34 mmol, 365.09 g/mol).

¹H-NMR (400 MHz, CDCl₃, δ/ppm): 3.18 (s, 1 H, CH), 5.50 (s, 2 H, CH₂), 6.48 (m, 1 H, ArH), 6.55 (m, 2 H, ArH), 7.61 (m, 4 H, ArH), 7.90 (m, 2 H, ArH), 8.41 (m, 1 H, ArH).

¹⁹F-NMR (376 MHz, CDCl₃, δ/ppm): -108.6 (m, 2 F, ArF).

¹³C-NMR (101 MHz, CDCl₃, δ/ppm): 67.24 (s), 78.79 (s), 82.96 (s), 97.31 (m), 98.84 (m), 122.64 (s), 123.42 (s), 126.94 (s), 129.10 (s), 131.68 (s), 132.20 (s), 132.95 (s), 138.21 (s), 141.16 (s), 147.28 (s), 159.89 (s), 162.43 (s), 165.04 (s).

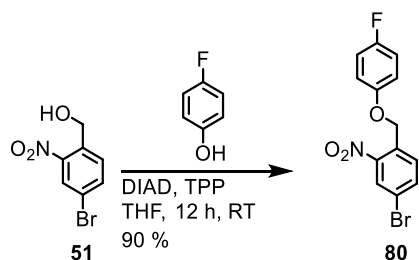
HRMS (ESI): *m/z* calcd for C₂₁H₁₃F₂NO₃: 365.0863 found 364.0785.

4-Bromo-2-nitro-1-((4-(trifluoromethyl)phenoxy)methyl)benzene (81)

The whole reaction was performed in the absence of light. A solution of 4-bromo-2-nitrophenylmethanol (**51**, 232 mg, 1.00 mmol, 1.0 equiv.), 4-(trifluoromethyl)phenol (195 mg, 1.20 mmol, 1.2 equiv.) and triphenylphosphine (318 mg, 1.20 mmol, 1.2 equiv.) in dry THF (5 ml) was cooled to 0 °C. DIAD (0.28 ml, 1.20 mmol, 1.2 equiv.) was added dropwise within 15 min. The reaction was allowed to warm to room temperature and stirred for 12 h. When TLC showed full conversion of the starting materials, the solvent was removed in vacuo and the remaining residue purified by column chromatography (silica gel, cyclohexane/ethyl acetate; 10:1) yielding 4-bromo-2-nitro-1-((4-(trifluoromethyl)phenoxy)methyl)benzene (**81**) as a colorless solid in 76 % yield (287 mg, 0.76 mmol, 374.97 g/mol).

¹H-NMR (400 MHz, CDCl₃, δ/ppm): 5.48 (s, 2 H, CH₂), 7.05 (d, ³J_{HH} = 8.5 Hz, 2 H, ArH), 7.59 (d, ³J_{HH} = 8.5 Hz, 2 H, ArH), 7.75 (d, ³J_{HH} = 8.4 Hz, 1 H, ArH), 7.82 (dd, ³J_{HH} = 8.4 Hz, ⁴J_{HH} = 2.0 Hz, 1 H, ArH), 8.34 (d, ⁴J_{HH} = 2.0 Hz, 1 H, ArH).

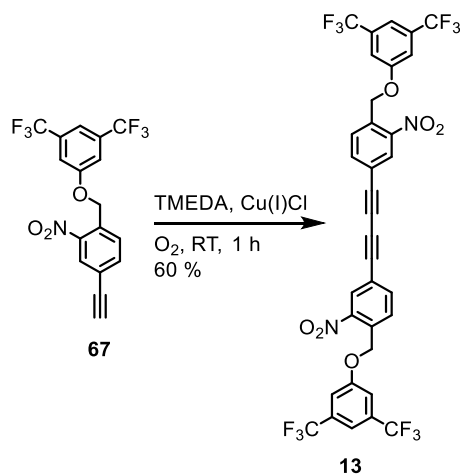
¹⁹F-NMR (376 MHz, CDCl₃, δ/ppm): -61.7 (s, 2 F, ArF).

4-Bromo-1-((4-fluorophenoxy)methyl)-2-nitrobenzene (80)

The whole reaction was performed in the absence of light. A solution of 4-bromo-2-nitrophenylmethanol (**51**, 232 mg, 1.00 mmol, 1.0 equiv.), 4-fluorophenol (135 mg, 1.20 mmol, 1.2 equiv.) and triphenylphosphine (318 mg, 1.20 mmol, 1.2 equiv.) in dry THF (5 ml) was cooled to 0 °C. DIAD (0.28 ml, 1.20 mmol, 1.2 equiv.) was added dropwise within 15 min. The reaction was allowed to warm to room temperature and stirred for 12 h. When TLC showed full conversion of the starting materials the solvent was removed *in vacuo* and the remaining residue purified by column chromatography (silica gel, cyclohexane/ethyl acetate; 10:1) yielding 4-bromo-1-((4-fluorophenoxy)methyl)-2-nitrobenzene (**80**) as a colorless solid in 90 % yield (295 mg, 0.91 mmol, 324.97 g/mol).

¹H-NMR (400 MHz, CDCl₃, δ/ppm): 5.39 (s, 2 H, CH₂), 6.96 (m, 4 H, ArH), 7.80 (m, 2 H, ArH), 8.32 (d, ⁴J_{HH} = 1.9 Hz, 1 H, ArH).

¹⁹F-NMR (376 MHz, CDCl₃, δ/ppm): -122.5 (s, 2 F, ArF).

1,4-Bis(4-((3,5-bis(trifluoromethyl)phenoxy)methyl)-3-nitrophenyl)buta-1,3-diyne (**13**)

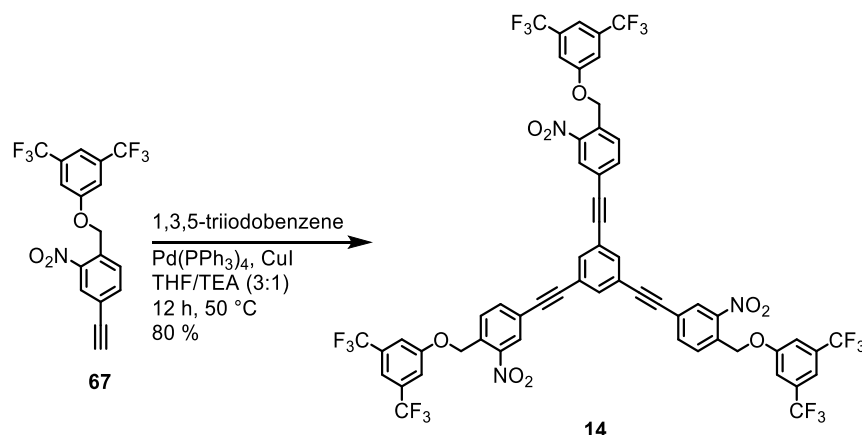
In an open Erlenmeyer-flask 1-((3,5-bis(trifluoromethyl)phenoxy)methyl)-4-ethynyl-2-nitrobenzene (**67**, 389 mg, 1.00 mmol, 1.0 equiv.) was dissolved in dichloromethane (200 ml). After stirring vigorously for 5 min TMEDA (4.5 ml, 30.0 mmol, 30 equiv.) was added, and the solution stirred under air for another 5 min. Then Cu(I)Cl (2.97 g, 30 mmol, 30 equiv.) was added and the reaction stirred for 50 min vigorously at air. After multiple washing of the solution with water and brine and drying over anhydrous Na₂SO₄, the solvent was removed under reduced pressure. The resulting solid was purified by column chromatography (silica gel, cyclohexane/ethyl acetate; 2:1 to ethyl acetate) obtaining the crude product as the last fraction. The crude was recrystallized from chloroform yielding 1,4-bis(4-((3,5-bis(trifluoromethyl)phenoxy)methyl)-3-nitrophenyl)buta-1,3-diyne (**13**) as a colorless solid in 60 % yield (233 mg, 0.30 mmol, 776.08 g/mol).

¹H-NMR (400 MHz, THF-*d*₈, δ/ppm): 5.71 (s, 4 H, CH₂), 7.66 (m, 6 H, ArH), 7.94 (m, 4 H, ArH), 8.40 (m, 2 H, ArH).

¹⁹F-NMR (376 MHz, THF-*d*₈, δ/ppm): -63.7 (s, 12 F, ArF).

¹³C-NMR (101 MHz, THF-*d*₈ CDCl₃, δ/ppm): 68.54 (s), 76.02 (s), 80.89 (s), 115.90 (m), 116.79 (s), 123.12 (s), 125.85 (s), 129.80 (s), 130.17 (s), 133.87 (q), 134.99 (s), 138.20 (s), 148.71 (s), 160.34 (s).

HRMS (MALDI/ESI): *m/z* calcd for C₃₄H₂₀F₁₂N₃O₆: 794.1155 found 794.1157.

1,3,5-Tris((4-((3,5-bis(trifluoromethyl)phenoxy)methyl)-3-nitrophenyl)ethynyl)benzene (**14**)

1,3,5-Triiodobenzene (65.2 mg, 0.14 mmol, 1.0 equiv.) was dissolved in THF/TEA (3:1, 20 ml) and degassed for 20 min in a constant argon stream. Copper(I)iodide (1.4 mg, 5 mol%) and tetrakis(triphenylphosphine)palladium(O) (8.4 mg, 5 mol%) were added and the solution degassed again for 10 min in a constant argon stream. 1-((3,5-Bis(trifluoromethyl)phenoxy)methyl)-4-ethynyl-2-nitrobenzene (**67**, 250 mg, 0.64 mmol, 4.5 equiv.) was added and the reaction mixture heated to 50 °C for 12 h. The completion of the reaction was checked by TLC. When all starting material was consumed the reaction mixture was cooled to room temperature and diluted with TBME. The organic phases was washed with water and brine, dried over anhydrous Na₂SO₄, and the solvent removed under reduced pressure. The crude was recrystallized from chloroform to obtain 1,3,5-tris((4-((3,5-bis(trifluoromethyl)phenoxy)methyl)-3-nitrophenyl)ethynyl)benzene (**14**) as a colorless solid in 80 % yield (142 mg, 1.54 mmol, 1239.15 g/mol).

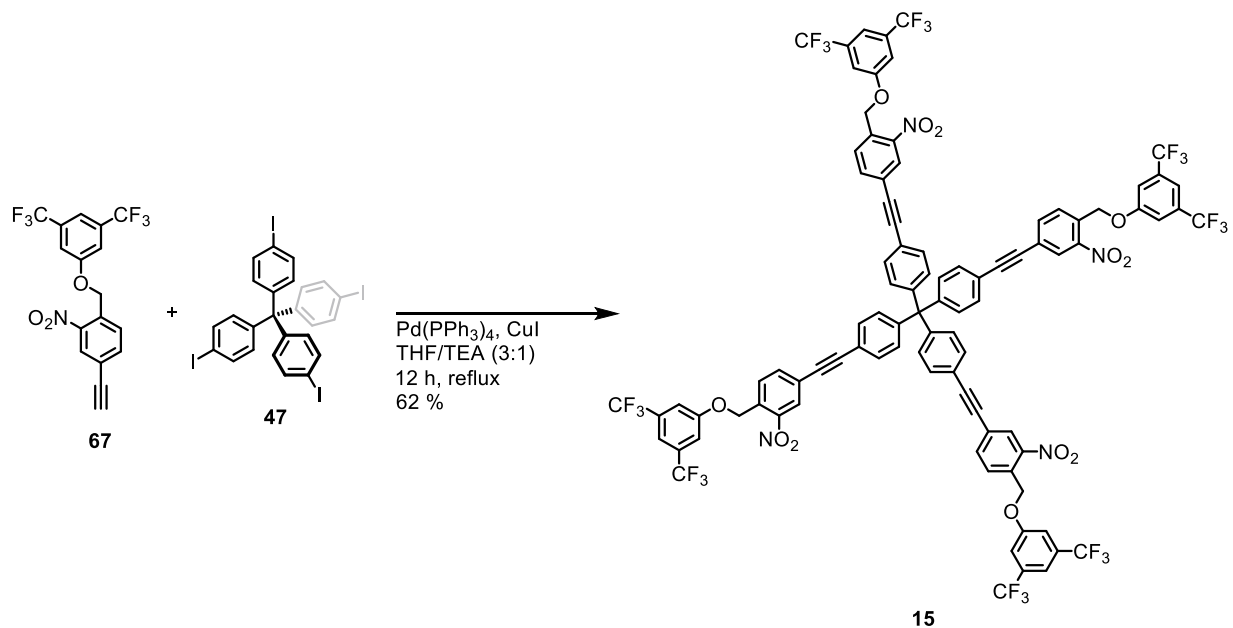
¹H-NMR (400 MHz, THF-*d*₈, δ/ppm): 5.72 (s, 6 H, CH₂), 7.67 (m, 9 H, ArH), 7.94 (s, 3 H, ArH), 7.94 (m, 6 H, ArH), 8.38 (m, 3 H, ArH).

¹⁹F-NMR (376 MHz, THF-*d*₈, δ/ppm): -63.7 (s, 18 F, ArF).

¹³C-NMR (101 MHz, THF-*d*₈, δ/ppm): 68.61 (s), 89.29 (s), 90.52 (s), 115.86 (m), 116.77 (s), 123.15 (s), 124.54 (s), 124.79 (s), 125.86 (s), 128.87 (s), 130.14 (s), 134.04 (q), 135.90 (s), 137.26 (s), 148.71 (s), 160.40 (s).

HRMS (MALDI/ESI): *m/z* calcd for C₅₇H₂₇F₁₈N₃NaO₉: 1262.1352 found 1262.1370.

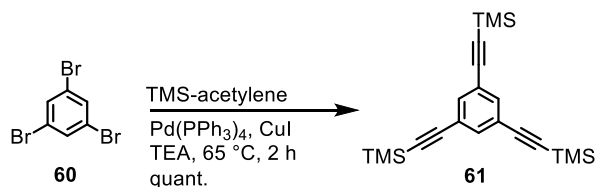
Tetrakis(4-((4-((3,5-bis(trifluoromethyl)phenoxy)methyl)-3-nitrophenyl)ethynyl)phenyl)methane (15)



Tetrakis(4-iodophenyl)methane (**47**, 84.9 mg, 0.10 mmol, 1.0 equiv.) was dissolved in THF/TEA (5:1, 48 ml) and degassed for 20 min in a constant argon stream. Copper(I)iodide (0.2 mg, 10 mol%) and tetrakis(triphenylphosphine)palladium(O) (0.6 mg, 5 mol%) were added and the solution degassed again for 10 min in a constant argon stream. 1-((3,5-Bis(trifluoromethyl)phenoxy)methyl)-4-ethynyl-2-nitrobenzene (**67**, 200 mg, 0.52 mmol, 5.0 equiv.) was added and the reaction mixture heated to reflux for 12 h. The completion of the reaction was checked by TLC. When all starting material was consumed the reaction mixture was cooled to room temperature and extracted with TBME. Combined organic phases were washed with water and brine, dried over anhydrous Na₂SO₄, and the solvent removed under reduced pressure. The resulting solid was purified by column chromatography (silica gel, cyclohexane/ethyl acetate; 2:1 to ethyl acetate) obtaining the crude product as the last fraction. The crude was recrystallized from chloroform to obtain tetrakis(4-((4-((3,5-bis(trifluoromethyl)phenoxy)methyl)-3-nitrophenyl)ethynyl)phenyl)methane (**15**) as a colorless solid in 62 % yield (119 mg, 0.06 mmol, 1869.29 g/mol).

¹H-NMR (400 MHz, THF-*d*₈, δ/ppm): 5.69 (s, 8 H, CH₂), 7.33 (d, ³J_{HH} = 8.7 Hz, 8 H, ArH), 7.55 (d, ³J_{HH} = 8.5 Hz, 8 H, ArH), 7.65 (s, 8 H, ArH), 7.89 (m, 12 H, ArH), 8.32 (s, 4 H, ArH).

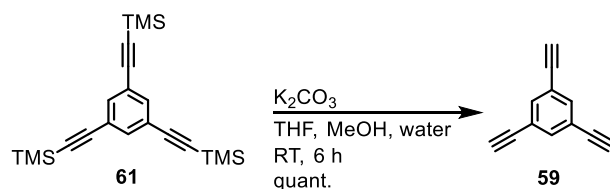
¹⁹F-NMR (376 MHz, THF-*d*₈, δ/ppm): -65.6 (s, 24 F, ArF).

1,3,5-Tris((trimethylsilyl)ethynyl)benzene (61)¹⁶⁰

1,3,5-Tribromobenzene (**60**, 5.01 g, 15.9 mmol, 1.0 equiv.), tetrakis(triphenylphosphine)-palladium (557 mg, 3 mol%), and CuI (91 mg, 3 mol%) were dissolved in TEA (100 ml) and degassed in a constant argon stream for 20 min. TMS-acetylene (9 ml, 63.6 mmol, 4.0 equiv.) was added and the reaction heated to 65 °C for 2 h. When TLC showed consumption of the starting materials hexane was added. The reaction mixture was filtered through a plug of silica. Solvents were removed under reduced pressure to yield 1,3,5-tris((trimethylsilyl)ethynyl)benzene (**61**) in quantitative yield as a yellow solid (5.83 g, 15.9 mmol, 366.17 g/mol).

¹H-NMR (400 MHz, CDCl₃, δ/ppm): 0.25 (s, 27 H, TMS), 7.52 (s, 3 H, ArH).

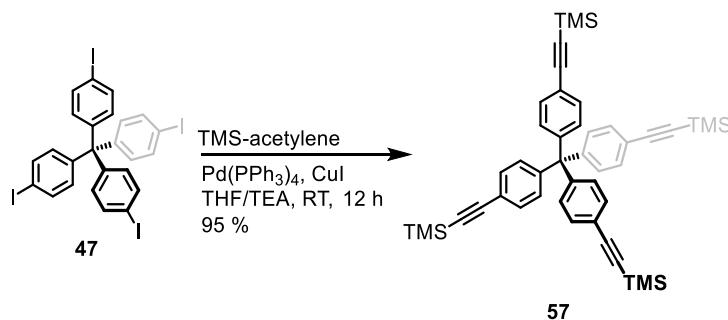
All analytical data were comparable to literature values.

1,3,5-Triethynylbenzene (59)¹⁶⁰

1,3,5-Tris((trimethylsilyl)ethynyl)benzene (**61**, 5.83 g, 16 mmol, 1.0 equiv.) and K_2CO_3 (332 mg, 2.40 mmol, 0.15 equiv.) were dissolved in a solvent mixture of THF (100 ml), MeOH (20 ml), and water (5 ml). The reaction was stirred for 6 h at room temperature. Water was added to the reaction mixture and the reaction mixture extracted with TBME. Combined organic phases were washed with water and brine and dried over anhydrous Na_2SO_4 . The solvent was removed under reduced pressure to obtain 1,3,5-triethynylbenzene (**59**) in quantitative yield as a colorless solid (2.40 g, 16 mmol, 150.05 g/mol).

1H -NMR (400 MHz, $CDCl_3$, δ /ppm): 3.10 (s, 3 H, CH), 7.57 (s, 3 H, ArH).

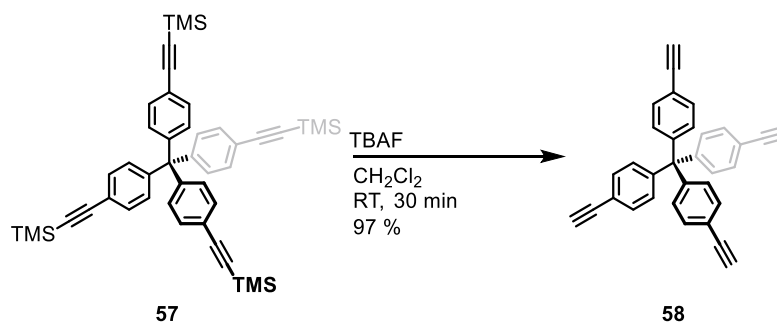
^{13}C -NMR (101 MHz, $CDCl_3$, δ /ppm): 78.81, 81.75, 123.09, 135.79.

Tetrakis(4-((trimethylsilyl)ethynyl)phenyl)methane (57)¹⁶¹

In an oven dried three neck flask tetrakis(4-iodophenyl)methane (**47**, 100 mg, 0.121 mmol, 1.0 equiv.), tetrakis(triphenylphosphine)-palladium (13 mg, 10 mol%), and CuI (1.00 mg, 4 mol%) were dissolved in THF (5 ml) and TEA (1 ml). The reaction mixture was degassed for 20 min in a constant argon stream. Trimethylsilylacetylene (0.180 ml, 1.21 mmol, 10 equiv.) was added and the reaction stirred at room temperature for 12 h. TBME was added and the combined organic phases were washed with water and brine. After drying over anhydrous Na₂SO₄ the solvent was removed under reduced pressure. The remaining dark brown solid was purified by column chromatography (silica gel, cyclohexane/ ethyl acetate, 10:1) yielding tetrakis(4-((trimethylsilyl)ethynyl)phenyl)methane (**57**) in 95 % as a yellow solid.

¹H-NMR (400 MHz, CDCl₃, δ/ppm): 0.25 (s, 27 H, TMS), 7.52 (d, ³J_{HH} = 8.6 Hz, 8 H, ArH), 7.33 (d, ³J_{HH} = 8.5 Hz, 8 H, ArH).

All analytical data were comparable to literature values.

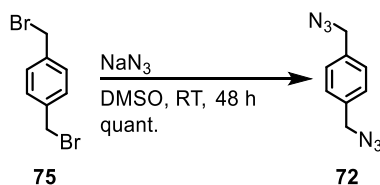
Tetrakis(4-ethynylphenyl)methane (58)¹⁶¹

Tetrakis(4-((trimethylsilyl)ethynyl)phenyl)methane (**57**, 458 mg, 0.649 mmol, 1.0 equiv.) was dissolved in dichloromethane (60 ml). TBAF (1 M in THF, 5.2 ml, 5.19 mmol, 8.0 equiv.) was added and the reaction stirred at room temperature for 30 min. The reaction was stopped by the addition of methanol (60 ml). After evaporation of the solvents, the crude was purified by column chromatography (Silica gel, cyclohexane/ ethyl acetate, 5:1) to yield tetrakis(4-ethynylphenyl)methane (**58**) as a colorless solid in 97 % yield (261 mg, 0.626 mmol, 416.16 g/mol).

¹H-NMR (400 MHz, CDCl₃, δ/ppm): 3.06 (s, 4 H, CH), 7.12 (d, ³J_{HH} = 8.7 Hz, 8 H, ArH), 7.39 (d, ³J_{HH} = 8.5 Hz, 8 H, ArH) ppm.

¹³C-NMR (101 MHz, CDCl₃, δ/ppm): 64.96, 77.76, 83.32, 120.45, 130.89, 131.80, 146.35.

HRMS (ESI/MALDI): *m/z* calcd for C₃₃H₂₀: 416.1560 found 416.1560 .

1,4-Bis(azidomethyl)benzene (72)¹⁶²

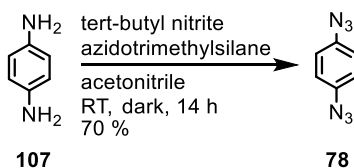
CAUTION: Azides are potential explosives, handle with care. Sodium azide is toxic and can be adsorbed through skin.

A stock solution of sodium azide (0.5 M in DMSO) was prepared by stirring over night at room temperature. To the stock solution of sodium azide (0.5 M in DMSO, 22 ml, 11.0 mmol, 2.2 equiv.) dibromo-*p*-xylol (**75**, 1.36 g, 5.00 mmol, 1.0 equiv.) was added and the solution stirred for 48 h. The reaction was quenched with water and extracted with diethylether. Combined organic phases were washed twice with water, with brine and dried over anhydrous Na₂SO₄. The solvent was removed under reduced pressure to give 1,4-bis(azidomethyl)benzene (**72**) as a colorless liquid in quantitative yield (941 mg, 5.00 mmol, 188.08 g/mol).

¹H-NMR (400 MHz, CDCl₃, δ/ppm): 4.36 (s, 4 H, CH₂), 7.34 (s, 4 H, ArH).

¹³C-NMR (101 MHz, CDCl₃, δ/ppm): 54.41 (s), 128.65 (s), 135.55 (s).

MS (EI-QMS): *m/z* (%): 188 (25) [M]⁺, 146 (100), 131 (14), 118 (62), 104 (31), 91 (83), 77 (49), 65 (28).

1,4-Diazidobenzene (78)¹⁶³

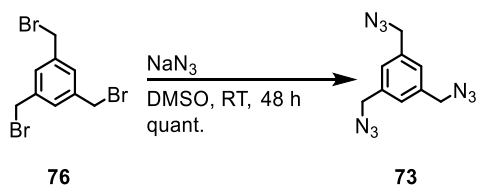
CAUTION: Azides are potential explosives, handle with care. Sodium azide is toxic and can be adsorbed through skin. Nitrogen is produced during the reaction, do not use closed systems.

p-Phenylenediamine (**107**, 541 mg, 5.00 mmol, 1.0 equiv.) was dissolved in acetonitrile (12 ml). After cooling to 0 °C *tert*-butyl nitrite (4 ml, 30.0 mmol, 9.0 equiv.) and azidotrimethylsilane (2.71 ml, 20.0 mmol, 4.0 equiv.) were added sequentially dropwise. The reaction was stirred for 14 h at room temperature in the dark. The solvent was removed under reduced pressure and the remaining residue purified by column chromatography (silica gel, hexane) to give 1,4-diazidobenzene (**78**) in 70 % yield as a colorless solid (561 mg, 3.50 mmol, 160.05 g/mol).

¹H-NMR (400 MHz, CDCl₃, δ/ppm): 7.01 (s, 4 H, ArH).

¹³C-NMR (101 MHz, CDCl₃, δ/ppm): 120.36 (s), 136.69 (s).

MS (EI-QMS): *m/z* (%): 160 (25) [M]⁺, 132 (15), 103 (35), 78 (55), 64 (18).

1,3,5-Tris(azidomethyl)benzene(73)¹⁶²

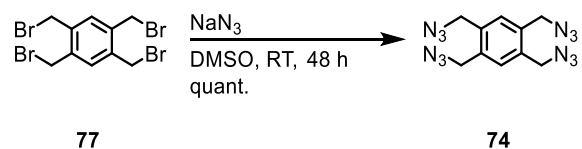
CAUTION: Azides are potential explosives, handle with care. Sodium azide is toxic and can be adsorbed through skin.

A stock solution of sodium azide (0.5 M in DMSO) was prepared by stirring over night at room temperature. To the stock solution of sodium azide (0.5 M in DMSO, 17.9 ml, 8.97 mmol, 3.3 equiv.) 1,3,5-tris(bromomethyl)benzene (**76**, 1.00 g, 2.72 mmol, 1.0 equiv.) was added and the solution stirred for 48 h. The reaction was quenched with water and extracted with diethylether. Combined organic phases were washed with water, brine, and dried over anhydrous Na₂SO₄. The solvent was removed under reduced pressure to give 1,3,5-tris(azidomethyl)benzene (**73**) as a colorless liquid in quantitative yield (661 mg, 2.72 mmol, 243.10 g/mol).

¹H-NMR (400 MHz, CDCl₃, δ/ppm): 4.40 (s, 6 H, CH₂), 7.25 (s, 3 H, ArH).

¹³C-NMR (101 MHz, CDCl₃, δ/ppm): 54.30 (s), 127.47 (s), 136.99 (s).

MS (EI-QMS): *m/z* (%): 243 (23) [M]⁺, 215 (18), 201 (64), 173 (42), 131 (26), 117 (64), 91 (75), 77 (100), 65 (61).

1,2,4,5-Tetrakis(azidomethyl)benzene (74)¹⁶²

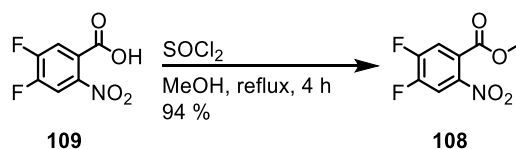
CAUTION: Azides are potential explosives, handle with care. Sodium azide is toxic and can be adsorbed through skin.

A stock solution of sodium azide (0.5 M in DMSO) was prepared by stirring over night at room temperature. To the stock solution of sodium azide (0.5 M in DMSO, 18.6 ml, 9.29 mmol, 4.4 equiv.) 1,2,4,5-tetrakis(bromomethyl)benzene (**77**, 1.00 g, 2.11 mmol, 1.0 equiv.) was added and the solution stirred for 48 h. The reaction was quenched with water and extracted with diethylether. Combined organic phases were washed with water, brine, and dried over anhydrous Na₂SO₄. The solvent was removed under reduced pressure to give 1,2,4,5-tetrakis(azidomethyl)benzene (**74**) as a colorless liquid in quantitative yield (630 mg, 2.11 mmol, 298.12 g/mol).

¹H-NMR (400 MHz, CDCl₃, δ/ppm): 4.60 (s, 8 H, CH₂), 7.37 (s, 2 H, ArH).

¹³C-NMR (101 MHz, CDCl₃, δ/ppm): 28.68 (s), 133.64 (s), 137.62 (s).

All other analytical data were comparable to literature values.

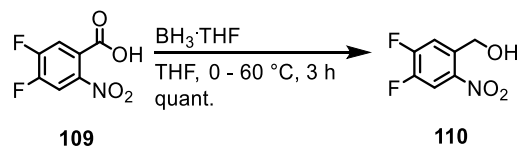
Methyl 4,5-difluoro-2-nitrobenzoate (108)

4,5-Difluoro-2-nitrobenzoic acid (**109**, 406 mg, 2.00 mmol, 1.0 equiv.) was dissolved in MeOH (10 ml) and cooled to 0 °C. Thionyl chloride (1.46 ml, 20.0 mmol, 10 equiv.) was added dropwise and the reaction heated to reflux for 4 h. The reflux condenser was removed and the solvent and remaining thionyl chloride were distilled off. The corresponding methyl 4,5-difluoro-2-nitrobenzoate (**108**) was obtained in 94 % yield as a colorless liquid (410 mg, 1.89 mmol, 517.02 g/mol).

¹H-NMR (400 MHz, CDCl₃, δ/ppm): 3.94 (s, 3 H, CH₃), 7.58 (dd, ³J_{HF} = 9.3 Hz, ⁴J_{HF} = 7.4 Hz, 1 H, ArH), 7.82 (dd, ³J_{HF} = 9.0 Hz, ⁴J_{HF} = 6.6 Hz, 1 H, ArH).

¹⁹F-NMR (376 MHz, CDCl₃, δ/ppm): -126.6 (d, ³J_{FF} = 20.8 Hz, 1 F, Ar-F), -127.6 (d, ³J_{FF} = 20.7 Hz, 1 F, Ar-F).

All other analytical data were comparable to literature values.

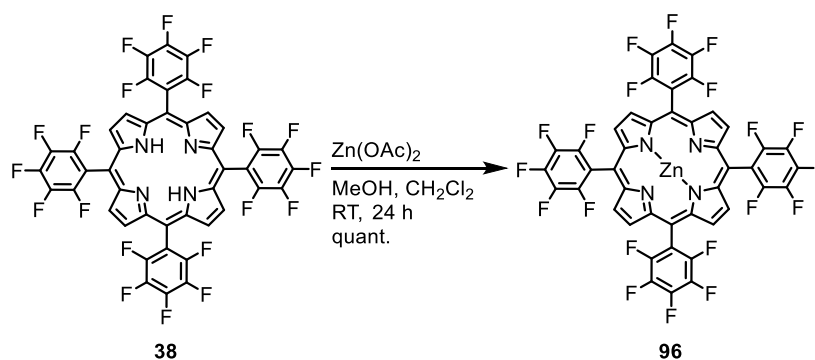
(4,5-Difluoro-2-nitrophenyl)methanol (110)

A solution of 4,5-difluoro-2-nitrobenzoic acid (**109**, 203 mg, 1.00 mmol, 1.0 equiv.) in THF (10 ml) was cooled to 0 °C. Borane-THF complex (1 M in THF, 2.5 ml, 2.50 mmol, 2.5 equiv.) was slowly added keeping the temperature below 0 °C. The cooling bath was removed and the reaction heated to reflux for 3 h. At 0 °C methanol was added and the reaction stirred at 0 °C for 10 min. Dilution with ethyl acetate was followed by washing of the combined organic phases with water and brine. After drying over anhydrous MgSO₄ the solvent was removed under reduced pressure and the crude purified by column chromatography (silica gel, cyclohexane/ethyl acetate; 2:1) to yield (4,5-difluoro-2-nitrophenyl)methanol (**110**) as a colorless solid in quantitative yield (188 mg, 0.99 mmol, 189.02 g/mol).

¹H-NMR (400 MHz, CDCl₃, δ/ppm): 2.76 (brs, 1 H, OH), 5.03 (s, 2 H, CH₂), 7.71 (dd, ³J_{HF} = 10.9 Hz, ⁴J_{HF} = 7.9 Hz, 1 H, ArH), 8.05 (dd, ³J_{HF} = 9.8 Hz, ⁴J_{HF} = 7.1 Hz, 1 H, ArH).

¹⁹F-NMR (376 MHz, CDCl₃, δ/ppm): -126.0 (d, ³J_{FF} = 21.6 Hz, 1 F, Ar-F), -135.5 (d, ³J_{FF} = 21.6 Hz, 1 F, Ar-F).

¹³C-NMR (101 MHz, CDCl₃, δ/ppm): 61.44 (s), 115.24 (dd, ³J_{CF} = 21.8 Hz, ⁴J_{CF} = 2.2 Hz), 117.74 (d, ³J_{CF} = 20.6 Hz), 136.18 (dd, ⁴J_{CF} = 6.7 Hz, ⁴J_{CF} = 3.8 Hz), 148.52 (dd, ²J_{CF} = 253.5 Hz, ³J_{CF} = 14.0 Hz), 153.81 (dd, ²J_{CF} = 259.9 Hz, ³J_{CF} = 12.3 Hz), 171.74 (s).

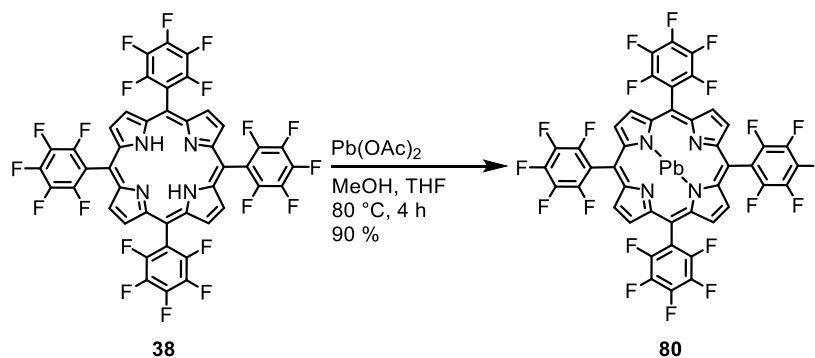
5,10,15,20-Tetrakis(perfluorophenyl)porphyrin-zinc (96)

A solution of zinc acetate (325 mg, 1.76 mmol, 5.7 equiv.) in MeOH (15 ml) was added to a solution of 5,10,15,20-tetrakis(perfluorophenyl)porphyrin (**38**, 300 mg, 0.31 mmol, 1.0 equiv.) in dichloromethane (70 ml). The reaction mixture was stirred for 24 h. The reaction was washed with water (150 ml) and the solvent removed under reduced pressure to yield 5,10,15,20-tetrakis(perfluorophenyl)porphyrin-zinc (**96**) in quantitative yield (319 mg, 0.31 mmol, 1035.97 g/mol).

¹H-NMR (400 MHz, CDCl₃, δ/ppm): 9.02 (s, 8 H, ArH).

¹⁹F-NMR (376 MHz, CDCl₃, δ/ppm): -136.8 (m, 8 F, Ar-F), -152.0 (m, 4 F, Ar-F), -161.8 (m, 8 F, Ar-F).

MS (MALDI-TOF): *m/z* (%): 1035.5 (100) [M]⁺, 1036.4 (41), 1037.4 (66), 1038.4 (28), 1039.4 (38), 1040.4 (10).

5,10,15,20-Tetrakis(perfluorophenyl)porphyrin-lead (80)

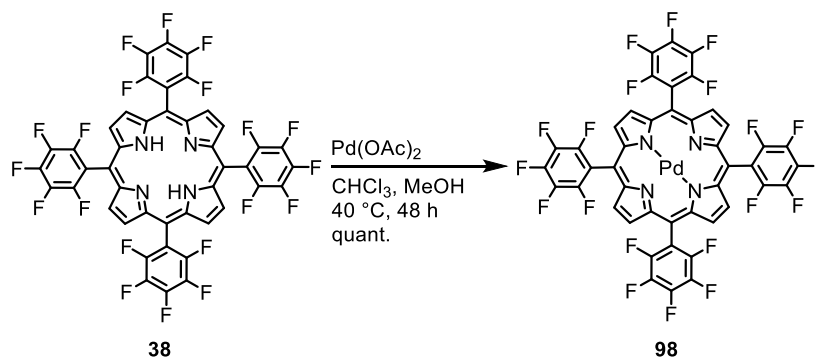
To a solution of 5,10,15,20-tetrakis(perfluorophenyl)porphyrin (**38**, 195 mg, 0.20 mmol, 1.0 equiv.) in THF (10 ml) a solution of lead acetate trihydrate (986 mg, 2.6 mmol, 13 equiv.) in methanol (10 ml) was added and the reaction mixture heated to reflux for 4 h. The reaction was stopped by the addition of water and extracted with TBME. Combined organic phases were washed with water and brine. The crude was dried over anhydrous Na_2SO_4 and the solvent removed under reduced pressure to yield 5,10,15,20-tetrakis(perfluorophenyl)porphyrin-lead (**80**) in 90 % yield (186 mg, 0.18 mmol, 1180.02 g/mol).

$^1\text{H-NMR}$ (400 MHz, CDCl_3 , δ/ppm): 9.03 (s, 8 H, ArH).

$^{19}\text{F-NMR}$ (376 MHz, CDCl_3 , δ/ppm): -136.8 (m, 8 F, Ar-F), -152.0 (m, 4 F, Ar-F), -161.8 (m, 8 F, Ar-F).

MS (MALDI-TOF): m/z (%): 1181.2 (20) $[\text{M}+\text{H}]^+$, 1182.0 (45), 1183.0 (100), 1183.8 (64), 1084.6 (33).

HRMS (MALDI/ESI): m/z calcd for $\text{C}_{44}\text{H}_8\text{F}_{20}\text{N}_4\text{Pb}$: 1180.0196 found 1180.0194.

5,10,15,20-Tetrakis(perfluorophenyl)porphyrin-palladium (98)

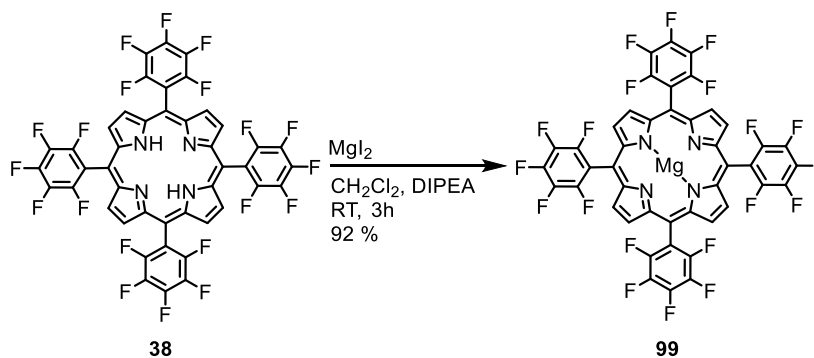
5,10,15,20-Tetrakis(perfluorophenyl)porphyrin (**38**, 150 mg, 0.15 mmol, 1.0 equiv.) was dissolved in chloroform (10 ml) and Pd(OAc)₂ (51 mg, 0.23 mmol, 1.5 equiv.) in MeOH (10 ml) was added. The reaction was heated to 40 °C for 48 h in the absence of light. The reaction mixture was diluted with dichloromethane, washed with water and brine, and dried over anhydrous Na₂SO₄. The solvent was removed under reduced pressure to yield 5,10,15,20-tetrakis(perfluorophenyl)porphyrin-palladium (**98**) in quantitative yield (166 mg, 0.15 mmol, 1077.95 g/mol).

¹H-NMR (400 MHz, CDCl₃, δ/ppm): 8.88 (s, 8 H, ArH).

¹⁹F-NMR (376 MHz, CDCl₃, δ/ppm): -136.4 (m, 8 F, Ar-F), -151.2 (m, 4 F, Ar-F), -161.2 (m, 8 F, Ar-F).

MS (MALDI-TOF): *m/z* (%): 1077.5 (23) [M]⁺, 1078.5 (66), 1079.4 (100), 1080.4 (51), 1081.3 (75), 1082.3 (39), 1083.3 (35), 1084.3 (18).

HRMS (MALDI/ESI): *m/z* calcd for C₄₄H₈F₂₀N₄Pd: 1077.9474 found 1077.9468.

5,10,15,20-Tetrakis(perfluorophenyl)porphyrin-magnesium (99)

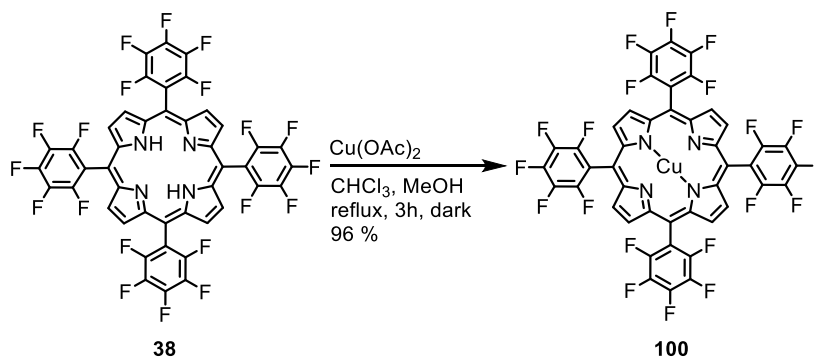
To a solution of 5,10,15,20-tetrakis(perfluorophenyl)porphyrin (**38**, 195 mg, 0.20 mmol, 1.0 equiv.) in dichloromethane (15 ml) MgI_2 (556 mg, 2.00 mmol, 10 equiv.) and DIPEA (1 ml) was added. The reaction stirred at room temperature for 3 h. The reaction mixture was extracted with dichloromethane, washed with water and brine, and dried over anhydrous Na_2SO_4 . The solvent was removed under reduced pressure to yield 5,10,15,20-tetrakis(perfluorophenyl)porphyrin-magnesium (**99**) in 92 % yield (183 mg, 0.184 mmol, 996.03 g/mol).

$^1\text{H-NMR}$ (400 MHz, CDCl_3 , δ/ppm): 8.84 (s, 8 H, ArH).

$^{19}\text{F-NMR}$ (376 MHz, CDCl_3 , δ/ppm): -137.0 (m, 8 F, Ar-F), -153.0 (m, 4 F, Ar-F), -162.5 (m, 8 F, Ar-F).

MS (MALDI-TOF): m/z (%): 996.3 (100) $[\text{M}]^+$, 997.3 (72), 998.3 (40).

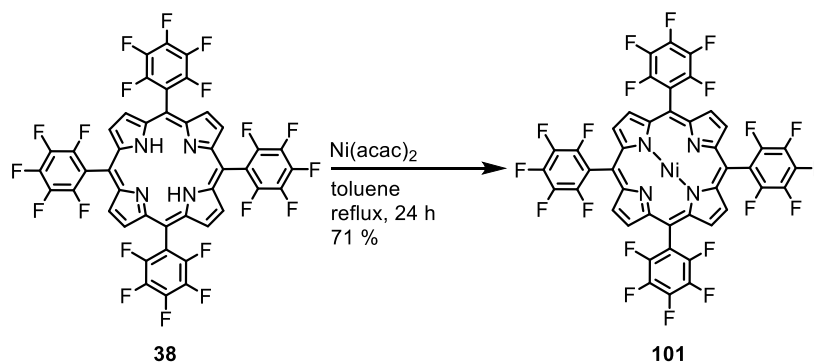
HRMS (MALDI/ESI): m/z calcd for $\text{C}_{44}\text{H}_8\text{F}_{20}\text{N}_4\text{Mg}$: 996.0275 found 996.0273.

5,10,15,20-Tetrakis(perfluorophenyl)porphyrin-copper (100)

A saturated solution of $\text{Cu}(\text{OAc})_2$ (55.9 mg, 0.308 mmol, 2.0 equiv.) in MeOH (15 ml) was mixed with a solution of 5,10,15,20-tetrakis(perfluorophenyl)porphyrin (**38**, 150 mg, 0.154 mmol, 1.0 equiv.) in chloroform (15 ml). The reaction mixture was heated to reflux for 3 h in the absence of light. After extraction with TBME combined organic phases were washed with water and brine and dried over anhydrous Na_2SO_4 . The solvent was removed under reduced pressure to yield 5,10,15,20-tetrakis(perfluorophenyl)porphyrin-copper (**100**) in 96 % yield (153 mg, 0.148 mmol, 1034.97 g/mol).

MS (MALDI-TOF): m/z (%): 1035.2 (31) $[\text{M}]^+$, 1036.2 (31), 1037.2 (100), 1038.2 (44), 1039.2 (38), 1040.2 (12).

HRMS (MALDI/ESI): m/z calcd for $\text{C}_{44}\text{H}_8\text{F}_{20}\text{N}_4\text{Cu}$: 1034.9720 found 1034.9718.

5,10,15,20-Tetrakis(perfluorophenyl)porphyrin-lead (101)

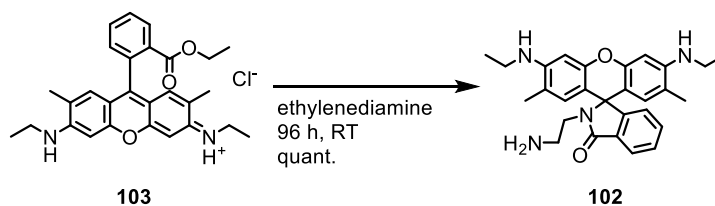
TPPF (150 mg, 0.154 mmol, 1.00 equiv.) was dissolved in toluene (20 ml). Nickel acetylacetonate (acac) (55,7 mg, 0.208mmol, 1.35 equiv.) was added. The solute was stirred under reflux in the dark. After 24 h the reaction was finished and water was added to the product. Then the product was extracted with dichloromethane. Combined organic phases were washed with water and brine and dried over anhydrous MgSO_4 . After drying under high vacuum 5,10,15,20-tetrakis(perfluorophenyl)porphyrin-lead (**101**) was obtained as a violet powder in 71 % yield (112 mg, 0.109 mmol, 1029.98 g/mol).

$^1\text{H-NMR}$ (400 MHz, CDCl_3 , δ/ppm): 8.79 (s, 8H, Ar-H).

$^{19}\text{F-NMR}$ (376 MHz, CDCl_3 , δ/ppm): -136.61 (q, 8 F, Ar-F), -151.28 (t, 4 F, Ar-F), -161.16 (m, 8 F, Ar-F).

MS (MALDI-TOF): m/z (%): 1031.6 (100)[$\text{M}+\text{H}$] $^+$, 1033.5 (60), 1032.5 (57), 1034.5 (31).

HRMS (MALDI/ESI): m/z calcd for $\text{C}_{44}\text{H}_8\text{F}_{20}\text{N}_4\text{Ni}$: 1029.9778 found 1029.9776.

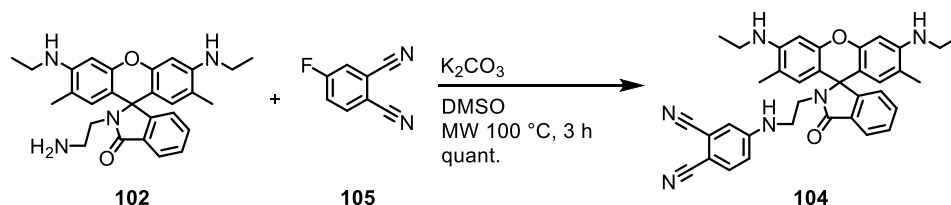
Rhodamine 6G spirolactame (102)¹⁶⁴

Rhodamine 6G (**103**, 9.58 g, 19.8 mmol, 1.0 equiv.) was dissolved in ethylenediamine (14 ml, 209 mmol, 11 equiv.) cooling the mixture in an ice bath. The solution was stirred vigorously at room temperature for 96 h in an atmosphere of argon. The pink precipitate was filtered off and washed excessively with water. After recrystallization from toluene and drying under high vacuum rhodamine 6G spirolactame (**102**) was obtained as a pink solid in quantitative yield. (9.04 g, 20 mmol, 456.59 g/mol).

¹H-NMR (400 MHz, CDCl₃, δ/ppm): 1.32 (t, ³J_{HH} = 7.1 Hz, 6 H, CH₃), 1.90 (s, 6 H, CH₃), 2.35 (t, ³J_{HH} = 6.7 Hz, 2 H, CH₂), 3.16 (t, ³J_{HH} = 6.8 Hz, 2 H, CH₂), 3.22 (dd, ³J_{HH} = 7.2 Hz, ³J_{HH} = 5.1 Hz, 4 H, CH₂), 3.50 (t, ³J_{HH} = 5.2 Hz, 2 H, NH), 6.22 (m, 2 H, Ar-H), 6.34 (m, 2 H, Ar-H), 7.05 (m, 1 H, Ar-H), 7.45 (m, 2 H, Ar-H), 7.93 (m, 1 H, Ar-H).

All analytical data were comparable to literature values.

4-((2-(3',6'-bis(ethylamino)-2',7'-dimethyl-3-oxospiro[isoindoline-1,9'-xanthen]-2-yl)ethyl)amino)phthalonitrile (104)

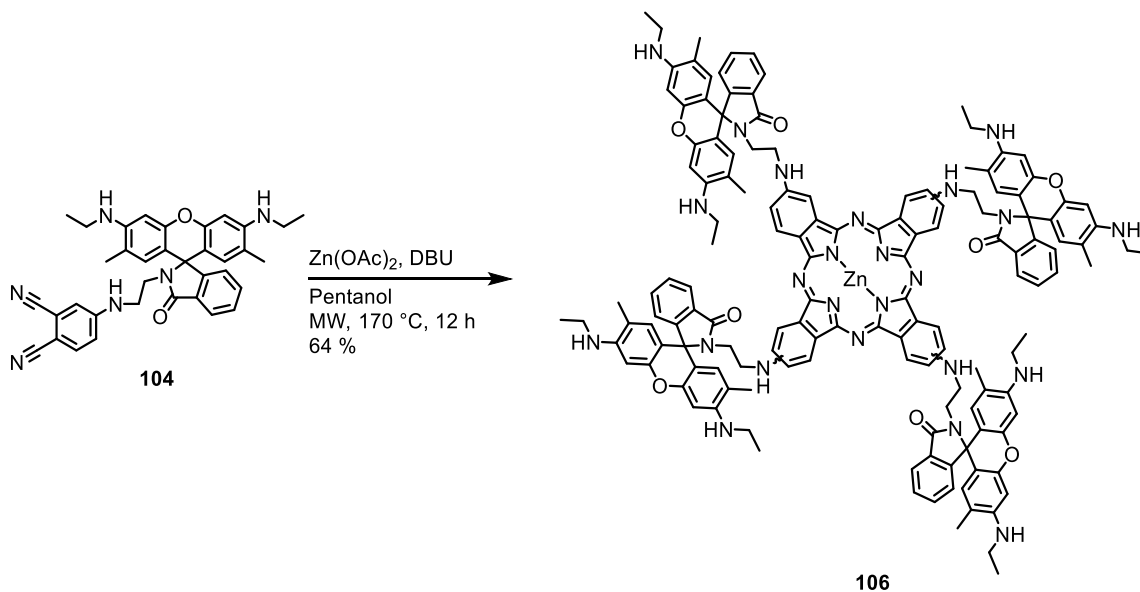


In a Biotage microwave tube (10-20 ml) 4-fluorophthalonitrile (**105**, 150 mg, 1.03 mmol, 1.0 equiv.), rhodamine 6G spirolactame (**102**, 1.41 g, 3.08 mmol, 3.0 equiv.) and potassium carbonate (430 mg, 3.08 mmol, 3.0 equiv.) were dissolved in dry DMSO (10 ml) and heated in the microwave apparatus for 3 h to 100 °C. After cooling to room temperature, water was added to the reaction mixture. The two-phase system was extracted with TBME. Combined organic phases were washed with water and brine. Solvents were removed under reduced pressure and the resulting residue purified by column chromatography (silica gel, cyclohexane/ethyl acetate, 5:1). The desired phthalonitrile 4-((2-(3',6'-bis(ethylamino)-2',7'-dimethyl-3-oxospiro[isoindoline-1,9'-xanthen]-2-yl)ethyl)amino)phthalonitrile (**104**) was obtained in quantitative yield as a light pink solid (597 mg, 1.03 mmol, 582.71 g/mol).

¹H-NMR (400 MHz, CDCl₃, δ/ppm): 1.26 (m, 6 H, CH₃), 1.34 (m, 6 H, CH₃), 1.77 (s, 6 H, CH₃), 2.03 (s, 2 H, CH₂).

¹³C NMR (126 MHz, CDCl₃, δ/ppm): 171.15, 169.64, 153.40, 151.77, 150.92, 147.71, 134.33, 133.06, 130.47, 128.39, 128.08, 123.98, 122.89, 118.18, 117.12, 116.61, 116.13, 105.07, 100.28, 96.43, 77.40, 77.14, 76.89, 65.49, 60.40, 42.62, 38.60, 38.35, 31.92, 29.70, 29.66, 29.36, 22.70, 21.05, 16.60, 14.65, 14.20, 14.14.

MS (MALDI-TOF): *m/z* (%): 581.41 (8), 582.21 (34), 583.42 (100) [M+H]⁺, 584.43 (35), 585.43 (6).

Tetrakis-(rhodamine 6G spirolactame)-zinc-phthalocyanine (**106**)

Phthalonitrile (**104**, 233 g, 0.4 mmol, 1.0 equiv.), zinc acetate (18 mg, 0.1 mmol, 0.25 equiv.) and DBU (12 μ l, 0.08 mmol, 0.20 equiv.) were added to dry DMF (3 ml) in a microwave tube (Biotage[®] microwave vial 2-5 ml). The sealed tube was heated in the microwave apparatus to 170 °C for 12 h. The dark blue solution was extracted with TBME and washed three times with water and brine. After drying over anhydrous Na₂SO₄ the solvent was removed under reduced pressure. The remaining green solid was dissolved in dichloromethane and washed with TBME. Remaining green solid was washed with THF from the silica. The solvent was removed under reduced pressure and tetrakis-(rhodamine 6G spirolactame)-zinc-phthalocyanine (**106**) obtained in 64 % yield as a dark blue solid. Due to poor solubility of the product only MALDI-TOF analysis were performed.

MS (MALDI-TOF): m/z (%): 2397.43 (100) [M+H]⁺.

8 List of Abbreviations

Ac	acetyl
acac	acetylacetonate
Bz	benzyl
DBU	1,8-diazabicycloundec-7-ene
DDQ	2,3-dichloro-5,6-dicyano-1,4-benzoquinone
DIAD	diisopropyl azodicarboxylate
DIPEA	<i>N,N</i> -diisopropylethylamine
DMF	dimethylformamide
DMSO	dimethyl sulfoxide
ϵ	extinction coefficient
equiv.	equivalent
ESI	electron spray ionization
HRMS	high-resolution mass spectrometry
KDTLI	Kapitsa-Dirac-Dalbot-Lau interferometer
L_T	Talbot-distance
MALDI	matrix assisted laser desorption ionization
MeOH	methanol
MS	mass spectrometry
NMR	nuclear magnetic resonance
PIFA	[bis(trifluoroacetoxy)iodo]benzene
Ph	phenyl
RT	room temperature
TBAF	tetra-butyl-ammonium-fluoride
TBOH	tetra-butyl-ammonium-hydroxide
TBME	<i>tert</i> -butyl methyl ether
TEA	triethylamine
TFA	trifluoroacetic acid
THF	tetrahydrofuran
TLC	thin layer chromatography
TLI	Talbot-Lau interferometer
TMEDA	tetramethylethylenediamine
TMS	trimethylsilyl
TOF	time of flight
TPP	tetraphenylporphyrin
TPPF	<i>meso</i> -tetrakis(pentafluorophenyl)porphyrin

9 Literature

- (1) Young, T. *Philos. Trans. R. Soc. Lond.* **1802**, 92, 12–48.
- (2) Young, T. *A course of lectures on natural philosophy and the mechanical arts.* By Thomas Young.; Printed for J. Johnson.; London :, 1807.
- (3) Walther, T.; Walther, H. *Was ist Licht?: von der klassischen Optik zur Quantenoptik*; C.H.Beck, 1999.
- (4) D. Meschede. *Optik, Licht und Laser*; Vieweg Teubner In Gwv Fachverlage: Wiesbaden, 2008.
- (5) De Broglie, L. *Nature* **1923**, 112, 540.
- (6) C. Davisson; L.H. Germer. *Nature*.
- (7) Estermann, I.; Stern, O. *Z. Für Phys.* **1930**, 61 (1-2), 95–125.
- (8) H. von Halban; P. Preiswerk. *C R Acad Sci Paris* **1936**, 203, 73–75.
- (9) Jönsson, C. *Z. Für Phys.* **1961**, 161 (4), 454–474.
- (10) Jönsson, C. *Am. J. Phys.* **1974**, 42 (1), 4–11.
- (11) Martin, J. P.; Jönsson, C. *Naturwissenschaften* **1966**, 53 (23), 609–609.
- (12) Zeilinger, A.; Gähler, R.; Shull, C. G.; Treimer, W.; Mampe, W. *Rev. Mod. Phys.* **1988**, 60 (4), 1067–1073.
- (13) Carnal, O.; Mlynek, J. *Phys. Rev. Lett.* **1991**, 66 (21), 2689–2692.
- (14) Keith, D. W.; Schattenburg, M. L.; Smith, H. I.; Pritchard, D. E. *Phys. Rev. Lett.* **1988**, 61 (14), 1580–1583.
- (15) Schöllkopf, W.; Toennies, J. P. *Science* **1994**, 266 (5189), 1345–1348.
- (16) Bordé, C. J.; Courtier, N.; du Burck, F.; Goncharov, A. N.; Gorlicki, M. *Phys. Lett. A* **1994**, 188 (3), 187–197.
- (17) Chapman, M. S.; Hammond, T. D.; Lenef, A.; Schmiedmayer, J.; Rubenstein, R. A.; Smith, E.; Pritchard, D. E. *Phys. Rev. Lett.* **1995**, 75 (21), 3783–3787.
- (18) Chapman, M. S.; Ekstrom, C. R.; Hammond, T. D.; Rubenstein, R. A.; Schmiedmayer, J.; Wehinger, S.; Pritchard, D. E. *Phys. Rev. Lett.* **1995**, 74 (24), 4783–4786.
- (19) Lisdat, C.; Frank, M.; Knöckel, H.; Almazor, M.-L.; Tiemann, E. *Eur. Phys. J. D* **2000**, 12 (2), 235–240.
- (20) Reisinger, T.; Patel, A. A.; Reingruber, H.; Fladischer, K.; Ernst, W. E.; Bracco, G.; Smith, H. I.; Holst, B. *Phys. Rev. A* **2009**, 79 (5), 053823.
- (21) Arndt, M.; Nairz, O.; Vos-Andreae, J.; Keller, C.; van der Zouw, G.; Zeilinger, A. *Nature* **1999**, 401 (6754), 680–682.
- (22) Born, M.; Wolf, E. *Principles of Optics: Electromagnetic Theory of Propagation, Interference and Diffraction of Light*; Cambridge University Press, 1999.
- (23) Clauser, J. F.; Li, S. *Phys. Rev. A* **1994**, 49 (4), R2213–R2216.
- (24) Kroto, H. W.; Heath, J. R.; O'Brien, S. C.; Curl, R. F.; Smalley, R. E. *Nature* **1985**, 318 (6042), 162–163.

-
- (25) Krätschmer, W.; Lamb, L. D.; Fostiropoulos, K.; Huffman, D. R. *Nature* **1990**, *347* (6291), 354–358.
- (26) Nairz, O.; Arndt, M.; Zeilinger, A. *Am. J. Phys.* **2003**, *71* (4), 319–325.
- (27) Nairz, O.; Arndt, M.; Zeilinger, A. *J. Mod. Opt.* **2000**, *47* (14–15), 2811–2821.
- (28) Arndt, M.; Nairz, O.; Petschinka, J.; Zeilinger, A. *Comptes Rendus Académie Sci. - Ser. IV - Phys.* **2001**, *2* (4), 581–585.
- (29) Nairz, O.; Brezger, B.; Arndt, M.; Zeilinger, A. *Phys. Rev. Lett.* **2001**, *87* (16), 160401.
- (30) Hackermüller, L.; Hornberger, K.; Brezger, B.; Zeilinger, A.; Arndt, M. *Appl. Phys. B* **2003**, *77* (8), 781–787.
- (31) Kapitza, P. L.; Dirac, P. a. M. *Math. Proc. Camb. Philos. Soc.* **1933**, *29* (02), 297–300.
- (32) Moskowitz, P. E.; Gould, P. L.; Atlas, S. R.; Pritchard, D. E. *Phys. Rev. Lett.* **1983**, *51* (5), 370–373.
- (33) Freimund, D. L.; Aflatooni, K.; Batelaan, H. *Nature* **2001**, *413* (6852), 142–143.
- (34) Cronin, A. D.; Schmiedmayer, J.; Pritchard, D. E. *Rev. Mod. Phys.* **2009**, *81* (3), 1051–1129.
- (35) Juffmann, T.; Nimmrichter, S.; Arndt, M.; Gleiter, H.; Hornberger, K. *Found. Phys.* **2010**, *42* (1), 98–110.
- (36) Juffmann, T.; Milic, A.; Müllneritsch, M.; Asenbaum, P.; Tsukernik, A.; Tüxen, J.; Mayor, M.; Cheshnovsky, O.; Arndt, M. *Nat. Nanotechnol.* **2012**, *7* (5), 297–300.
- (37) H. Talbot. *Philos. Mag. Ser. 3* **1836**, *9* (56), 401–407.
- (38) Lau, E. *Ann. Phys.* **1948**, *437* (7-8), 417–423.
- (39) Case, W. B.; Tomandl, M.; Deachapunya, S.; Arndt, M. *Opt. Express* **2009**, *17* (23), 20966–20974.
- (40) Brezger, B.; Arndt, M.; Zeilinger, A. *J. Opt. B Quantum Semiclassical Opt.* **2003**, *5* (2), S82.
- (41) Moiré pattern - Oxford Reference
<http://www.oxfordreference.com/view/10.1093/acref/9780199233991.001.0001/acref-9780199233991-e-1955> (accessed Jul 31, 2015).
- (42) Brezger, B.; Hackermüller, L.; Uttenthaler, S.; Petschinka, J.; Arndt, M.; Zeilinger, A. *Phys. Rev. Lett.* **2002**, *88* (10), 100404.
- (43) Hackermüller, L.; Uttenthaler, S.; Hornberger, K.; Reiger, E.; Brezger, B.; Zeilinger, A.; Arndt, M. *Phys. Rev. Lett.* **2003**, *91* (9), 090408.
- (44) Stibor, A.; Stefanov, A.; Goldfarb, F.; Reiger, E.; Arndt, M. *New J. Phys.* **2005**, *7* (1), 224.
- (45) Gerlich, S.; Hackermüller, L.; Hornberger, K.; Stibor, A.; Ulbricht, H.; Gring, M.; Goldfarb, F.; Savas, T.; Müri, M.; Mayor, M.; Arndt, M. *Nat. Phys.* **2007**, *3* (10), 711–715.
- (46) Gerlich, S.; Gring, M.; Ulbricht, H.; Hornberger, K.; Tüxen, J.; Mayor, M.; Arndt, M. *Angew. Chem. Int. Ed.* **2008**, *47* (33), 6195–6198.
- (47) Hornberger, K.; Gerlich, S.; Ulbricht, H.; Hackermüller, L.; Nimmrichter, S.; Goldt, I. V.; Boltalina, O.; Arndt, M. *New J. Phys.* **2009**, *11* (4), 043032.
-

-
- (48) Gring, M.; Gerlich, S.; Eibenberger, S.; Nimmrichter, S.; Berrada, T.; Arndt, M.; Ulbricht, H.; Hornberger, K.; Müri, M.; Mayor, M.; Böckmann, M.; Doltsinis, N. L. *Phys. Rev. A* **2010**, *81* (3), 031604.
- (49) Tüxen, J.; Gerlich, S.; Eibenberger, S.; Arndt, M.; Mayor, M. *Chem. Commun.* **2010**, *46* (23), 4145–4147.
- (50) Deachapunya, S.; Stefanov, A.; Berninger, M.; Ulbricht, H.; Reiger, E.; Doltsinis, N. L.; Arndt, M. *J. Chem. Phys.* **2007**, *126* (16), 164304.
- (51) Deachapunya, S.; Fagan, P. J.; Major, A. G.; Reiger, E.; Ritsch, H.; Stefanov, A.; Ulbricht, H.; Arndt, M. *Eur. Phys. J. D* **2007**, *46* (2), 307–313.
- (52) Dreas-Wlodarczyk, A.; Müllneritsch, M.; Juffmann, T.; Cioffi, C.; Arndt, M.; Mayor, M. *Langmuir* **2010**, *26* (13), 10822–10826.
- (53) Marksteiner, M.; Haslinger, P.; Sclafani, M.; Ulbricht, H.; Arndt, M. *J. Phys. Chem. A* **2009**, *113* (37), 9952–9957.
- (54) Gerlich, S.; Eibenberger, S.; Tomandl, M.; Nimmrichter, S.; Hornberger, K.; Fagan, P. J.; Tüxen, J.; Mayor, M.; Arndt, M. *Nat. Commun.* **2011**, *2*, 263.
- (55) Eibenberger, S.; Gerlich, S.; Arndt, M.; Tüxen, J.; Mayor, M. *New J. Phys.* **2011**, *13* (4), 043033.
- (56) Hornberger, K.; Gerlich, S.; Haslinger, P.; Nimmrichter, S.; Arndt, M. *Rev. Mod. Phys.* **2012**, *84* (1), 157–173.
- (57) Tüxen, J.; Eibenberger, S.; Gerlich, S.; Arndt, M.; Mayor, M. *Eur. J. Org. Chem.* **2011**, *2011* (25), 4823–4833.
- (58) Schmid, P.; Stöhr, F.; Arndt, M.; Tüxen, J.; Mayor, M. *J. Am. Soc. Mass Spectrom.* **2013**, *24* (4), 602–608.
- (59) Eibenberger, S.; Gerlich, S.; Arndt, M.; Mayor, M.; Tüxen, J. *Phys. Chem. Chem. Phys.* **2013**, *15* (35), 14696–14700.
- (60) Arndt, M.; Hornberger, K. *Nat. Phys.* **2014**, *10* (4), 271–277.
- (61) Arndt, M. *Nat. Phys.* **2011**, *7* (5), 375–376.
- (62) Dörre, N.; Rodewald, J.; Geyer, P.; von Issendorff, B.; Haslinger, P.; Arndt, M. *Phys. Rev. Lett.* **2014**, *113* (23), 233001.
- (63) Cotter, J. P.; Eibenberger, S.; Mairhofer, L.; Cheng, X.; Asenbaum, P.; Arndt, M.; Walter, K.; Nimmrichter, S.; Hornberger, K. *Nat. Commun.* **2015**, *6*.
- (64) Arndt, M.; Gerlich, S.; Hornberger, K.; Mayor, M. *Phys. J.* **2010**, *10*, 37–43.
- (65) P. Crease. The most beautiful experiment - physicsworld.com
<http://physicsworld.com/cws/article/print/2002/sep/01/the-most-beautiful-experiment>
(accessed Jul 30, 2015).
- (66) Zhao, B. S.; Meijer, G.; Schöllkopf, W. *Science* **2011**, *331* (6019), 892–894.
- (67) Tonomura, A.; Endo, J.; Matsuda, T.; Kawasaki, T.; Ezawa, H. *Am. J. Phys.* **1989**, *57* (2), 117–120.
- (68) Merli, P. G.; Missiroli, G. F.; Pozzi, G. *Am. J. Phys.* **1976**, *44* (3), 306–307.
- (69) Eastwood, D.; Edwards, L.; Gouterman, M.; Steinfeld, J. *J. Mol. Spectrosc.* **1966**, *20* (4), 381–390.
-

-
- (70) Alzeer, J.; Roth, P. J. C.; Luedtke, N. W. *Chem. Commun.* **2009**, No. 15, 1970.
- (71) Wöhrle, D.; Eskes, M.; Shigehara, K.; Yamada, A. *Synthesis* **1993**, 1993 (02), 194–196.
- (72) Juffmann, T.; Milic, A.; Müllneritsch, M.; Asenbaum, P.; Tsukernik, A.; Tüxen, J.; Mayor, M.; Cheshnovsky, O.; Arndt, M. *Nat. Nanotechnol.* **2012**.
- (73) Wöhrle, D.; Schnurpfeil, G.; Knothe, G. *Dyes Pigments* **1992**, 18 (2), 91–102.
- (74) Balaz, M.; Collins, H. A.; Dahlstedt, E.; Anderson, H. L. *Org. Biomol. Chem.* **2009**, 7 (5), 874.
- (75) Lee, C.-H.; S. Lindsey, J. *Tetrahedron* **1994**, 50 (39), 11427–11440.
- (76) Michael E. Peach, A. M. S. *J. Fluor. Chem.* **1974**, 4 (4), 399–408.
- (77) Musial, B. C.; Peach, M. E. *J. Fluor. Chem.* **1976**, 7 (5), 459–469.
- (78) Chambers, R. D.; Musgrave, W. K. R.; Waterhouse, J. S.; Williams, D. L. H.; Burdon, J.; Hollyhead, W. B.; Tatlow, J. C. *J. Chem. Soc. Chem. Commun.* **1974**, No. 6, 239–240.
- (79) Crowell, T. R.; Peach, M. E. *J. Fluor. Chem.* **1982**, 21 (4), 469–477.
- (80) O’Hagan, D. *Chem. Soc. Rev.* **2008**, 37 (2), 308–319.
- (81) Fathalla, M.; Jayawickramarajah, J. *Eur. J. Org. Chem.* **2009**, 2009 (35), 6095–6099.
- (82) Wagner, R. W.; Lindsey, J. S.; Turowska-Tyrk, I.; Scheidt, W. R. *Tetrahedron* **1994**, 50 (38), 11097–11112.
- (83) Wagner, R. W.; Johnson, T. E.; Li, F.; Lindsey, J. S. *J. Org. Chem.* **1995**, 60 (16), 5266–5273.
- (84) S. Lindsey, J.; Prathapan, S.; E. Johnson, T.; W. Wagner, R. *Tetrahedron* **1994**, 50 (30), 8941–8968.
- (85) Glaser, C. *Berichte Dtsch. Chem. Ges.* **1869**, 2 (1), 422–424.
- (86) Hay, A. S. *J. Org. Chem.* **1962**, 27 (9), 3320–3321.
- (87) Dahlstedt, E.; Collins, H. A.; Balaz, M.; Kuimova, M. K.; Khurana, M.; Wilson, B. C.; Phillips, D.; Anderson, H. L. *Org. Biomol. Chem.* **2009**, 7 (5), 897.
- (88) Kamada, K.; Ogawa, K.; Ohta, K.; Kobuke, Y. *Chem. Commun.* **2012**.
- (89) Drobizhev, M.; Meng, F.; Rebane, A.; Stepanenko, Y.; Nickel, E.; Spangler, C. W. *J. Phys. Chem. B* **2006**, 110 (20), 9802–9814.
- (90) Pawlicki, M.; Morisue, M.; Davis, N. K. S.; McLean, D. G.; Haley, J. E.; Beuerman, E.; Drobizhev, M.; Rebane, A.; Thompson, A. L.; Pascu, S. I.; Accorsi, G.; Armaroli, N.; Anderson, H. L. *Chem. Sci.* **2012**, 3 (5), 1541.
- (91) Pawlicki, M.; Collins, H. A.; Denning, R. G.; Anderson, H. L. *Angew. Chem. Int. Ed.* **2009**, 48 (18), 3244–3266.
- (92) Fomina, L.; Vazquez, B.; Tkatchouk, E.; Fomine, S. *Tetrahedron* **2002**, 58 (33), 6741–6747.
- (93) Fenn, J. B.; Mann, M.; Meng, C. K.; Wong, S. F.; Whitehouse, C. M. *Science* **1989**, 246 (4926), 64–71.
- (94) Tanaka, K.; Waki, H.; Ido, Y.; Akita, S.; Yoshida, Y.; Yoshida, T.; Matsuo, T. *Rapid Commun. Mass Spectrom.* **1988**, 2 (8), 151–153.
- (95) Golovlev, V. V.; Allman, S. L.; Garrett, W. R.; Chen, C. H. *Appl. Phys. Lett.* **1997**, 71 (6), 852–854.
-

-
- (96) Golovlev, V. V.; Allman, S. L.; Garrett, W. R.; Taranenko, N. I.; Chen, C. H. *Int. J. Mass Spectrom. Ion Process.* **1997**, *169–170*, 69–78.
- (97) Bald, I.; Dąbkowska, I.; Illenberger, E. *Angew. Chem. Int. Ed.* **2008**, *47* (44), 8518–8520.
- (98) Crawford, K. E.; Campbell, J. L.; Fiddler, M. N.; Duan, P.; Qian, K.; Gorbaty, M. L.; Kenttämaa, H. I. *Anal. Chem.* **2005**, *77* (24), 7916–7923.
- (99) Asenbaum, P.; Kuhn, S.; Nimmrichter, S.; Sezer, U.; Arndt, M. *Nat. Commun.* **2013**, *4*.
- (100) Peng, W.-P.; Lin, H.-C.; Lin, H.-H.; Chu, M.; Yu, A. L.; Chang, H.-C.; Chen, C.-H. *Angew. Chem. Int. Ed.* **2007**, *46* (21), 3865–3869.
- (101) Sezer, U.; Wörner, L.; Horak, J.; Felix, L.; Tüxen, J.; Götz, C.; Vaziri, A.; Mayor, M.; Arndt, M. *Anal. Chem.* **2015**, *87* (11), 5614–5619.
- (102) Zinovev, A. V.; Veryovkin, I. V.; Moore, J. F.; Pellin, M. J. *Anal. Chem.* **2007**, *79* (21), 8232–8241.
- (103) Juffmann, T.; Ulbricht, H.; Arndt, M. *Rep. Prog. Phys. Phys. Soc. G. B.* **2013**, *76* (8), 086402.
- (104) Arndt, M. *Phys. Today* **2014**, *67* (5), 30–36.
- (105) Calvert, C. R.; Belshaw, L.; Duffy, M. J.; Kelly, O.; King, R. B.; Smyth, A. G.; Kelly, T. J.; Costello, J. T.; Timson, D. J.; Bryan, W. A.; Kierspel, T.; Rice, P.; Turcu, I. C. E.; Cacho, C. M.; Springate, E.; Williams, I. D.; Greenwood, J. B. *Phys. Chem. Chem. Phys.* **2012**, *14* (18), 6289–6297.
- (106) Chen, J.; Jia, L.; Zhao, L.; Lu, X.; Guo, W.; Weng, J.; Qi, F. *Energy Fuels* **2013**, *27* (4), 2010–2017.
- (107) Antoine, R.; Compagnon, I.; Rayane, D.; Broyer, M.; Dugourd, P.; Sommerer, N.; Rossignol, M.; Pippen, D.; Hagemester, F. C.; Jarrold, M. F. *Anal. Chem.* **2003**, *75* (20), 5512–5516.
- (108) van de Meerakker, S. Y. T.; Bethlem, H. L.; Vanhaecke, N.; Meijer, G. *Chem. Rev.* **2012**, *112* (9), 4828–4878.
- (109) Felix, L.; Sezer, U.; Arndt, M.; Mayor, M. *Eur. J. Org. Chem.* **2014**, *2014* (31), 6884–6895.
- (110) Gil-Ramírez, G.; Karlen, S. D.; Shundo, A.; Porfyraakis, K.; Ito, Y.; Briggs, G. A. D.; Morton, J. J. L.; Anderson, H. L. *Org. Lett.* **2010**, *12* (15), 3544–3547.
- (111) Odom, S. A.; Webster, S.; Padilha, L. A.; Peceli, D.; Hu, H.; Nootz, G.; Chung, S.-J.; Ohira, S.; Matichak, J. D.; Przhonska, O. V.; Kachkovski, A. D.; Barlow, S.; Brédas, J.-L.; Anderson, H. L.; Hagan, D. J.; Van Stryland, E. W.; Marder, S. R. *J. Am. Chem. Soc.* **2009**, *131* (22), 7510–7511.
- (112) Odom, S. A.; Kelley, R. F.; Ohira, S.; Ensley, T. R.; Huang, C.; Padilha, L. A.; Webster, S.; Coropceanu, V.; Barlow, S.; Hagan, D. J.; Van Stryland, E. W.; Brédas, J.-L.; Anderson, H. L.; Wasielewski, M. R.; Marder, S. R. *J. Phys. Chem. A* **2009**, *113* (40), 10826–10832.
- (113) Drobizhev, M.; Stepanenko, Y.; Dzenis, Y.; Karotki, A.; Rebane, A.; Taylor, P. N.; Anderson, H. L. *J. Phys. Chem. B* **2005**, *109* (15), 7223–7236.
-

- (114) Retsek, J. L.; Medforth, C. J.; Nurco, D. J.; Gentemann, S.; Chirvony, V. S.; Smith, K. M.; Holten, D. *J. Phys. Chem. B* **2001**, *105* (27), 6396–6411.
- (115) Aujard, I.; Baltaze, J.-P.; Baudin, J.-B.; Cogné, E.; Ferrage, F.; Jullien, L.; Perez, É.; Prévost, V.; Qian, L. M.; Ruel, O. *J. Am. Chem. Soc.* **2001**, *123* (34), 8177–8188.
- (116) Shaw, J. L.; Garrison, S. A.; Alemán, E. A.; Ziegler, C. J.; Modarelli, D. A. *J. Org. Chem.* **2004**, *69* (22), 7423–7427.
- (117) Achelle, S.; Couleaud, P.; Baldeck, P.; Teulade-Fichou, M.-P.; Maillard, P. *Eur. J. Org. Chem.* **2011**, *2011* (7), 1271–1279.
- (118) Lou, X.; van Dongen, J. L. J.; Meijer, E. W. *J. Am. Soc. Mass Spectrom.* **2010**, *21* (7), 1223–1226.
- (119) Winter, J. D.; Deshayes, G.; Boon, F.; Coulembier, O.; Dubois, P.; Gerbaux, P. *J. Mass Spectrom.* **2011**, *46* (3), 237–246.
- (120) Fenn, J. B.; Mann, M.; Meng, C. K.; Wong, S. F.; Whitehouse, C. M. *Science* **1989**, *246* (4926), 64–71.
- (121) Cai, Y.; Peng, W.-P.; Kuo, S.-J.; Sabu, S.; Han, C.-C.; Chang, H.-C. *Anal. Chem.* **2002**, *74* (17), 4434–4440.
- (122) Breuker, K.; Knochenmuss, R.; Zhang, J.; Stortelder, A.; Zenobi, R. *Int. J. Mass Spectrom.* **2003**, *226* (1), 211–222.
- (123) Glückmann, M.; Karas, M. *J. Mass Spectrom.* **1999**, *34* (5), 467–477.
- (124) Tomalová, I.; Frankevich, V.; Zenobi, R. *Int. J. Mass Spectrom.* **2014**, *372*, 51–53.
- (125) Sezer, U.; Schmid, P.; Felix, L.; Mayor, M.; Arndt, M. *J. Mass Spectrom.* **2015**, *50* (1), 235–239.
- (126) Grottemeyer, J.; Boesl, U.; Walter, K.; Schlag, E. *Org. Mass Spectrom.* **1986**, *21* (9), 595–597.
- (127) Grottemeyer, J.; Boesl, U.; Walter, K.; Schlag, E. W. *J. Am. Chem. Soc.* **1986**, *108* (14), 4233–4234.
- (128) Schlag, E. W.; Grottemeyer, J.; Levine, R. D. *Chem. Phys. Lett.* **1992**, *190* (6), 521–527.
- (129) Marksteiner, M.; Haslinger, P.; Sclafani, M.; Ulbricht, H.; Arndt, M. *J. Phys. Chem. A* **2009**, *113* (37), 9952–9957.
- (130) Marksteiner, M.; Haslinger, P.; Ulbricht, H.; Sclafani, M.; Oberhofer, H.; Dellago, C.; Arndt, M. *J. Am. Soc. Mass Spectrom.* **2011**, *19* (7), 1021–1026.
- (131) Haslinger, P.; Dörre, N.; Geyer, P.; Rodewald, J.; Nimmrichter, S.; Arndt, M. *Nat. Phys.* **2013**, *9* (3), 144–148.
- (132) Reiger, E.; Hackermüller, L.; Berninger, M.; Arndt, M. *Opt. Commun.* **2006**, *264* (2), 326–332.
- (133) Nimmrichter, S.; Haslinger, P.; Hornberger, K.; Arndt, M. *New J. Phys.* **2011**, *13* (7), 075002.
- (134) Klán, P.; Šolomek, T.; Bochet, C. G.; Blanc, A.; Givens, R.; Rubina, M.; Popik, V.; Kostikov, A.; Wirz, J. *Chem. Rev.* **2013**, *113* (1), 119–191.
- (135) Il'ichev, Y. V.; Wirz, J. *J. Phys. Chem. A* **2000**, *104* (33), 7856–7870.
- (136) Schwörer, M.; Wirz, J. *Helv. Chim. Acta* **2001**, *84* (6), 1441–1458.

- (137) Cummings, R. T.; DiZio, J. P.; Krafft, G. A. *Tetrahedron Lett.* **1988**, 29 (1), 69–72.
- (138) Cummings, R. T.; Krafft, G. A. *Tetrahedron Lett.* **1988**, 29 (1), 65–68.
- (139) Corrie, J. E. T.; Trentham, D. R. *J. Chem. Soc. [Perkin 1]* **1995**, No. 16, 1993–2000.
- (140) Robertson, S. A.; Ellman, J. A.; Schultz, P. G. *J. Am. Chem. Soc.* **1991**, 113 (7), 2722–2729.
- (141) Singh, A. K.; Khade, P. K. *Tetrahedron* **2005**, 61 (42), 10007–10012.
- (142) Patchornik, A.; Amit, B.; Woodward, R. B. *J. Am. Chem. Soc.* **1970**, 92 (21), 6333–6335.
- (143) Pillai, V. N. R. *Synthesis* **1980**, 1980 (01), 1–26.
- (144) Schmierer, T.; Laimgruber, S.; Haiser, K.; Kiewisch, K.; Neugebauer, J.; Gilch, P. *Phys. Chem. Chem. Phys.* **2010**, 12 (48), 15653–15664.
- (145) Miyaura, N.; Suzuki, A. *J. Chem. Soc. Chem. Commun.* **1979**, No. 19, 866–867.
- (146) Miyaura, N.; Yamada, K.; Suzuki, A. *Tetrahedron Lett.* **1979**, 20 (36), 3437–3440.
- (147) Miyaura, N.; Suzuki, A. *Chem. Rev.* **1995**, 95 (7), 2457–2483.
- (148) Ishiyama, T.; Murata, M.; Miyaura, N. *J. Org. Chem.* **1995**, 60 (23), 7508–7510.
- (149) Lemasson, F.; Tittmann, J.; Hennrich, F.; Stürzl, N.; Malik, S.; Kappes, M. M.; Mayor, M. *Chem. Commun.* **2011**, 47 (26), 7428–7430.
- (150) Mitsunobu, O.; Yamada, M. *Bull. Chem. Soc. Jpn.* **1967**, 40 (10), 2380–2382.
- (151) Mitsunobu, O. *Synthesis* **1981**, 1981 (01), 1–28.
- (152) Surry, D. S.; Buchwald, S. L. *Angew. Chem. Int. Ed.* **2008**, 47 (34), 6338–6361.
- (153) Li, J.; Huang, P. *Beilstein J. Org. Chem.* **2011**, 7, 426–431.
- (154) Schweinfurth, D.; Pattacini, R.; Strobel, S.; Sarkar, B. *Dalton Trans.* **2009**, No. 42, 9291–9297.
- (155) Lindsey, J. S.; Woodford, J. N. *Inorg. Chem.* **1995**, 34 (5), 1063–1069.
- (156) Gouterman, M. *J. Mol. Spectrosc.* **1961**, 6, 138–163.
- (157) Gouterman, M.; Wagnière, G. H.; Snyder, L. C. *J. Mol. Spectrosc.* **1963**, 11 (1–6), 108–127.
- (158) Weiss, C.; Kobayashi, H.; Gouterman, M. *J. Mol. Spectrosc.* **1965**, 16 (2), 415–450.
- (159) Eberhardt, W.; Hanack, M. *Synthesis* **1997**, 1997 (01), 95–100.
- (160) Kobayashi, N.; Kijima, M. *J. Mater. Chem.* **2008**, 18 (9), 1037–1045.
- (161) Schilling, C. I.; Plietzsch, O.; Nieger, M.; Müller, T.; Bräse, S. *Eur. J. Org. Chem.* **2011**, 2011 (9), 1743–1754.
- (162) Alvarez, S. G.; Alvarez, M. T. *ChemInform* **1997**, 28 (39).
- (163) Luo, L.; Frisbie, C. D. *J Am Chem Soc* **2010**, 132 (26), 8854–8855.
- (164) Kuznetsova, N.; Makarov, D.; Derkacheva, V.; Savvina, L.; Alekseeva, V.; Marinina, L.; Slivka, L.; Kaliya, O.; Lukyanets, E. *J. Photochem. Photobiol. Chem.* **2008**, 200 (2–3), 161–168.

11 Appendix

11.1 Contributions

All molecules were synthesized and analyzed by Lukas Felix in the Group of Prof. Dr. Marcel Mayor at the organic institute of the University of Basel. The described QIE in near-field and far-field regime, the thermal stability tests, the desorption experiments and the LIAD experiments were performed in the group of Prof. Dr. Markus Arndt at the physical institute of the University of Vienna by Uğur Sezer, Nadine Dörre, Johannes Horak, Lisa Wörner, Philipp Schmid, and Christian Knobloch.

11.2 Publications

Parts of the work presented in this doctoral thesis have been published in the following articles:

Uğur Sezer, Lisa Wörner, Johannes Horak, Lukas Felix, Jens Tüxen, Christoph Götz, Alipasha Vaziri, Marcel Mayor, Markus Arndt

Laser-Induced Acoustic Desorption of Natural and Functionalized Biochromophores

Analytical Chemistry **2015**, 87, 11, 5614–5619.

Uğur Sezer, Philipp Schmid, Lukas Felix, Marcel Mayor, Markus Arndt

Stability of high-mass molecular libraries: the role of the oligoporphyrin core

Journal of Mass Spectrometry **2015**, 50, 1, 235-239.

Lukas Felix, Uğur Sezer, Markus Arndt, Marcel Mayor

Synthesis of Highly Fluoroalkyl-Functionalized Oligoporphyrin Systems

European Journal of Organic Chemistry **2014**, 31, 6884-6895.

Publications

Uğur Sezer, Lisa Wörner, Johannes Horak, Lukas Felix, Jens Tüxen, Christoph Götz, Alipasha Vaziri, Marcel Mayor, Markus Arndt

Laser-Induced Acoustic Desorption of Natural and Functionalized Biochromophores

Analytical Chemistry **2015**, 87, 11, 5614–5619.

Uğur Sezer, Philipp Schmid, Lukas Felix, Marcel Mayor, Markus Arndt

Stability of high-mass molecular libraries: the role of the oligoporphyrin core

Journal of Mass Spectrometry **2015**, 50, 1, 235-239.

Lukas Felix, Uğur Sezer, Markus Arndt, Marcel Mayor

Synthesis of Highly Fluoroalkyl-Functionalized Oligoporphyrin Systems

European Journal of Organic Chemistry **2014**, 31, 6884-6895.